

I Università Iuav
- - - di Venezia
U
- - -
A
- - -
V

ON URBAN FORM AND URBAN RESILIENCE

Examining the underlying politics and advancing the role of
immaterial technology and typomorphology in assessing
urban resilience to heat stress

by

Ahmed Hazem Eldesoky
PhD curriculum in Urbanism

Supervisor

Prof. Eugenio Morello
Politecnico di Milano

August 2022

Abstract

This thesis focuses on one of the emerging research topics within the field of urban morphology that investigates how the concept of resilience, which has recently become a buzzword very favored to address the complexity and future uncertainty in cities, can be integrated into the study of urban form, as the raw material of urban design and a key element that can guide cities towards more sustainable trajectories.

More specifically, the thesis tackles some of the theoretical and methodological challenges for integrating resilience thinking into urban morphology, where two main research gaps have been addressed. The first, is the need to understand the core meaning of resilience in urban morphology and systematically examine its underlying politics (e.g. resilience of/through what? To what? For whom? How? When? Where?) so that it can be effectively operationalized.

The second is the need to support urban planning and design decisions with tools and methods that provide an improved understanding of the impact of urban form on urban resilience to different stresses and shocks. In particular, the thesis, through the use of *immaterial technology* (e.g. Geographical Information Systems, machine learning and remote sensing techniques), focuses on improving and developing quantitative methods to better understand the impact of urban form on urban resilience to heat stress, as one of the most pressing challenges in cities nowadays that has been demonstrated to be exacerbated by urban form. And assessing their applicability in growing contemporary cities in arid areas, as the most vulnerable to the impacts of climate change, and where little research has been conducted. At the core of these methods are the typomorphological classifications, which have been demonstrated to be powerful descriptive-analytical as well as normative/prescriptive means of *understanding* and *designing* cities.

Keywords: Urban morphology; space-morphology; urban resilience; typomorphology; arid cities; heat stress; GIS; machine learning; remote sensing

Preface

The work presented in this thesis is an original scientific product of the author, A. H. Eldesoky. Out of the ten chapters that make up this thesis, versions and materials of four key ones have been published in international peer-reviewed scientific journals and conference proceedings, and there is one manuscript under preparation.

An extended abstract of Chapter 3 has been accepted for publication in the proceeding of the International Seminar of Urban Form (ISUF 2022) and a full-length journal article is under preparation:

Eldesoky, A. H., Abdeldayem, W., 2022. Disentangling the relationship between urban form and urban resilience: A systematic review of the literature

A version of Chapter 5 has been peer-reviewed and published:

Eldesoky, A.H., Colaninno, N., Morello, E., 2021. High-resolution air temperature mapping in a data-scarce, arid area by means of low-cost mobile measurements and machine learning. J Phys Conf Ser 2042, 012045. <https://doi.org/10.1088/1742-6596/2042/1/012045>

A version of Chapter 6 has been peer-reviewed and published:

Eldesoky, A.H., Colaninno, N., Morello, E., 2019. Improving local climate zones automatic classification based on physic-morphological urban features. Int Conf Virtual City Territ 0, 0–3. <https://doi.org/10.5821/ctv.8663>

A version of Chapter 8 has been peer-reviewed and published:

Eldesoky, A.H., Gil, J., Berghauser Pont, M., 2021. The suitability of the urban local climate zone classification scheme for surface temperature studies in distinct macroclimate regions. Urban Clim 37, 100823. <https://doi.org/10.1016/j.uclim.2021.100823>

A version of Chapter 9 has been peer-reviewed and published:

Eldesoky, A. H., Gil, J., Berghauser Pont, M., 2022. Combining environmental and social dimensions in the typomorphological study of urban resilience to heat stress. Sustain Cities Soc 83, 103971. <https://doi.org/10.1016/j.scs.2022.103971>

Table of contents

Abstract iii

Preface iv

List of figures ix

List of tables xvi

Acknowledgment xviii

1. Introduction 1

- 1.1 Background: Cities, current and future challenges and the role of urban planning and design 1
- 1.2 Problem statement: Missing links between urban morphology and urban resilience and the need for research and decision-support tools and methods 2
- 1.3 Research aim and questions 5
- 1.4 Research context and the role of the case study 6
- 1.5 Thesis outline: The organization and the contribution of the thesis chapters 10

Part I: Background and literature review 13

2. On urban morphology and urban resilience: An introduction 14

- 2.1 Urban morphology: The study of the physical form of cities 14
 - 2.1.1. Defining urban morphology 14
 - 2.1.2. Schools and approaches in urban morphology: The standpoint of the thesis (a quantitative approach to urban form) 16
- 2.2 Urban resilience 25
 - 2.2.1. What is resilience? 25
 - 2.2.2. The concept of resilience in urban planning and design 28

3. Disentangling the relationship between urban form and urban resilience: A systematic literature review 33

- 3.1 Aim and the scope of the review 33
- 3.2 Review method 33
 - 3.2.1. Search strategy and data extraction 34
 - 3.2.2. Study selection and bibliometrics 35
 - 3.2.3. Review questions 36
- 3.3 Synthesis of the review results 38
 - 3.3.1. Bibliometrics 38

- 3.3.2. The underlying politics of resilience in urban morphology 39
- 3.3.3. Resilience as a positive/negative concept and existing definitions of urban form resilience (or resilient urban forms) 53
- 3.4 Discussion 60
 - 3.4.1. The nature of the relationship between urban form and urban resilience 60
 - 3.4.2. Towards an integrated definition of urban form resilience to heat stress 61
 - 3.4.3. Limitations of the review 62

Part II: Methods and techniques 63

4. Quantitative methods for studying the impact of urban form on urban climate: An overview 64

- 4.1 Climatological-/Environmental-based methods 64
 - 4.1.1. Field observations 65
 - 4.1.2. Empirical modelling/generalization 69
- 4.2 Typomorphological methods 70
 - 4.2.1. Typomorphological research within urban climatology 71
 - 4.2.2. The local climate zone (LCZ) classification scheme for urban temperature studies 74

5. Combining field observations and empirical modelling for describing the impact of urban form on urban temperatures in Sixth of October, Egypt 78

- 5.1 Challenges of high-resolution air temperature mapping in urban areas 78
- 5.2 Data and methods 80
 - 5.2.1. Mobile air temperature data collection and processing 80
 - 5.2.2. Calculating multi-spectral, multi-scalar remote sensing indices 84
 - 5.2.3. Empirical modelling of air temperature 85
- 5.3 Results of the empirical models and the spatial patterns of air temperature 86
- 5.4 Discussion: The scope and role of the resulting air temperature maps, limitations of the method and future improvements 90

6. Improving the local climate zone mapping of cities by means of remote sensing- and GIS-based techniques 92

- 6.1 Overview, existing LCZ mapping methods and limitations 92
- 6.2 Data and methods 94
 - 6.2.1. Test case study and data 94
 - 6.2.2. The LCZ classification procedure 95
 - 6.2.3. Accuracy assessment 97
- 6.3 The resulting LCZ map and map accuracy 97

- 6.4 Discussion: The potentials and limitations of the proposed method and future improvements 101

Part III: Testing methods and techniques, gap of knowledge and proposed innovation—The integrated multi-dimensional typomorphological classification 102

7. How well does the local climate zone classification scheme discern the thermal differences between different areas in Sixth of October, Egypt? 103

- 7.1 The LCZ classification scheme in contemporary arid cities 103
- 7.2 Data and methods 104
 - 7.2.1. LCZ sample sites 104
 - 7.2.2. Air temperature data 105
 - 7.2.3. Statistical analysis 105
- 7.3 Results: The significance of the air temperature differences between LCZ types 107
- 7.4 Conclusions: The need for a wider suitability assessment of the LCZ classification scheme 109

8. Assessing the suitability of the local climate zone classification scheme for urban temperature studies in distinct macroclimate regions 110

- 8.1 Introduction to the aim and scope of the assessment 110
- 8.2. Data and methods 111
 - 8.2.1. World macroclimate regions 112
 - 8.2.2. LCZ sample sites 113
 - 8.2.3. LST retrieval 119
 - 8.2.4. Statistical analysis 122
- 8.3. Results of the statistical analyses 123
 - 8.3.1. Intra-macroclimate region variability of LST within LCZs 123
 - 8.3.2. Intra-macroclimate region LST differences between LCZs 125
 - 8.3.3. Influence of macroclimate on the LST/SUHI characteristics of LCZs 126
- 8.4. Discussion 130
 - 8.4.1. LCZs and LSTs 130
 - 8.4.2. Extending LCZs with land cover properties to address arid regions 132
 - 8.4.3. Limitations of the study 133
 - 8.4.4. Further investigations 135

9. Combining environmental and social dimensions in the typomorphological study of urban resilience to heat stress in Sixth of October, Egypt 136

- 9.1. Inadequacies of the existing typomorphological classifications for studying heat-stress resilience 136

- 9.2. A multi-dimensional approach to the typomorphological study of heat-stress resilience 137
 - 9.2.1. A conceptual morphological framework to study heat-stress resilience 138
 - 9.2.2. Urban form characteristics and measures associated with the social dimension of heat-stress resilience 139
- 9.3. A quantitative GIS- and ML-based method for typomorphological classification of the social dimension of heat-stress resilience 142
 - 9.3.1. Introduction to the study neighborhoods in Sixth of October 142
 - 9.3.2. Data and methods 143
 - 9.3.3. Resulting typomorphological classification describing the social dimension of heat-stress resilience 147
- 9.4. Discussion 150
 - 9.4.1. An integrated multi-dimensional typomorphological classification 150
 - 9.4.2. The scope and role of the developed typomorphological classification 151
 - 9.4.3. Towards general typomorphological classifications 152

10. Discussion of research results and conclusions 153

- 10.1. Theoretical and methodological contributions 153
- 10.2. Implications for urban planning and design practice 160
- 10.3. Final considerations and directions for future research 163

References 166

Appendices 201

- Appendix A A matrix of the relationship between the urban form elements/attributes (rows) and different disturbances (columns) that they provide resilience to
- Appendix B Results of the normality and homogeneity of variance tests conducted in Chapter 7
- Appendix C Results of the normality and homogeneity of variance tests conducted in Chapter 8
- Appendix D Data sources, processing steps and the calculation of the urban form measures selected in Chapter 9 for the statistical clustering of neighborhoods

List of figures

- Figure 1.** Calthorpe’s TOD model as an example of a sustainable urban development pattern and growth. TOD was developed based on Calthorpe’s earlier pedestrian pocket concept (1989) that envisaged the neighborhood as comfortably walkable (within 400 meters), mixed-used and with medium- to high-density housing to provide a more compact urban form. The concept thus preserves open space and facilitates public transit provision that, in turn, decreases people’s dependence on driving. The TOD concept extends the pedestrian pocket to include an outer secondary area around the dense core, where there is a transit stop, to accommodate low-density housing and other large-scale developments. TODs are located at strategic locations along the regional transit network.2
- Figure 2.** The location of the existing (first, second and third generation), planned (fourth generation) and under study desert cities in Egypt. Readapted from (Angélil and Malterre-Barthes, 2018) using official data from the Egyptian Ministry of Housing and the New Urban Communities Authority (NUCA).8
- Figure 3.** The location of Sixth of October (top), readapted form (Angélil and Malterre-Barthes, 2018), and the original 1979 linear master plan and its similarity with Le Corbusier *Ville Radieuse* of 1930 (bottom); however, the green areas that were planned in the original master plan remain desert today.9
- Figure 4.** Flowchart of the chapters of this thesis in relation to each of the research questions (RQs), research problems (RPs) and the appended papers. 12
- Figure 5.** Conzen’s fundamental elements of the town plan. Reproduced from (Moudon, 1994, p. 297). 17
- Figure 6.** Conzen’s plan unit and the compositeness of the town plan. Reproduced from (Moudon, 1994, p. 298). 18
- Figure 7.** Caniggia’s typological process. The progressive transformation of the elementary domus and its ancillary spaces into a medieval courtyard house. Reproduced from (Moudon, 1994, p. 292). 18
- Figure 8.** The diachronic mutation of house types in Florence. Rome and Genoa is reconstructed in a schematic way. Reproduced from (Moudon, 1994, p. 293). 19
- Figure 9.** An overview of the categorization of urban morphology research based on Gauthier and Gilliland (2006) and Moudon (1992). *Externalist* approaches refer to contributions that consider urban form as the resulting product of external forces such as socio-economic, political and historical conditions. Reproduced from (Berghauser Pont, 2018, p. 103).20
- Figure 10.** Fresnel’s diagram: All concentric squared annuluses have the same surface area, which is equal to the area of the central square (Martin and March, 1975, p. 19).22
- Figure 11.** Two basic building types, i.e. pavilions (left) and courts (right), with the same percentage of ground coverage, building height and total floor space area. Reproduced from (Martin and March, 1975, p. 20).22

Figure 12. Martin and March’s radical proposal to replace Manhattan’s 36-stories towers in New York with large courtyard buildings only eight stories high. Reproduced from (Martin and March, 1975, pp. 20–21).	22
Figure 13. Figure-ground (top) and axial map representation (bottom) of the city of London. Reproduced from (Hillier, 1996, p. 117).	23
Figure 14. The ball-in-cup representation of the difference between engineering and ecological resilience (Carpenter et al., 1999; Scheffer et al., 1993). Reproduced from (Liao, 2012, p. 3).	26
Figure 15. A graphical representation of the metaphor of the “Adaptive Cycle”. The figure refers to four distinct phases of change in the structures and function of SESs: (r) growth or exploitation; (k) conservation; (Ω) release or creative destruction; and (α) reorganization (Gunderson and Holling, 2002). Retrieved from: http://www.resalliance.org/adaptive-cycle (Accessed June 2022).	27
Figure 16. The Panarchy model representing the interactive dynamics of a nested set of adaptive cycles. Reproduced from (Folke, 2006, p. 258).	27
Figure 17. An unbuilt project for the extension of the Zachęta art gallery in Warsaw, Poland (1958) by Polish architect and urban planner Oskar Hansen representing his concept of the open form. The building has a system of movable stairs and slabs that allow for a continuous reconfiguration of the different floors.	29
Figure 18. A project for an office complex in Apeldoorn, the Netherlands (1968–1972) by Dutch architect Herman Hertzberger representing his idea of the polyvalent space. The office space was intentionally left partially unfinished to allow users to complete it in ways that suit their working needs.	29
Figure 19. Flow diagram of the systematic review process.	34
Figure 20. The network of keywords occurrence/co-occurrence formed using the VOSviewer software based on the 106 included publications from Scopus and WoS.	38
Figure 21. The distribution of the publications based on the distinction between resilience <i>through</i> and <i>of</i> urban form.	40
Figure 22. The distribution of the publications based on the type of resilience they discuss (general versus specified).	41
Figure 23. The most recurring urban resilience actors in the reviewed literature. The bigger and bolder the word, the more frequent it was mentioned in the literature.	47
Figure 24. The most recurring urban resilience beneficiaries. The bigger and bolder the word, the more frequent it was mentioned in the literature.	47
Figure 25. The distribution of the reviewed publications based on the pathway of resilience they focus on.	48
Figure 26. The distribution of the reviewed publications based on the type of adaptability performance they discuss (people adapt versus urban form adapts).	48

Figure 27. The distribution of the reviewed publications based on the temporal scale of resilience they discuss from the authors' point of view.....	50
Figure 28. The geographical distribution of the number of publications focusing on the relationship between urban form and urban resilience.	52
Figure 29. The different atmospheric layers over a city during daytime (left) and nighttime (right). Readapted from (Oke et al., 2017, p. 31).	65
Figure 30. Conceptual diagram of ground-based, aerial and remote-sensing observational platforms, sorted by their suitability to sample the entire urban boundary layer (UBL, left), the surface layer (SL, center) or the urban canopy layer (UCL, right), and their sampling approach (upright side). Most importantly, within the UCL, fixed platforms (along the front) include a Stevenson (thermometer) Screen (1), and mobile/traversing approaches (along the back) include vehicles such as cars and cargo bikes (9). Satellite remote sensing can characterize the surface or atmosphere across a range of scales including the UCL (12). Readapted from (Oke et al., 2017, p. 53). ...	66
Figure 31. Examples of fixed weather stations (top) and a network of fixed weather stations in the Lombardy region, Italy (bottom).	67
Figure 32. Example of a low-cost (around 190\$) personal weather station manufactured by Netatmo company.	67
Figure 33. Examples of mobile traverse systems that have been used in previous studies. (a) A mobile monitoring setup composed of a radiation shield containing a temperature sensor, a portable weather station and a video camera (Tsin et al., 2016); (b) A light-colored vehicle equipped with several sensors, a Global Positioning System (GPS) and a video camera (Shi et al., 2018); (c) A wearable monitoring system with several embedded sensors as well as a camera and a GPS (Pigliautile and Pisello, 2018); (d) A semi-stationary weather station composed of a portable weather station, rotating vane mount, tripod, and signboard (Kim and Macdonald, 2016); (e) A local transport bus in Aachen, Germany, equipped with a self-built measurement device consisting of a temperature sensor and a GPS (Buttstädt et al., 2011); (f) A bicycle equipped with a temperature sensor and a GPS (Yokoyama et al., 2018); (g) A bicycle equipped with different sensors of air pollutants (Samad and Vogt, 2020).	68
Figure 34. Representation of the instrumental configurations when instruments are carried by humans during mobile measurements. (a) Wearable instrument; (b) portable instrument; (c) Movable instrument; (d) Semi-stationary instrument. Reproduced from (Requena-Ruiz et al., 2019, p. 4).	69
Figure 35. Chandler's classification of local climate regions in London (I = Central; II = Inner suburban; III = Outer suburban; IV = Northern heights). Reproduced from (Chandler, 1965, p. 243).	72
Figure 36. Auer's meteorologically-oriented LULC classification of the Metropolitan St. Louis area (I1 = Heavy industrial; I2 = Light moderate industrial; C1 = Commercial; R1 = Common residential; R2 = Compact residential (single-family dwellings); R3 = Compact residential (multi-family dwellings); R4 = Estate residential; A1 = Metropolitan natural; A2 = Agricultural rural; A3 = Undeveloped; A4 = Undeveloped rural; A5 = Water surfaces). Reproduce from (Auer, 1978, p. 637).	72

Figure 37. The distinctive features of Ellefsen’s UTZ type A1 (the core area). Reproduced from (Ellefsen, 1991, p. 1041).....	73
Figure 38. Oke’s UCZ classification scheme. Reproduced from (Oke, 2004, p. 11). 73	
Figure 39. Logical division of the universe type by roughness objects (buildings, plants), object height (high, mid, low, nil), object density (O = open; C = close) and land cover (I = impervious; P = pervious). Sample derivative types are shown at the bottom. The close high-rise type (bottom left) derives from landscape division into buildings of maximum height and density, and surrounding surfaces of impervious cover. Reproduced from (Stewart, 2011, p. 163).....	75
Figure 40. The LCZ classification scheme. Reproduced from (Stewart, 2011, p. 196).	76
Figure 41. Interpolation of air temperature at 1500-m spatial resolution for the metropolitan city of Milan (Italy) implemented by <i>Agenzie Regionali per la Protezione dell’Ambiente (ARPA)</i> (top); and Geographically Weighted Regression (GWR) modelling of air temperature at 30-m spatial resolution by <i>Laboratorio di Simulazione Urbana Fausto Curti</i> (bottom).....	79
Figure 42. Schematic overview of the air temperature modelling procedure.	80
Figure 43. The Pasco portable weather station used to collect air temperature data during the four measurement campaigns.	81
Figure 44. The morphologically different built-up areas crossed during the four automobile-based measurement campaigns on September 2nd, 29th and 30th, 2020. 82	
Figure 45. Geolocating the processed air temperature mobile measurements for each of the measurement campaigns using the latitude and longitude coordinates collected by the GPS sensor.	83
Figure 46. A multi-spectral image at 30-m spatial resolution for the study area (Sixth of October, Egypt) acquired from Landsat 8 on September 14, 2020.	84
Figure 47. Spatial distribution, with isotherm lines, of the modelled air temperature data at 30-m spatial resolution for the 2nd (at 19:00 LT, left) and 29th (at 14:30 LT, right) of September 2020. The dotted white lines denote the routes of the measurement campaigns.	88
Figure 48. Spatial distribution, with isotherm lines, of the modelled air temperature data at 30-m spatial resolution for the 30th of September 2020 at 13:30 LT (left) and 19:30 LT (right). The dotted white lines denote the routes of the measurement campaigns.	88
Figure 49. Close-up views with isotherm lines showing the impact of urban form on the spatial variability of air temperature on the 2nd of September 2020 during the nighttime (19:00 LT).....	89
Figure 50. Close-up views, with isotherm lines, showing that the central urban areas with relatively higher building density are cooler than the surrounding desert during daytime (left) but warmer at nighttime (right).	89

Figure 51. The LCZ classification of Sixth of October generated using the LCZ generator (left), and the LCZ classification accuracy measures (right), where OA, OA _u , OA _{bu} and OA _w refer to the overall accuracy, the overall accuracy of the urban LCZ types only, the overall accuracy of the built versus natural LCZ types only and the overall weighted accuracy, respectively.	94
Figure 52. The location of the metropolitan city of Milan (highlighted in red) within the Lombardy region (left), and a multi-spectral image acquired from Landsat 8 (right).	95
Figure 53. The training samples used for creating the supervised LCZ classification of the metropolitan city of Milan. The LCZ samples were digitized using Google Earth imagery following the instruction provided by WUDPAT.....	96
Figure 54. The resulting LCZ map of the metropolitan city of Milan using the proposed method and a post-classification majority filter of a 4-pixel radius. The raw and filtered (at different radii) LCZ maps are made open access and can be downloaded from https://doi.org/10.6084/m9.figshare.19646781.v1	98
Figure 55. Boxplots of the distribution of the accuracy measures across the 25 iterations. (a) Overall accuracy for all testing polygons; (b) Kappa coefficient for all testing polygons; (c) Overall accuracy of all built polygons; and (d) Overall accuracy of all built polygons (excluding LCZs 3 and 9).	99
Figure 56. Boxplots for the certainty of the results over the entire domain. (a) Built LCZs; (b) Non-built LCZs.	99
Figure 57. The producer accuracy (%) for each LCZ type. (a) The WUDAPT level 0 product; (b) The proposed method.....	100
Figure 58. The total number of digitized polygons per LCZ type in Sixth of October, Egypt.	105
Figure 59. Box plots of the distribution of the air temperature for each LCZ type during nighttime (top) and daytime (bottom).	107
Figure 60. Results of the post-hoc tests to compare LCZ types for the different dates/times considered in the analysis. Black cells indicate no significant difference between LCZ types ($p > .05$), while colors ranging from red to yellow via green indicate higher to lower significance levels at ($p < .05$). The number of hits (N. hits) in significance per LCZ type is reported twice at the end of each row: once considering all the LCZ types and once considering only the urban/built LCZ types. The percentage of hits in all pairwise comparison tests is indicated for each date/time as a (%) value in the bottom right corner.....	108
Figure 61. Köppen–Geiger climate classification map (1980–2016) at 1-km spatial resolution. Reproduced from (H. E. Beck et al., 2018, p. 3).	112
Figure 62. Examples of the quality control and the processed WUDAPT raw training data. (a) Excluded unrepresentative/heterogeneous LCZ polygons; (b) Excluded LCZ polygon representing site that is not persistent over time; (c) Reclassified LCZ polygons; (d) Range of LCZ polygons across Madrid, Spain distinguished for processing; (e) Final LCZ polygons after quality control and processing.	116

Figure 63. The distribution of the total number of polygons (5392) per LCZ and macroclimate region; the tropical (745), the arid (718), the temperate (2918) and the cold (1011). 117

Figure 64. The geographic distribution of LCZ polygons (grouped by city) for each macroclimate region. Circled dots indicate the newly added locations. 118

Figure 65. Examples of multi-year LST images (top) and NDVI images (bottom) calculated from Landsat 7 and Landsat 8 imagery between 2017 and 2019 by applying a SC algorithm in Google Earth Engine. 120

Figure 66. (a) Average percentage of monthly missing data in LCZ polygons per macroclimate region, calculated for every polygon as the ratio between the number of cloudy pixels in a polygon and the total number of pixels in that polygon. Bars represent the standard error of the mean. (b) Comparison between the mean LST values calculated per LCZ type and macroclimate region using different samples of LCZ polygons with varying levels of missing data, from no more than 20% up to 80% of missing data in all months (see Figure 1 in Appendix C for a more detailed plot). .. 121

Figure 67. Box plots of the distribution of the LST for each LCZ type per macroclimate region. 124

Figure 68. Results of the post-hoc tests to compare LCZ types within each macroclimate region. Black cells indicate no significant difference between LCZ types ($p > .05$), while colors ranging from red to yellow via green indicate higher to lower significance levels at ($p < .05$). The number of hits (N. hits) in significance per LCZ type is indicated at the end of each row. The percentage of hits in all pairwise comparison tests is indicated for each macroclimate region as a (%) value in the bottom right corner. 126

Figure 69. The mean LST of each LCZ type across the tropical (red), the temperate (sea green) and the cold (slate blue) climate regions. Bars represent standard deviation, NS stands for not significant and asterisks indicate significant differences between group pairs at ($p < .05$), as calculated by the post-hoc tests. 128

Figure 70. The mean SUHI intensity of each LCZ type across the tropical (red), the temperate (sea green) and the cold (slate blue) climate regions. Bars represent standard deviation, NS stands for not significant and asterisks indicate significant differences between group pairs at ($p < .05$), as calculated by the post-hoc tests. 129

Figure 71. The LST–NDVI scatterplots with marginal histograms for the different macroclimate regions. The black solid lines are the dry (upper) and wet (lower) limiting edges considering all the observations from all macroclimate regions, while the black dashed lines are the limiting edges considering only observations from the underlying macroclimate region. 133

Figure 72. Refrigerated trucks stored bodies during the 1995 heatwave (left); Chicagoans sleeping outdoor during the heatwave (right). Source: Chicago Sun-Times. 138

Figure 73. Conceptual framework representing the contribution of urban form to heat-stress resilience: (a) urban form characteristics modify urban climate and result in increased heat stress; (b) excessive heat stress impacts people’s health and comfort; (c)

various social processes can increase people’s adaptation capacity to heat stress; (d) urban form characteristics influence these social processes; and (e) people can redesign/manage urban form to better mitigate or adapt to heat stress..... 139

Figure 74. The case study area and the neighborhoods selected for the analysis and the typomorphological classification. Study neighborhoods were classified into LCZ types based on the local knowledge of the author and using subtypes that represent a combination of built and land cover types. 143

Figure 75. The GIS model of the study area showing the main layers included in the analysis and the typomorphological classification. 144

Figure 76. Hierarchical clustering dendrogram with a heatmap. Colors ranging from dark to light blue indicate higher to lower values. The dendrogram suggests a division of the neighborhoods into five clusters. H, L and N/A stand for high, low and not applicable, respectively. 148

Figure 77. Box plots showing the distribution of urban form numeric measures per neighborhood cluster (top), the spatial distribution of clusters (middle) and examples of representative neighborhoods with schematic visualizations (bottom). Boxes in red colors represent the measures of public space characteristics and in blue colors accessibility to social infrastructure. Boxplot values are standardized using Z-scores, where the values of DSINF and DSINF (SD) are inverted so that positive values (above the mean) indicate a positive contribution to heat-stress resilience..... 149

List of tables

Table 1. Examples of the different conditions that were found in previous studies to increase/decrease people’s resilience to extreme heat events.....	4
Table 2. A selection of definitions of urban morphology. Reproduced form (Marshall and Çalışkan, 2011, p. 412).	15
Table 3. A selection of definitions of urban resilience. Reproduced form (Meerow et al., 2016).	30
Table 4. Search blocks used in Scopus and WoS databases to retrieve relevant publications eligible for the systematic literature review.	35
Table 5. The urban form elements/attributes that were discussed in the reviewed literature in relation to resilience performances and/or properties to face general/specified disturbances.	40
Table 6. The contexts where the relationship between urban form and urban resilience was discussed and studied. Countries are listed in descending order based on the number of publications.	51
Table 7. The number of publications (per continent in descending order) focusing on the relationship between urban form and urban resilience, as well as the top most discussed urban form elements and disturbances.	53
Table 8. A selection of definitions of urban form resilience (or resilient urban form) identified in the 106 reviewed publications.	54
Table 9. Summary of the processed air temperature data.	83
Table 10. Summary of the RF model results.....	86
Table 11. Accuracy measures of the LCZ classification.....	99
Table 12. Summary of the preliminary analyses of variance showing the significance of the difference between LCZ types in terms of air temperature for each date/time analyzed.	107
Table 13. Quality control and processing steps for the WUDAPT training data.....	114
Table 14. Summary of the preliminary analyses of variance showing the significance of the difference between LCZ built types in terms of LST within each macroclimate region, where statistic is the test statistics, reported as χ^2 in case of Kruskal–Wallis test and F in case of Welch’s Heteroscedastic F Test with Trimmed Means and Winsorized Variances.....	125
Table 15. Summary of the preliminary analyses of variance showing the significance of the difference between the macroclimate regions, other than the arid, in terms of LST within each LCZ built type, where statistic is the test statistics, reported as χ^2 in case of Kruskal–Wallis test and F in case of Welch’s Heteroscedastic F Test with Trimmed Means and Winsorized Variances.....	127

Table 16. Summary of the preliminary analyses of variance showing the significance of the difference between the macroclimate regions, other than the arid, in terms of SUHI within each LCZ built type, where statistic is the test statistics, reported as χ^2 in case of Kruskal–Wallis test and F in case of Welch's Heteroscedastic F Test with Trimmed Means and Winsorized Variances.....	127
Table 17. LCZs' rank in terms of mean LST from 1 (highest) to 10 (lowest) within the tropical, the temperate and the cold climate regions.....	130
Table 18. Overview of the urban form measures selected for the statistical clustering of neighborhoods. More details are provided in Appendix D.	145
Table 19. Contingency table between the LCZ types and the identified neighborhood clusters.	151

Acknowledgment

I am deeply indebted to many people without whom this work could not have been possible. I would like to express my sincere thanks and gratitude to:

- My main supervisor and mentor Professor Eugenio Morello who gave me all the possible academic support and sound guidance during this PhD journey. He has motivated me, believed in my research capabilities and offered me the opportunity to engage in the research projects run by his research lab.
- My supervisors during my research visiting period at Chalmers University of Technology (2020–2021): Professor Meta Berghauer Pont who offered me the possibility to join the Spatial Morphology Group and whose writings have inspired me intellectually and opened up my horizons in the world of space-morphology; and Professor Jorge Gil for his excellent supervision and for helping me taking my research and data analytics skills to the next level. My gratitude to them extends beyond words.
- My thesis reviewers, Professors Sergio Porta and Alexander Wandl for their availability to review this work, highly valuable comments and feedback.
- The journal editors, conference organizers and the many peer reviewers involved for their comments and feedback that undoubtedly improved the quality of this work.
- The Spatial Morphology Group at Chalmers University of Technology for providing a research-friendly and welcoming environment. Special thanks to Job van Eldijk, Jonathan Cohen, Gianna Stavroulaki, Alexander Hellervik, Professor Lars Marcus and Jane Bobkova, and also to my other Chalmers colleagues, Elke Miedema and Giliam Dokter.
- My colleagues at Laboratorio di Simulazione Urbana at Politecnico di Milano, especially Nicola Colaninno to whom I owe my fondness of GIS science.
- My friends: Mohamed Yadem, Walid Samir, Abdelrahman Elmahdy, Mahmoud Nagy, Mohamed Elgohary, Somaya Aboelnaga, Sara Eltokhy, Ebraheem Imam, Mohamed Abolilah, Yasmin Samak, Ahmed Said Amer, Marika Fior, Janett Vucidolov and Giacomo Magnabosco.
- My family members: my beloved father and mother; my little brothers; and my aunts. Thank you very much for your unconditional love, support, encouragement and strong faith in me.
- And a heartfelt thank you to Maia for joining my life and being with me at this very important moment.

Last but not least, I would like to dedicate this thesis to my late grandfather who would have been very proud and happy to see me finish this work.

This research was made possible through a Doctoral Scholarship from Università IUAV di Venezia (the PhD curriculum in Urbanism).

Chapter 1

Introduction

This first chapter of the thesis gives an overview of the research project by setting the background to the research problem, formulating the research aim and questions, introducing the research context and presenting the individual chapters of the thesis.

1.1 Background: Cities, current and future challenges and the role of urban planning and design

Cities occupy only 3% of the Earth's land; however, in 2018 they were home to more than 55% of the world's population (around 4.2 billion people) with expectations to reach around 70% by 2050 (United Nations, 2019). As a result, cities, especially in the developing countries where 86% of the world's urban population is expected to be living by 2050 (United Nations, 2019), are facing unprecedented pressing challenges and have become more prone than ever to various chronic stresses and acute shocks. This includes for instance high unemployment, lack of affordable housing, poor air quality, food shortages, water scarcity, inefficient infrastructure and transport systems, disease outbreaks, heatwaves and flooding.

To address these challenges, there is a need for new models of governance and innovative approaches to the planning and design of cities (Albrechts et al., 2020). In particular, in the fields of urban planning and design, several models and approaches have been proposed since the 1980s to provide patterns of urban development and growth that are socially, economically and environmentally sustainable (Raman, 2010). This includes, for instance: the compact city (Jenks et al., 1996); the polycentric city (Frey, 2003); the eco-neighborhood (Barton, 2000); the urban village (Aldous, 1992); smart growth (Farris, 2001); the sustainable urban neighborhood (Rudlin and Falk, 1999); transit-oriented development (TOD) (Calthorpe, 1993; Cervero, 1998) (Figure 1); and the new urbanism development (Jabareen, 2006; Talen, 1999).

More recently, the concept of urban resilience defined as “the ability of an urban system . . . to maintain or rapidly return to desired functions in the face of a disturbance, to adapt to change, and to quickly transform systems that limit current or future adaptive capacity” (Meerow et al., 2016, p. 39) has become mainstream in urban research and policy to prepare cities for the future uncertainty and indeterminism in “a world of transformations” (Folke et al., 2002), and contribute to the broader sustainable development goals (Meerow and Newell, 2016; Zhang and Li, 2018).

This new way of resilience thinking has been widely adopted and promoted by many national and supranational organizations and was integrated into global policy documents such as the UN 2030 Agenda for Sustainable Development, specifically goals 9 (industry, innovation and infrastructure) and 11 (sustainable cities and communities), and the New Urban Agenda, adopted by Habitat III in Quito, Ecuador. Furthermore, several international initiatives have been promoted to support cities

worldwide in integrating resilience thinking into planning and design practices. Examples of these initiatives include the Making Cities Resilient (MCR) campaign by the United Nations Office for Disaster Risk Reduction (UNDRR) and the 100 Resilient Cities (100RC) program launched in 2013 by the Rockefeller Foundation¹.

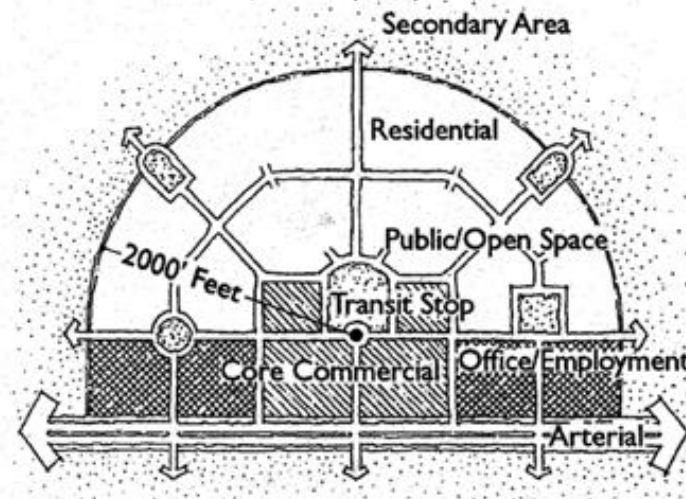


Figure 1. Calthorpe's TOD model as an example of a sustainable urban development pattern and growth. TOD was developed based on Calthorpe's earlier pedestrian pocket concept (1989) that envisaged the neighborhood as comfortably walkable (within 400 meters), mixed-used and with medium- to high-density housing to provide a more compact urban form. The concept thus preserves open space and facilitates public transit provision that, in turn, decreases people's dependence on driving. The TOD concept extends the pedestrian pocket to include an outer secondary area around the dense core, where there is a transit stop, to accommodate low-density housing and other large-scale developments. TODs are located at strategic locations along the regional transit network.

1.2 Problem statement: Missing links between urban morphology and urban resilience and the need for research and decision-support tools and methods

The concept of resilience has been introduced in urban planning and design almost two decades ago, and since then there have been several efforts to better integrate the concept into the theory and practice of urban planning and design (Sharifi, 2019a; Sharifi and Yamagata, 2016a).

In particular, in urban planning and design, the interest in better understanding how resilience thinking can be integrated into the study of urban form or the physical form of cities (i.e. in urban morphology) has been growing. As a result, several studies have been published to better establish this urban form-resilience relationship (e.g. Feliciotti et al., 2016; Marcus and Colding, 2014; Sharifi, 2019b, 2019a, 2019c; Sharifi and Yamagata, 2018a). The motivation for studying this relationship is twofold. Firstly,

¹ <https://www.rockefellerfoundation.org/>

urban form has various implications for the economic (Bobkova et al., 2019b), social (Legeby, 2013) and environmental (Ratti et al., 2003) performance of cities, and hence it can direct them towards either sustainable or unsustainable trajectories (Feliciotti et al., 2016; Sharifi and Yamagata, 2018a). Secondly, most of the instruments that urban planners and designers have at hand to intervene in cities and influence different urban processes “are physical in form and intent” (Batty and Longley, 1994, p. 1), where they primarily act upon the shaping of urban elements (e.g. buildings, streets, open and green spaces) and their relationships (Carmona, 2021; Marcus and Colding, 2011).

The ambiguity of the meaning of resilience in urban morphology

However, resilience is a polysemic concept (Galderisi et al., 2020; Norris et al., 2008; Sharifi and Yamagata, 2018b) and can be interpreted in a multitude of ways (Meerow et al., 2016). For example, as persistence/robustness to maintain the system’s status quo against a disturbance (i.e. engineering resilience) but also as the ability of the system to incrementally adapt (i.e. ecological resilience) or more radically transform to a new equilibrium status (i.e. evolutionary resilience). Hence, there is a “need to examine the underlying politics of resilience” (Meerow and Newell, 2016, p. 6) and adjust its meaning “depending on the specific research question(s)” (Sharifi and Yamagata, 2018a, p. 168) so that it can be effectively operationalized. This requires thinking critically through a set of relevant wh-questions (Brown, 2014; Carpenter et al., 2001; Meerow and Newell, 2016; Vale, 2014).

More specifically, in urban morphology, this requires questioning what elements of urban form (e.g. buildings, plots, streets, blocks) can be resilient (or can provide resilience) to what (e.g. climate change, natural disasters, disease outbreaks, terrorism)? Who does benefit/lose from this resilience (e.g. general or special populations)? Who does determine (plan/design for) the resilience (e.g. policymakers, urban planners, designers)? And how or in which mechanism (e.g. by maintaining the system’s status quo, incrementally adapting or radically transforming)? Where (in which geographical context)? And when (for short term or long term)? However, to date, there has been little effort to understand these aforementioned politics of resilience in urban morphology and improve the intelligibility in the field about this emerging research topic, and it is this the preliminary research problem that this thesis addresses.

The need for urban resilience planning and design decision-support tools and methods

Another challenge to integrating resilience thinking into urban planning and design practices in general, and providing evidence-based design principles and guidelines is the need for tools and methods to study (e.g. describe, analyze, measure and assess) urban resilience to different stresses and shocks (da Silva et al., 2012; Feliciotti, 2018; Forgaci and van Timmeren, 2014; Hassler and Kohler, 2014). In urban morphology, these tools and methods do not aim to provide a full understating of all the complex dynamics of cities, such as the different processes that influence urban resilience to specific stresses or shocks. Rather, they are “concerned with describing, defining and

theorizing a single segment of urban knowledge” (Scheer, 2016, p. 3), i.e. the physical form of cities (or urban form) and explaining how it relates to urban resilience.

More specifically, this thesis addresses how urban resilience to heat stress—as one of the most pressing challenges in cities nowadays that has been demonstrated to be exacerbated by urban form characteristics (Fahed et al., 2020; Martins et al., 2016; Salata et al., 2017; Shareef and Abu-Hijleh, 2020)—can be studied. Excessive heat stress is not only associated with high discomfort levels but also results in increased heat-related mortality and hospitalization, as well as an increased chance of death from other diseases such as respiratory illness (Hatvani-Kovacs et al., 2016; Heaviside et al., 2017; Pyrgou and Santamouris, 2018).

On the one hand, although there are several methods to study the impact of urban form on urban resilience to heat stress, there is a need to (1) extend their application to cover entire cities and urban areas; and (2) improve their output in terms of spatial resolution and accuracy, thus better supporting strategic urban planning and design decisions at multiple scales and levels. Furthermore, there is a need to assess the applicability of these methods in growing contemporary (modernist) cities in arid areas as the most vulnerable to the impacts of climate change and global warming, and where little research has been conducted.

On the other hand, most of the existing methods focus primarily on the environmental dimension of heat-stress resilience, i.e. address the urban form characteristics and measures that influence the environmental conditions in cities and overlook other important ones for heat-stress resilience, such as the social, economic and institutional conditions (Table 1). Indeed, whilst urban form does not influence all these conditions, some have shown to be related to urban form characteristics, such as the conditions of social interaction and the state of social ties and solidarities in urban neighborhoods, as will be discussed in detail in Chapter 9. Therefore, there is a need for improved methods to better study the broader impact of urban form on urban resilience to heat stress.

Table 1. Examples of the different conditions that were found in previous studies to increase/decrease people’s resilience to extreme heat events.

Conditions	Description	Reference
Environmental	Refer to the indoor and outdoor thermal conditions (e.g. air temperature, relative humidity) that determine human physiological responses during extreme heat events. In addition to the background climate characteristics, these conditions are largely influenced by urban form characteristics, such as building dimensions, construction materials properties, and land cover types and properties.	(Hu et al., 2019; Huynen et al., 2001; Madrigano et al., 2015; van Loenhout et al., 2016)

(continued)

Table 1 (continued)

Conditions	Description	Reference
Social	Refer to the extent to which people are integrated into social networks/relationships and have access to enough social support during extreme heat events. They are influenced by different factors, among which are the urban form characteristics that can, e.g. facilitate/impede access to potential social infrastructure as will be discussed in Chapter 9.	(Klinenberg, 2018, 2002, 2001, 1999; Naughton et al., 2002; Seebaß, 2017)
Economic	Reflect the financial capacity of individuals or households to survive or adapt to extreme heat events (e.g. by affording air conditioning, hospitalization expenses, health insurance and means to access information, such as mobile phones and internet connection). They are primarily determined by the economic characteristics of the population (e.g. measured by household income).	(Curriero et al., 2002; Harlan et al., 2006; Kim and Joh, 2006; Naughton et al., 2002)
Health and demographic	Reflect the physiological capacity of individuals to survive or adapt to extreme heat events. They are primarily determined by the health (e.g. the presence of chronic diseases, such as respiratory- and cardiovascular-related diseases) and demographic characteristics (e.g. age and sex) of the population.	(Ando et al., 1997; Baccini et al., 2008; D'Ippoliti et al., 2010; Hertel et al., 2009; Rocklöv et al., 2014; Semenza et al., 1996)
Institutional	Refer to the institutional/governance capacity and the degree of preparedness of cities (or city officials) to deal with extreme heat events. They are determined by the effectiveness of different institutional services, such as emergency services (e.g. ambulance services and cooling centers), hospitalization and social care services, life support systems (e.g. electricity and drinking water systems), and communication and early-warning systems.	(Ebi et al., 2004; Klinenberg, 2018, 2002, 1999)

1.3 Research aim and questions

Besides clarifying the core meaning of resilience in urban morphology and systematically examining its underlying politics, this thesis aims to improve (in terms of scale and accuracy) and develop methods to better study the impact of urban form on urban resilience to heat stress as well as assessing their applicability in contemporary arid cities. These methods are aimed to be:

- Descriptive and analytical (explanatory), i.e. not only explaining the *what is* but also the *why*;
- Suitable for climate-vulnerable areas (e.g. arid climate regions);
- Context-sensitive as well as systematic, i.e. adaptable to different contexts; and
- Multi-dimensional, i.e. addressing the broad foundation of the problem and not only its environmental dimension.

Specifically, the thesis aims to answer the following research questions (RQs):

- What is the core meaning of resilience in urban morphology? Or, in other words, what urban form elements can be resilient (or can provide resilience) to what? For whom? How? When? Where? Why?
- What are the existing quantitative methods that can be used for studying the impact of urban form on urban resilience to heat stress? What are their potentials and limitations?
- How can we improve the output of these methods in terms of scale (i.e. extent and spatial resolution) and accuracy to better support urban planning and design decisions?
- What is the applicability of these methods in contemporary cities in arid areas (e.g. Cairo desert cities)?
- What other important urban form characteristics and quantitative measures (not considered in existing methods) do we need to consider when studying heat-stress resilience from a broader perspective (e.g. including both environmental and social dimensions)?
- How can these urban form characteristics and quantitative measures be employed to better study urban resilience to heat stress in contemporary cities in arid areas (e.g. Cairo desert cities)?

1.4 Research context and the role of the case study

This section introduces the specific case study that will serve in this thesis as the testbed where the different concepts, methods, findings and conclusions will be viewed.

In general, as anticipated earlier, the geographical context of this thesis is arid climate regions and, in particular, the new desert cities (or the emerging desert urbanity) in Egypt. The reasons for this choice are as follows. Firstly, arid regions cover more than 30% of the Earth's land and are home to more than a third of the world's population who lives mostly in developing countries (Arup, 2018). Secondly, arid regions are highly vulnerable to global climate change effects and are already experiencing extreme climate events such as a high increase in the temperature of the hottest days (Masson-Delmotte et al., 2021). Hence, addressing arid climate cities is an urgent challenge to test resilience pathways and can be a reference for other urban latitudes that will experience severe climate conditions in the (near) future. Lastly, most of the

contemporary cities in arid regions, which have been exponentially growing over the last decades, are planned and designed based on outdated global western modernist models that rely on strict zoning, large-scale urban schemes and car-centric plans (Arup, 2018). The result is sprawling, unsustainable cities that are poorly adapted to arid climate conditions, which exacerbates their vulnerability to global climate change effects.

These above-mentioned models are well represented in the case of the new desert cities in Egypt, which, since the 1950s, has adopted a long-lasting national policy to urbanize desert land (land reclamation) and produce housing to decentralize existing dense cities. The result of this policy is about 44 cities of which 16 are around Cairo (within the greater Cairo region) (Figure 2). The planning of these cities is inspired by western modernist models (e.g. *ville fonctionnelle* and American suburbia) that rely on functional zoning and geometric layouts to create ordered urban environments (Combeau and Greco, 2018).

The specific case study of this work is Sixth of October new desert city, Egypt, located approximately 32 km west of Cairo (29.9° N, 30.9° E) in the hot desert climate zone (BWh) according to the Köppen–Geiger climate classification system (H. E. Beck et al., 2018; Köppen and Geiger, 1936). The city occupies a total area of about 220 km² and had a population of around 348,870 inhabitants in 2017.

Sixth of October is one of the first-generation new cities (the second oldest) and it is regarded as a relatively successful city both in attracting industry and population, even though it has never reached its initial target population (500,000 inhabitants) (Angélil and Malterre-Barthes, 2018). Further, it represents a typical example where “modernist urban planning, economic liberalization and crony capitalism meet and overlap, with unfortunate results” (Angélil and Malterre-Barthes, 2018, p. 27). The city has a functionalist, linear plan similar to that of the Soviet cities of the early 1920s and the functionalist schemes of 1930s CIAM (*Congrès Internationaux d’Architecture Moderne*), where residential districts are separated from industrial areas and are organized around a major service spine. Each residential district is composed of six to eight of the so-called neighborhoods that target different income groups (Figure 3).

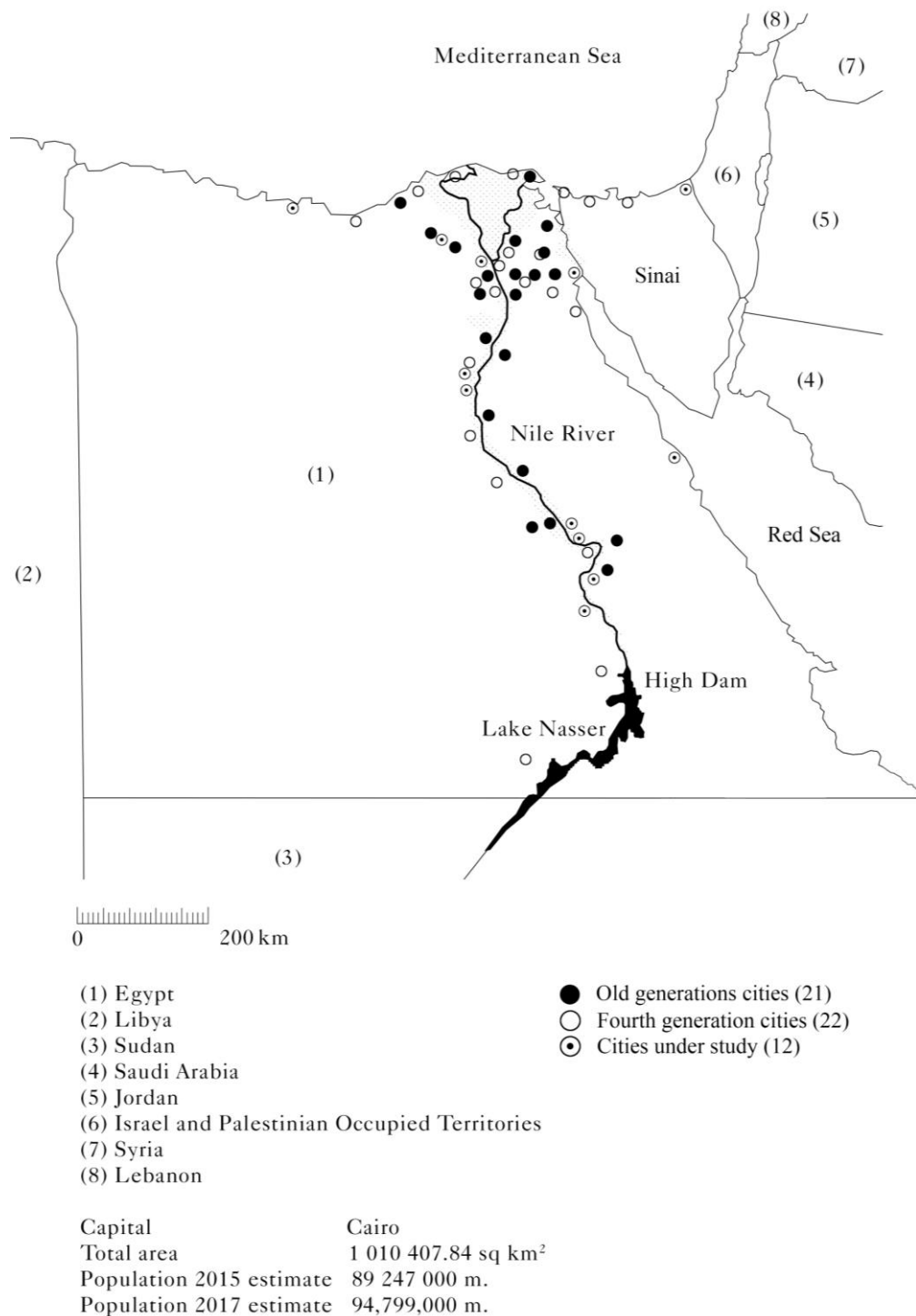


Figure 2. The location of the existing (first, second and third generation), planned (fourth generation) and under study desert cities in Egypt. Readapted from (Angéilil and Malterre-Barthes, 2018) using official data from the Egyptian Ministry of Housing and the New Urban Communities Authority (NUCA).

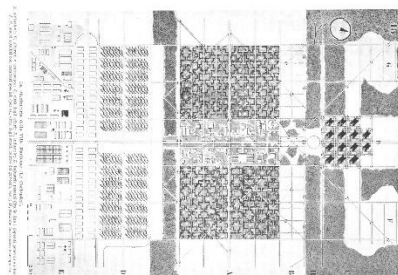
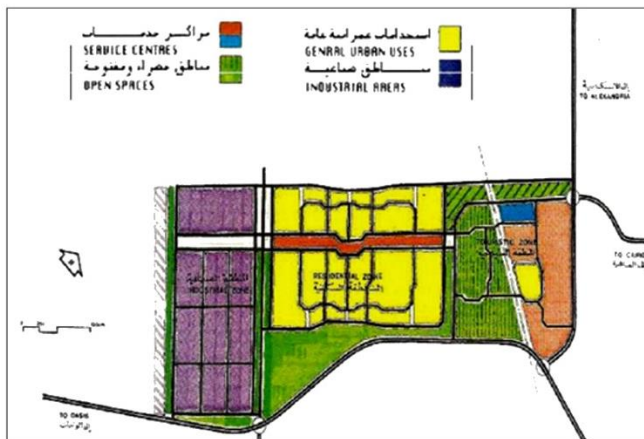
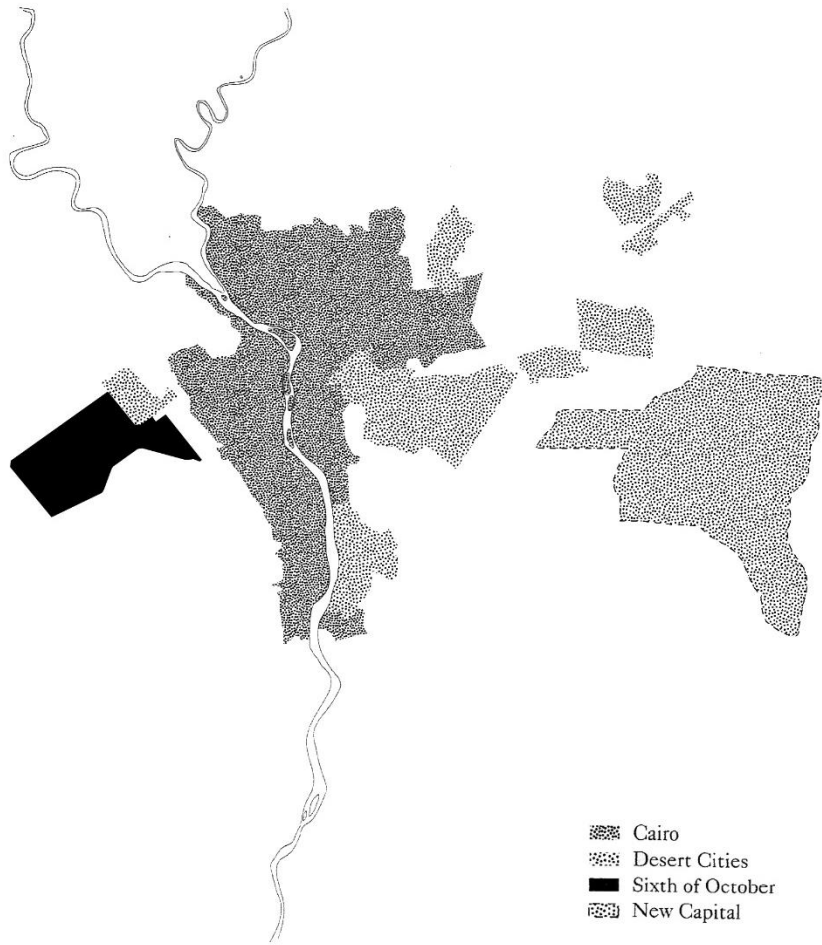


Figure 3. The location of Sixth of October (top), readapted form (Angéilil and Malterre-Barthes, 2018), and the original 1979 linear master plan and its similarity with Le Corbusier *Ville Radieuse* of 1930 (bottom); however, the green areas that were planned in the original master plan remain desert today.

1.5 Thesis outline: The organization and the contribution of the thesis chapters

This section gives an overview of the structure of the thesis and provides a summary of its individual chapters.

Besides the introduction and conclusion (Chapters 1 and 10), the thesis divides logically into three parts: (1) Chapters 2 and 3 cover background material on urban morphology and urban resilience; (2) Chapters 4–6 explore the different tools and methods for studying the impact of urban form on urban resilience to heat stress; and (3) Chapters 7–9 focus on testing and advancing these tools and methods.

More specifically, after the introductory Chapter 1, Chapter 2 provides a synthetic introduction to both urban morphology and urban resilience. It starts with defining urban morphology. Then, considering that urban morphology is open to be approached by various disciplines with different schools and methods, the chapter clarifies the specific position and standpoint of this thesis. Next, the concept of resilience is introduced and an understanding of its meaning and definition in urban planning and design is provided.

In Chapter 3, a systematic literature review is conducted to clarify the core meaning of resilience in urban morphology and examine its underlying politics in light of growing literature on the topic.

Chapter 4 gives an overview of the different quantitative methods that can be used for studying the impact of urban form on urban climate (with a focus on urban heating) and, in turn, the possibility of determining its impact on people's health and thermal sensation (i.e. what will be referred to later as the environmental/engineering dimension of heat-stress resilience). The methods discussed in this chapter aim to provide scientifically sound answers to the following questions:

- Do urban climate effects (of urban form) in terms of heating exist and, if so, what is their nature?
- What are the specific causes (or the urban form characteristics responsible for) of such effects?

In particular, the chapter discusses two different groups of methods, i.e. climatological-/environmental-based methods and typomorphological methods, and highlights their potentials and limitations.

In Chapter 5, the (descriptive) climatological-/environmental-based methods for studying, or more precisely describing, the impact of urban form on air temperatures are investigated in the context of the case study (i.e. Sixth of October new desert city, Egypt). Specifically, the effectiveness of combining in-situ climate campaigns and empirical modelling, to provide urban micro- and local climate substantive descriptive information (i.e. air temperature maps) at high spatial resolution (30 m) in such a data-scarce, arid area, is explored and assessed. The resulting maps are then used to describe the spatial patterns of air temperature across the city, thus providing empirical evidence

on the impact of urban form on air temperatures. The data and maps produced in this chapter are made open access for public, non-commercial use and will be further used in Chapter 7.

Chapters 6 and 7 explore the (analytical) typomorphological methods for studying the impact of urban form on urban climate and focus, more specifically, on the so-called local climate zone (LCZ) classification scheme, as one of the most advanced and widely used typomorphological classifications in urban climate. Chapter 6 starts by giving an overview of the methods and challenges in applying the LCZ classification scheme to cities and, then, proposes an approach to improve its application to cover entire cities and urban areas at a fine spatial resolution and accuracy. On the other hand, in Chapter 7, the LCZ classification scheme is applied to the case study to assess how well it discerns the thermal differences between different neighborhoods/areas within the city, thus determining its applicability for urban temperature studies in contemporary arid cities.

Chapters 8 and 9 offer a comprehensive assessment and an analysis of the inadequacies of the existing typomorphological methods in studying urban resilience to heat stress and propose improvements. More specifically, Chapter 8 assesses the global suitability of the LCZ scheme for urban temperature studies by examining its effectiveness in discerning temperature differences between the different LCZ types across and within different macroclimate regions (i.e. assessing its global suitability for addressing the environmental/engineering dimension of heat-stress resilience). On the other hand, Chapter 9 addresses the shortcomings of the LCZ scheme and the other typomorphological classifications in addressing the broader perspective of urban resilience to heat stress. It proposes a broader, multi-dimensional approach to the classification of urban form types, in Sixth of October, that combines environmental and social dimensions of importance to heat-stress resilience. The proposed approach gives new insights for planning and designing cities not only to reduce high temperatures but also to recognize the added value of communities, through social ties and solidarities, in handling extreme events as a collaborative challenge, thus better enhancing urban resilience to heat stress. However, the integrated approach proposed in this chapter does not constitute a validation study, i.e. does not build empirical evidence on the elements of urban form that are best correlated with social resilience. Rather, that association is assumed from literature, not measured on the ground.

Lastly, Chapter 10 highlights the original theoretical/conceptual and methodological contribution of this thesis by revisiting and trying to provide an answer to each of the initial research questions formulated in Section 1.3. Furthermore, it discusses how the work carried out and the acquired knowledge about the role of urban form in enhancing urban resilience to heat stress can be integrated into urban resilience planning frameworks and translated into city climate policies and design guidelines to inform urban practices. The chapter closes by identifying new directions for future research.

Figure 4 shows a flowchart of the chapters of this thesis in relation to each of the research questions, research problems and the appended papers.

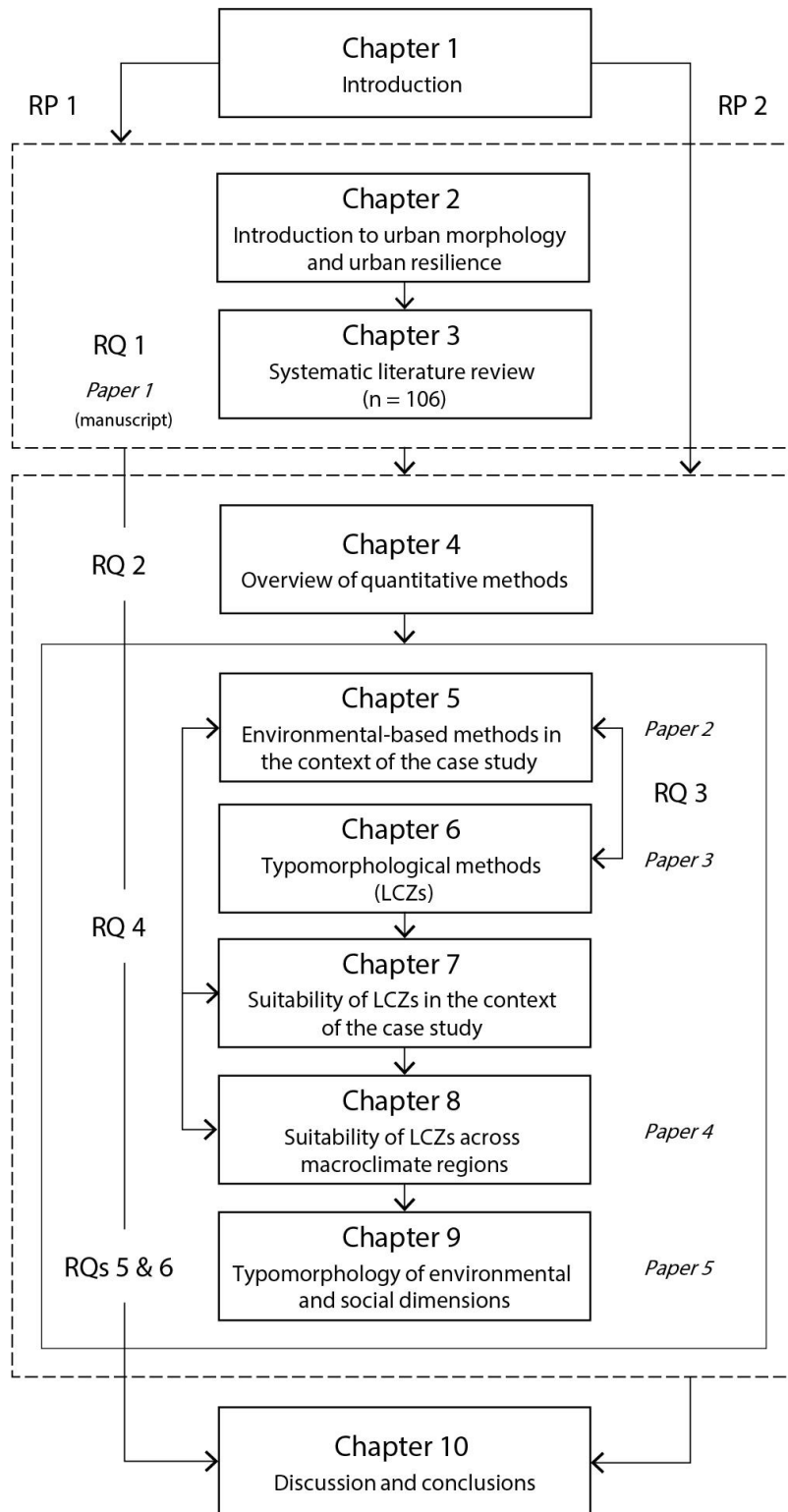


Figure 4. Flowchart of the chapters of this thesis in relation to each of the research questions (RQs), research problems (RPs) and the appended papers.

Part I
Background and literature review

Chapter 2

On urban morphology and urban resilience: An introduction

As indicated in Chapter 1, the aim of this chapter is not to conduct a comprehensive literature review on urban morphology (see instead, e.g. Oliveira, 2018, 2016) and/or urban resilience (see instead, e.g. Meerow et al., 2016). Rather, to synthetically introduce each of them and set the stage for Chapter 3, where a systematic literature review to better understand the relationship between urban form, as the object of study in urban morphology, and urban resilience will be conducted. The chapter is in two sections. Section 2.1 provides a concise definition of urban morphology, introduces the different schools and approaches within the field and clarifies the specific position and the standpoint of this thesis. Section 2.2 concisely introduces the concept of resilience and discusses its use and definition in urban planning and design.

2.1 Urban morphology: The study of the physical form of cities

2.1.1. Defining urban morphology

The term *morphology* was first introduced in the 18th century in biology by the German literary figure Johann Wolfgang Von Goethe to describe the study of natural forms/formations (Marshall and Çalışkan, 2011; Oliveira, 2016). However, because of the abstract and general nature of morphology as a science of form, the concept has been used in many other fields, such as geology, geography, linguistics and in the study of cities or urban sciences in general (and henceforth called *urban morphology*) (Marshall and Çalışkan, 2011; Oliveira, 2018). However, considering the complex dynamics of cities as an object of study (Batty, 2008; Jabareen, 2013), urban morphology contains contributions from different fields such as architecture, planning, geography and history (Oliveira, 2018). As a result, urban morphology is open to different research approaches and methods (both qualitative and quantitative); covers a wide range of scales or different levels of resolution (from buildings to metropolitan areas); and has different applications (Marshall and Çalışkan, 2011), as will be discussed in the next section. Hence, it is hard to find a common definition of urban morphology and there are several definitions (see Table 2).

In particular, this thesis draws on a basic and general definition of urban morphology that is “the study of urban forms, and of the agents and processes responsible for their transformation, and that urban form refers to the main physical elements that structure and shape the city . . .” (Oliveira, 2016, p. 2). On the one hand, these main physical (or urban form) elements are the buildings, the plots, the streets and the street blocks which correspond to different levels of resolution or scales of urban morphological research (Moudon, 1997; Oliveira, 2016). On the other hand, the agents and processes of urban transformations refer to those who are involved, directly or indirectly, in the continuous

change of urban forms, and the complex processes through which they interact. This includes, for instance, developers, architects, builders, planners and politicians, among many others (Oliveira, 2016).

Table 2. A selection of definitions of urban morphology. Reproduced form (Marshall and Çalışkan, 2011, p. 412).

	Definition	Sources as cited in (Marshall and Çalışkan, 2011)
General	“The study of urban form.”	(Cowan, 2005)
	“The science of form, or of various factors that govern and influence form”	(Lozano, 1990, p. 209)
	“The study of the physical (or built) fabric of urban form, and the people and processes shaping it.”	(Urban Morphology Research Group, 1990)
	“Morphology literally means ‘form-lore’, or knowledge of the form . . . what is the essence of that form; does certain logic in spatial composition apply, certain structuring principles?”	(Meyer, 2005, p. 125)
Focus on the object of study (urban form)	“. . . an approach to conceptualising the complexity of physical form. Understanding the physical complexities of various scales, from individual buildings, plots, street blocks, and the street patterns that make up the structure of towns helps us to understand the ways in which towns have grown and developed.”	(Larkham, 2005)
	“Urban morphology . . . is not merely two dimensional in scope. On the contrary, it is through the special importance which the third dimension assumes in the urban scene that much of its distinctiveness and variety arise.”	(Smailes, 1955, p. 101; cited in Chapman, 2006, p. 24)
Focus on the manner and purpose of study	“A method of analysis which is basic to find[ing] out principles or rules of urban design.”	(Gebauer and Samuels, 1981; cited in Larkham, 1998)
	“. . . the study of the city as human habitat . . . Urban morphologists . . . analyse a city’s evolution from its formative years to its subsequent transformations, identifying and dissecting its various components.”	(Moudon, 1997)

(continued)

Table 2 (continued)

	Definition	Source
Focus on the manner and purpose of study	“First, there are studies that are aimed at providing explanations or developing explanatory frameworks or both (i.e. cognitive contributions); and secondly, there are studies aimed at determining the modalities according to which the city should be planned or built in the future (i.e. normative contributions).”	(Gauthier and Gilliland, 2006, p. 42)

2.1.2. Schools and approaches in urban morphology: The standpoint of the thesis (a quantitative approach to urban form)

Although there is a general agreement about the object of study in urban morphology, there is a debate over how and for what purpose urban form should be studied (Gauthier and Gilliland, 2006). The reason is that, as discussed in the previous section, urban morphology is an emerging interdisciplinary field of knowledge (Moudon, 1997) and it is “open to approach by various disciplines with their own methods” (Choay and Merlin, 1986, pp. 433–434).

In her paper “Urban Morphology as an Emerging Interdisciplinary Field”, Moudon (1997) discussed three mainstream schools of urban morphology that emerged in England, Italy and France and have provided different and distinct contributions to the field. These schools were mainly influenced by the seminal works of the German geographer Michael Robert Günter Conzen (1907–2000), most famous by his study of Alnwick (1960), and the Italian architect Saverio Muratori (1910–1973), known by his studies of Venice (Muratori, 1959) and Rome (Muratori et al., 1963). These three schools are also known as the Conzenian (British), the Muratorian (Italian) and the Versailles (French) schools, respectively. However, although the contributions from these three schools agree in their *internalist* approach to the study of urban form, i.e. they “consider urban form as a relatively independent system” (Gauthier and Gilliland, 2006, p. 44) that undergoes transformation and change over time following “laws that urban morphology tries to identify” (Levy, 1999, p. 79), they differ in their approach and purpose for studying urban form.

In general, while the Conzenian and Muratorian Schools have developed two distinct scholarly approaches to urban morphology, i.e. *descriptive-analytical* to develop “a theory of city building” (p. 8) and *normative/prescriptive* to develop “a theory of city design” (p. 8), respectively, the Versailles School has been influenced by both schools and stood in between (Moudon, 1997). In particular, the Conzenian School primarily focuses on the description of urban forms through the use of basic plan elements (i.e. buildings, plots and streets) and their unique combinations (i.e. plan unit or urban fabric) (Figures 5 and 6), and on the development of analytical (explanatory) methods

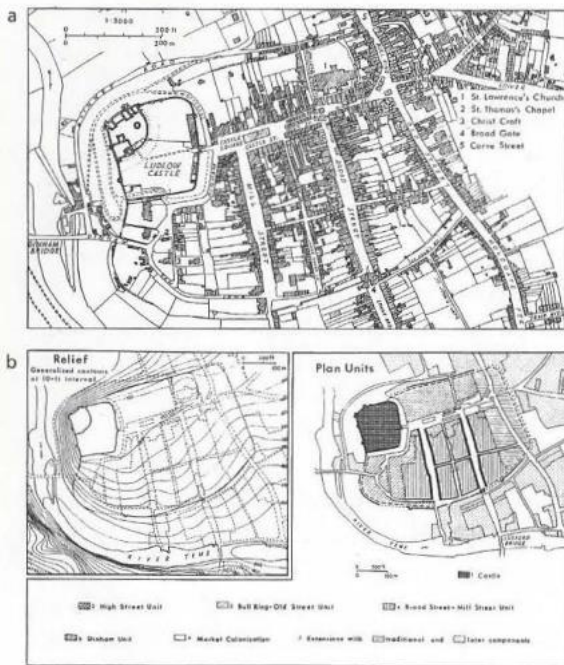
for explaining how urban forms are built and why without being directly concerned with the future city and its design (Moudon, 1994).

On the other hand, the Italian tradition focuses on the study of building types and their mutations over time and space as the basis of the urban morphological analysis (known as the *procedural/process typology* or the *typological process*. See Figures 7 and 8) to understand the fundamental principles of city-making, i.e. how cities were built, transformed and adapted; and hence how cities and their architecture should be designed and built (Moudon, 1997, 1994). Nevertheless, some researchers from the Muratorian school, especially in the second generation such as Gianfranco Caniggia (1933–1987), have not only been concerned with urban design but also worked towards knowledge production and developed explanatory frameworks in their urban morphological analysis (Gauthier and Gilliland, 2006). Therefore, Gauthier and Gilliland (2006) suggested making a more clear distinction between the different internalist approaches in the field by classifying the individual contributions as either being *cognitive* or *normative* studies. By cognitive studies, they refer to “contributions that aim to produce knowledge . . . or develop theoretical and analytical tools” (p. 44) to produce such knowledge, while normative studies refer to “contributions aimed at articulating a vision of the future” (p. 44).



16-5
Conzen's fundamental elements of the town plan (source: J.W.R. Whitehand, ed. 1981, "The Urban Landscape: Historical Development and Management, Papers by M.R.G. Conzen." In Institute of British Geographers, special publication no. 13, p. 26)

Figure 5. Conzen's fundamental elements of the town plan. Reproduced from (Moudon, 1994, p. 297).



16-6

Conzen's plan units and the compositeness of the town plan (source: H.J. Dyos, ed. 1968, *The Study of Urban History*, St. Martin's Press, pp. 123, 125)

a. Ludlow town plan 1926; lays out streets, lots, and building footprints

b. Topography and plan units; demonstrates how the town plan emerged in response to topographical conditions and to the gradual accretion of seven plan units

The compact medieval towns we know today are an aggregate of areas (plan units) built over time. The case of Ludlow shows how an original castle area was consolidated into a town. Focusing on the walled core, the successive addition of plan units reads as follows: The High Street unit (unit number 2) is laid out on axis with the castle (unit number 1). The Bull Ring Old Street (unit number 3) is developed perpendicularly to the main axis, along the main access road. Units number 4 and 5, Broad Street and Dinham units, come next. While the Broad Street unit is clearly a planned addition with regular streets laid out perpendicularly to High Street, the Dinham unit fits into space left over in the walled city. It comes last because its rugged topography made building difficult and costly.

Figure 6. Conzen's plan unit and the compositeness of the town plan. Reproduced from (Moudon, 1994, p. 298).

16-3

Caniggia's typological process (source: P. Maretto 1986, *La casa veneziana nella storia della città, dalle origini all'ottocento*, Marsilio Editori, pp. 29-30). This diagram illustrates the progressive transformation of the elementary domus and its ancillary spaces into a medieval courtyard house. Starting at top left and reading across: the basic domus type was perpendicular to the street with a side court; depending on the solar orientation of the lot, an alternative type has a front court parallel to the street; mutations through the thirteenth century include the addition of porches, the building of new stories, and the infill of side yards along the street to form L-shaped courtyards.

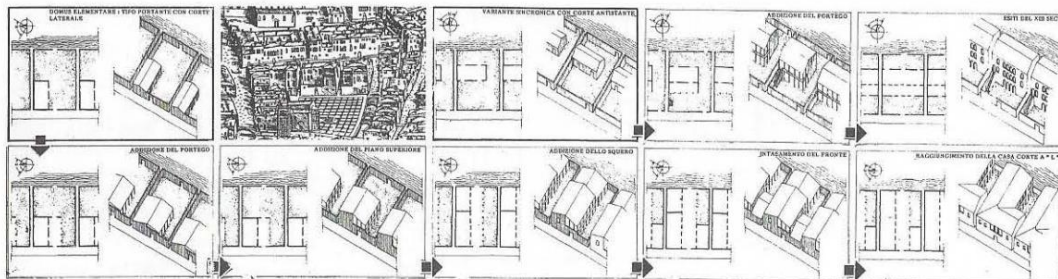


Figure 7. Caniggia's typological process. The progressive transformation of the elementary domus and its ancillary spaces into a medieval courtyard house.

Reproduced from (Moudon, 1994, p. 292).

16-4

Human action and environmental reaction (source: G. Caniggia and G.L. Maffei 1979, *Composizione architettonica e tipologia edilizia*, 1. *Lettura dell'edilizia di base*, Marsilio Editori, p. 101). The diachronic mutation of house types in Florence, Rome, and Genoa is reconstructed in a schematic way.

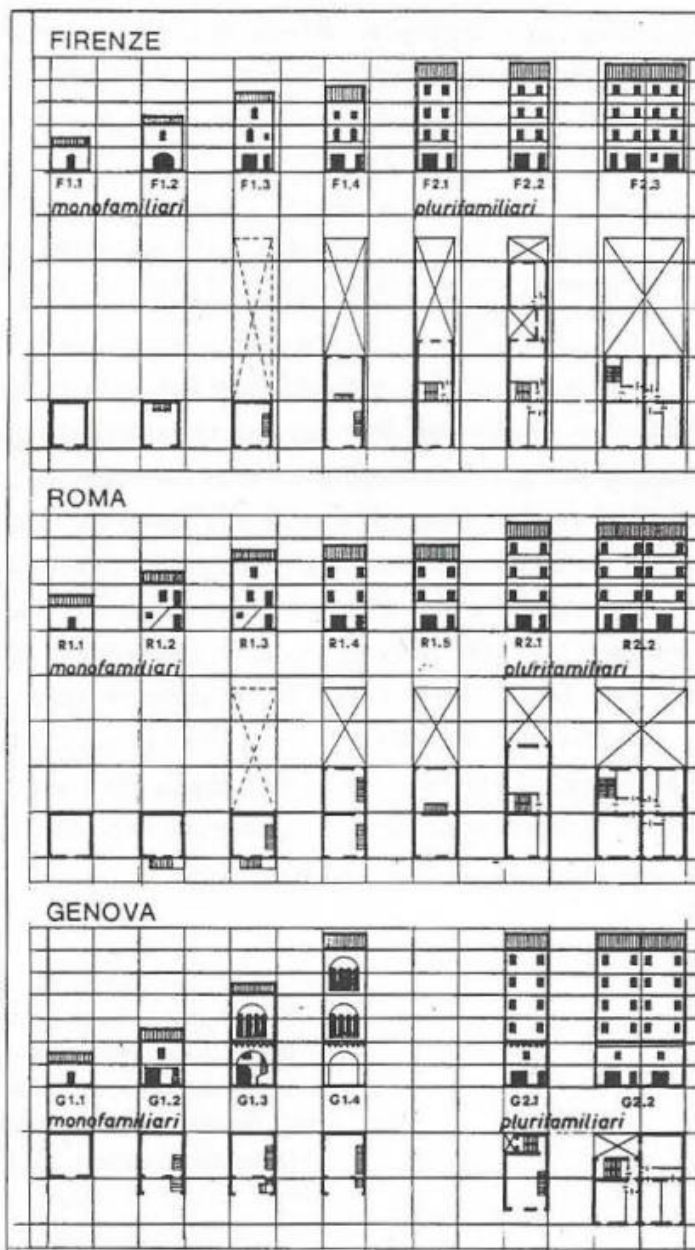


Figure 8. The diachronic mutation of house types in Florence. Rome and Genoa is reconstructed in a schematic way. Reproduced from (Moudon, 1994, p. 293).

Furthermore, to better distinguish between the different studies in urban morphology and clarify the position and standpoint of this thesis, one can further classify urban morphological studies based on their specific area of concentration and/or the similarity of their research questions rather than the methods they apply. In general, Moudon (1992) identified, at least, nine areas of concentration in urban design; these are (1) urban history studies; (2) picturesque studies; (3) image studies; (4) environment-behavior studies; (5) place studies; (6) material cultural studies; (7) typology-morphology studies; (8) space-morphology studies; and (9) nature-ecology studies. Figure 9 shows an overview of the categorization of urban morphology research, following both the criteria proposed by Gauthier and Gilliland (2006) and the specific areas of concentration suggested by Moudon (1992).

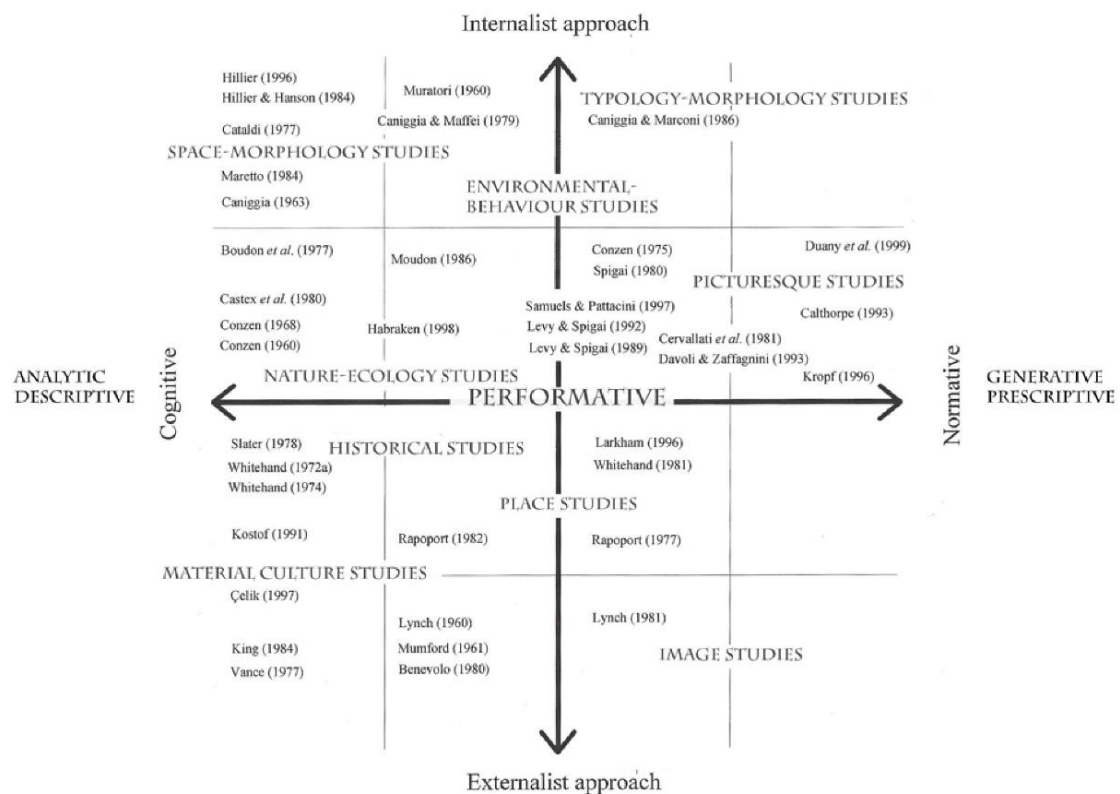


Figure 9. An overview of the categorization of urban morphology research based on Gauthier and Gilliland (2006) and Moudon (1992). *Externalist* approaches refer to contributions that consider urban form as the resulting product of external forces such as socio-economic, political and historical conditions. Reproduced from (Berghauser Pont, 2018, p. 103).

In particular, this thesis acknowledges the importance of substantive descriptive information (i.e. explaining the *what is* and maybe also the *why*) for evaluating normative decisions and better designing (prescribing) cities, and hence reducing the gap between knowledge and action (Moudon, 1992), which risks urban design becoming a pseudoscience (Marshall, 2012). Such substantive descriptive knowledge requires developing descriptive and analytical (explanatory) tools and methods to describe and analyze the impact of different design proposals on urban processes

(Berghauser Pont, 2018; Berghauser Pont et al., 2017; Kropf, 2011; Whitehand, 2001). To this point, the thesis also acknowledges the potential of describing and analyzing urban form quantitatively (i.e. *measuring urban form*) for providing empirical and valid evidence that can support planning and design decisions and provide measurable design outcomes (Berghauser Pont, 2018). In other words, measuring urban form or doing *urbanism by numbers* allows urban designers to “practice their art with its due precision” (Moudon and Lee, 2009, p. 73) and ensures that “what is proposed will also deliver the city, neighborhood or building that is aimed for, be it a more sustainable, healthier or more just” (Berghauser Pont, 2018, p. 117).

Based on the above, one can identify this thesis as generally belonging to the cognitive studies of urban morphology and, more specifically, to the area of concentration of space morphology. According to Moudon (1992), space morphology aims to “uncover the fundamental characteristics of urban geometries” (p. 344) by quantifying the urban form elements and their relations, and thus “enrich[ing] the description of built form in ways that express aspects of performance and function and bring[ing] them within the purview of systematic design intention” (Peponis, 2013, p. 2). In quantifying urban form, space-morphology studies use mathematical reasoning. This is well exemplified in the works of two pioneering research centers that originated in England in the seventies, i.e. the Centre of Land Use and Built Form (now known as the Martin Centre) at the Department of Architecture at Cambridge University directed by Leslie Martin and Lionel March and the Unit for Architectural Studies at the Bartlett School of Architecture at University College London (UCL) directed by Bill Hillier which is widely known now as the Space Syntax Laboratory (Berghauser Pont, 2018).

In particular, Martin and March, in their seminal book *Urban Space and Structure* (1975), raised the question of “what building forms make the best use of land?” where *best* is understood in terms “of access, of how the free space is distributed around them [buildings] and what natural lighting and view the rooms within them [buildings] might have” (Martin and March, 1975, p. 20). By analyzing and comparing two basic building types with different geometry, i.e. courtyards and pavilions, which geometrically represent the outer annulus and the central square in Fersnel’s diagram (Figure 10), respectively, Martin and March (1975) showed that at the same quantifiable building parameters such as percentage of ground coverage, building height and total floor space area, one can design two different urban environments in terms of access, open space distribution and daylight (Figure 11). Their findings led to their radical proposal for the Manhattan’s center in New York that replaces all the 36-stories towers with large courtyard buildings only eight stories high while providing the same floor space contained in towers and at the same time creating larger central open spaces, each is almost as large as Washington Square (Figure 12).

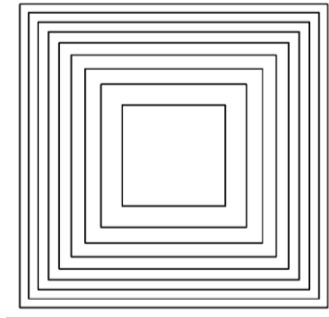


Figure 10. Fresnel's diagram: All concentric squared annuluses have the same surface area, which is equal to the area of the central square (Martin and March, 1975, p. 19).

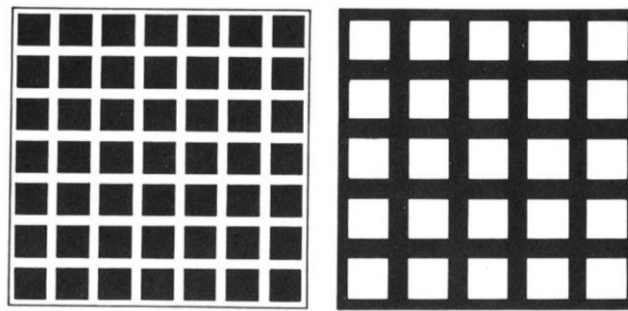


Figure 11. Two basic building types, i.e. pavilions (left) and courts (right), with the same percentage of ground coverage, building height and total floor space area.
Reproduced from (Martin and March, 1975, p. 20).

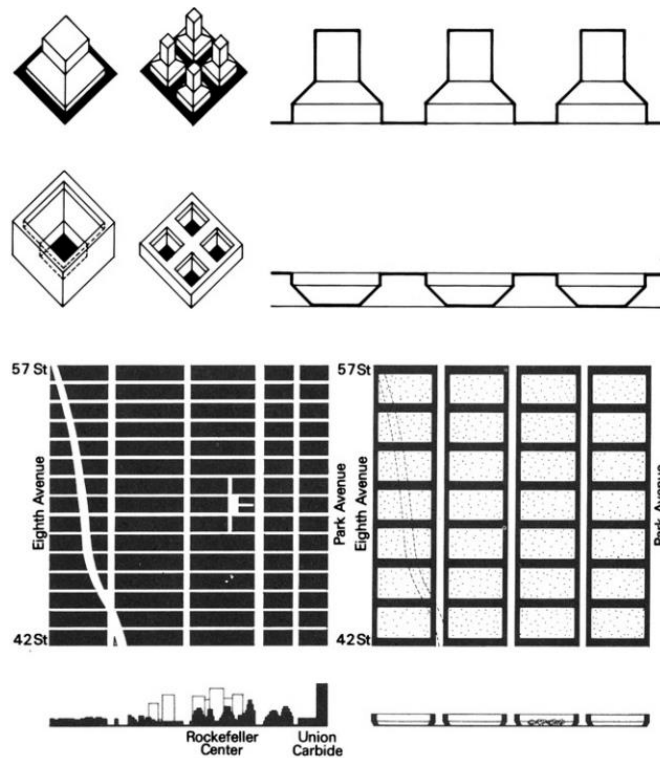


Figure 12. Martin and March's radical proposal to replace Manhattan's 36-stories towers in New York with large courtyard buildings only eight stories high.
Reproduced from (Martin and March, 1975, pp. 20–21).

On the other hand, Bill Hillier and the Space Syntax group have been primarily concerned with the relationship between urban forms and the social processes they afford or, in other words, in understanding *the social logic of space*. As a result, in their description and representation of urban form, Hillier and Hanson (1984) have not focused on the geometry of the individual components of urban form (i.e. urban form geometric characteristics) as, for instance, did Martin and March, but rather on the geometric *relations* between urban spaces (i.e. urban form configurational characteristics) to capture what emerges from the dynamic interaction between humans in motion and the physical environment or what James Gibson has coined as *affordances* (1986, 1977). Hence, the forms of geometric representation developed in space syntax aim to integrate both the human conception of space and the reality of the physical environment into one representation or description of urban form (Marcus, 2018). Of particular importance here is the axial map representation (Figure 13) which is “a representation of continuous urban space, structured by built form such as buildings, infrastructure and landscape elements, which specifically captures a vital set of affordances (accessibility and visibility) that the environment gives rise to in relation to a moving human subject” (Marcus, 2018, p. 5). The axial map is constructed by drawing “the least amount of straight lines that cover all accessible open space in the area of analysis, where each straight line (here called axial line) in the map represents an urban space that is possible to visually overlook and physically access” (Berghauser Pont, 2018, p. 107).



Figure 13. Figure-ground (top) and axial map representation (bottom) of the city of London. Reproduced from (Hillier, 1996, p. 117).

As such, axial maps can be considered the simplest geometrical representation of a set of accessibility and visibility affordances that the urban environment offers (Marcus, 2018). This geometric representation of affordances through axial lines offers the possibility for better studying urban form and quantitatively measuring it from a perspective of human perception and cognition, and hence it contributes to better understating the relationship between urban form and human behavior or social processes in general. For instance, one can topologically measure how central or close a space in the spatial system is to all the other spaces by counting the number of axial steps that have to be made from this space to reach all the other spaces, using the shortest path (Hillier and Hanson, 1984). In this way, we “capture both the energy effort and the informational effort for a moving subject in an urban area” (Berghauser Pont, 2018, p. 107), and it is this *cognitive distance* that explains why space syntax representations are better than other distance measures (e.g. metric walking distance) in capturing human behavior, not least pedestrian movement (Hillier and Iida, 2005; Marcus, 2018).

The work of the two aforementioned pioneering centers has inspired a generation of researchers and recently several studies in the area of space-morphology have sought to combine one or both of these approaches with Geographical Information systems (GIS-) and machine learning (ML-) based methods (referred to in this thesis as *immaterial technology*) that allow working with large-scale data sets and multiple urban form measures simultaneously and systematically, thus better studying urban form quantitatively (Berghauser Pont, 2018). This combination has resulted in the advancement of the so-called *typological*, or more specifically *typomorphological*, research within the area of space-morphology.

In general, the concept of typology is used in architecture, urban design and urban planning to classify objects based on “certain internal structural similarities” (Moneo, 1978, p. 23), where typomorphology, from a space-morphology perspective, is a specific typology developed based on the physical characteristics (e.g. geometric, configurational) (Berghauser Pont, 2018; Moudon, 1992, 1994). Because types within typomorphologies perform and function in specific ways due to their shared characteristics, they are regarded as powerful descriptive-analytical and normative/pre-scriptive tools in urban planning and design research and practice. Examples of previous typomorphological studies that have employed GIS- and ML-based methods include (Barthelemy, 2017; Berghauser Pont et al., 2019a, 2019b; Bobkova et al., 2019b, 2019a; Colaninno et al., 2011; Fleischmann et al., 2021; Fusco and Araldi, 2018; Gil et al., 2012; Hausleitner and Berghauser Pont, 2017; Lee et al., 2019; Maiullari et al., 2021; Song and Knaap, 2007; Steiniger et al., 2008).

In this thesis, the use of typomorphology, as a descriptive and analytical (explanatory) tool to better study the impact of urban form on urban resilience, and specifically on heat-stress resilience, will be explored in detail in the next chapters.

2.2 Urban resilience

2.2.1. What is resilience?

The word resilience has a very long history (see Alexander, 2013 for a detailed review of the historical etymology of the term). It originally stems from the Latin verb *resilio* (present infinitive *resilire*), i.e. to leap/spring back, rebound, recoil and retreat (Alexander, 2013; Klein et al., 2003). However, as an academic and scientific concept, its roots are more ambiguous (Adger, 2016; Friend and Moench, 2013; Lhomme et al., 2013; Meerow et al., 2016; Pendall et al., 2010).

Roots of resilience as a scientific concept

In general, many believe that resilience as a scientific concept was most developed in the field of ecology and, in particular, was brought to prominence by the ecologist Crawford Stanley Holling after his 1973 seminal paper “Resilience and Stability of Ecological Systems” (Alexander, 2013). In his paper, Holling (1973) distinguished between two kinds of behaviors of ecological systems, i.e. *stability* and *resilience*. On the one hand, stability “represents the ability of a system to return to an equilibrium state after a temporary disturbance; the more rapidly it returns and the less it fluctuates, the more stable it would be” (Holling, 1973, p. 14). On the other hand, resilience is “a measure of the persistence of systems and of their ability to absorb change and disturbance and still maintain the same relationships between populations or state variables” (Holling, 1973, p. 14). In a later paper, Holling (1996a) termed these behaviors or aspects of the system’s stability *engineering* and *ecological* resilience, respectively (Figure 14). Engineering resilience refers to the system’s ability to return (or bounce back) to the near-equilibrium steady state after being disturbed (i.e. maintain the *efficiency* of function), while ecological resilience is the system’s ability to maintain key functions after disturbance by moving to another stability domain or bouncing forward (i.e. maintain the *existence* of function). In other words, ecological resilience focuses on “the ability to persist and the ability to adapt” (Adger, 2003a, p. 1), and hence it “emphasizes conditions far from any equilibrium steady state” (Holling, 1996a, p. 33), but rather the existence of multi-stable states.

However, despite the difference between the aforementioned views of resilience, i.e. engineering and ecological, what they have in common is the existence of the notion of stability, be it the near-equilibrium state or the new stability domain. Figure 14 illustrates the difference between engineering and ecological resilience using the ball-in-cup representation (Carpenter et al., 1999; Scheffer et al., 1993). In particular, in this representation “the ball represents the system state and the cup represents the stability domain. . . . An equilibrium exists when the ball sits at the bottom of the cup and disturbances shake the marble to a transient position within the cup. Engineering resilience refers to characteristics of the shape of the cup—the slope of the sides dictates the return time of the ball to the bottom. Ecological resilience suggests that more than one cup exists, and resilience is defined as the width at the top of the cup” (Gunderson, 2003, p. 427).

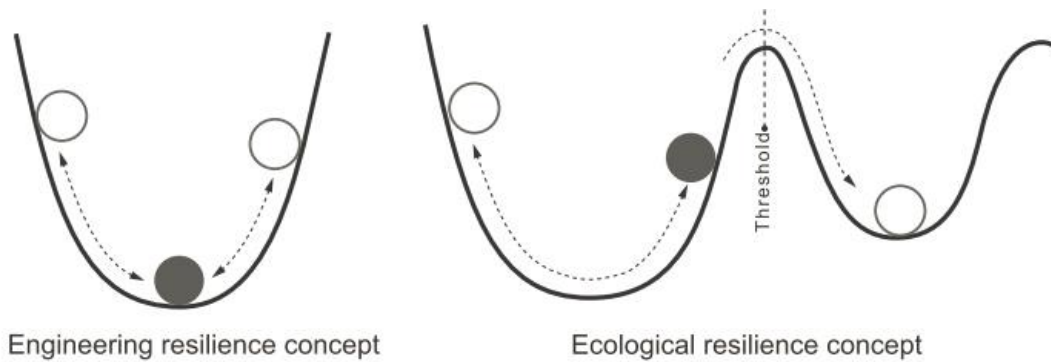


Figure 14. The ball-in-cup representation of the difference between engineering and ecological resilience (Carpenter et al., 1999; Scheffer et al., 1993). Reproduced from (Liao, 2012, p. 3).

From ecological to social-ecological resilience

The latter ecological understanding of resilience, in which natural systems—or ecosystems—were viewed as dynamic and adaptive, was key to the development of the so-called social-ecological (Folke, 2006), evolutionary (Davoudi et al., 2012) or progressive (Vale, 2014) approach to resilience.

In the theory of social-ecological systems (SESs), “the delineation between social and natural systems is artificial and arbitrary” (Berkes and Folke, 1998, p. 4), and hence “humans and nature are studied as an integrated whole, not as separated parts” (Folke et al., 2016, p. 9). Such interdependent, integrated SESs are “complex, non-linear and self-organizing” (Berkes and Folke, 1998, p. 12), where agents (or the system’s parts) “interplay in complex ways with relations, interactions, and feedbacks that emerge across temporal and spatial levels and scales, often with unexpected outcomes and surprises” (Walker et al. 2009, Homer-Dixon et al. 2015, as cited in Folke et al., 2016, p. 6). SESs thus keep evolving and adapting over time in the face of change, be it fast or slow or due to external or internal disturbances (Gunderson and Holling, 2002). This dynamic change of SESs over time can be best explained by the metaphor of the “Adaptive Cycle” (Figure 15) and the “Panarchy” model (Figure 16); however, a detailed explanation of these is beyond the focus of this thesis, and interested readers can refer to (e.g. Gunderson and Holling, 2002) for more details.

In this perspective, unlike the engineering and ecological understanding of resilience, social-ecological resilience challenges the whole idea of equilibrium, stability or return to normality (Davoudi et al., 2012; Scheffer, 2009). It can be defined by one or more of the following definitions:

- “. . . the ability of a complex socio-ecological system to change, adapt, and, crucially, transform in response to stresses and strains” (Carpenter et al., 2005, as cited in Davoudi et al., 2012, p. 302).
- “. . . the capacity of a system to absorb disturbance and reorganize while undergoing change so as to still retain essentially the same function, structure, identity, and

feedbacks—in other words, stay in the same basin of attraction” (Walker et al., 2004, p. 6).

- “. . . the capacity to adapt or transform in the face of change in social-ecological systems, particularly unexpected change, in ways that continue to support human wellbeing” (Chapin et al. 2010, Biggs et al. 2015 as cited in Folke et al., 2016, p. 2).

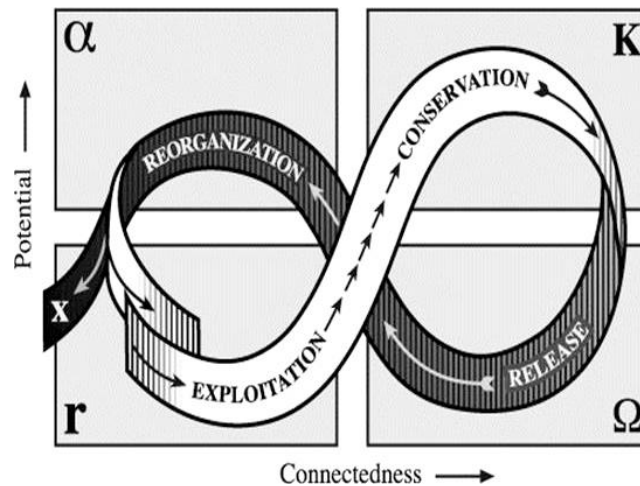


Figure 15. A graphical representation of the metaphor of the “Adaptive Cycle”. The figure refers to four distinct phases of change in the structures and function of SESs: (r) growth or exploitation; (k) conservation; (Ω) release or creative destruction; and (α) reorganization (Gunderson and Holling, 2002). Retrieved from: <http://www.resalliance.org/adaptive-cycle> (Accessed June 2022).

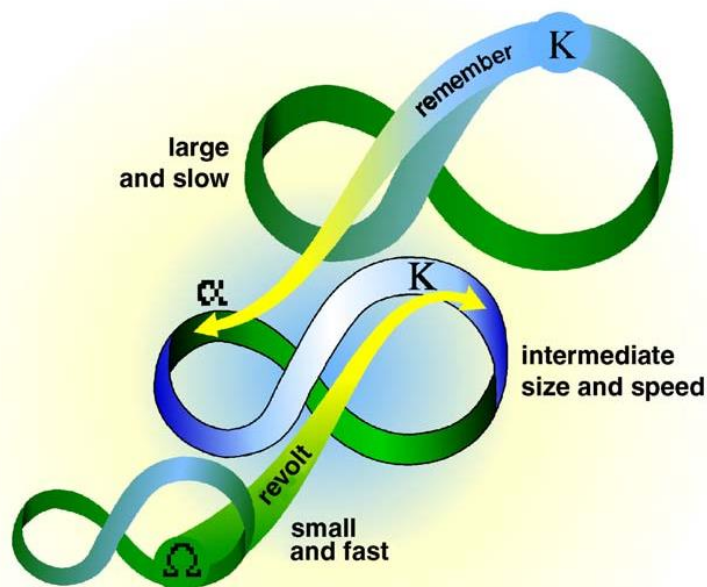


Figure 16. The Panarchy model representing the interactive dynamics of a nested set of adaptive cycles. Reproduced from (Folke, 2006, p. 258).

Resilience performances, attributes and assets

In the previous paragraphs, we have discussed the roots of resilience as a scientific concept and a range of different responses that a resilient system is capable to implement when facing a disturbance, namely persistence, adaptability and transformability. Feliciotti (2018) coined these as resilience *performances*, i.e. “what a resilient system should do or be able to do” (p.116), and distinguished them from resilience *attributes*, i.e. “what a resilient system should be” (p.116) and *assets*, i.e. “what a resilient system should have” (p. 117). Example of the resilience attributes include: diversity, i.e. the simultaneous availability of multiple distinct components contributing to a variety of non-overlapping functions, and hence the system’s capacity to deal with multiple disturbances at the same time (Sharifi and Yamagata, 2016b; Wardekker et al., 2010); redundancy, i.e. the availability of different (substitutable) components performing the same (overlapping) function, thus maintaining the system’s functionality in case of a damage or loss (Roggema, 2014; Rose, 2007; Sharifi and Yamagata, 2016b); connectivity, i.e. the extent to which different systems or components are linked, where both high (that facilitates knowledge exchange and fast recovery) and low (that works against the spread of risk) connectivity can be beneficial for resilience (Feliciotti et al., 2016; Marcus and Colding, 2014); and modularity, i.e. the distribution and spread, usually in form of clusters or modules, of functions across the different scales of the system to ensure autonomy and self-sufficiency (Anderies, 2014; Feliciotti, 2018; Walker and Salt, 2012). These attributes are general in nature, meaning that they can characterize any kind of complex system and are not related to a specific disturbance (Feliciotti, 2018). However, the presence, or not, of these attributes can influence the system’s effectiveness in dealing with disturbances (Arup, 2014, as cited in Feliciotti, 2018). On the other hand, resilience assets are the translations of the general attributes in a specific system or the “resources that systems possess or can implement in order to operationalize attributes” (Feliciotti, 2018, p. 117).

In the next section, we will explore how the concept of resilience, be it performance, attribute or asset, has been used and defined in urban planning and design.

2.2.2. The concept of resilience in urban planning and design

The parallels to resilience in the history of urban planning and design

In urban planning and design, the concept of resilience has a long history as a metaphor to deal with the unknown future and the indefinite growth and change of cities (Dhar and Khirfan, 2017). More specifically, it has been used since the beginning of postmodern urbanism, around the mid of the 20th century, to reflect the need for flexibility and adaptability in architecture and urbanism in opposition to the rigidity, fragility, radical abstraction, strong functionalism and universalization of the architectural product of the 1930s modernism (Ellin, 2007). This anti-rigidity movement had taken various forms and its intellectual streams have been visible in the work of many architects, urban designers and planners at the time, such as the members of Team X (also known as Team 10) (1953–1981) and the Italian *La Tendenza* group

(1965–1985), and lasted for decades after. Examples of the different trends and concepts that emerged during this period as parallels to resilience in reaction to the modernism's rigidity of both the architectural mode of production and its product include: the aesthetic of number, formulated by Aldo Van Eyck in 1959 (Ligtelijn and Strauven, 2008); open aesthetic (Voelcke, 1959); open architecture (Habraken, 1961, 1972); open form (Hansen, 1961) (Figure 17); mat building/urbanism (Smithson, 1974); and polyvalent space (Hertzberger, 1991) (Figure 18). What is common among these trends and concepts is that they all aimed at creating a new type of architecture and urbanism that can grow and change.

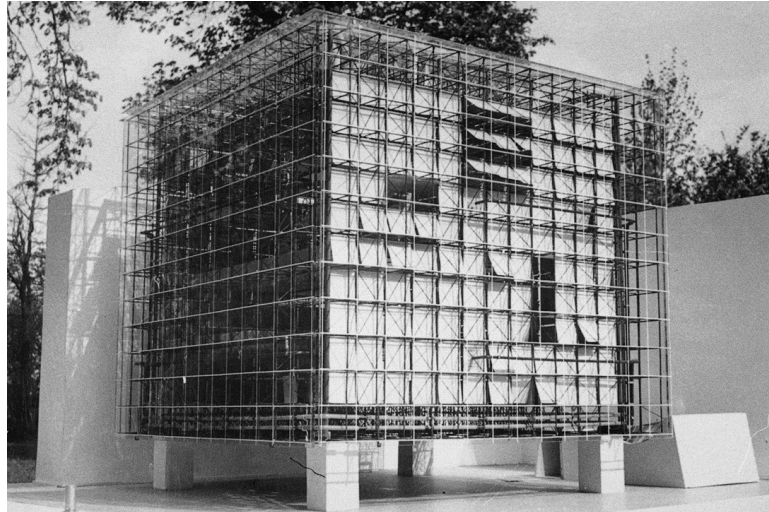


Figure 17. An unbuilt project for the extension of the Zachęta art gallery in Warsaw, Poland (1958) by Polish architect and urban planner Oskar Hansen representing his concept of the open form. The building has a system of movable stairs and slabs that allow for a continuous reconfiguration of the different floors.



Figure 18. A project for an office complex in Apeldoorn, the Netherlands (1968–1972) by Dutch architect Herman Hertzberger representing his idea of the polyvalent space. The office space was intentionally left partially unfinished to allow users to complete it in ways that suit their working needs.

Resilience and its contemporary use and definition in urban planning and design

More recently, and particularly over the last two decades (Sharifi, 2019d), the use of the resilience concept in urban planning and design has increased (Leichenko, 2011; Meerow et al., 2016) and extended from a metaphor and a descriptive concept to a mode of thinking or a paradigm to deal with the complexity of cities and prepare them for future uncertainty (Meerow and Newell, 2016). This is because cities are considered “example par excellence of complex systems” (Batty, 2008, p. 769). However, because, as discussed earlier, complex systems (e.g. SESs) exhibit resilience performance in a multitude of ways, i.e. persistence, adaptability and transformability, there has been an ambiguity of the core meaning of resilience in urban studies, as well as “a tapestry of definitions and meanings with little orthodoxy in its conceptualization and application” (Cutter, 2016, p. 742). This ambiguity works against the operationalization, benchmarking and measurement of the concept in urban studies (Meerow and Newell, 2016; Pizzo, 2015), and a common definition is needed. Therefore, Meerow et al. (2016) conducted an extensive review of the different existing definitions of urban resilience across different disciplines and fields of study (Table 3) and proposed the following integrative definition of urban resilience:

“Urban resilience refers to the ability of an urban system—and all its constituent socio-ecological and socio-technical networks across temporal and spatial scales—to maintain or rapidly return to desired functions in the face of a disturbance, to adapt to change, and to quickly transform systems that limit current or future adaptive capacity” (p. 39).

Nevertheless, despite the inclusiveness and the flexibility that the aforementioned definition offers, the ambiguity of the meaning of resilience still persists in other related realms or fields such as urban morphology, where the relationship between resilience and urban form, as the main object of study, is rather unclear. Therefore, in the next chapter, a systematic literature review will be conducted to understand the core meaning of resilience in urban morphology and examine its underlying politics in light of the growing literature on the topic.

Table 3. A selection of definitions of urban resilience. Reproduced from (Meerow et al., 2016).

Definition	Source as cited in (Meerow et al., 2016)
“. . . the degree to which cities tolerate alteration before reorganizing around a new set of structures and processes” (p. 1170).	(Alberti et al., 2003)
“. . . a sustainable network of physical systems and human communities” (p. 137).	(Godschalk, 2003)
“. . . the ability of a system to adjust in the face of changing conditions” (p. 373).	(Pickett et al., 2004)

(continued)

Table 3 (continued)

Definition	Source as cited in (Meerow et al., 2016)
“To sustain a certain dynamic regime, urban governance also needs to build transformative capacity to face uncertainty and change” (p. 533).	(Ernstson et al., 2010)
“. . . the capacity of a city to rebound from destruction” (p. 141).	(Campanella, 2006)
“. . . a system that can tolerate disturbances (events and trends) through characteristics or measures that limit their impacts, by reducing or counteracting the damage and disruption, and allow the system to respond, recover, and adapt quickly to such disturbances” (p. 988).	(Wardekker et al., 2010)
“. . . the capacity of systems to reorganize and recover from change and disturbance without changing to other states . . . systems that are “safe to fail” (p. 341).	(Ahern, 2011)
“. . . the ability . . . to withstand a wide array of shocks and stresses” (p. 164).	(Leichenko, 2011)
“. . . encourages practitioners to consider innovation and change to aid recovery from stresses and shocks that may or may not be predictable” (p. 312).	(Tyler and Moench, 2012)
“. . . the capacity of the city to tolerate flooding and to reorganize should physical damage and socioeconomic disruption occur, so as to prevent deaths and injuries and maintain current socioeconomic identity” (p. 5).	(Liao, 2012)
“. . . the capacity of the city to tolerate flooding and to reorganize should physical damage and socioeconomic disruption occur, so as to prevent deaths and injuries and maintain current socioeconomic identity” (p. 5).	(Brown et al., 2012)
“. . . encompasses the idea that towns and cities should be able to recover quickly from major and minor disasters” (p. 63).	(Lamond and Proverbs, 2009)
“. . . the ability of a city to absorb disturbance and recover its functions after a disturbance” (p. 222).	(Lhomme et al., 2013)
“A disaster resilient city can be understood as a city that has managed. . . to: (a) reduce or avoid current and future hazards; (b) reduce current and future susceptibility to hazards; (c) establish functioning mechanisms and structures for disaster response; and (d) establish functioning mechanisms and structures for disaster recovery” (p. 71).	(Wamsler et al., 2013)
“. . . should be framed within the resilience (system persistence), transition (system incremental change) and transformation (system reconfiguration) views” (p. 287).	(Chelleri, 2012)

(continued)

Table 3 (continued)

Definition	Source as cited in (Meerow et al., 2016)
“ability to recover and continue to provide their main functions of living, commerce, industry, government and social gathering in the face of calamities and other hazards” (p. 109).	(Hamilton, 2009)
“the ability of an urban asset, location and/or system to provide predictable performance – benefits and utility and associated rents and other cash flows – under a wide range of circumstances” (p. 217).	(Brugmann, 2012)
“. . . the capacity to withstand and rebound from disruptive challenges . . .” (p. 323).	(Coaffee, 2013)
“ability to absorb, adapt and respond to changes in urban systems” (p. 89).	(Desouza and Flanery, 2013)
“. . . the ability of a city to absorb disturbance while maintaining its functions and structures” (p. 200).	(Lu and Stead, 2013)
“. . . a capacity of urban populations and systems to endure a wide array of hazards and stresses” (p. 358).	(Romero-Lankao and Gnatz, 2013)
“. . . capacity to adapt or respond to unusual often radically destructive events” (p. 4069).	(Asprone and Latora, 2013)
“A climate-resilient city . . . has the capacity to withstand climate change stresses, to respond effectively to climate-related hazards, and to recover quickly from residual negative impacts” (p. 178).	(Henstra, 2012)
“. . . a general quality of the city’s social, economic, and natural systems to be sufficiently future-proof” (p. 2).	(Thornbush et al., 2013)
“. . . the general capacity and ability of a community to withstand stress, survive, adapt and bounce back from a crisis or disaster and rapidly move on” (p. 114).	(Wagner and Breil, 2013)

Chapter 3

Disentangling the relationship between urban form and urban resilience: A systematic literature review²

In the previous chapter, we have provided a synthetic review of both urban morphology and urban resilience to introduce fundamental concepts and lay the theoretical foundation of this thesis. Here, we take a step further and conduct a systematic literature review to understand the core meaning of resilience in urban morphology and examine its underlying politics in light of growing interest and the publication of several studies on the topic as discussed in Chapter 1.

3.1 Aim and the scope of the review

The synthetic review conducted in Chapter 2 (Section 2.2) about the concept of resilience and its roots as a scientific concept and meaning in urban planning and design literature has revealed that the concept has “a tapestry of definitions and meanings with little orthodoxy in its conceptualization and application” (Cutter, 2016, p. 742). This makes the concept difficult to operationalize (Meerow and Newell, 2016) and risks it becoming an “empty signifier” (Weichselgartner and Kelman, 2015), and therefore a systematic review of the literature is conducted in this chapter. In this thesis, since the focus is specifically on the relationship between urban form and urban resilience, this systematic review will focus only on publications (e.g. journal articles, papers in conference proceedings, book chapters) that explicitly or implicitly speak of urban form (or, more generally, the built environment) in relation to a resilience performance, i.e. “what a resilient system should do or be able to do” (Felicciotti, 2018, p. 117) (e.g. persistence, adaptability, transformability) or property/attribute, i.e. “what a resilient system should be” (Felicciotti, 2018, p. 117) (e.g. diversity, connectivity, redundancy, modularity).

The remainder of this chapter is organized as follows. Firstly, the review method is presented in Section 3.2. Then, in Section 3.3, a synthesis of the review results is given and finally, these results and their implications, as well as the limitations of the review are discussed in Section 3.4.

3.2 Review method

The systematic literature review includes three main steps (Figure 19):

1. Searching scientific databases, using relevant search terms, to retrieve potentially eligible publications for the review.

² This chapter is based on the journal manuscript (in preparation): **Eldesoky, A. H.**, Abdeldayem, W., 2022. Disentangling the relationship between urban form and urban resilience: A systematic review of the literature.

2. Excluding irrelevant publications using clearly-defined inclusion/exclusion criteria and conducting a preliminary bibliometric analysis;
3. The reading and analysis of the full publications guided by specific review questions.

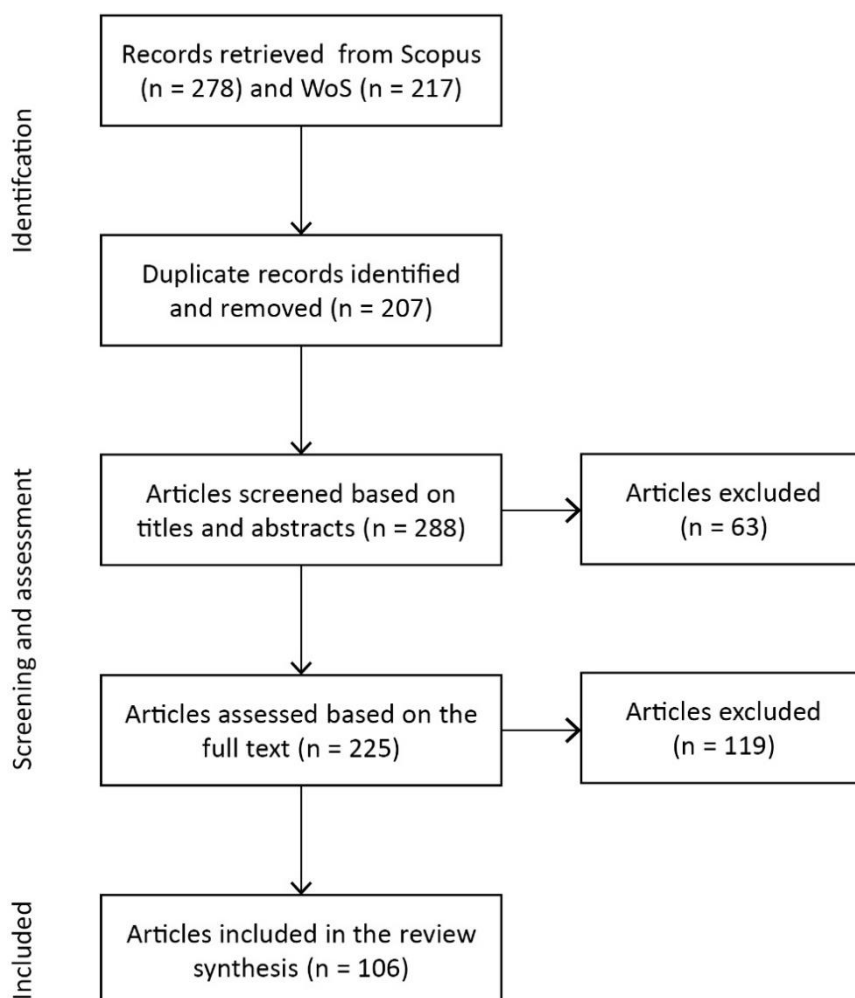


Figure 19. Flow diagram of the systematic review process.

3.2.1. Search strategy and data extraction

To retrieve relevant peer-reviewed publications eligible for the systematic review and analysis, two scientific databases, i.e. Scopus and Thompson Reuters Web of Science (WoS), were searched using a combination of relevant search keywords (see Table 4).

The search was restricted to peer-review publications written in English and published between database inception and July 31, 2021. However, given that this is a rapidly growing research topic, additional publications may have been published since the search was conducted. The initial search using the search blocks shown in Table 4 yielded 278 and 217 publications in Scopus and WoS, respectively, which when combined resulted in a total of 288 unique publications after excluding duplicates (207 publications).

Table 4. Search blocks used in Scopus and WoS databases to retrieve relevant publications eligible for the systematic literature review.

Database	Search block in titles, abstracts and keywords	Results
Scopus	(TITLE-ABS-KEY (((built OR urban OR city OR spatial) W/2 form) OR ((built OR urban OR city OR spatial) W/2 morphology) OR ((built OR urban OR city OR spatial) W/2 fabric) OR ((built OR urban OR city OR spatial) W/2 tissue) OR ((built OR urban OR city OR spatial) W/2 geometry) OR (built W/1 environment))) AND (TITLE-ABS-KEY (urban W/2 resilien*)) AND (LIMIT-TO (LANGUAGE , "English"))	278
WoS	TS= (((built OR urban OR city OR spatial) NEAR/2 form) OR ((built OR urban OR city OR spatial) NEAR/2 morphology) OR ((built OR urban OR city OR spatial) NEAR/2 fabric) OR ((built OR urban OR city OR spatial) NEAR/2 tissue) OR ((built OR urban OR city OR spatial) NEAR/2 geometry) OR (built NEAR/1 environment)) AND (TS= (urban NEAR/2 resilien*)) and English (Languages)	217

3.2.2. Study selection and bibliometrics

As a next step, the titles and abstracts of the 288 retrieved publications were screened on a case-by-case basis to exclude obviously-irrelevant publications based on the criteria of the topic relevance and the type of study. Publications were only included if they were found to discuss a physical dimension of the city in relation to a resilience performance or property to face a disturbance. Furthermore, only primary literature (e.g. research papers, method papers, theory papers, case studies, viewpoint/commentary papers) was included in this systematic review and secondary sources, such as narrative reviews, systematic reviews and meta-analyses that are based on original research publications, were excluded. This step reduced the number of publications to be fully read and assessed to 225 (63 publications were excluded). Finally, after reading these 225 publications other 119 publications, which did not meet the aforementioned criteria, were excluded. Therefore, the results presented in Section 3.3 are based on a sample of 106 publications.

Furthermore, in order to provide a preliminary analysis of the 106 included publications and to identify the different research themes (or clusters) on the topic, the bibliometric information, specifically the authors' keywords, retrieved from Scopus and WoS databases was analyzed using the VOSviewer software (van Eck and Waltman, 2010) to develop a visual representation of the most common keywords (based on their occurrence/co-occurrence in titles, abstracts and keywords). The resulting visualization is a distance-based map with clustered, colored keywords of different sizes indicating the density of their occurrence in all publications. The line between two keywords refers to their co-occurrence and the thickness of the line indicates the density of this co-occurrence. Keywords are clustered based on their co-occurrence frequencies. For this analysis, we only considered keywords that occurred at least 10 times.

3.2.3. Review questions

To clarify the core meaning of resilience in urban morphology and understand how the relationship between urban form and urban resilience is addressed across the different fields and studies, the 106 included publications were fully read in an attempt to clarify “conceptual tensions” (Meerow et al., 2016) and answer a number of recurring questions in the resilience literature (Carpenter et al., 2001; Meerow and Newell, 2016; Vale, 2014; Weichselgartner and Kelman, 2014). These are:

1. What elements and attributes of urban form are discussed as being resilient or can provide resilience? In this regard, we made a distinction between resilience *through* and *of* urban form. By resilience *through* urban form, we mean that urban form is studied as a vehicle for resilience performance either by enhancing people’s persistence during a disturbance (e.g. providing direct protection from extreme heat) (i.e. *people persist*) or by providing them with opportunities to adapt and maintain basic functions during and after a disturbance, such as providing access to basic services after a flood or an earthquake (i.e. *people adapt*). According to Masnavi et al. (2019), one can call this a “non-structured” resilience performance aiming at “creating a system that offers behavioral adaptation of people to change” (p. 10).

On the other hand, resilience *of* urban form means that urban form is studied as being resilient in itself, i.e. exhibiting a “structured resilience” performance (Masnavi et al., 2019) either by (1) being persistent (e.g. earthquake-/flood-proof buildings) (i.e. *urban form persists*); (2) being adaptable without experiencing major physical changes to maintain the existence of function (e.g. spaces that their design can be adapted to house temporary and emergency shelters) (i.e. *urban form adapts*); or (3) behaving as a complex system that can accommodate “minor but continuous adjustments” (Romice et al., 2018, p. 2) over time to adapt to ever-changing socio-economic, cultural, demographic or technological conditions (i.e. *urban form changes/transforms*).

2. Resilience to what? For this question, we distinguished between the so-called *general* and *specified* (or targeted) resilience. According to Folke et al. (2010), general resilience refers to the “resilience of any and all parts of a system to all kinds of shocks, including novel ones” (p. 3), whereas specified resilience refers to the “resilience of some particular part of a system . . . to one or more identified kinds of shocks” (p. 3). The different specified disturbances that were discussed in the literature in relation to urban form were identified.
3. Who are the different actors involved in the planning process of resilience? Who does take part in determining what is desirable for an urban system?
4. Resilience for whom? Or whose resilience is addressed/prioritized? Or who does benefit/lose from this resilience?
5. What is the resilience performance discussed (or the pathway towards a resilient state)? For this question, we distinguished between three different resilience

performances that were discussed in Chapter 2. These are (1) persistence, to maintain the efficiency of function or system's status quo (i.e. to bounce back) in correspondence with the engineering understanding of resilience, and where there is a collapse point after which the system breaks down (Holling, 1996b, 1973); (2) adaptability, to maintain the existence of key functions (i.e. to bounce forward), and which corresponds to the ecological understanding of resilience (Holling, 1996b; Walker et al., 2004). As discussed above, adaptability can either be a characteristic of the urban form itself (i.e. urban form adapts) or an opportunity that urban form offers to people (i.e. people adapt); and (3) transformability, to maintain the system's ability to radically change or transform (i.e. to transform forward). Transformability reflects the resilience performance of social-ecological systems (also known as evolutionary or progressive resilience) (Davoudi et al., 2012; Folke, 2006; Vale, 2014).

6. Resilience for when? In this review, we distinguished between resilience to short-term disruptions that usually have a short duration and are caused by rapid-onset events (or shocks) such as earthquakes; and long-term disruptions with a longer duration that are caused by slow-onset events (or stresses) such as the temperature or precipitation changes caused by climate change.
7. Resilience for where? Although this question is usually addressed in the resilience literature to understand “the spatial boundaries of the urban system” (Meerow et al., 2016, p. 4) and “how fostering resilience at one spatial scale affects those at others” (Meerow and Newell, 2016, p. 11), the aim here is to understand where research on the topic is most active or in which contexts there is more acknowledgment and attention to the relationship between urban form and urban resilience.
8. Is resilience being discussed/defined as a positive concept? This is an important question because although there is consensus “that resilience is a positive trait that contributes to sustainability” (Brown et al., 2012, p. 534), there is a debate about whether it should be always conceptualized as such (Cote and Nightingale, 2012; Meerow et al., 2016; Nelson et al., 2007). For instance, when the original state of the system is undesirable (e.g. poverty, dictatorships), then a resilient state can be “self-defeating” (Hassler and Kohler, 2014).
9. Did the author(s) explicitly/implicitly define what urban form resilience is or what resilient urban forms are? As pointed out in Chapter 2, agreeing on a common definition of urban form resilience is an important step to operationalizing resilience in urban morphology and avoiding it from becoming an empty signifier (Meerow et al., 2016; Meerow and Newell, 2016; Weichselgartner and Kelman, 2014). Therefore, this question aims to provide an understanding of how the combination of urban form and urban resilience is defined across different fields and studies and, from there, propose a refined and inclusive definition of urban form resilience to heat stress, which is the specific focus of this thesis.

3.3 Synthesis of the review results

This section provides a synthesis of the review results. The section is organized as follows: firstly, the results of the bibliometric analysis of the 106 included publications are presented in Section 3.3.1; then, in Section 3.3.2 the answer to each of the review questions put forward in Section 3.2.3 is provided based on the systematic reading of the 106 selected publications; and finally, a selection of definitions of urban form resilience (or resilient urban forms) that were identified in the reviewed publications is provided in Section 3.2.3.

3.3.1. Bibliometrics

Figure 20 shows the network of keywords occurrence/co-occurrence based on the 106 included publications from Scopus and WoS. Four clusters of keywords were formed based on their co-occurrence frequencies. These clusters represent different research themes on the topic of urban form and urban resilience: Cluster 1 focuses on urban resilience and urban planning and their relation to other general topics like sustainability and governance; Cluster 2 focuses mainly on the trio of the built environment, resilience and sustainable development, as well as on risk assessment/management; Cluster 3 takes more an urban design and morphology perspective and focuses on the urban form of cities and neighborhoods as well as on urban population (or humans); Cluster 4 focuses on climate change, atmospheric temperature and the urban heat island effect.

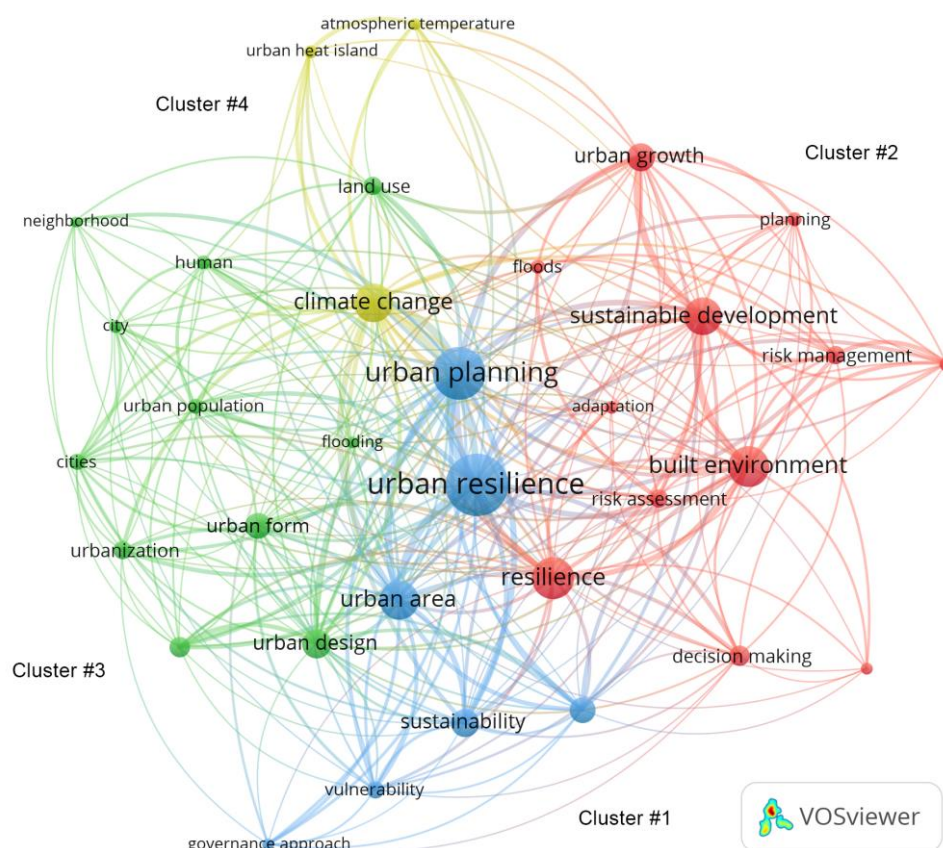


Figure 20. The network of keywords occurrence/co-occurrence formed using the VOSviewer software based on the 106 included publications from Scopus and WoS.

3.3.2. The underlying politics of resilience in urban morphology

3.3.2.1. Resilience of what or through what?

The review of the 106 included publications has shown that there are at least 11 urban form elements and attributes that can enhance urban resilience to different stresses and shocks (Table 5). In this section, we give an overview of these elements and attributes, and in Section 3.3.2.2, we further associate them with specific stresses and shocks.

In general, one can address these urban form elements and attributes at two/three main scales as suggested by Sharifi and Yamagata (2018a), namely the macro-scale and the meso-/micro-scales. At the macro-scale “urban form concerns the whole structure of the city, its existing position, and its future development in relation to other cities and settlements in the broader network of cities and city regions” (Sharifi and Yamagata, 2018a, p. 170). On the other hand, at the meso- and micro-scales urban form concerns, respectively, “the general structure of neighborhoods and districts” (Sharifi and Yamagata, 2018a, p. 173), and “the structure of buildings, how they are located in relation to each other (on the site), and their relative position with respect to the pedestrian and traffic networks in a finer level of granularity” (Sharifi and Yamagata, 2018a, p. 174). Table 5 lists these different-scale urban form elements and attributes and indicates whether they are discussed in the literature as being resilient in themselves (i.e. resilience *of* urban form) or as means for providing resilience to people to face different disturbances (i.e. resilience *through* urban form).

More specifically, around 34% of publications (36) focused on the macro-scale level of urban form by discussing either the attributes of the built environment as a whole system (19 publications) or the type of the urban development, for instance, in terms of the growth pattern (e.g. compact versus dispersed or planned versus informal); shape (star, hexagonal, rectangular); and degree of clustering (e.g. polycentric versus monocentric) (17 publications).

On the other hand, around 46% of the publications (49) focused on the meso-/micro-scale level of urban form, where buildings (14), open/green spaces (13) and neighborhoods/sanctuary areas³ (8) were the most discussed urban form elements in relation to resilience performances and/or properties. Four meso-/micro-scale urban form elements were discussed in the literature more than once but not more than five times. These include streets (5), land uses (3), blocks (2) and the so-called urban project (2). The latter refers to the form of urban projects that are not built based on a rigid and prohibitive set of rules and regulations such as those typically found in flood-risk prevention plans, but rather with a certain degree of flexibility and attention to local contexts that can enhance urban resilience (Rode et al., 2018; Rode and Gralepois, 2017). There are two urban form elements that were discussed only once in the reviewed literature, namely the underground space (or the subsurface) and the plot.

³ Assemblages of meso-/micro-scale urban form elements such as buildings, plots, blocks and streets (Felicetti, 2018).

The remaining 21 publications discussed a combination of the aforementioned urban form elements and attributes. These were marked as *varied* in Table 5.

As for the distinction between resilience *through* and *of* urban form, Table 5 and Figure 21 show that the large majority of publications (76) addressed providing resilience *through* urban form, where almost all the urban form elements were involved. On the other hand, 26 publications discussed the resilience *of* the urban form elements themselves with a focus on buildings and development types. There are only four publications that discussed both resilience *through* and *of* urban form, as they discussed a variety of urban form elements that can contribute to resilience via both mechanisms.

Table 5. The urban form elements/attributes that were discussed in the reviewed literature in relation to resilience performances and/or properties to face general/specified disturbances.

Scale	Urban form element/attribute	Number of publications			
		Through	Of	Through and of	Total
Macro-scale	General/Not-specified	13	5	1	19
	Development type	11	5	1	17
Meso-/Micro-scale	Building	8	6	-	14
	Open/Green space	12	1	-	13
	Neighborhood/Sanctuary area	7	1	-	8
	Street	5	-	-	5
	Land use	3	-	-	3
	Block	2	-	-	2
	The urban project	1	1	-	2
	Underground space	1	-	-	1
	Plot	0	1	-	1
Varied		13	6	2	21
Total		76	26	4	106

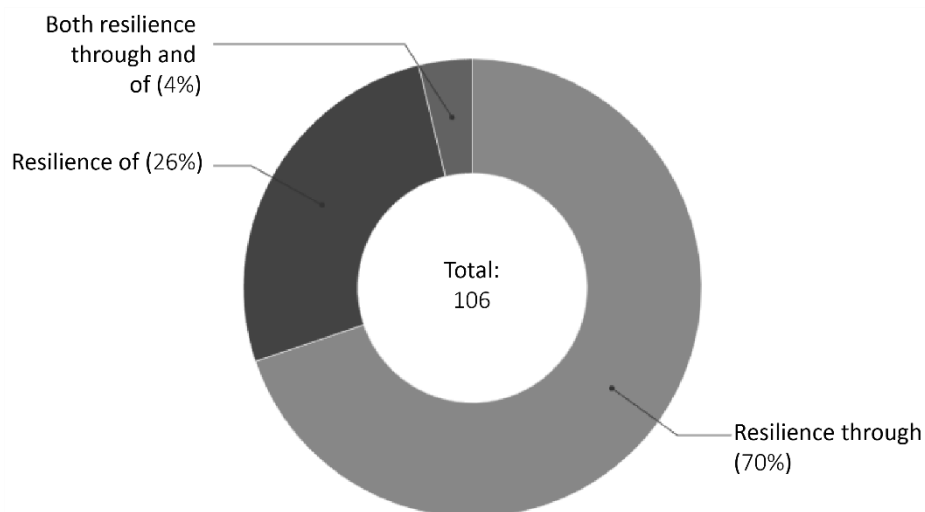


Figure 21. The distribution of the publications based on the distinction between resilience *through* and *of* urban form.

3.3.2.2. Resilience to what?

Regarding the type of stresses and shocks that the urban form elements and attributes, discussed in the previous section, can provide resilience to, the review has shown that there are a great many. In general, the large majority (86%) of the publications (91) discussed resilience to a specific disturbance, while only 15 publications (14%) discussed resilience to general unforeseen disturbances (Figure 22).

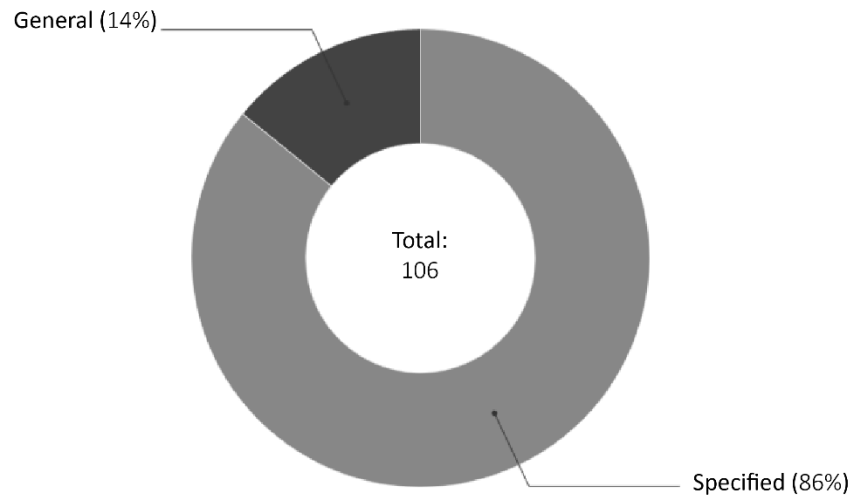


Figure 22. The distribution of the publications based on the type of resilience they discuss (general versus specified).

More specifically, there are 17 different types of stresses and shocks that urban form elements and attributes can provide resilience to, where floods (22), earthquakes (15) and high temperatures (10) are the most discussed disturbances in the literature in relation to urban form. And disturbances such as terrorist attacks, ill-being, warfares/armed conflicts, water scarcity, and gentrification are the least discussed ones with only one publication addressing each. Appendix A shows the full list of these stresses and shocks as well as the urban form elements and attributes that are associated with each. And is discussed below in more detail.

Floods, earthquakes and related general structural collapses

22 and 15 of the reviewed publications focused on resilience to floods and earthquakes, respectively, where, in most cases, they were discussed in relation to three specific urban form attributes and elements, namely the type of development, buildings and open/green spaces.

On the one hand, it was found that compact growth patterns of urban development (also known as smart growth) can lead to an overall reduction, at the city scale, in flood losses compared to low-density urban sprawls (Brody et al., 2013; Xu et al., 2020). This can be returned to the concentration of the urban development in the most suitable land available while avoiding flood-prone areas (Stevens et al., 2010). However, at the neighborhood scale, high-density developments can increase surface runoff due to the relatively high fraction of impervious surface cover. Therefore one should account for

this tradeoff between the neighborhood and the city scales when it comes to runoff/flood mitigation (Xu et al., 2020).

On the other hand, compact developments were found to be less seismic-resilient (where polycentric compact developments are favored over monocentric ones) compared to urban sprawls. This is because in urban sprawls “only a small share of the city will be exposed to an earthquake at a time” (Wang, 2020). Also, the shape of the city (e.g. rectangular, hexagonal, star, circular) was found to influence its resilience, in terms of the number of damaged buildings, when hit by an earthquake. More specifically, Bozza et al. (2015) found that the star shape is the most seismic-resilient shape and the circular one is the least resilient.

As for buildings, it was found that building characteristics such as the geometry of structural elements (e.g. columns and beams) (Cimellaro et al., 2018; Schinke et al., 2016) and building heights and density (Rezende et al., 2019) are key determinants of the resilience, or more precisely the persistence, of buildings to both floods and earthquakes.

Open/Green spaces were also discussed in several publications as being important urban form elements for enhancing people's resilience during floods (Miguez et al., 2019) and earthquakes (Villagra et al., 2014), for instance, by acting as emergency evacuation directing points, temporary shelters and distribution points for essential goods and emergency medical services, among other survival needs.

Besides the many reviewed studies that focused on the relationship between urban form and resilience to floods and earthquakes, there is another study that discussed resilience to general structural collapses (e.g. because of earthquakes, floods and fires). More specifically, Cutini and Pezzica (2020) discussed how the characteristics of the street network (e.g. number of connections and availability of path alternatives) can play an important role in “maintain[ing] the operation of urban functional assets by redistributing movement after a physical perturbation” (p. 2).

High temperatures

Ten studies focused on providing resilience to extremely high temperatures. This was mainly associated with the characteristics of open/green spaces, such as the coverage of tree canopy and soft/natural landscape materials (Romano et al., 2020; Sharifi et al., 2020; Sharifi and Boland, 2017; Swapan, 2017), and with the urban form characteristics of neighborhoods/sanctuary areas. The latter include, for example: the shape, dimensions (e.g. height, width and length), spacing and arrangement of urban elements (e.g. buildings, streets); construction materials and their thermal, roughness, radiative and moisture properties; and land cover types (e.g. vegetation, bare rock, sand) and their properties (e.g. dry or wet ground) (Tayebi et al., 2019; Wang et al., 2015, 2016; Williams et al., 2020).

Climate change

Eight studies focused on the relationship between urban form and resilience to various effects of climate change, where different macro- and meso-/micro-scale urban form elements were discussed. For instance, Wang and Foley (2021) discussed how the proper location, design and management of urban open/green spaces (e.g. urban parks) can improve the delivery of ecosystem services (e.g. carbon sequestration, temperature reduction, water purification), thus stabilizing rapidly changing climate conditions. Dhar and Khirfan (2017) discussed the potential role that the built environment, as a whole complex adaptive system, can play “to accommodate new or retrofitted forms (and/or functions) through [an] incremental transformation so as to adapt to climate change and its ensuing uncertainty (Lennon et al., 2014; León and March, 2014)” (p.73). Tablada and Zhao (2016) showed that different block types (e.g. point block, slab block, contemporary block) can have different potentials to achieve food and energy self-sufficiency, which are at high risk because of climate change.

Energy shortages

Five studies focused on resilience to energy shortages, which was discussed in relation to a variety of urban form elements and attributes. These include, for instance, land use, streets, buildings, blocks and development types, where Ragheb et al. (2017) related each of these elements and attributes to specific energy resilience properties (e.g. diversity, redundancy, flexibility) based on a review of different energy efficiency frameworks in urban planning. For instance, an energy-resilient city should be diverse in terms of land uses to ensure the functionality of the system in case of energy supply disruptions (Sharifi and Yamagata, 2016b).

Disease outbreaks

Two studies focused on the relationship between urban form and urban resilience to disease outbreaks. For instance, Lak et al. (2020) pointed out that a pandemic-resilient urban form can minimize the risk of virus spread at three different scales. These are (1) the building (e.g. by designing semi-open spaces in housings, such as balconies for planting and pleasure, and sanitation facilities shared by multiple households); (2) the neighborhood (e.g. by providing semi-public and semi-private or shared open spaces in residential buildings for planting, playing and working out in pandemic situations); and (3) the city (e.g. by creating less dense urban centers to decelerate the spread of diseases and avoiding locating cities at short distances).

Economic recessions and financial crises

Two studies focused on the relationship between resilience to economic recessions or financial crises and urban form. More specifically, in the first study, Rao et al. (2018) discussed how certain types of retail buildings/shops can offer, through their design such as building size and degree of land sub-division, opportunities for adaptation to shocks, such as boom-bust cycles “while fostering a viable retail economy and strong public urban life simultaneously (Rao and Summers, 2016)” (p. 553). For instance,

financial crises can leave retailers with big boxes and large land holdings under single ownerships underperforming, bankrupt, dead and ghosted (Hahn, 2000; Parlette and Cowen, 2011). In the other study, Nielsen (2015) discussed how the design of the street network can facilitate access to retail concentration, thus allowing households to “adapt their behavior and possibly reduce travel in response to the changing economic climate” (p. 10).

Immigration/Migration

Two studies discussed how the urban form of *arrival cities* (Saunders, 2012) can enhance their capacity for “ingesting immigration, adapting to the on-going changes and successfully responding to the needs of immigrants” (Salem, 2021, p. 768). For instance, Asikin et al. (2017) showed that the spatial adaptability/flexibility of some urban form elements in Malang, Indonesia, has enhanced its resilience. This includes, for instance, streets that could be used by migrants as spaces for business and social gatherings/events (e.g. weddings) and dwelling spaces that could be easily adjusted to the lifestyle and needs of the new migrants.

Fires

Two studies discussed the relationship between urban form and resilience to fires, where the focus was primarily on buildings and their characteristics, such as heights, structure and uses, as well as their proximity to fire stations (Kumar et al., 2020; Mota et al., 2017).

Urban poverty

The relationship between resilience to the effects of urban poverty and urban form was discussed in two studies and, specifically, in relation to building characteristics. For instance, Sanders et al. (2008) argued that while poverty itself cannot be eliminated, improving the quality of housing (e.g. in terms of heating and ventilation) can foster resilience to its harmful health effects. On the other hand, Avogo et al. (2017) showed that the transformation⁴ of housing in Accra, Ghana, has increased the capacity of the urban poor households to survive and be more resilient to the rapidly growing socio-economic conditions by using newly added buildings' extensions as home-based enterprises to foster family income (e.g. retail shops, food/water vending, charcoal selling and drinking bars).

Air pollution

Two studies focused on the relationship between resilience to air pollution and urban form, where different urban form characteristics were discussed as having an impact on outdoor air quality by influencing traffic emissions, pollutant concentrations and population exposure to air pollution. These include, for instance, built density, land use

⁴ In the form of “alterations [i.e. internal changes in the building layout] or extensions [i.e. addition of space to the building] involving construction activity and using materials and technology in use in the locality” (Tipple, 1992, p. 4).

types and the roughness of the urban form elements (e.g. height/compactness of buildings) (Cariolet et al., 2018).

Ill-being

According to Merriam-Webster's online dictionary, ill-being is "a condition of being deficient in health, happiness, or prosperity". There is a single study (i.e. Samuelsson et al., 2019) that focused on the relationship between well-being/ill-being and urban form, where the configurational characteristics of open spaces, and specifically their spatial integration⁵, were found to influence the diversity and connectivity of positive human experiences (e.g. calmness, escape from one's routine and nature) that contribute to people's well-being. It was found that people's well-being, or what they referred to as "resilience at eye level"⁶, can be promoted through "a diversity of experiences and . . . [an intermediate] level of connectivity between them" (Samuelsson et al., 2019, p. 71).

Warfares/armed conflicts

One reviewed study pointed out the importance of urban form in supporting various survival practices of civilians during urban warfares. In this study, Kittana and Meulder (2019) found that the spatial characteristics of the *kasbah*⁷ of Nablus, Palestine, enabled the local residents to survive and make living during the Israeli invasion of Nablus in 2002. More specifically, three spatial elements of the *kasbah* were discussed. These are (1) *nodes* such as houses, factories, mosques and other buildings that, due to their physical or spatial characteristics such as materials, size and orientation, could provide sheltering, hiding, medical care and storing facilities, as well as places for people to meet and interact, thus forming strong social bonds and feeling of togetherness; (2) *sneaks* defined as "alternative routes of movement [e.g. tunnel-like streets, narrow passages, back doors] that are concealed from the Israeli fields of view" (Kittana and Meulder, 2019, p. 709). Sneaks played an important role during the 2002 invasion because they provided civilians with opportunities for "escaping, delivering items and people, rescuing wounded people, recovering dead bodies, conveying news and communicating information" (Kittana and Meulder, 2019, p. 710); and (3) *edges*, which refer to the "three-dimensional imagined lines [e.g. formed by the building's architectural features such as height and windows] that separate exposed and protected spaces [from the fields of fire]" (Kittana and Meulder, 2019, p. 710).

Water scarcity

A single study focused on the role of urban form, and specifically buildings, in providing resilience to water scarcity. More specifically, Paschoalin et al. (2020) examined the potential of rainwater harvesting in heritage buildings in Wellington, New

⁵ Spatial integration is a measure of network centrality that determines how close a space is to all other spaces (Hillier and Hanson, 1984).

⁶ The level where people experience the city (Marcus and Colding, 2014).

⁷ The fortified quarter of the old islamic city.

Zealand, where they found that roof spaces can collect a significant amount of water per year that could potentially be used, for example, in favor of irrigation, toilet flushing and emergency water for fighting fires, thus enhancing residents' resilience to water scarcity.

Terrorist attacks

There is only one study that referred to the potential role of urban form in combating terrorism⁸. More specifically, Fischer et al. (2018) discussed how different development patterns, such as compact and linear developments, may exhibit different degrees of susceptibility to terrorist attacks. It was found that in compact developments, there may exist several hotspots with a relatively high susceptibility compared to the linear ones, which exhibit low susceptibility due to the clear separation between the different uses and the relatively low density.

Gentrification

There is a single study that discussed the relationship between resilience to gentrification—as a form of the inevitable future change and transformation in cities—and urban form. More specifically, Venerandi et al. (2017) hypothesized that “traditional, fine-grained urban forms are more capable than others of responding to small-scale, largely self-organized dynamics of socio-cultural nature, in this case, gentrification by ‘collective action’” (p. 1061). They found that there are shared urban form characteristics, especially at the unit of the street edge⁹, between five neighborhoods in London, England, that have undergone a process of gentrification by collective action. These include, for instance, the area of the street edge; the centrality of the street that defines the street edge; the average height of all buildings in a street edge; and the total amount of gross floor area over the street edge area. However, this, in their words, does not imply “any causal or universal relationship between morphological and social dynamics [due to the number and size of the cases investigated, and the confinement within this study to only cases of a single-type of gentrified neighborhoods]” (Venerandi et al., 2017, p. 1056).

3.3.2.3. Who does determine resilience?

The review has shown that there are a great many urban actors that are involved in the planning and decision-making process of resilience through/of urban form. Examples of the most recurring urban resilience actors in the reviewed literature are depicted in Figure 23, where the bigger and bolder the word, the more frequent it was mentioned in the reviewed literature.

⁸ “. . . unpredictable destruction to attack the citizens of governments they oppose, causing uneasiness and fear in those societies” (Lin et al., 2007, p. 149).

⁹ “The sum total of all the plots on one block which face the same street (i.e., having their main entrance on it)” (Venerandi et al., 2017, p. 1063).



Figure 23. The most recurring urban resilience actors in the reviewed literature. The bigger and bolder the word, the more frequent it was mentioned in the literature.

3.3.2.4. Resilience for whom?

The review of the literature has shown that most of the research carried out focused on the resilience of the general population, where terms such as society, city residents, community, ecosystem and stakeholders were the most used (Figure 24). Examples of the specified population that was addressed in a few of the reviewed publications include: the low-income population in Acra, Ghana (Avogo et al., 2017); the Madurese migrants in Indonesia (Asikin et al., 2017); the African Americans in the US (Sanders et al., 2008); the tsunami-affected communities in Sri Lanka (Jayakody and Amaratunga, 2020); and the local residents of Nablus, Palestine (Kittana and Meulder, 2019).

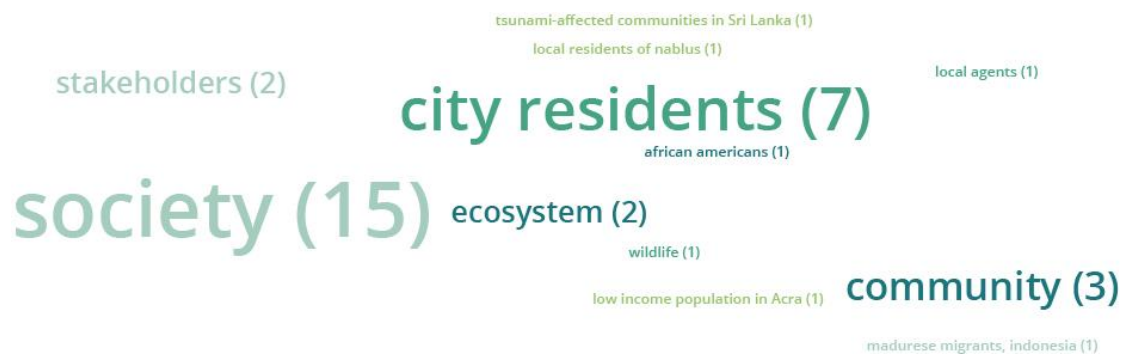


Figure 24. The most recurring urban resilience beneficiaries. The bigger and bolder the word, the more frequent it was mentioned in the literature.

3.3.2.5. Pathways to urban resilience

Figure 25 shows that 38 out of 106 of the reviewed publications focused on the adaptability pathway to resilience, 33 focused on persistence, 18 did not take an explicit position (or are unclear), nine discussed a combination of pathways and eight focused on transformability.

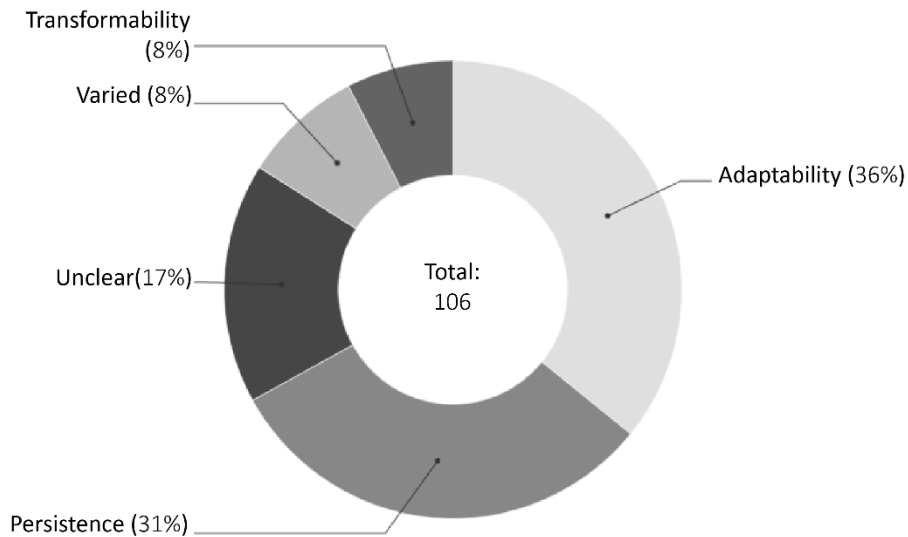


Figure 25. The distribution of the reviewed publications based on the pathway of resilience they focus on.

Adaptability (people adapt vs urban form adapts)

34 out of the 38 publications on adaptability focused on the opportunities that urban form offers to people to adapt and maintain basic functions during and after a disturbance (i.e. people adapt) (Figure 26). In the reviewed literature, this was best exemplified by the capacity of the urban form elements, especially streets and open spaces, to enable people to access safe destinations after disturbances (e.g. floods and earthquakes), where they can get survival needs such as temporary sheltering, medical care, basic goods as well as information and awareness (Abdulkareem and Elkadi, 2018; Cutini and Pezzica, 2020; Jayakody and Amaratunga, 2020; Villagra et al., 2014).

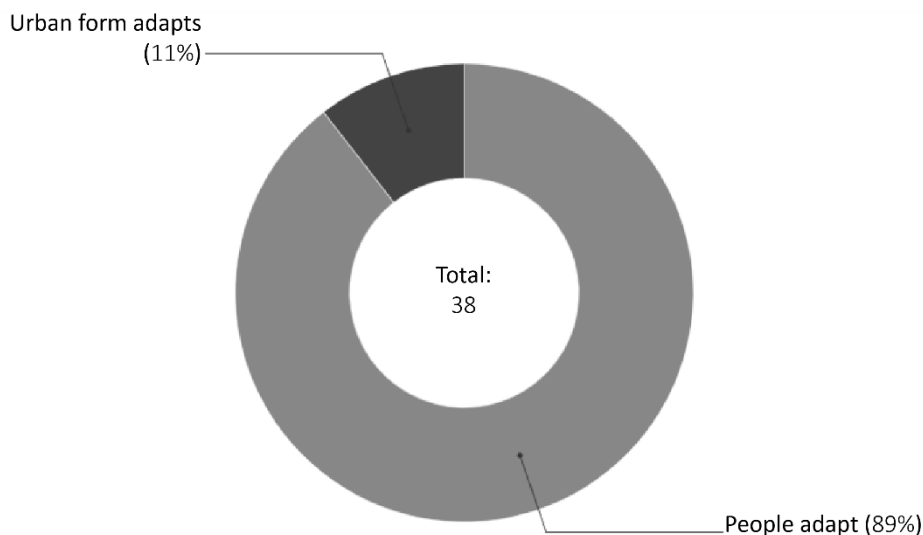


Figure 26. The distribution of the reviewed publications based on the type of adaptability performance they discuss (people adapt versus urban form adapts).

On the other hand, only four publications focused on the capacity of the urban form elements to be adapted without experiencing major physical changes to serve diverse

key functions during and/or after a disturbance (i.e. urban form adapts). This includes, for instance, buildings with polyvalent/unlabeled (Hertzberger, 1991), indeterminant/half-determinant/unfinished (Habracken, 1972) or flexible spaces that can allow new users (e.g. immigrants/migrants) to adjust and re-organize the available space to meet their lifestyle, societal and cultural needs (Asikin et al., 2017); or enable existing users to add extensions that work, for example, as home-based enterprises (e.g. retail shops, selling and drinking bars) to foster family income in the time of economic crises (Avogo et al., 2017).

Other typical examples of the adaptability capacity of urban form (that were not discussed in the included publications) include streets or open spaces that can be temporarily used to store stormwater runoff during flooding (by functioning as bioswales) or to house temporary and emergency shelters after disasters such as earthquakes (Allan et al., 2013; Moudon, 1986; Roggema et al., 2012).

Persistence (people persist vs urban form persists)

20 out of the 34 publications on persistence discussed how urban form can enhance people's persistence capacity during a disturbance. In particular, half of these publications (10) focused on the role of different urban form elements (referred to in Section 3.3.2.2) in providing resilience to high-temperature events by keeping outdoor temperatures below what Sharifi and Boland (2017) called the "critical thermal threshold" (CTT). CTT is associated with zero human activity and can lead to severe health consequences. On the other hand, 13 publications focused on the persistence of the urban form elements themselves (i.e. urban form persists) with more than half (8 out of 13) focusing on earthquake-/flood-/fire-proof buildings and development patterns.

Transformability (urban form changes/transforms)

Six of the eight publications on transformability addressed resilience to general unanticipated disruptions or future unknown urban change (i.e. general resilience), while only two discussed resilience to specified disturbances, namely climate change (Dhar and Khirfan, 2017) and gentrification by collective action (Venerandi et al., 2017). In all of these publications, the focus was primarily on the capacity of different urban form elements, such as plots (Barbour et al., 2016) and open/green spaces (Roggema, 2018), or the built environment as a whole system (Dhar and Khirfan, 2017; Du Plessis et al., 2015) to behave as a complex system. Complex systems "change and evolve over time at different speed[s] and different scales" (Romice et al., 2018) and so is urban form with a combination of long-lasting (e.g. streets) and changeable (e.g. buildings) constituent elements, each has its own adaptive cycle at a different speed. According to Romice et al. (2018), "it is this dynamic relationship between fast and slow, changeable and permanent that has always enabled cities to respond to challenges of different nature: from local fast-paced changes to large-scale events" (p. 3).

3.3.2.6. Resilience for when?

Figure 27 shows the distribution of the reviewed publications based on the temporal scale of resilience they discuss (as explicitly expressed by authors), where in more than half of the publications (55), authors explicitly expressed long-term resilience targets. However, only two publications explicitly expressed short-term resilience targets. In around 46% of the publications (49), the authors' points of view regarding the temporal scale of resilience discussed were not clear. Nonetheless, one can generally expect that the focus is on short-term resilience when the discussed pathway to resilience (Section 3.3.2.5) is through persistence, whereas long-term resilience would likely require some degree of adaptability or transformability performances (Chelleri et al., 2012; Meerow and Newell, 2016). Also, building short-term resilience is usually associated with disturbances that are rapid/sudden-onset and have a short duration (i.e. shocks), such as earthquakes and terrorist attacks, while building long-term resilience is usually associated with slow-onset events that result from incremental changes over time and have a protracted duration (i.e. stresses), such as irregular migration and changes in precipitation and temperature caused by climate change.

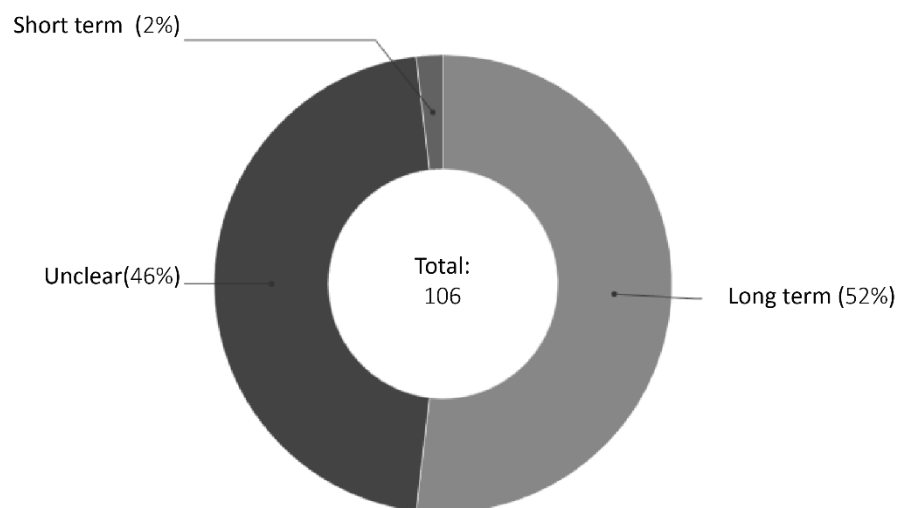


Figure 27. The distribution of the reviewed publications based on the temporal scale of resilience they discuss from the authors' point of view.

3.3.2.7. Resilience for where?

In general, only 73 out of the 106 publications were geographically contextualized (i.e. investigated the relationship between urban form and urban resilience in a specific context). Table 6 and Figure 28 show these different contexts (indicating the number of publications per country). Furthermore, Table 7 shows the top most discussed urban form elements and the disturbances per continent.

More specifically, most of these publications were in the European context (29 publications), where the top most discussed urban form element/attribute is the type of development, and it was specifically discussed in relation to floods. On the other hand, Africa is the continent with the least number of publications on the topic with only two publications focusing on the role that different urban form elements (e.g. buildings,

streets and open/green spaces) play in providing resilience to two specific disturbances, namely urban poverty and floods.

Table 6. The contexts where the relationship between urban form and urban resilience was discussed and studied. Countries are listed in descending order based on the number of publications.

Country	Number of publications
Australia	7
Iran	7
Italy	7
France	5
China	4
UK	3
Canada	3
Chile	3
Brazil	3
Vietnam	2
Greece	2
Spain	2
Germany	2
USA	2
Oman	2
Portugal	2
Japan	2
Bangladesh	1
Ireland	1
Sweden	1
North Macedonia	1
Ghana	1
India	1
Sri Lanka	1
Israel and Palestine occupied territories	1
Taiwan	1
Indonesia	1
Barbados	1
Scotland	1
Denmark	1
Singapore	1
Nigeria	1

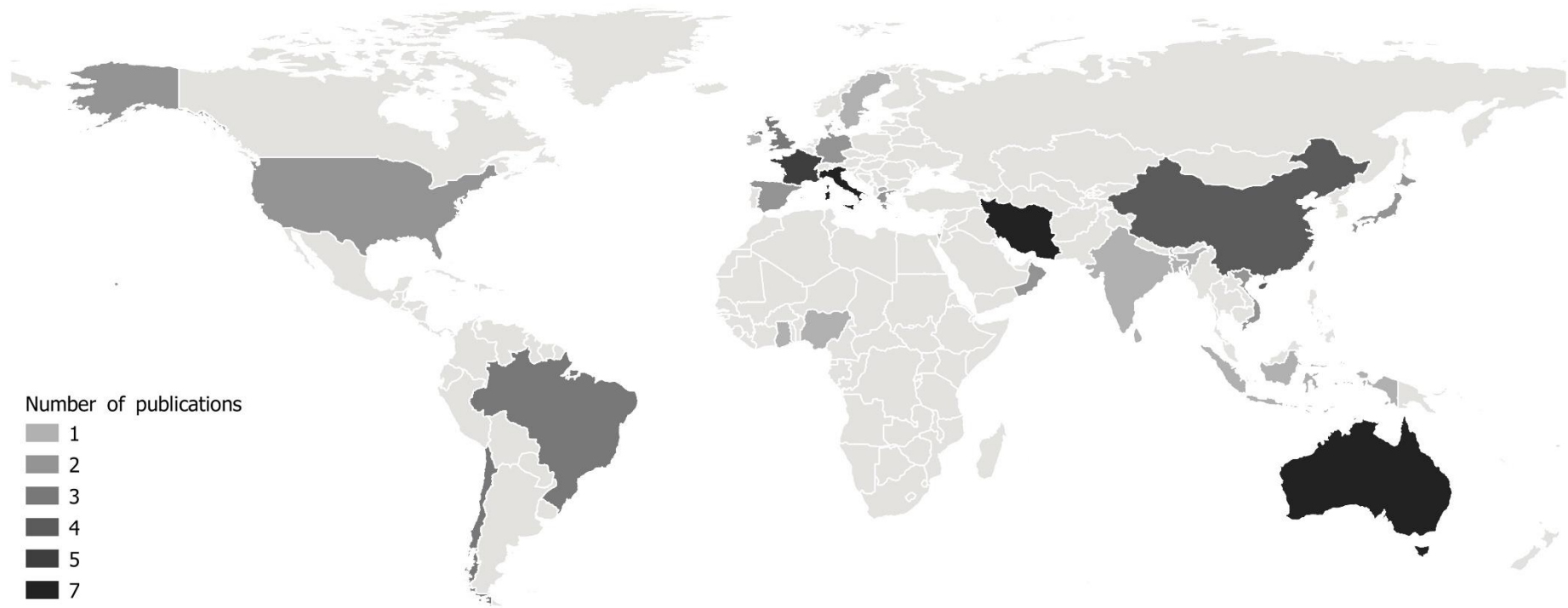


Figure 28. The geographical distribution of the number of publications focusing on the relationship between urban form and urban resilience.

Table 7. The number of publications (per continent in descending order) focusing on the relationship between urban form and urban resilience, as well as the top most discussed urban form elements and disturbances.

Continent	Number of publications	The top most discussed urban form element(s)	The top most discussed disturbance(s)
Europe	29	Type of development (6)	Floods (8)
Aisa	23	Type of development (6)	Earthquakes (6)
South America	7	Type of development (2) and open/green spaces (2)	Floods (5)
Australia	7	Open/Green spaces (3)	High temperatures (3)
North America	5	Neighborhood/Sancturay areas (3)	High temperatures (3)
Africa	2	Buildings, streets and open/green spaces (2)	Urban poverty (1) and floods (1)

3.3.3. Resilience as a positive/negative concept and existing definitions of urban form resilience (or resilient urban forms)

Resilience as a positive concept

In general, all the 106 reviewed publications discussed resilience as a positive concept, a desirable state or a “politically significant notion” (Hassler and Kohler, 2014). Nevertheless, a single study (i.e. Felicioni et al., 2020) pointed out that the planning for increased resilience (or more precisely persistence) of buildings to earthquakes may result in increased environmental impacts at the construction stage. Furthermore, when urban form resilience to gentrification was viewed as a good thing in (Venerandi et al., 2017), this was because gentrification was discussed as a form of the inevitable future change and transformation in cities. But what if we want to combat the negative effects of gentrification such as the forced displacement of the population? Then an urban form that accommodates physical changes and facilitates transformation might be undesirable. Such controversy highlights that there is a cost of resilience and while some may benefit, others may lose. Hence, the question of “resilience for whom” (Section 3.3.2.4) is essential for operationalizing resilience and cannot be overlooked.

Existing definitions of urban form resilience

Out of the 106 reviewed publications, only 31 (29%) explicitly/implicitly defined (or used other scholars’ definitions) urban form resilience or resilient urban forms. Table 8 lists 41 identified definitions, where we have distinguished between general definitions (20) that focus on resilience to ever-changing conditions (e.g. socio-economic, cultural, demographic and technological) or to general unforeseen disturbances and those that focus on specific stresses/shocks and/or urban form elements/attributes (21).

Table 8. A selection of definitions of urban form resilience (or resilient urban form) identified in the 106 reviewed publications.

	Definition	Source
General	“. . . facilitates recovery after disasters and increases the adaptive capacity of the urban system with a degree of shock absorption” (p. 312).	(Sharifi, 2019e) in (Roosta et al., 2022)
	“. . . [evolves] with spatial-temporal dynamics and . . . [is] constantly changing under the influence of social, economic and environmental conditions” (p. 312).	(Sharifi and Yamagata, 2018a) in (Roosta et al., 2022)
	“. . . provide[s] diversity of options and resources for recovery, flexibility to adapt to changed conditions and new functions . . .” (p. 1368).	(Tumini et al., 2017)
	“. . . [is] capable, over time, of embracing change and modulating the new with the existing, without a loss of overall coherence, diversity and, ultimately, resilience” (p. 19); “. . . enable[s] and support[s] a virtuous cycle of gradual investment, capable of meeting changing human needs over time in a flexible and responsive manner” (p. 20).	(Barbour et al., 2016)
	“. . . accommodate[s] new or retrofitted forms (and/or functions) through incremental transformation so as to adapt to climate change and its ensuing uncertainty . . .” (p.73); “. . . [reduces] shocks . . . facilitate[s] incremental and generative urban development . . . [and] strengthen[s] the innate ability of the urban system to be transformed physically, functionally, and spatially in a manner that accommodates new changes in society, economy, and/or environment over time” (p. 81); “. . . reduce[s] an area's specific risks, but also . . . addresses our ever-changing environment and complex urban systems in a continuous bid for sustainable development” (p. 88).	(Dhar and Khirfan, 2017)

(continued)

Table 8 (continued)

	Definition	Source
General	<p>“... accommodate[s] adaptation through incremental changes that facilitate transformation and diversity. . . . These adaptations cannot be satisfactorily implemented at a single scale. Rather, they form part of a hierarchical continuum of interacting systems (for example, metropolis, neighbourhood and street) that adapt at different rates and require a variety of approaches to facilitate improved resilience” (p. 183-184).</p>	(Du Plessis et al., 2015)
	<p>“... adapt[s] to fluctuating economic, environmental and social circumstances [due] to the dynamic interplay between [its fundamental] scales [namely, plots, street edges, blocks, streets and sanctuary areas/districts]” (p. 25).</p>	(Felicciotti et al., 2016)
	<p>Responds and allows for change (or disturbance) by improving spatial connectedness and accessibility “... so that information, people, and biotic components . . . can access each other and construct new constellations . . .” (p. 7);</p> <p>“... support[s] and develop[s] differences in human activity . . .” (p. 7-8) by creating spatial diversity (i.e. multiple, distinct spaces); allows for self-organization, i.e. the ability of the urban form elements to spatially re-organize and structure when facing change, e.g. the presence of “shops [that] typically respond to new market demands by reconfiguring in new geographic clusters” (p. 8); and carries knowledge (or learning), for instance, by creating not only highly integrated spaces but also segregated ones that “... can work as pockets of memory for survival in crises and from which the system can be retrieved if the right connections are present” (p. 9).</p>	Authors’ formulation based on (Marcus and Colding, 2014)
	<p>“The capacity of . . . urban form to provide a fertile environment for economic prosperity and social cohesion . . .” (p. 1056);</p> <p>“... [is capable] of responding to small-scale, largely self-organized dynamics of socio-cultural nature . . . [such as] gentrification by ‘collective action’” (p. 1061).</p>	(Venerandi et al., 2017)

(continued)

Table 8 (continued)

	Definition	Source
General	<p>“ . . . the capacity of the form of the physical city to adapt to everchanging social, economic, and technical contexts” (p. 593);</p> <p>“ . . . the ability of the city’s physical forms to adapt and transform in the presence of urban change, without requiring heavy operations, such as the destruction and reconstruction of entire neighbourhoods” (p. 594);</p> <p>“ . . . the capacity of the physical city to avoid obsolescence (often even early obsolescence) through self-organized processes of adaptation to change” (p. 594);</p> <p>“ . . . the potential adaptability and transformability (or, conversely, with the potential fragility) of the present forms of the physical city when confronted with future socioeconomic and technical changes that urban societies constantly produce endogenously . . . for example, in lifestyles, work organization, and use of technology, in the urban space” (p. 594).</p>	(Fusco and Venerandi, 2020)
	<p>“ . . . enable[s] local agents to respond to adverse events (disasters, disorder) or promising opportunities (new technologies) at any time in the future” (p. 353).</p>	(Roggema, 2018)
	<p>“ . . . the capacity of [the] built environment to maintain acceptable structural safety levels during and after unforeseeable events, such as earthquakes, as well as to recover their original functionality” (p. 291).</p>	(Ferreira et al., 2016)
Focus on specific stresses/shocks and/or urban form elements	<p>“ . . . enhance[s] the coastal cities’ resilience to tsunamis [by providing a system of open spaces that act] as an emergency evacuation directing point, as a primary place for emergency rescue, as an agent for temporary sheltering, as a facilitator for tsunami disaster mitigation and as a mediator to provide tsunami awareness” (p. 471).</p>	(Jayakody and Amaratunga, 2020)
	<p>“ . . . [keeps] residential buildings out of the water thanks to a combination of technical solutions, and . . . [encourages] risk awareness by resorting to the visible presence of water” (p. 19).</p>	(Rode et al., 2018)

(continued)

Table 8 (continued)

	Definition	Source
Focus on specific stresses/shocks and/or urban form elements	“ . . . progressively absorb[s] the flood impact to uphold new critical stability . . . [and] maintains a minimum required level of functionality, a safe-to-fail strategy with a bounce-forth perspective” (p. 182); “ . . . [enables] people to access safety destination and for the surface runoff to gently flow towards natural downstream without disturbing the urban context with inundation” (p. 189).	(Abdulkareem and Elkadi, 2018)
	“ . . . the ability [of retail buildings/shops or urban shopping centers] to adapt to shocks while fostering a viable retail economy and strong public urban life simultaneously . . .” (p. 553).	(Rao et al., 2018)
	“ . . . allows households to adapt their behavior and possibly reduce travel in response to the changing economic climate” (p. 10).	(Nielsen, 2015)
	“ . . . compact form[] of development [that is] . . . better able to [reduce flood-related losses by] . . . focus[ing] development intensity on the most suitable land available . . . deter[ing] the release and subsequent development of flood-prone land elsewhere . . . [and] have[ing] in place a flood mitigation infrastructure that can appropriately handle large amounts of runoff” (p. 791).	(Brody et al., 2013)
	“ . . . [a polycentric, compact urban development pattern that] cause[s] less total seismic damage by shifting floor areas from the city center to . . . subcenters away from most historical earthquakes” (p. 98).	(Wang, 2020)
	“ . . . dense and diverse urban [development] pattern[] . . . [that provides] a redundancy of functions . . . networkability and response diversity to disturbances . . .” (p. 96).	(Lim and Kain, 2016)
	“ . . . [provides] outdoor spaces with more tree canopy, grass cover, and shadow coverage [that] tend to facilitate more frequent extended outdoor activities during summer . . .” (p. 2).	(Sharifi et al., 2020)

(continued)

Table 8 (continued)

	Definition	Source
Focus on specific stresses/shocks and/or urban form elements	“. . . [possesses] passive preventive design features that do not require energy. [This includes, for instance,] . . . reflective roofing, ceiling insulation, reflective foil in the roof cavity . . . ceramic floor covering . . . heavyweight walls . . . slab-on-ground structures in warm climates . . . garden vegetation, shading and appropriate orientation . . .” (p. 280).	(Hatvani-Kovacs et al., 2016)
	“. . . the capability of the built environment to support outdoor activities during heat stress conditions” (p. 944).	(Sharifi and Boland, 2017)
	“. . . [promotes] climate responsive and socially interactive spaces” (p. 122).	(Ray and Shaw, 2018)
	“. . . [includes] a dormant network of streets, squares and parks, among other open areas, which in times of crisis can be prepared to adapt to uncertainty . . . and provide temporal refuge, information, goods and medical care, among other survival needs” (p. 65).	(Villagra et al., 2014)
	“. . . the capacity of an urban grid to maintain the operation of urban functional assets by redistributing movement after a physical perturbation” (p. 2).	(Cutini and Pezzica, 2020)
	“. . . [supports] civilian survival practices during urban warfare” (p. 698).	(Kittana and Meulder, 2019)
	“. . . [is] capable of ingesting immigrations, adapting to the on-going changes and successfully responding to the needs of immigrants” (p. 768).	(Salem, 2021)
	“. . . provides psychological and physiological benefits to people by adding motivations to interact with the environment . . .” (p. 3).	(Song and Li, 2019)

(continued)

Table 8 (continued)

	Definition	Source
Focus on specific stresses/shocks and/or urban form elements	“. . . [affords] a diversity of [positive human] experiences and a level of connectivity between them that limits adverse outcomes” (p. 187).	(Samuelsson et al., 2019)
	Minimizes the risk of virus spread at three different scales: (1) the building (e.g. by designing semi-open spaces in housing design like balconies for planting and pleasure, designing sanitation facilities shared by multiple households); (2) the neighborhood (e.g. by providing semi-public and semi-private or shared open spaces in residential buildings for planting, playing and working out in pandemic situations); (3) and the city (e.g. by creating less dense urban centers to decelerate the spread of diseases and avoiding locating cities at short distances).	Authors’ formulation based on (Lak et al., 2020)
	“. . . [promotes an increased] capacity for health resilience in the face of severe poverty” (p. 1104).	(Sanders et al., 2008)

3.4 Discussion

In urban research and policy, the concept of resilience has recently become a buzzword very favored to address the complexity and future uncertainty in cities. However, as repeatedly discussed in the previous chapters, resilience is a polysemic concept and can be interpreted in a multitude of ways, which works against its operationalization. Operationalizing resilience requires examining its underlying politics by specifying what will be made resilient to what, for whom, when and where, among many other relevant questions in the resilience literature. Specifically in urban morphology, there has been little effort to examine these underlying politics of resilience. Therefore, in this chapter, we have conducted a systematic literature review ($n = 106$ peer-reviewed publications) to improve the intelligibility in the field and better understand how resilience can be operationalized and integrated into the study of urban form.

3.4.1. The nature of the relationship between urban form and urban resilience

Our systematic literature review confirms and adds to the existing evidence that urban form has various implications for the resilience of cities, and hence it can direct them towards either sustainable or unsustainable trajectories. More specifically, the review suggests that the relationship between urban form and urban resilience is rather complex and multifaceted. This complexity is a result of the existence of many urban form elements (ranging from the macro- to the meso- and micro-scales) that were found in the reviewed literature to enhance urban resilience, or the resilience of the urban population (both general and specified), to a great many disturbances. These disturbances can be general unanticipated disruptions or specific existing threats but also can be rapid-onset shocks (short-term disruptions) or slow-onset stresses (long-term disruptions). Furthermore, in responding to these disturbances, urban form elements were found to exhibit different resilience performances, namely persistence, adaptability and transformability depending on the kind of disturbance and its temporal scale of effect (e.g. persistence for short-term disruptions and transformability for long-term ones). In relation to these resilience performances, it was found that urban form can be either persistent, adaptable or changeable in itself (i.e. resilience *of* urban form) or can enhance people's persistence or provide them with opportunities to adapt and maintain basic functions during a disturbance (i.e. resilience *through* urban form).

Another part of this complexity of the relationship between urban form and urban resilience stems from the diversity of agents (direct and indirect) and agencies that were found in the literature to determine urban form resilience such as urban planners, designers, policy- and decision-makers, politicians and architects, with each has its own goals, priorities but also different degree of power to make the decisions about how resilience is applied, whose resilience is prioritized and where.

The review has also shown that in enhancing urban form resilience, there are some potential trade-offs, and resilience may have different kinds of costs. For instance, fostering resilience at one scale can negatively affect resilience at others. Take, for

example, the case of the compact urban development patterns (smart growth) that can reduce the overall flood losses at the city scale due to the concentration of the urban development in the most suitable land available but significantly increase surface runoff at the neighborhood scale due to the relatively high fraction of impervious surface cover. The review has also shown that while some specific populations may benefit from urban form resilience, others may lose as explained in the case of gentrification, where an urban form that accommodates minor but continuous adjustments over time and facilitates transformation might be undesirable for the original inhabitants who often face forced displacement. Furthermore, other examples from the resilience literature have pointed out that too much focus on the system's resilience to specific disturbances can lessen the effectiveness of its general resilience, as this reduces the system's diversity and flexibility among many other general resilience properties (Walker and Salt, 2006; Wu and Wu, 2014). Likewise, achieving long-term resilience targets comes at the cost of short-term ones (Walker and Salt, 2006). These aforementioned trade-offs illustrate that "planning for resilience is inherently a struggle" (Wagenaar and Wilkinson, 2015 as cited in Meerow and Newell, 2016, p. 9) and confirm earlier arguments in the literature regarding the importance of thinking through questions related to who, what, when, where and why, if resilience is to be effectively operationalized.

3.4.2. Towards an integrated definition of urban form resilience to heat stress

The systematic literature review conducted in this chapter has improved our understanding of the underlying politics of resilience in urban morphology. This, which aside from being an important contribution per se, sets the stage for the forthcoming chapters of this thesis, where we will particularly focus on studying the relationship between urban form and urban resilience to heat stress. More specifically, based on (1) our understanding of the different resilience performances that urban form can exhibit to face disturbances; (2) our review of the existing definitions of urban form resilience (Table 8); and (3) our earlier identification of the different conditions that are important for heat stress resilience and can be related to urban form (see Table 1.1, Chapter 1), we propose the following extended definition of urban form resilience to heat stress.

A resilient urban form to heat stress is able, through its geometric, configurational and/or surficial characteristics, to:

- Enhance people's persistence during extreme heat events by maintaining desirable (within the acceptable ranges) outdoor/indoor thermal conditions (both physiological and psychological). This corresponds to the engineering definition of resilience (i.e. to maintain the system's status quo against a disturbance) and is henceforth referred to in this thesis as the *environmental/engineering* dimension of heat stress resilience. This is the most common approach in the reviewed literature to discuss the relationship between urban form and urban resilience, and is regarded in this thesis as the baseline on which the concept of resilience will be addressed in the next chapters.

- Increases people's adaptation capacity during extreme heat events, e.g. by facilitating access to potential social infrastructure (e.g. libraries, open/green spaces, community organizations, places of worship), where people can meet, interact and get enough social support (e.g. emotional, informational, instrumental). This, in principle, corresponds to the ecological definition of resilience discussed in Chapter 2, which focuses on the ability to maintain the existence of the function. In this thesis, this is coined as the *social/ecological* dimension of heat-stress resilience and will be discussed in more detail in Chapter 9.

3.4.3. Limitations of the review

Although the systematic literature review conducted in this chapter aimed to provide a comprehensive understanding of the relationship between urban form and urban resilience, it has a number of limitations that might have caused some biases, and therefore the results should be interpreted with caution.

First, this systematic review has relied only on two databases for the identification of potentially eligible studies, namely Scopus and WoS. Although these are the widest multidisciplinary databases available at the moment, and which together provide relevant scientific content from 1956 to the present, some relevant studies may have not been included. Furthermore, these databases focus mainly on publications written in English, which gives the results an Anglo-American bias (Newell and Cousins, 2015), and they do not generally include books. For these reasons, other supplementary databases could have been used in the review, such as PubMed, Dimensions and Google Scholar.

In addition to these database limitations, the search script used in this review to retrieve relevant publications may have caused an unintentional exclusion of important studies. For instance, the search term 'resilien*' (i.e. resilience, resiliency, resilient) does not ensure the inclusion of studies that implicitly speak of resilience; use parallels to the concept of resilience (as discussed in Chapter 2); or focus only on specific resilience performances (i.e. persistence, adaptability and transformability) or properties (e.g. diversity, redundancy). Furthermore, searching for potentially eligible publications only using titles, abstracts and keywords, and not the full text, is another major limitation that may have resulted in the exclusion of relevant studies. This is because titles, abstracts and keywords include only limited information (Penning de Vries et al., 2020). These limitations in the search script and in the search method have indeed eliminated some important studies that discuss, for instance, the importance of plots (e.g. Bobkova et al., 2019b; Byahut and Mittal, 2017; Salat, 2017) and blocks (e.g. Siksna, 1997) for enhancing urban resilience to different specified and general disturbances.

Finally, considering that systematic reviews are time-consuming, several other publications might have been published since the end date set for our search (July 31, 2021). Obviously, these were not included in the review.

Part II
Methods and techniques

Chapter 4

Quantitative methods for studying the impact of urban form on urban climate: An overview

This chapter gives an overview of the different quantitative methods that can be used for studying the impact of urban form on urban climate (with a focus on urban heating) and, in turn, the possibility of determining its impacts on people's health and thermal sensation¹⁰ (i.e. what we have referred to in Chapter 3 as the environmental/engineering dimension of heat-stress resilience). As outlined in Chapter 2, this thesis takes a quantitative approach to studying urban form with an overarching aim to provide urban planners and designers with empirically-derived and valid evidence on which they can base their decisions when intervening in cities or planning/designing new ones. Therefore, qualitative methods (also known as person-based approaches) to studying urban climate effects are not discussed here and interested readers can, instead, refer to (e.g. Lenzholzer et al., 2018; Requena-Ruiz et al., 2019) for more details.

In particular, the chapter discusses two groups of quantitative methods and underlines their potentials and limitations: climatological-/environmental-based methods (Section 4.1) and typomorphological methods (Section 4.2). These methods aim to provide scientifically sound answers to the following important questions in urban climatology:

- Do urban climate effects (of urban form) in terms of heating exist and, if so, what is their nature?
- What are the specific causes (or the urban form characteristics responsible for) of such effects?

4.1 Climatological-/Environmental-based methods

This section discusses those methods that are widely used in urban climatological/environmental sciences to quantitatively study urban climate effects in general. They are usually used to observe and measure a specific meteorological/climatological parameter (e.g. air temperature, relative humidity) or simulate different atmospheric processes and, from there, calculate different physiological thermal indices to determine human physiological responses to heat stress and their associated health consequences (i.e. the environmental/engineering dimension of heat-stress resilience). Examples of these indices include: the physiological index (PMV) (Fanger, 1972); the physiological equivalent temperature (PET) (Matzarakis et al., 1999; Mayer and Höppe, 1987); and the universal thermal climate index (UTCI) (Höppe, 2002). Hence, these methods are coined in this thesis as *descriptive* methods that emphasize *what is* the problem and provide empirical information on the phenomena under question (i.e. urban heating and its related health/thermal sensation consequences).

¹⁰ The physiological dimension of human thermal comfort/perception (Auliciems, 1981, p. 110).

Generally, one can classify climatological-/environmental-based methods into four groups: (1) field observations using physical devices (i.e. sensors); (2) physical modelling using scaled-representation of the real world (i.e. physical models or hardware); (3) numerical modelling/simulation using mathematical equations (e.g. energy balance, micro-scale computational fluid dynamics (CFD), meso-scale numerical weather prediction (NWP) and coupled models); and (4) empirical modelling/generalization using statistical methods. In particular, in this thesis, we will primarily focus on field observations and empirical modelling/generalization methods. This is because using physical and/or numerical modelling methods to study urban micro- and local climate for entire cities and urban areas at a high spatial resolution can be challenging or not possible due to their high expenses (both monetary and computational) as well as the complexity and the large amount of data required by numerical models (Shahraiyni and Sodoudi, 2017). However, interested readers can refer to (e.g. Oke et al., 2017, chap. 3) for more details about these methods.

4.1.1. Field observations

Filed observations are the most common methods to study urban climate effects quantitatively. They rely on measuring different surface and atmospheric properties using “physical devices (sensors) that respond to changes in the environment to which they are exposed” (Oke et al., 2017, p. 45) and store measurements at defined time intervals on a so-called data logger. In general, there are two main approaches for conducting field observations using sensors, namely fixed and mobile measurements. For each of these approaches, different platforms (e.g. vehicles, satellites, towers, airplanes, drones) can be used to carry the sensors depending on their type and the atmospheric layer under study. Figure 29 shows the different atmospheric layers that are making up the urban climate system and Figure 30 shows the different platforms that can be used to carry sensors and conduct measurements within these layers.

Considering that our main focus in this thesis is on the impact of urban form on urban micro- and local climate and, in turn, people’s health and thermal sensation, we will discuss only field observations (using either fixed or mobile measurements) within the urban canopy layer (UCL), which is the layer beneath buildings’ roof level and where most of the human activity takes place.

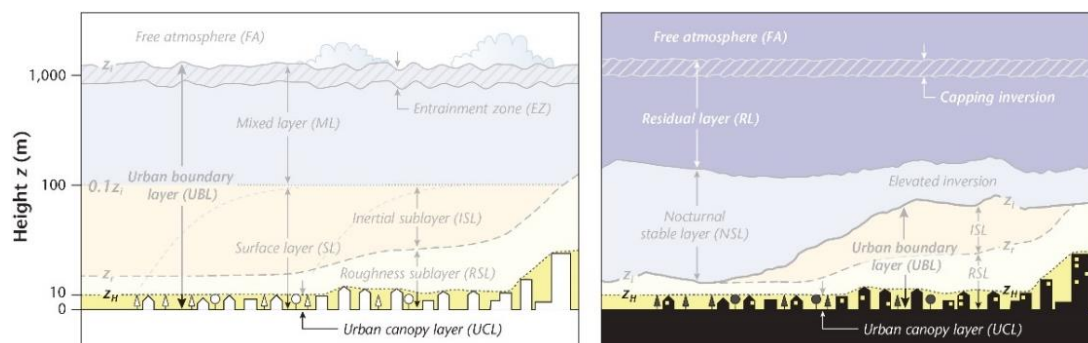


Figure 29. The different atmospheric layers over a city during daytime (left) and nighttime (right). Readapted from (Oke et al., 2017, p. 31).

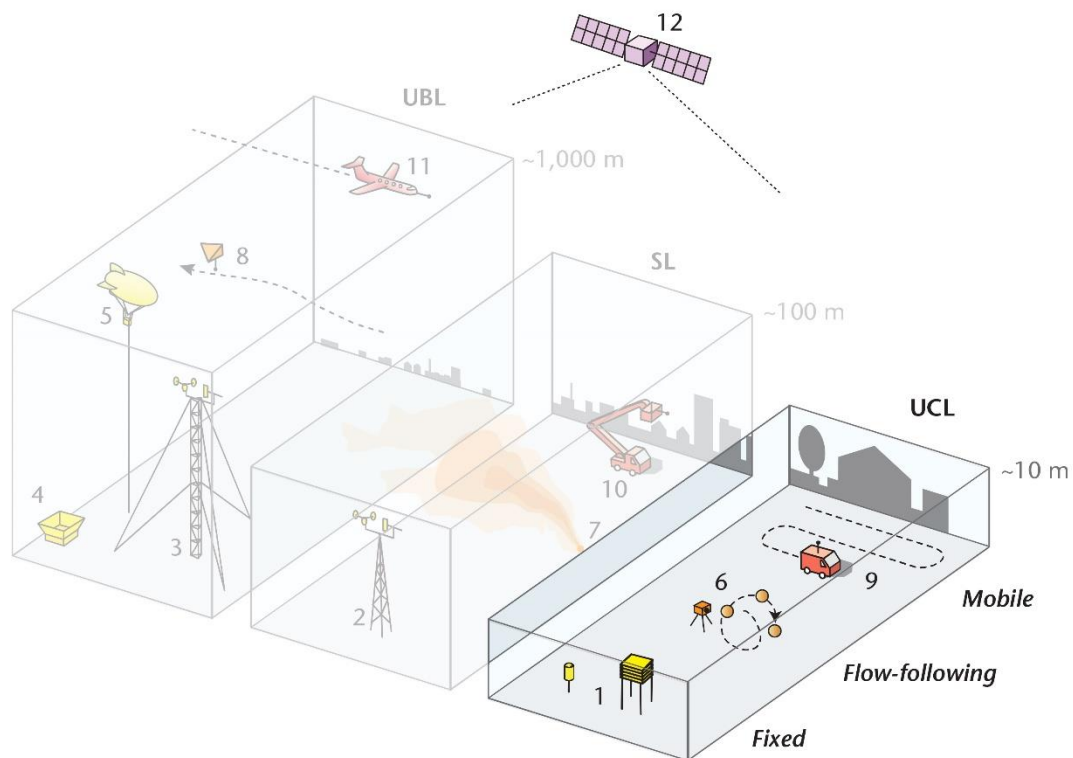
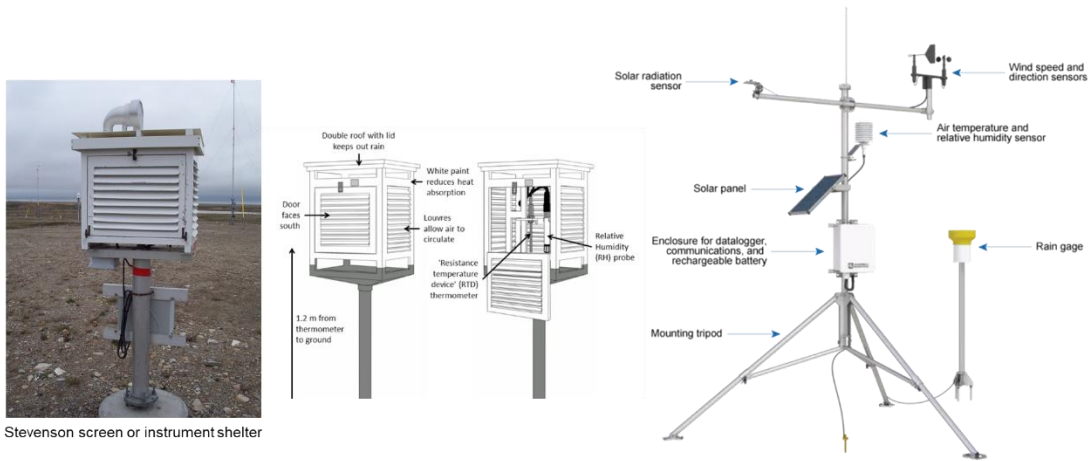


Figure 30. Conceptual diagram of ground-based, aerial and remote-sensing observational platforms, sorted by their suitability to sample the entire urban boundary layer (UBL, left), the surface layer (SL, center) or the urban canopy layer (UCL, right), and their sampling approach (upright side). Most importantly, within the UCL, fixed platforms (along the front) include a Stevenson (thermometer) Screen (1), and mobile/traversing approaches (along the back) include vehicles such as cars and cargo bikes (9). Satellite remote sensing can characterize the surface or atmosphere across a range of scales including the UCL (12). Readapted from (Oke et al., 2017, p. 53).

Measurements at fixed stations

On the one hand, measurements at fixed weather stations (Figure 31) are designed for long-term observations of climate properties such as air temperature, precipitation and wind. They usually exist within a wider network and are managed by official weather authorities in a city, region or country since they are relatively expensive and require site-specific requirements to be located correctly, and hence they have limited spatial coverage (Oke et al., 2017). However, with the advances in sensor technology and the *Internet of Things* (IoT)¹¹, it has become very popular to find fixed personal weather stations across many cities, which can complement official weather stations and provide better spatial coverage of climate data (Figure 32).

¹¹ “The term Internet of Things (IoT) is used as an umbrella that covers several topics, related to the application of technological means to monitor, measure and act upon the environment” (Di Martino et al., 2018, p. 99).



Stevenson screen or instrument shelter

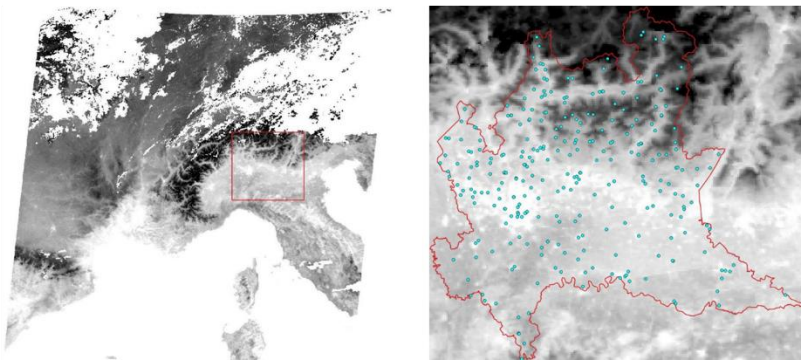


Figure 31. Examples of fixed weather stations (top) and a network of fixed weather stations in the Lombardy region, Italy (bottom).

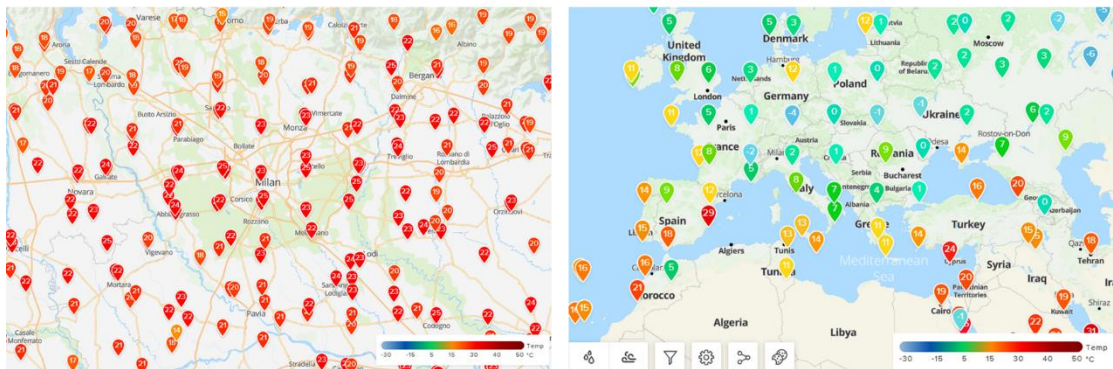


Figure 32. Example of a low-cost (around 190\$) personal weather station manufactured by Netatmo company.

Mobile measurements

On the other hand, mobile measurements are suitable for short-term measurements and can be used to complement observations from fixed weather stations or to observe places that are rarely explored or with spatial heterogeneity of climate properties such as air temperature (Oke et al., 2017). They are usually conducted under normal weather conditions and using sensors or instruments mounted on vehicles (e.g. cars, bicycles) or carried by humans to cross different microclimates (Figure 33). When instruments are carried by humans, they can take different forms as depicted in Figure 34 (e.g. wearable, portable, movable or semi-stationary to conduct *stop and go* campaigns).



Figure 33. Examples of mobile traverse systems that have been used in previous studies. (a) A mobile monitoring setup composed of a radiation shield containing a temperature sensor, a portable weather station and a video camera (Tsin et al., 2016); (b) A light-colored vehicle equipped with several sensors, a Global Positioning System (GPS) and a video camera (Shi et al., 2018); (c) A wearable monitoring system with several embedded sensors as well as a camera and a GPS (Pigliatile and Pisello, 2018); (d) A semi-stationary weather station composed of a portable weather station, rotating vane mount, tripod, and signboard (Kim and Macdonald, 2016); (e) A local transport bus in Aachen, Germany, equipped with a self-built measurement device consisting of a temperature sensor and a GPS (Buttstädt et al., 2011); (f) A bicycle equipped with a temperature sensor and a GPS (Yokoyama et al., 2018); (g) A bicycle equipped with different sensors of air pollutants (Samad and Vogt, 2020).

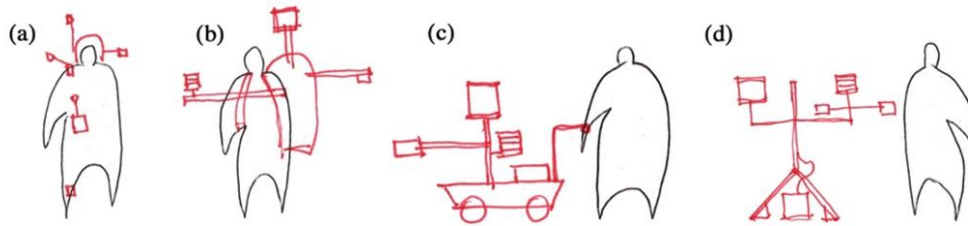


Figure 34. Representation of the instrumental configurations when instruments are carried by humans during mobile measurements. (a) Wearable instrument; (b) portable instrument; (c) Movable instrument; (d) Semi-stationary instrument. Reproduced from (Requena-Ruiz et al., 2019, p. 4).

Despite this variety of approaches and techniques for conducting field observations, it should be noted that whatever the approach or the technique used, one should make sure to (1) choose the appropriate instruments and sensors for the objectives of the study (e.g. thermometer for air temperature, anemometer for wind speed and vane for wind direction, hygrometer for humidity, rain gauge for rainfall); (2) know sensor properties (e.g. accuracy, resolution, response rate, logging frequency, memory size, battery capacity); (3) carefully position sensors in the field both vertically (e.g. air temperature is measured at around 1.5 m above ground and wind speed is measured at 10 m above ground) and horizontally (within a homogenous part of the landscape to avoid mixed signals in the surface area seen by the sensor, known as the *source area*); and (4) choose the appropriate time for the measurements depending on the purpose of the study (e.g. day, night, afternoon, summer, winter) as well as to ensure that measurements are taken during steady-state conditions so that they are not influenced by large-scale weather changes and can be attributed to the characteristics of the place (Oke et al., 2017).

4.1.2. Empirical modelling/generalization

Empirical modelling/generalization methods are used to determine meteorological/climatological parameters (dependent variables) such as air temperature based on their pre-established statistical relationship (usually using regression models) with other climatological, geographical or landscape parameters, such as vegetation or surface temperature (independent/explanatory variables). Therefore, these methods require pre-existing observational data of both the dependent and independent variables (e.g. obtained from field observations or numerical modelling) to fit regression models and predict the dependent variable elsewhere.

Although empirical methods are relatively cost-efficient, less complicated to apply, compared to, e.g. numerical methods, and provide a useful summary of climatological relationships that are often quite complex (Hjort et al., 2011; Shahraiyni and Sodoudi, 2017), they (1) require a large amount of data to train algorithms; (2) have little diagnostic insight (i.e. only descriptive) because “they are restricted by the information upon which they are based” (Oke et al., 2017, p. 74); and (3) have little transferability to other locations, where their application should be limited to conditions similar to those under which the statistical relationship was established (Oke et al., 2017).

There are great many regression models that can be used to model climatological parameters such as air temperature, and which can be linear (simple or multiple) regression models (e.g. Fung et al., 2009; Guo et al., 2020; Kawashima et al., 2000; Nichol et al., 2009; Vogt et al., 1997) or non-linear models. In general, using global linear regression models (i.e. a single linear regression equation) to predict non-stationary data (e.g. climate data) at high spatial and temporal resolution can produce a high level of error (Shahraiyini and Sodoudi, 2017), and hence geographically weighted regression (GWR) models and/or non-linear models are favored for this purpose. GWR models are extensions of linear regression models that allow for the analysis to vary over space (Fotheringham et al., 1998), and have been used in previous studies (e.g. Colaninno and Morello, 2019; Eldesoky et al., 2020; Zhou et al., 2019). On the other hand, several non-linear regression models can be used to model climatological parameters such as the support vector regression (SVR) (Bruzzone and Melgani, 2005; Camps-Valls et al., 2006; Durbha et al., 2007; Ho et al., 2014; Shahraiyini et al., 2012); the adaptive network-based fuzzy inference system (Jang, 1993; Taheri Shahraiyini et al., 2015); the multivariate adaptive regression splines (MARS) (Friedman, 1991; Shahraiyini et al., 2015); and the random forest (RF) regression (e.g. Ho et al., 2014; Pan et al., 2018; Shandas et al., 2019; Voelkel et al., 2016).

In Chapter 5, a combination of field observations (using mobile measurements) and empirical modelling (using RF regression) will be used for describing the impact of urban form on urban temperatures in Sixth of October desert city, Egypt.

4.2 Typomorphological methods

This section discusses the second group of quantitative methods for studying the impact of urban form on urban climate and, in turn, on people's health and thermal sensation, namely the typomorphological methods. Unlike the climatological-environmental-based methods that were coined in the previous section as *descriptive* methods (i.e. emphasizing *what is* the problem and providing relevant empirical information on it), typomorphological methods are coined here as *analytical* (explanatory) methods. This is because they explain the causes (by describing the urban form characteristics) responsible for this problem (i.e. emphasizing the *why* and/or the *how*). Furthermore, typomorphological methods were regarded in Chapter 2 as normative/prescriptive methods (i.e. emphasizing *what should be*) because types within typomorphologies perform and function in specific ways due to their similar characteristics, and thereby they are central to informing urban planning and design decisions.

In the next sections, we will, first, give an overview of typomorphological research within urban climatology (Section 4.2.1) and, then, introduce the most developed typomorphological classification in urban climatology, namely the local climate zone (LCZ) classification scheme (Stewart and Oke, 2012) from which this thesis departs and aims to add to (Section 4.2.2).

4.2.1. Typomorphological research within urban climatology

Within urban climatology, typomorphological research has been growing in response to the need for (1) a common language between climatology and other related fields, such as urban planning and design, that conveys urban climate principles “through spatial scales (micro, local) and design elements (e.g. building height, “green” cover ratio)” (Stewart and Oke, 2012, p. 1894); (2) better characterizing the effect of urban form on micro- and local climates rather than the simple urban-rural classifications typically used in urban heat island (UHI) studies (Stewart and Oke, 2012).

As a result, several typomorphological classifications (also known as typologies of urban surface properties) have been developed to describe, in an integrative way, the urban form characteristics that can exacerbate heat stress and influence people’s health and thermal sensation (i.e. the environmental/engineering dimension of heat-stress resilience). These urban form characteristics include for instance: the shape, dimensions (e.g. height, width and length), spacing and arrangement of urban elements (e.g. buildings, streets); construction materials and their thermal, roughness, radiative and moisture properties; and land cover types (e.g. vegetation, bare rock, sand) and their properties (e.g. dry or wet ground) (Fahed et al., 2020; Martins et al., 2016; Salata et al., 2017; Shareef and Abu-Hijleh, 2020).

Examples of such typomorphological classification, which are synthetically reviewed in (Stewart, 2011; Stewart and Oke, 2012), include:

- The early classification of London’s climate regions developed by Chandler’s (1965) (Figure 35);
- Auer’s meteorologically-oriented land use/land cover (LULC) classification of the Metropolitan St. Louis area (1978) (Figure 36);
- The *climatope* (i.e. local areas with distinct climates) maps of Hannover (Wilmers, 1990) and Basel (Scherer et al., 1999);
- The urban terrain zones (UTZs) developed by Ellefsen (1991) for several U.S cities (Figure 37); and
- The urban climate zones (UCZs) generic classification scheme designed by Oke (2004) (Figure 38).

What is common among these classifications is that they include different urban form characteristics (e.g. building dimensions and construction materials properties) to distinguish between various zones within the city in terms of their micro- or local climate.

Most recently, Stewart (2011) and Stewart and Oke (2012) developed the so-called LCZ classification scheme to overcome the shortcomings of the previous classifications in terms of description and communication. Namely, it has become popular among architects, urban designers, urban planners, ecologists and engineers, contributing remarkably to the advancement of urban heat studies, and is discussed in more detail in the next section.

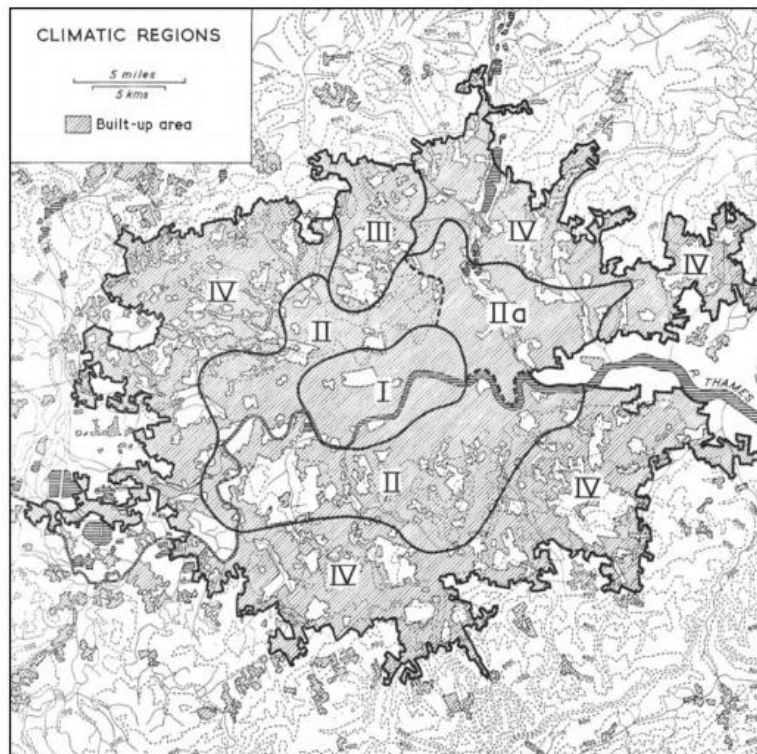


Figure 35. Chandler's classification of local climate regions in London (I = Central; II = Inner suburban; III = Outer suburban; IV = Northern heights). Reproduced from (Chandler, 1965, p. 243).

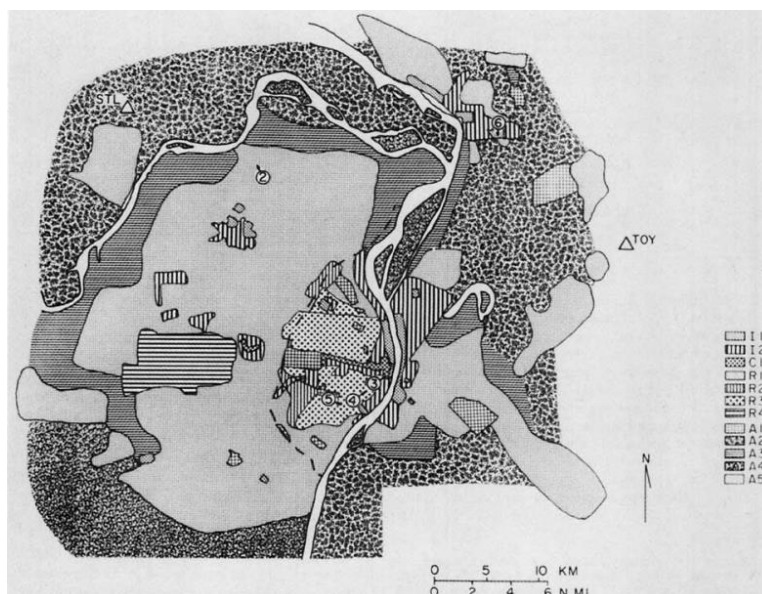


Figure 36. Auer's meteorologically-oriented LULC classification of the Metropolitan St. Louis area (I1 = Heavy industrial; I2 = Light moderate industrial; C1 = Commercial; R1 = Common residential; R2 = Compact residential (single-family dwellings); R3 = Compact residential (multi-family dwellings); R4 = Estate residential; A1 = Metropolitan natural; A2 = Agricultural rural; A3 = Undeveloped; A4 = Undeveloped rural; A5 = Water surfaces). Reproduce from (Auer, 1978, p. 637).

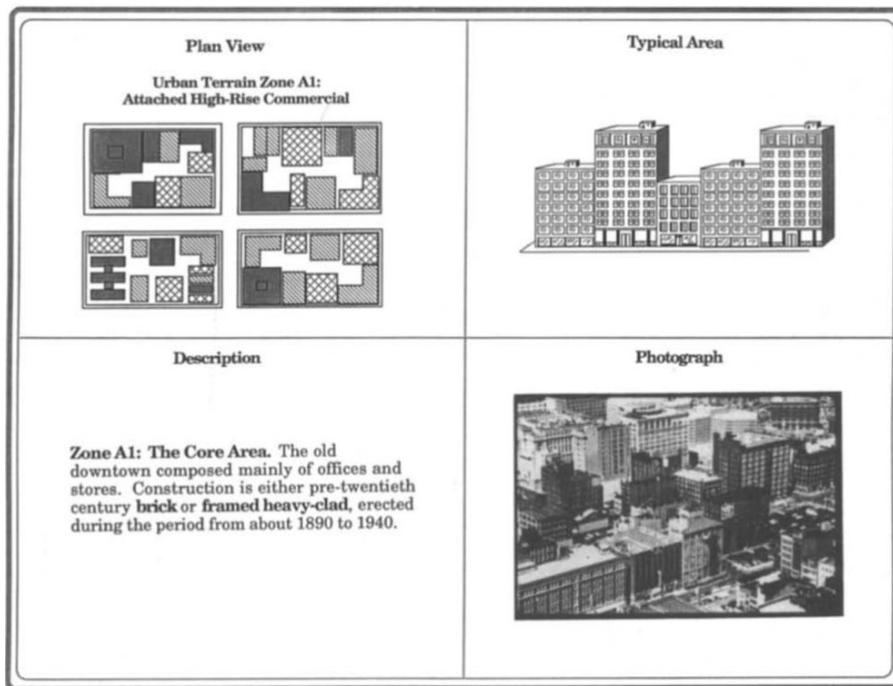


Figure 37. The distinctive features of Ellefsen's UTZ type A1 (the core area). Reproduced from (Ellefsen, 1991, p. 1041).

Urban Climate Zone, UCZ ¹	Image	Roughness class ²	Aspect ratio ³	% Built (impermeable) ⁴
1. Intensely developed urban with detached close-set high-rise buildings with cladding, e.g. downtown towers		8	> 2	> 90
2. Intensely developed high density urban with 2 – 5 storey, attached or very close-set buildings often of brick or stone, e.g. old city core		7	1.0 – 2.5	> 85
3. Highly developed, medium density urban with row or detached but close-set houses, stores & apartments e.g. urban housing		7	0.5 – 1.5	70 - 85
4. Highly developed, low or medium density urban with large low buildings & paved parking, e.g. shopping mall, warehouses		5	0.05 – 0.2	70 - 95
5. Medium development, low density suburban with 1 or 2 storey houses, e.g. suburban housing		6	0.2 – 0.6, up to >1 with trees	35 - 65
6. Mixed use with large buildings in open landscape, e.g. institutions such as hospital, university, airport		5	0.1 – 0.5, depends on trees	< 40
7. Semi-rural development, scattered houses in natural or agricultural area, e.g. farms, estates		4	> 0.05, depends on trees	< 10

Key to image symbols: buildings; vegetation; impervious ground; pervious ground

Figure 38. Oke's UCZ classification scheme. Reproduced from (Oke, 2004, p. 11).

4.2.2. The local climate zone (LCZ) classification scheme for urban temperature studies

As anticipated in the previous section, the LCZ classification scheme was developed by Stewart (2011) and Stewart and Oke (2012) to overcome the shortcomings of the earlier typomorphological classifications in terms of description and communication. In particular, the aforementioned typomorphological classifications have the following limitations:

- Climatic relevance: not all classifications use a full set of the urban form characteristics that influence urban micro- and local climate.
- Urban and rural representation: some of the classifications do not include rural types, which makes them not suitable for UHI investigations, where the most common approach to establish an experimental control and isolate the urban climate effects is to calculate the urban-rural temperature difference.
- Nomenclature: most type names include terms that can vary with culture, time and location, which make them open to misinterpretation. In other words, there is no standardization and consistency in naming and describing types in a simple and logical way, which is crucial to the validity and acceptance of a classification system (Grigg, 1965).
- Origin and scope: most of the classifications have limited transferability and function poorly outside the contexts in which they were developed (i.e. they are locationally specific).
- Quantification: most of the classifications do not provide quantifications of the urban form characteristics that influence urban micro- and local climate.

Taking into account these limitations and several other criteria (see Stewart, 2011, sec. 5.1.1.2), the LCZ classification scheme was developed as an organized system of 17 generic, logical and comprehensible types (ten built and seven land cover) at the local/neighborhood scale, where each type is distinguished based on buildings' geometric characteristics (e.g. heights, spacings), construction materials properties, land cover (e.g. vegetation) and land use (human activity). Based on these characteristics, each LCZ type describes specific local climate conditions, and hence the LCZ classification scheme is very relevant to various urban practices.

These 17 types were derived by *logical division*, i.e. starting with a *universe* type, which is then divided into subtypes based on certain differentiating factors, namely the aforementioned urban form characteristics that influence urban micro- and local climate. This classification process has initially resulted in 26 hypothetical types (Figure 39) that were reduced to the final 17 after excluding some types that are difficult to find in real-world (e.g. compact buildings on pervious cover such as grass) or that are unlogical (e.g. dense trees on impervious cover such as asphalt), and including other relevant ones.

The resulting types were coined as LCZs because they are “local in scale, climatic in nature, and zonal in representation” (Stewart and Oke, 2012, p. 1884), where each LCZ type was assigned a simple, concise name (Figure 40) and its characteristics were quantified based on the literature and by conducting several field visits in different cities across the world. A full and detailed description of each of the 17 LCZ types and their quantifiable characteristics can be found in (Stewart, 2011, sec. 5.2.1; Stewart and Oke, 2012, pp. 1885–1887).

Furthermore, the extent to which each of these LCZ types exhibits significantly different thermal characteristics was confirmed in several studies using observational (e.g. from fixed and mobile measurements) and modelled (e.g. numerical and empirical) air temperature data (see, e.g. Alexander and Mills, 2014; C. Beck et al., 2018; Fenner et al., 2017; Kwok et al., 2019; Richard et al., 2018; Stewart et al., 2014), as well as using land surface temperature (LST) data, e.g. from satellites (see, e.g. Bartesaghi Koc et al., 2018; Budhiraja et al., 2017; Cai et al., 2018; Geletič et al., 2019, 2016; Gémes et al., 2016; Lin and Xu, 2016; Nassar et al., 2016; Ochola et al., 2020; Shih, 2017; C. Wang et al., 2018; Wang et al., 2017; Zhao, 2018).

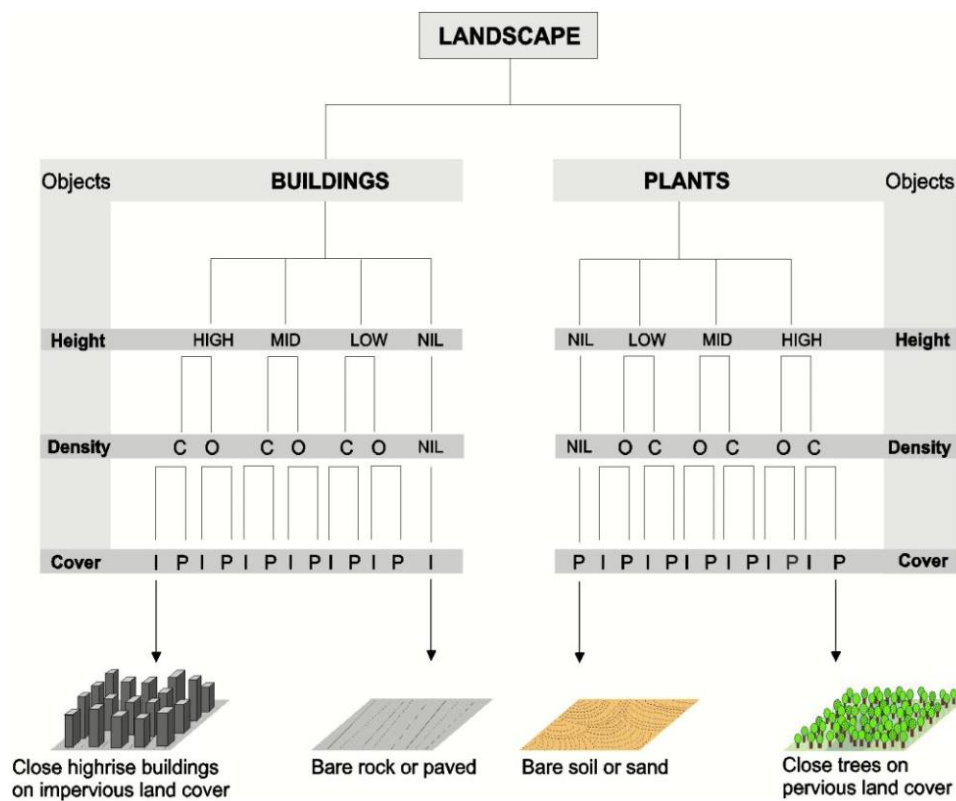


Figure 39. Logical division of the universe type by roughness objects (buildings, plants), object height (high, mid, low, nil), object density (O = open; C = close) and land cover (I = impervious; P = pervious). Sample derivative types are shown at the bottom. The close high-rise type (bottom left) derives from landscape division into buildings of maximum height and density, and surrounding surfaces of impervious cover. Reproduced from (Stewart, 2011, p. 163).

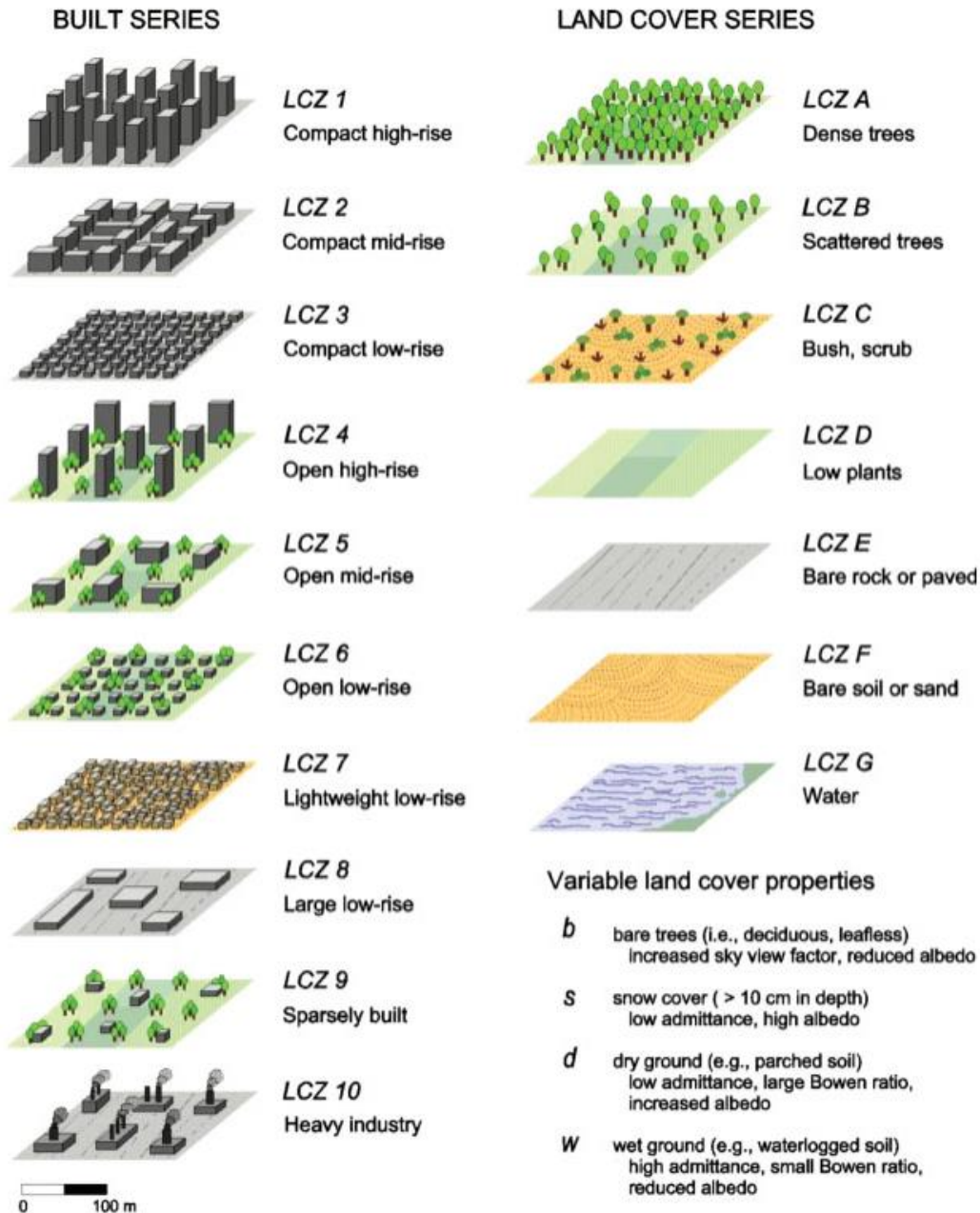


Figure 40. The LCZ classification scheme. Reproduced from (Stewart, 2011, p. 196).

Based on the above, the LCZ classification scheme has been widely used in various urban temperature studies for different applications and several methods have been proposed to better apply the concept and map entire cities into LCZs (an overview of these methods will be given in Chapter 6). Examples of these applications include: UHI assessment, where the UHI magnitude is calculated as a temperature difference between a certain LCZ type and LCZ D (low plants), and not as an urban-rural difference (Leconte et al., 2015; Siu and Hart, 2013); evaluating outdoor thermal sensation conditions (Das et al., 2020; Lau et al., 2019); and studying heat-related health issues (Brousse et al., 2019).

Nevertheless, the LCZ classification scheme has been also used for other applications, for example, to assess: building anthropogenic heat (Santos et al., 2020); building energy demand and consumption (Benjamin et al., 2021; Kotharkar et al., 2022; Yang et al., 2020); carbon emissions (Wu et al., 2018); urban ventilation (Shi et al., 2022; Zhao et al., 2020); air quality (Lu et al., 2021; Steeneveld et al., 2018); and urban vegetation phenology (Kabano et al., 2021).

In the next chapters, both the climatological-/environmental-based methods (specifically field observations and empirical modelling) and typomorphological methods (specifically using the LCZ classification scheme) will be examined in the context of the case study to (1) improve their outputs in terms of scale (i.e. spatial resolution and extent) and accuracy, and hence better support urban planning and design decisions; (2) to better understand their applicability in contemporary cities in arid areas (on which little research has been conducted), thus better supporting the development and implementation of their heat-resilience plans.

Chapter 5

Combining field observations and empirical modelling for describing the impact of urban form on urban temperatures in Sixth of October, Egypt¹²

In this chapter, the descriptive climatological-/environmental-based methods that can be used for studying, or more precisely describing, the impact of urban form on urban temperatures, and hence the possibility for assessing urban form-related risk to people's health and thermal sensation (i.e. the environmental/engineering dimension of heat-stress resilience), are investigated in the context of the case study (i.e. Sixth of October new desert city, Egypt). Specifically, the effectiveness of combining field observations and empirical modelling, to provide urban micro- and local climate substantive descriptive information (i.e. air temperature maps) at high spatial resolution (30 m) in such a data-scarce, arid area, is explored and assessed. The resulting maps are used to describe the spatial patterns of air temperature across the city, thus providing empirical evidence on the impact of urban form on air temperatures. The data and maps produced in this chapter are made open access¹³ for public, non-commercial use, and will be further used in the next chapters.

The chapter is organized as follows: firstly, the challenges in mapping air temperature at high spatial resolution in urban areas are discussed in Section 5.1; then, the data and methods utilized for modelling air temperature in the study area are presented in Section 5.2; Section 5.3 presents the resulting air temperature maps and describes the impact of urban form on the spatial variability of air temperature in Sixth of October; and finally, Section 5.4 discusses the scope and role of the resulting air temperature maps, as well as the limitations of the method and possible future improvements.

5.1 Challenges of high-resolution air temperature mapping in urban areas

With heatwaves becoming more severe and frequent across many parts of the world (Perkins-Kirkpatrick and Lewis, 2020), the interest in better understanding the urban micro- and local climate phenomena has been growing both in research and practice of urban planning and design. Furthermore, air temperature, measured at screen-level height (~ 1.5 m above ground), is an important variable for many fields such as climatology, ecology, hydrology and epidemiology (Bunker et al., 2016; Ho et al., 2014; Shahraini and Sodoudi, 2017). However, as discussed in the previous chapter, monitoring air temperature in the urban canopy layer (UCL, beneath the roof level) has

¹² A version of this chapter has been peer-reviewed and published: **Eldesoky, A.H.**, Colaninno, N., Morello, E., 2021. High-resolution air temperature mapping in a data-scarce, arid area by means of low-cost mobile measurements and machine learning. *J Phys Conf Ser* 2042, 012045. <https://doi.org/10.1088/1742-6596/2042/1/012045>

¹³ Available at <https://doi.org/10.6084/m9.figshare.17049053.v2>

been always limited by the availability and spatial coverage of air temperature data from fixed weather stations (Cai et al., 2018; Hooker et al., 2018). And setting up a meteorological network of fixed weather stations can be expensive or not possible in some locations (Oke et al., 2017). This is the case of Sixth of October, Egypt, where none of the national meteorological weather stations is located in the vicinity. Alternatively, we pointed out in Chapter 4 that mobile measurements, using instruments mounted on vehicles (e.g. cars, bicycles) or carried by humans, can be used to complement observations from fixed weather stations or to observe places that are rarely explored or with spatial heterogeneity of air temperature (Oke et al., 2017) and have been used in many studies (Alonso and Renard, 2020; Cassano, 2014; Leconte et al., 2015; Rajkovich and Larsen, 2016; Shandas et al., 2019; Shi et al., 2018; Tsin et al., 2016; Voelkel et al., 2016; Voelkel and Shandas, 2017).

Nevertheless, air temperature data obtained either from fixed weather stations or using mobile measurements are collected as point samples and cannot continuously describe the spatial variability of air temperature. Hence, providing gridded air temperature data at high spatial resolution has become of great importance and different modelling approaches have been used for this purpose such as interpolation, regression and simulation (Shahraiyni and Sodoudi, 2017) (Figure 41).

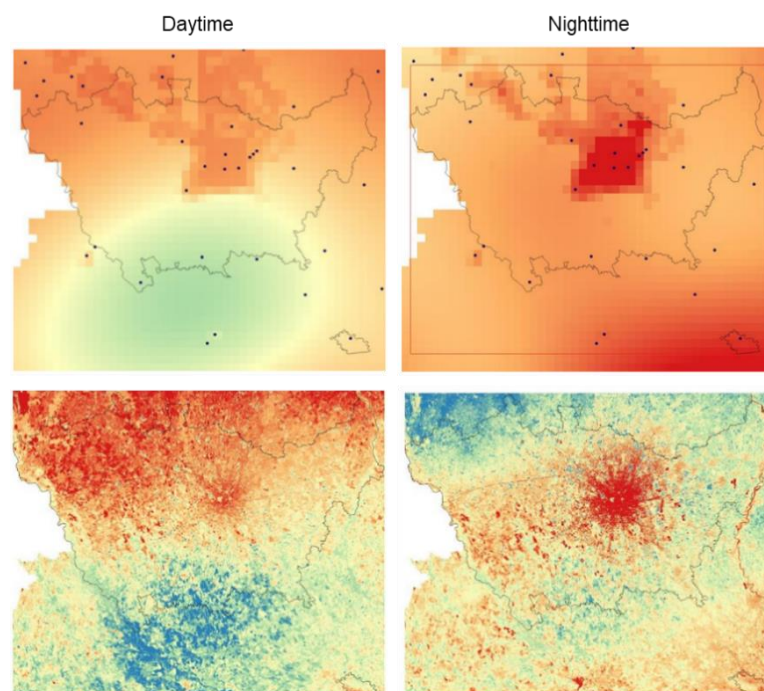


Figure 41. Interpolation of air temperature at 1500-m spatial resolution for the metropolitan city of Milan (Italy) implemented by *Agenzie Regionali per la Protezione dell’Ambiente (ARPA)*¹⁴ (top); and Geographically Weighted Regression (GWR) modelling of air temperature at 30-m spatial resolution by *Laboratorio di Simulazione Urbana Fausto Curti*¹⁵ (bottom).

¹⁴ https://www.arpalombardia.it/Pages/ARPA_Home_Page.aspx

¹⁵ <http://www.labsimurb.polimi.it/>

In particular, the random forest (RF) regression—a non-parametric machine learning model—is among the most recently investigated regression modelling techniques that have proven high predictive performance in many studies when using mobile measurements (Alonso and Renard, 2020; Shandas et al., 2019; Voelkel et al., 2016; Voelkel and Shandas, 2017). Therefore, in this chapter, we will explore the effectiveness of the RF regression in modelling air temperature in the study area, using sample air temperature data, collected from low-cost mobile measurement campaigns (as dependent variable), and multiple spectral indices, derived from freely-available satellite imagery (as explanatory variables). The end aim, as discussed earlier, is to provide and make publicly available gridded air temperature data at high spatial resolution for a data-scarce area where, to our knowledge, no such data are available, thus providing empirical evidence on the impact of urban form on air temperature.

5.2 Data and methods

Three main steps were required to map air temperature at high spatial resolution. Firstly, mobile air temperature data were collected and processed. Secondly, satellite data were acquired and multi-spectral, multi-scalar indices were derived. Finally, RF regression models were fitted and used to produce air temperature maps at high spatial resolution. Figure 42 shows an overview of the air temperature modelling procedure and Sections 5.2.1, 5.2.2 and 5.2.3 explain the aforementioned steps in more detail.

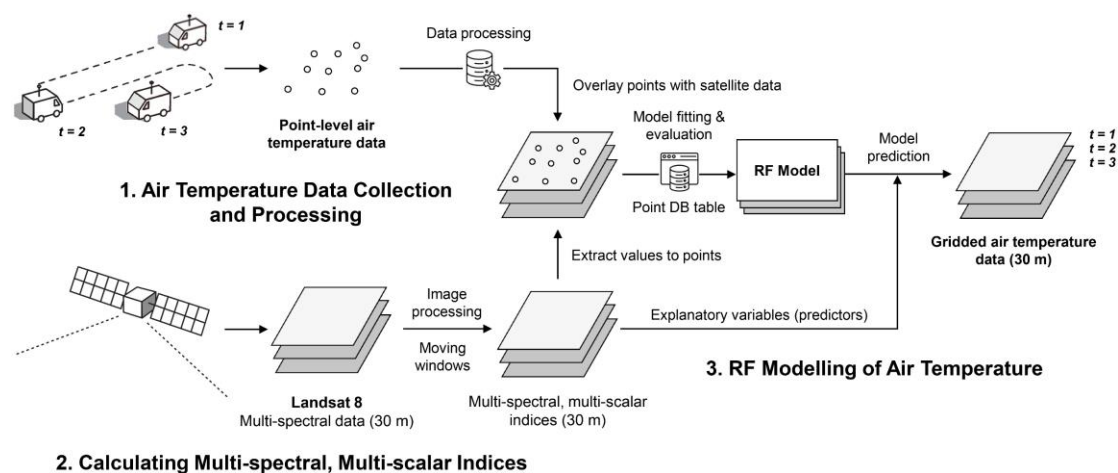


Figure 42. Schematic overview of the air temperature modelling procedure.

5.2.1. Mobile air temperature data collection and processing

In this study, a total of four automobile-based measurement campaigns were carried out on September 2nd, 29th and 30th, 2020 under suitable meteorological conditions of low nebulosity and low wind speed (below 9 m/s at 10-m height). The measurement campaigns were conducted using a relatively low-cost (~ \$400) portable, wireless weather station with Global Positioning System (GPS), manufactured by PASCO (PS-3209) (Figure 43), to measure the ambient air temperature at a one-second interval along a predefined route that crosses different land uses/covers (LULCs) and morphologically different built-up areas (Figure 44). Each measurement campaign was completed

between two and three hours to minimize any changes in the background climate conditions during the campaign time (Leconte et al., 2015; Shi et al., 2018). In particular, the temperature sensor has an accuracy of ± 0.2 °C and 0.1 °C resolution and it was mounted, at a screen-level height, on top of a car and shaded by a cardboard sheet. The car moved at an average speed of 20 to 30 km/h (minimum 15 km/h and maximum 60 km/h) which was sufficient to (1) ensure adequate ventilation for the sensor to rapidly adjust to local temperature changes (Cassano, 2014; Unger et al., 2001); (2) minimize any radiation-induced errors (Cassano, 2014); and (3) reduce the influence of vehicular anthropogenic heat (Leconte et al., 2015; Shi et al., 2018).

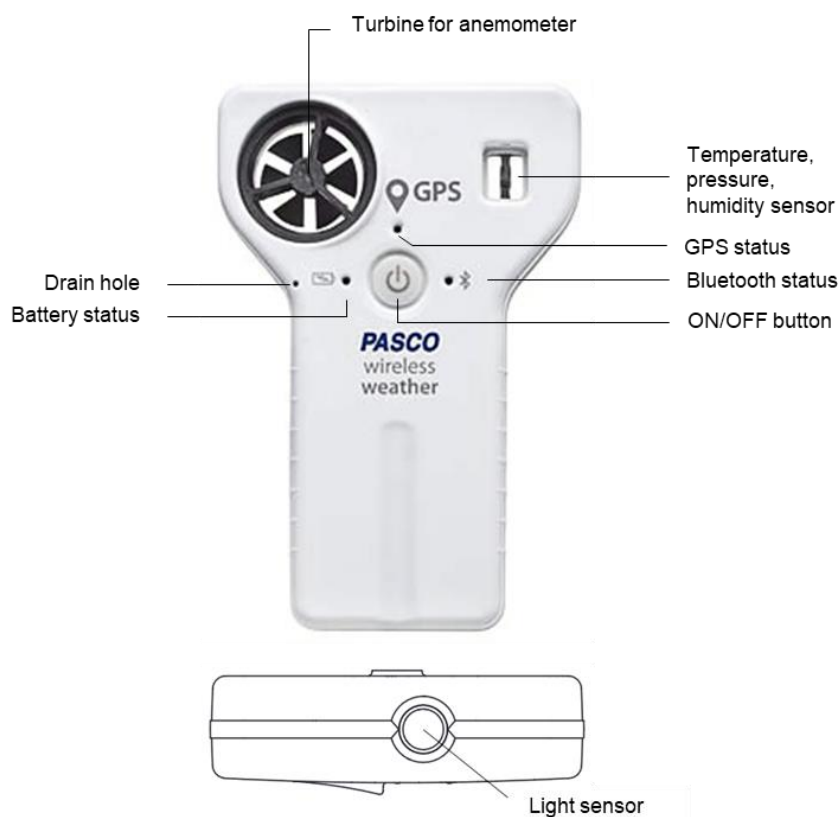


Figure 43. The Pasco portable weather station used to collect air temperature data during the four measurement campaigns.

Further, in order to remove any confounding effects in the collected temperature data, three processing steps were applied as recommended by Oke et al. (2017). This included, firstly, correcting for the local temperature changes that occurred during the time of the campaign. This was done by returning to the measurement starting point and calculating an average cooling/warming rate to adjust all the temperature records to the reference start time. Secondly, removing the effect of altitude changes by applying an average lapse rate of 0.64 K per 100 m (Oke et al., 2017). Thirdly, excluding measurements recorded when the car speed was very low/high (below 15 km/h and above 60 km/h). Table 9 shows the summary of the air temperature data for each measurement campaign after applying all the aforementioned steps.



Figure 44. The morphologically different built-up areas crossed during the four automobile-based measurement campaigns on September 2nd, 29th and 30th, 2020.

Table 9. Summary of the processed air temperature data.

Run no.	Date	Reference start time (HH:MM)	Descriptive statistics (°C)			
			Mean	Std.Dev.	Min.	Max.
1	2 September 2020	19:00 LT	31.36	0.45	30.35	32.60
2	29 September 2020	14:30 LT	36.01	0.50	34.59	37.92
3	30 September 2020	13:30 LT	35.34	0.62	32.88	37.68
4	30 September 2020	19:30 LT	29.35	0.38	28.49	30.53

Finally, all the processed air temperature data were exported to Geographical Information Systems (GIS), using the location information collected by the GPS sensor, and assigned a projection (Figure 45).

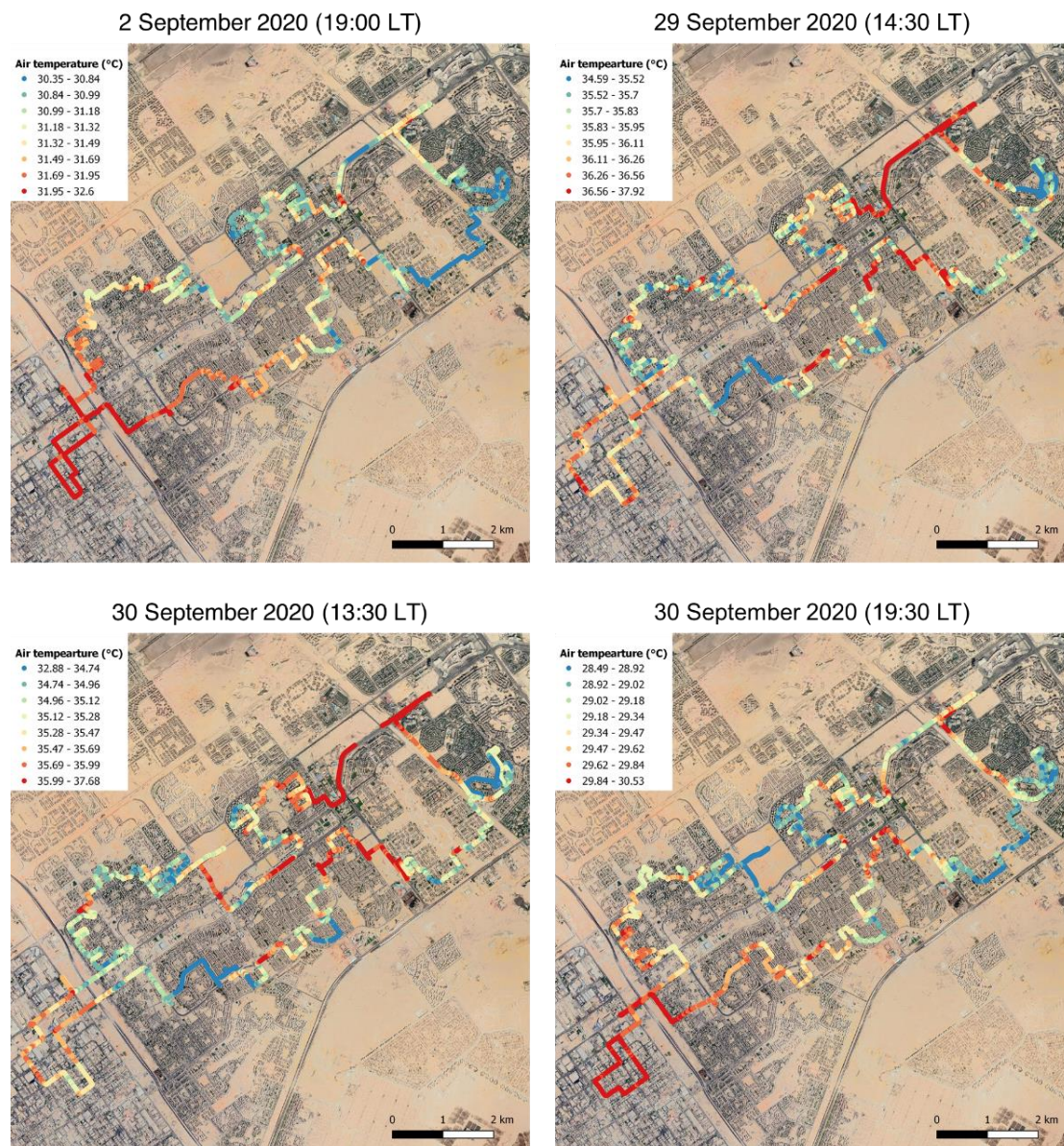


Figure 45. Geolocating the processed air temperature mobile measurements for each of the measurement campaigns using the latitude and longitude coordinates collected by the GPS sensor.

5.2.2. Calculating multi-spectral, multi-scalar remote sensing indices

Modelling air temperature employing regression approaches requires using one or more variables as predictors (explanatory variables). However, there are many factors that influence air temperature (e.g. LULC, land surface temperature (LST), anthropogenic heat, solar radiation, altitude) (Ho et al., 2014; Shahraiyini and Sodoudi, 2017). In this regard, remotely-sensed data (e.g. from satellites) can provide information on many of the surface properties that influence air temperature (Ho et al., 2014). For instance, several studies have statistically modelled air temperature based on satellite-derived LST and other spectral indices that distinguish LULC types such as the vegetation indices (Cristóbal et al., 2008; e.g. Ho et al., 2014).

Here, we used spectral indices, derived from Landsat 8 imagery, to model air temperature based on LULC characteristics. Landsat 8 carries two sensors, namely the Operational Land Imager (OLI) and the Thermal Infrared Sensor (TIR), which provide eight spectral bands at 30-m spatial resolution, one panchromatic band (15 m) and two thermal bands (collected at 100 m and resampled at 30 m) (USGS, 2015). For this study, a Landsat 8 level-1 image of the study area, acquired on September 14, 2020, was freely downloaded from the United States Geological Survey (USGS) and atmospherically corrected (Figure 46).

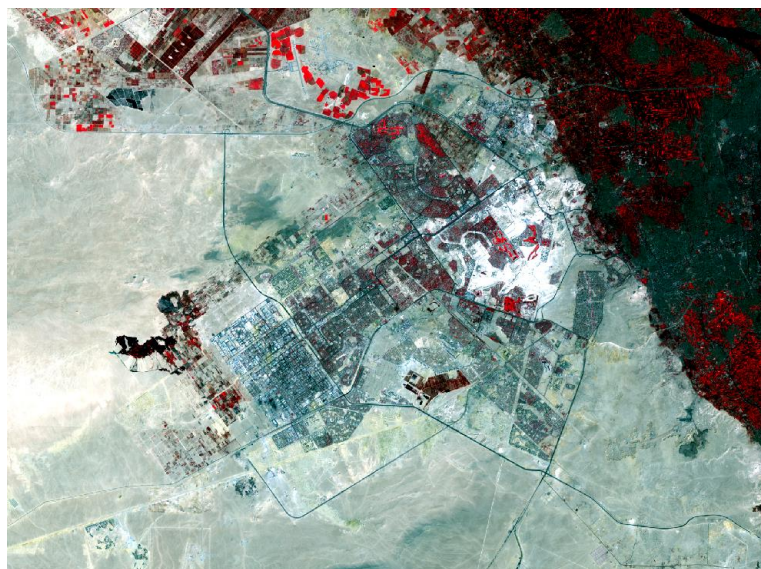


Figure 46. A multi-spectral image at 30-m spatial resolution for the study area (Sixth of October, Egypt) acquired from Landsat 8 on September 14, 2020.

In particular, three spectral indices, that distinguish LULC types in arid areas (e.g. vegetation cover, impervious surfaces and sandy desert) were derived (Pan et al., 2018; Yang et al., 2017). These are the Soil Adjusted Vegetation Index (SAVI) (Huete, 1988), the Normalized Difference Built-up Index (NDBI) (Zha et al., 2003) and the Normalized Difference Sand Index (NDSI) (Pan et al., 2018).

More specifically, SAVI is a measure of vegetation density, and it is used in areas where vegetation cover is low (e.g. arid areas) to correct for the soil brightness. SAVI is defined as:

$$SAVI = \left(\frac{B_5 - B_4}{B_5 + B_4 + L} \right) \times (1 + L) \quad (1)$$

where B_5 is the near-infrared (NIR) band, B_4 is the visible red band and L is a soil brightness correction factor ($L = 0.5$). On the other hand, NDBI is used to characterize built-up areas and bare soil, which reflect more shortwave infrared (SWIR) than NIR, and is defined as:

$$NDBI = \left(\frac{B_6 - B_5}{B_6 + B_5} \right) \quad (2)$$

where B_6 is the SWIR 1 band (1.57-1.65 μm) and B_5 is the NIR band. Furthermore, to better distinguish between the sandy desert and the built-up areas or bare soil, Pan et al. (2018) have proposed the NDSI based on Landsat 8 spectral bands 1 and 4. NDSI is defined as:

$$NDSI = \left(\frac{B_4 - B_1}{B_4 + B_1} \right) \quad (3)$$

where B_4 is the visible red band and B_1 is the coastal aerosol band (0.43-0.45 μm).

Nevertheless, air temperature can be influenced by LULC characteristics at multiple scales (varying radii) (Shandas et al., 2019; Voelkel et al., 2016). To account for this spatial dependence in the regression models, several studies have further applied focal operations (also called neighborhood operations) to the spectral indices using a moving window approach with different radii (Alonso and Renard, 2020; e.g. Ho et al., 2014; Shandas et al., 2019; Voelkel et al., 2016; Voelkel and Shandas, 2017). This creates a new dataset of the spectral indices where the value of each pixel is a function of the values of all the neighboring pixels within a specific radius (e.g. mean, minimum, maximum, median). One approach to identify the most appropriate spatial scales (radii) is to calculate the correlation coefficient between each predictor (calculated at each potential spatial scale) and air temperature and select the scale with the highest correlation coefficient or lowest Akaike information criterion (AIC) (Alonso and Renard, 2020; Bradter et al., 2013). Alternatively, one can use multi-spectral, multi-scalar indices, where each spectral index is calculated at multiple meaningful scales (Ho et al., 2014; Shandas et al., 2019; Voelkel and Shandas, 2017).

In this study, we calculated each of the three derived spectral indices at multiple spatial scales using a moving average algorithm. More specifically, we used 15 potential radii that range from 50 to 1000 m as proposed by Voelkel and Shandas (2017) and Shandas et al. (2019), and hence a total of 45 predictors were used in modelling air temperature.

5.2.3. Empirical modelling of air temperature

RF is a non-parametric machine learning algorithm that uses ensemble learning for both classification and regression tasks and has a nonlinear nature (Breiman, 2001). It operates by constructing n_{tree} decision trees using n_{tree} bootstrap samples of the dataset with replacement and m_{try} random subset of candidate variables (predictors) at each node.

Each new data point can be predicted by running it down through each of the n_{tree} decision trees and averaging all the predicted values from all trees (in case of regression) or taking the majority of votes (in case of classification).

To fit RF regression models and predict air temperature, the processed air temperature data points from each measurement campaign (Section 5.2.1) were overlaid with the multi-spectral, multi-scalar indices (Section 5.2.2), and each point was assigned the value of the pixels that it overlays. The result is four tables, each with 46 columns (the measured air temperature and 45 predictors) and a number of rows equaling the number of observations made in each measurement campaign. The tables were used as input in the `randomForest` function (Liaw and Wiener, 2002) in R (Team, 2019) to fit RF models using the default number of trees (n_{tree}) and variables (m_{try}), i.e., 500 and 15 (the total number of variables divided by three), respectively.

The RF models were then evaluated using the out-of-bag (OOB) dataset, i.e. the data that were not included in the bootstrap samples (around one-third), and two measures for goodness of fit were calculated, namely the coefficient of determination (R^2) and the Root Mean Square Error (RMSE). Finally, the obtained RF models were used to predict an air temperature value for each location that was not visited by the vehicle, based on the values of the multi-spectral, multi-scalar indices, and air temperature maps (at 30-m spatial resolution) were produced for the entire city.

5.3 Results of the empirical models and the spatial patterns of air temperature

All four models showed high performance with R^2 more than 0.87 and RMSE below 0.18 °C (Table 10). More specifically, the nighttime models outperform the afternoon ones which is in agreement with previous studies that recommended including other predictors (e.g. building heights) for better modelling air temperature during the afternoon time (Shandas et al., 2019; Voelkel and Shandas, 2017).

Table 10. Summary of the RF model results.

Run no.	Date	Reference start time (HH:MM)	Model goodness of fit	
			R^2	RMSE (°C)
1	2 September 2020	19:00 LT	0.96	0.09
2	29 September 2020	14:30 LT	0.87	0.18
3	30 September 2020	13:30 LT	0.92	0.18
4	30 September 2020	19:30 LT	0.93	0.10

Figures 47–50 show the resulting maps at 30-m spatial resolution, where the impact of LULC, as well as other urban form characteristics such as building density and green cover ratio, is apparent on the spatial variability of air temperature. From these maps, one can observe the following:

- There is a consistency in the diurnal and nocturnal spatial patterns of air temperature for the different days and times modelled, where the isotherm lines

correspond with the built-up outline and the degree and type of the urban development (Figures 47 and 48).

- In general, during the nighttime, there is a difference of about 1.7 to 2 °C between the maximum and minimum modelled air temperature compared to a difference of about 3 to 4 °C during the daytime (Figures 47 and 48).
- The extensive industrial area located in the southwest of the city (Figures 47 and 48) exhibits higher daytime and nighttime air temperatures compared to the surrounding areas due to the extensive impervious cover, low-albedo construction materials and anthropogenic heat from industrial activity.
- The latter is also the case in the commercial areas such as large shopping centers that are commonly found in new desert cities in Egypt (see area a, Figure 49). These areas do not only exhibit relatively high air temperatures during both nighttime and daytime but also amplify heat in their surroundings.
- Low-density residential areas with an abundance of vegetation cover (see, e.g. areas b, c and d, Figure 49) are cooler than areas with sparse or without vegetation (e.g. areas e and f, Figure 49) during both daytime and nighttime.
- During the daytime, central urban areas with relatively higher building density are cooler than the surrounding desert (urban cool island) but warmer at nighttime, which is typical for arid cities (see, e.g. areas a, b and c, Figure 50). This can be returned to the shadows cast by tall and compact buildings, which reduce the amount of absorbed solar radiation by surfaces. Exceptions are high-density areas with an abundance of urban green spaces, which regulate micro- and local climate during both daytime and nighttime (see area d, Figure 50).

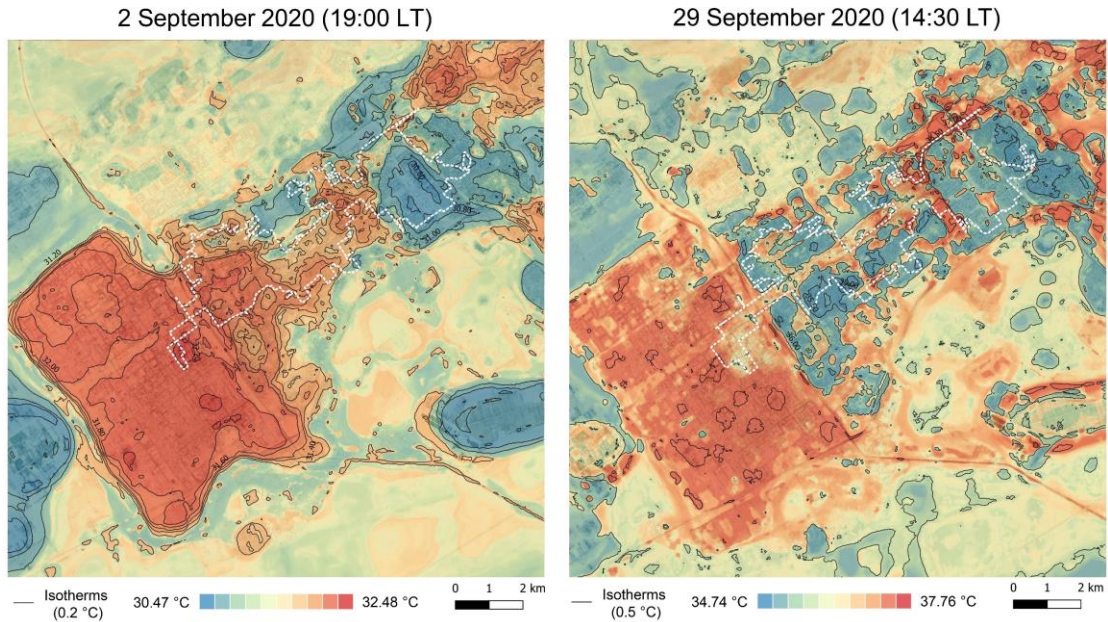


Figure 47. Spatial distribution, with isotherm lines, of the modelled air temperature data at 30-m spatial resolution for the 2nd (at 19:00 LT, left) and 29th (at 14:30 LT, right) of September 2020. The dotted white lines denote the routes of the measurement campaigns.

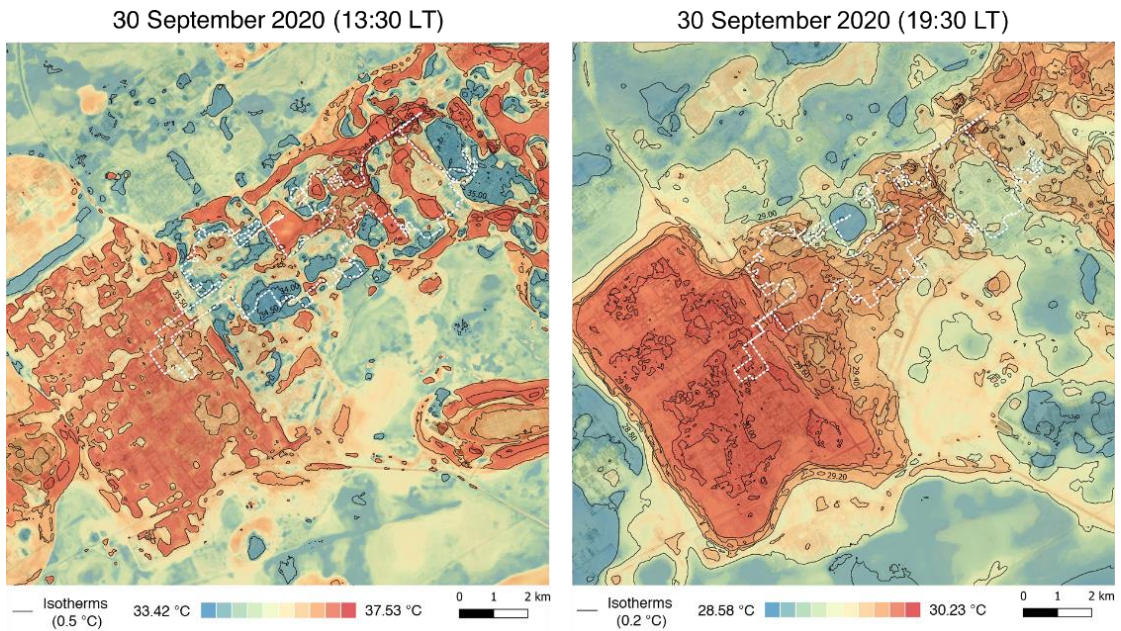


Figure 48. Spatial distribution, with isotherm lines, of the modelled air temperature data at 30-m spatial resolution for the 30th of September 2020 at 13:30 LT (left) and 19:30 LT (right). The dotted white lines denote the routes of the measurement campaigns.

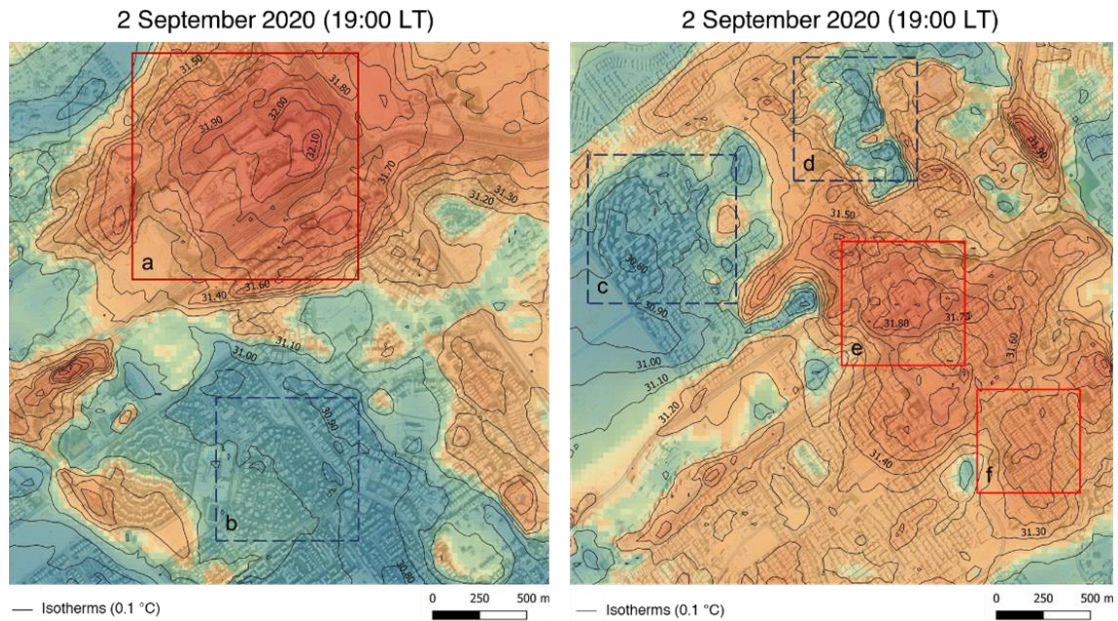


Figure 49. Close-up views with isotherm lines showing the impact of urban form on the spatial variability of air temperature on the 2nd of September 2020 during the nighttime (19:00 LT).

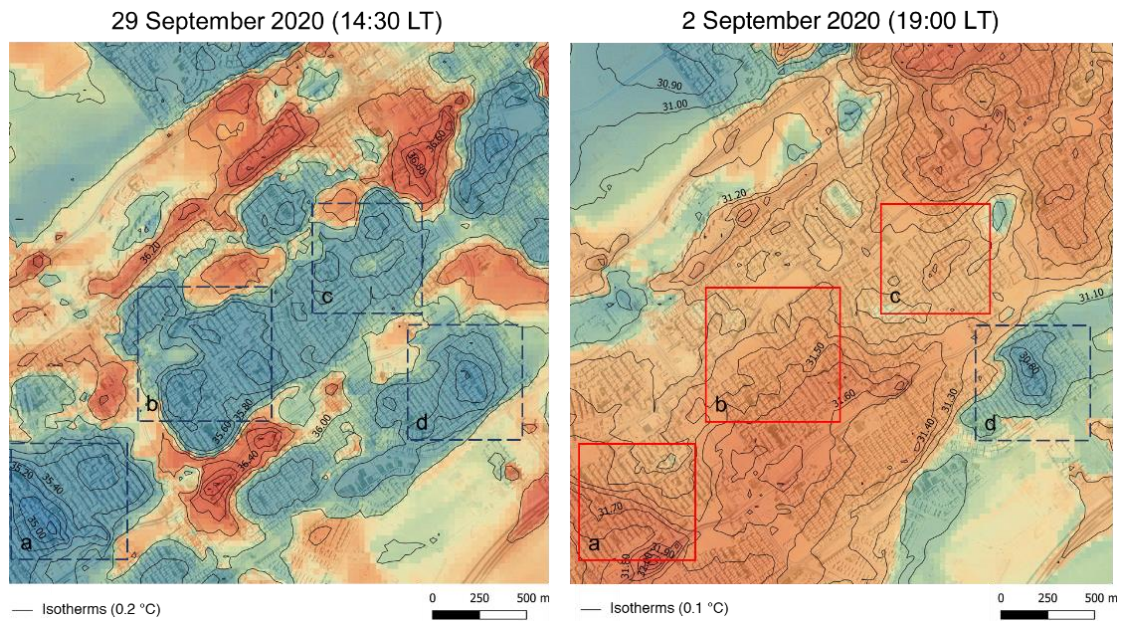


Figure 50. Close-up views, with isotherm lines, showing that the central urban areas with relatively higher building density are cooler than the surrounding desert during daytime (left) but warmer at nighttime (right).

5.4 Discussion: The scope and role of the resulting air temperature maps, limitations of the method and future improvements

In this chapter, we have explored the effectiveness of combining two climatological-/environmental-based methods, i.e. field observations (using low-cost mobile measurements) and empirical modelling (using RF regression), to provide urban micro- and local climate substantive descriptive information (i.e. gridded air temperature data or air temperature maps) at high spatial resolution in a data-scarce, arid city (i.e. Sixth of October, Egypt).

The results showed a high predictive power of the RF models with R^2 more than 0.87 and RMSE below 0.18 °C. The resulting air temperature maps are useful for various urban applications such as providing urban designers and planners with empirically-derived and valid evidence about the possible impacts of urban form characteristics on urban micro- and local temperatures and, in turn, on people's health and thermal sensation (i.e. the environmental/engineering dimension of heat-stress resilience). For instance, by applying a similar methodology to the one presented in this chapter for modelling air temperature, one can model other environmental parameters such as relative humidity and dew point (which are also collected by the PASCO weather station). And use a simple combination of temperature and humidity, or temperature and dew point, to calculate and map, at a high spatial resolution, simple thermal indices for assessing urban form-related extreme temperatures that may have public health consequences. Examples of these indices include the humidex (Masterton and Richardson, 1979) and the heat index (Steadman, 1979). For instance, Environment Canada¹⁶ uses five different levels of the humidex to inform and advise the general public about the degree of comfort: (1) no discomfort (less than 29 °C); (2) some discomfort (30 to 39 °C); (3) great discomfort (40 to 45 °C), where exertion should be avoided; (4) dangerous (46 to 54 °C), where heatstroke is possible; and very dangerous (above 54 °C), where a heat stroke is unavoidable if physical activity continues.

Furthermore, research has shown that there is a documented association between high ambient air temperature and human mortality in different locations around the world (Lo et al., 2022). For example, according to Health Canada¹⁷, when the daily average temperature is higher than 20 °C, for each degree increase in the air temperature, there is an expected increase in mortality by 2.3% (Wang et al., 2016). In the Netherlands, this can reach up to a 2.72% increase in mortality (Huynen et al., 2001; Wang et al., 2016). Hence, beyond urban planning and design applications, one can use the high-resolution air temperature maps produced in this study (and produce others during summertime over longer periods) to find the association between ambient air temperature and observed heat-related deaths. These associations can be used as a basis to develop

¹⁶ <https://ec.gc.ca/meteo-weather/meteo-weather/default.asp?lang=En&n=6C5D4990-1>

¹⁷ <https://www.canada.ca/en/health-canada.html>

statistical models to monitor and project future heat-related mortality at the local scale. These models can be used to provide useful information for public health agencies to prepare local heat-health action plans, and hence reduce the mortality impacts of heat.

Finally, it is worth highlighting that the proposed method for modelling air temperature in this chapter has a number of limitations that may influence the accuracy of the produced maps and should be considered in future studies. Firstly, although the temperature sensor of the PASCO weather station is not directly exposed to sunlight and was further shaded by a cardboard sheet, some radiation-induced errors may remain, thus it is better placed in a solar radiation shield to ensure the highest data accuracy. Secondly, there is some uncertainty over using an average cooling/warming rate to correct for the local temperature changes that occurred during the campaign time, since different local areas may have different cooling/warming rates. One solution would be to calibrate the temperature data using observations from fixed weather stations along the route if they exist. Also, limiting the campaign time by using a shorter route or employing multiple vehicles can help to reduce this source of error. Lastly, although the RF algorithm has proven very effective in both classification and regression tasks, it is prone to overfitting. Hence, it is recommended to use an external dataset of air temperature for better evaluating the model performance rather than the OOB dataset. Cross-validation, using training and test subsets of the original dataset, can also be used for this purpose. Further measurement campaigns should be conducted over longer time periods and during different seasons for developing a dataset of air temperature at finer temporal resolution and thus allowing for better monitoring of air temperature.

Chapter 6

Improving the local climate zone mapping of cities by means of remote sensing- and GIS-based techniques¹⁸

From this chapter on, we will be focusing on the analytical typomorphological methods for studying the impact of urban form on urban climate and, in turn, the possibility of determining its impact on people's health and thermal sensation (i.e. the environmental/engineering dimension of heat-stress resilience). More specifically, Chapters 6, 7 and 8 focus on the local climate zone (LCZ) classification scheme that was introduced in Chapter 4 as one of the most advanced and widely used typomorphological classifications for urban temperature studies. In particular, in this chapter, the aim is to give a concise overview of the existing methods for mapping cities into LCZs and present a proposal for improving their output in terms of scale (i.e. extent and spatial resolution) and accuracy (in answering RQ 3) by using a combination of two different LCZ mapping methods, namely remote sensing- and Geographical Information Systems (GIS) -based methods. The chapter comprises four main sections. Section 6.1 provides an overview of existing LCZ mapping methods and their limitations. Section 6.2 presents the different data and methods that will be used for improving the LCZ mapping of cities. Sections 6.3 and 6.4 present and discuss the results, respectively.

6.1 Overview, existing LCZ mapping methods and limitations

As discussed in Chapter 4, the LCZ classification scheme was originally introduced by Stewart (2011) and Stewart and Oke (2012) to advance urban temperature studies by providing a standardized method to objectively describe the internal structure of urban areas using the concept of typomorphology, thus facilitating the comparison of the thermal characteristic of different local areas within and between cities. As a result, the LCZ classification scheme has become popular among architects, urban designers, urban planners, ecologists and engineers and has been used in various applications (see Chapter 4, Section 4.2.2) among which the most important to this thesis is studying the impact of urban form on urban temperatures and, in turn, on people health and thermal sensation (i.e. the environmental/engineering dimension of heat-stress resilience).

To apply the concept of LCZs to cities, most ideally, field sites should be classified into LCZs based on in-situ measurements of LCZ-relevant geometric and surface cover parameters as provided in (Stewart, 2011; Stewart and Oke, 2012) and following the guidelines set in (Stewart, 2011, sec. 6.2.4). However, field surveys are time-consuming and sometimes are not possible, especially when considering entire cities or urban areas (Jiang et al., 2021). Hence, several methods have been proposed for LCZ mapping. This

¹⁸ A version of this chapter has been peer-reviewed and published: **Eldesoky, A.H.**, Colaninno, N., Morello, E., 2019. Improving local climate zones automatic classification based on physic-morphological urban features. *Int. Conf. Virtual City Territ.* 3. <https://doi.org/10.5821/ctv.8663>.

includes, for instance, subjective manual mapping based on the user's knowledge and experience (e.g. using secondary resources such as aerial photographs and satellite imagery) and GIS- and/or remote sensing-based methods (Ren et al., 2016; R. Wang et al., 2018). In particular, the GIS- and remote sensing-based methods or the combination of both (referred to as combined or hybrid methods) are the most widely used LCZ mapping methods because they offer the possibility of systematically mapping entire cities and large geographical areas with good accuracy, and have been used in several studies. A comprehensive and detailed review of these studies can be found, for instance, in (Jiang et al., 2021) and/or (Lehnert et al., 2021).

Among the most ambitious initiatives to build a worldwide urban climate database and generate automatic, remote sensing-based classifications of LCZs based on publicly available satellite data, is the World Urban Database and Access Portal Tools (WUDAPT) project (Mills et al., 2015). The WUDAPT project presents three-level products of urban climate data: level 0, at regional and city scale; level 1, at neighborhood scale; and level 2, at building scale (Mills et al., 2015). In the WUDAPT level 0 product, each LCZ is described and classified based on the characteristics of some key urban parameters consistent with different urban micro- and local climates (e.g. surface cover, materials, building geometry). This is done by conducting a supervised classification, using freely available multi-spectral and thermal satellite imagery and training samples, defined based on high-resolution aerial or satellite imagery.

Recently, the LCZ Generator¹⁹ was developed by Demuzere et al. (2021) as a web application to substitute and fully automate the WUDAPT procedure using only valid training samples and some metadata as inputs. For instance, Figure 51 shows the LCZ map and the classification accuracy of the study area (i.e. Sixth of October, Egypt) as created by the author using the LCZ generator.

Although the results of the WUDAPT procedure (and the LCZ Generator) provide a multi-categorical, comprehensive classification, LCZ maps are relatively rough (Ren et al., 2016) and frequent quality assessments demonstrate moderate overall accuracy, i.e. 50% to 60% (Bechtel et al., 2019a). Besides, only a few freely available satellite data provide thermal imagery. Furthermore, and most importantly, LCZ maps generated based on thermal data from satellite imagery imply some uncertainty when using these maps in subsequent studies to study the relationship between LCZs and urban temperatures. On the other hand, although GIS-based methods provide high-accuracy LCZ maps, they require high-quality GIS data, which are not always available or open-sourced (Lehnert et al., 2021).

Therefore, in this chapter, the aim is to investigate the possibility of improving the quality of LCZ maps both in terms of spatial resolution and accuracy without the use of thermal satellite imagery or high-quality GIS data. This is done by conducting a pixel-based supervised LCZ classification using (1) relatively small-sized LCZ training samples to account for some small-scale urban units (e.g. big buildings, elongated or

¹⁹ <https://lcz-generator.rub.de/>

wide urban canyons and urban blocks) that can influence the micro- and local climate (Oke et al., 2017); and (2) fine-scale classification variables that are a combination of LCZ-relevant multi-spectral indices (calculated from freely-available satellite imagery) and morphological indices (calculated from basic GIS building data). More specifically, four indices are used in this chapter to conduct the LCZ classification: surface albedo²⁰ (both narrow and broadband albedo); Normalized Difference Vegetation Index²¹ (NDVI); building heights; and the sky view factor²² (SVF).

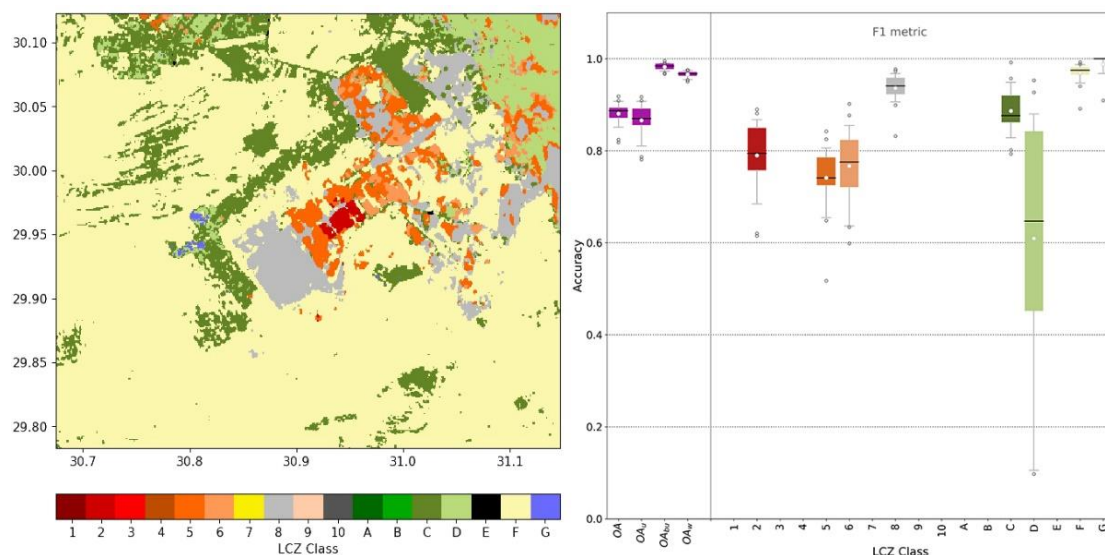


Figure 51. The LCZ classification of Sixth of October generated using the LCZ generator (left), and the LCZ classification accuracy measures (right), where OA, OA_u, OA_{bu} and OA_w refer to the overall accuracy, the overall accuracy of the urban LCZ types only, the overall accuracy of the built versus natural LCZ types only and the overall weighted accuracy, respectively.

6.2 Data and methods

6.2.1. Test case study and data

In this chapter, because the aim is to propose a method that improves the quality of LCZ maps in general and not in a specific context or area, we selected a test case study where all the 17 LCZ types are present and a complete GIS building data are available. These criteria were not met in Sixth of October, where only a few LCZ types are present and the GIS building data could not be obtained for the entire city.

The test case study is the metropolitan city of Milan (Figure 52), which includes the city of Milan and other 133 municipalities. It covers a surface area of about 1,575 km² and has a population of around 3.254 million inhabitants. According to the National

²⁰ The ability of surfaces to reflect sunlight (heat from the sun).

²¹ A measure of vegetation intensity and it ranges from -1 to 1 . High NDVI values ($\sim .60-.90$) indicate dense vegetation, while low values, close to zero, correspond to built-up areas, bare soil or sand.

²² Ratio of the amount of sky hemisphere visible from ground level to that of an unobstructed hemisphere.

Plan of Adaptation to the Climate Change (PNACC), the metropolitan city of Milan is one of the most vulnerable areas in Italy to the risk of extreme heatwaves.

In this study, we used a Landsat 8 satellite image for the study area (Figure 52) acquired on a summer day (15 August 2018) during daytime (10:10 AM), and where the cloud cover over the region of interest (ROI) was less than 10%. Landsat 8, as highlighted in Chapter 5, carries two sensors, i.e. the Operational Land Imager (OLI) and the Thermal Infrared Sensor (TIR), which provide eight spectral bands at 30-m spatial resolution, one panchromatic band (15 m) and two thermal bands (collected at 100 m and resampled at 30 m) (USGS, 2015). Also, high quality digital topographic database (DTDB) of building footprints, where building heights information is available, was obtained from Geoportale Lombardia²³. The DTDB is freely available for most of the Lombardian municipalities.

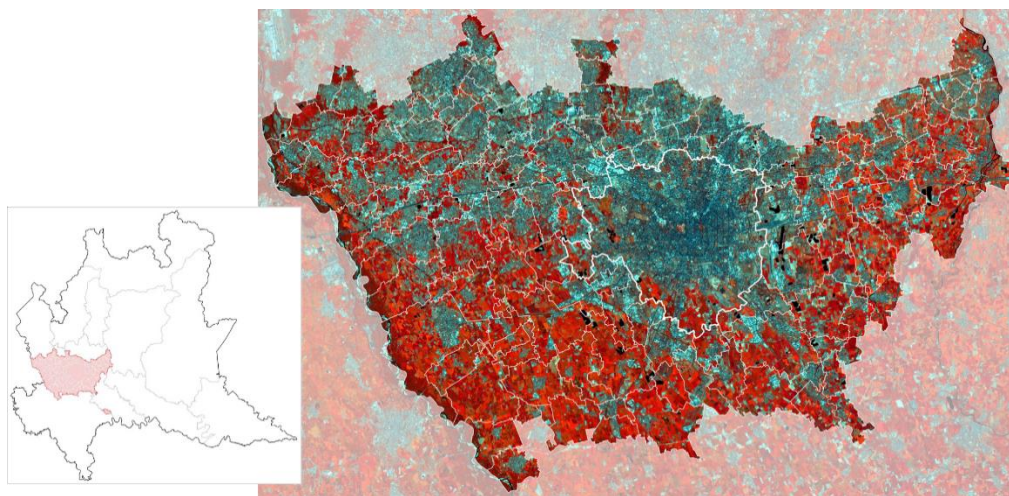


Figure 52. The location of the metropolitan city of Milan (highlighted in red) within the Lombardy region (left), and a multi-spectral image acquired from Landsat 8 (right).

6.2.2. The LCZ classification procedure

The proposed method for improving the output of the LCZ maps includes four main steps. Firstly, the Landsat 8 image (referred to above) was downloaded from the United States Geological Survey (USGS), pre-processed (i.e. calibrated and atmospherically corrected) and clipped to the ROI. Then, training samples (Figure 53) for each LCZ type were digitized in Google Earth following the instructions provided by WUDPAT. However, as mentioned earlier, we digitized relatively smaller-sized training samples for creating a fine-scale LCZ map as well as for considering the effect of the small-scale urban units on the micro- and local climate. More specifically, urban blocks of about 250 m in horizontal scale are commonly the smallest urban units where homogeneity can be found, and hence they were regarded as LCZs in this study (Kotharkar and Bagade, 2018; Oke et al., 2017).

²³ <https://www.geoportale.regione.lombardia.it/>



Figure 53. The training samples used for creating the supervised LCZ classification of the metropolitan city of Milan. The LCZ samples were digitized using Google Earth imagery following the instruction provided by WUDPAT.

Next, the multi-spectral and morphological indices were calculated. More specifically, the broadband albedo was calculated based on Landsat 8 bands 2, 4, 5, 6 and 7 using the conversion formulae described in (Liang, 2001), while the NDVI was calculated by using Landsat 8, NIR (5) and Red (4) bands (Rouse et al., 1974). On the other hand, building heights and SVF were calculated using the DTDB and resampled consistently with the spatial resolution of Landsat 8 data (30 m). Finally, a LCZ map was created using the random forest (RF) classifier (Ho, 1998) in SAGA GIS (the Local Climate Zone Classification tool) based on 64 decision trees as recommended by Oshiro et al. (2012). And a post-classification majority filter of a 4-pixel radius was applied to the output map to obtain more homogenous LCZs (of about 270 m in horizontal length scale). In fact, in this study, we created a LCZ map of the study area twice, first, as instructed by WUDAPT, i.e. using Landsat 8 multi-spectral and thermal bands, and, then, by using the Landsat 8 multi-spectral indices and the morphological indices. The WUDAPT map will be used in this chapter as a benchmark to determine the degree of improvement in the accuracy of the LCZ map created using the proposed method.

6.2.3. Accuracy assessment

Assessing the level of accuracy of the LCZ classification maps has been always challenging since this requires enough, independent test dataset (ground truth), and using the same training dataset for model validation and calibration is not appropriate. Accordingly, in the WUDAPT level 0 method, three approaches are usually used to assess the accuracy of the LCZ maps before they are disseminated on the online platform; these are cross-validation (rotation estimation), manual review, and cross-comparison with other data (Bechtel et al., 2019a). In this chapter, we used the repeated holdout cross-validation approach, using different subsamples for 25 iterations as recommended by Bechtel et al. (2019a). In particular, in the repeated holdout method, the original sample data are separated into two portions, i.e. training and testing data (we used half of the original data for training and the other half for testing), where, for each iteration, a different random subset of the data is used. Subsequently, standard accuracy measures (Bechtel et al., 2017) were calculated for each run of the 25 iterations, using a confusion matrix. In particular, we considered four measures: the overall classification accuracy (OA) for all polygons, the Kappa coefficient (Cohen, 1960), the OA for built polygons only and the producer accuracy calculated for each LCZ type. The producer accuracy is the likelihood that a pixel in a certain type was classified correctly. An additional certainty measure (Bechtel et al., 2019a) was calculated to determine how often each pixel was assigned to the most frequent LCZ type (as obtained by calculating the majority value of the 25 iterations).

6.3 The resulting LCZ map and map accuracy

Figure 54 shows the resulting LCZ map of the metropolitan city of Milan as obtained by the proposed method, where the built and the non-built (or land cover) LCZ types occupy around 24.5% and 75.5% of the total metropolitan area, respectively. In particular, LCZ types B, D, 6, 10, E and A are the most present in the metropolitan city

of Milan. However, by considering only the most urbanized area, i.e. the city of Milan, it is noticeable that the urban structure is mostly occupied by the open and the compact mid-rise built types (i.e. LCZs 5 and 2) and the land cover types of scattered trees and bare rock or paved (i.e. LCZs B and E).

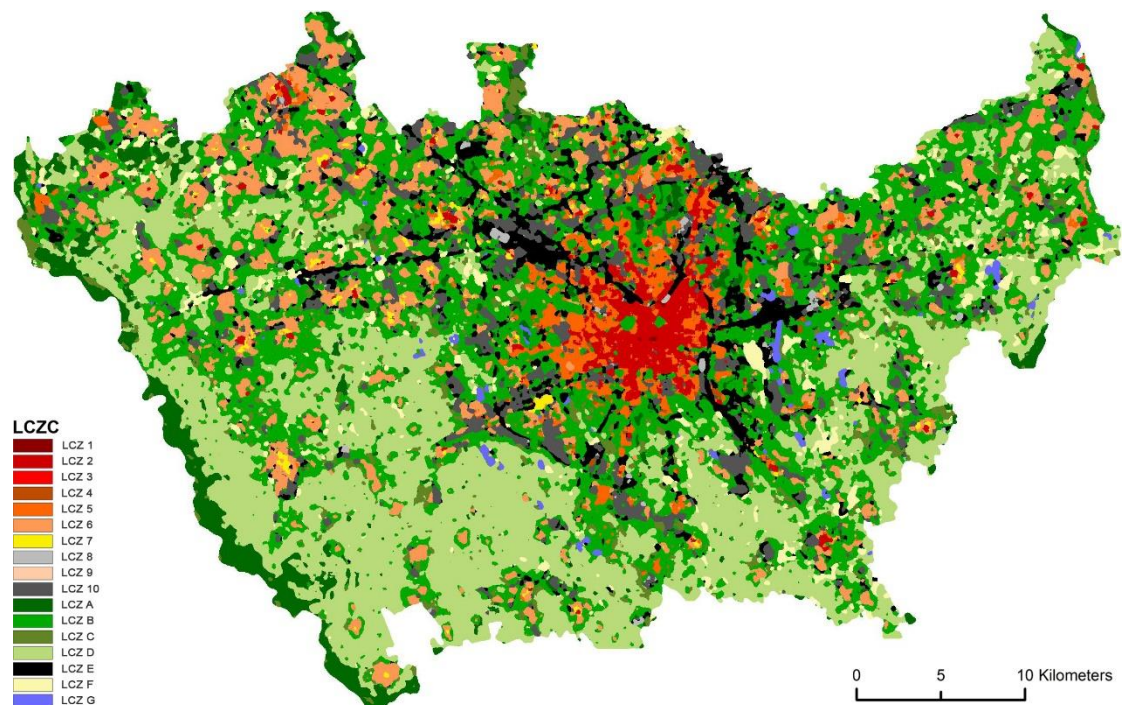


Figure 54. The resulting LCZ map of the metropolitan city of Milan using the proposed method and a post-classification majority filter of a 4-pixel radius. The raw and filtered (at different radii) LCZ maps are made open access and can be downloaded from <https://doi.org/10.6084/m9.figshare.19646781.v1>.

Table 11 and Figure 55 show the results of the accuracy assessment based on the four standard measures referred to in Section 6.2.3. In general, both the WUDAPT level 0 method and the developed method achieved an accuracy above 50%. However, it is noticeable that there is an overall improvement in the classification output of the proposed method with an OA of 67% compared to 55% using the WUDAPT method. Similarly, the Kappa coefficient for all the testing polygons is 0.61 using the proposed method, which implies a good agreement according to McHugh (2012), compared to a moderate agreement of 0.47 for the WUDAPT level 0 product. Also, considering only the quality of the built LCZ types, where misclassification mostly occurs, the OA for all the built polygons as obtained by the proposed method is 48% compared to 33% using the WUDAPT method; however, this is increased to 54% and 38%, respectively by excluding the least representative LCZ types (i.e. LCZs 3 and 9). Likewise, the output classification of the proposed method has a higher certainty of the results over the entire built domain (0.68) compared to that of the WUDAPT (0.58); however, both the output maps have almost the same certainty over the non-built classes (0.65) as shown in Figure 56. In general, according to Bechtel et al. (2019a), results are considered of acceptable quality if they achieve a minimum average accuracy of 50%.

Table 11. Accuracy measures of the LCZ classification.

Measure (average of 25 iterations)	WUDAPT level 0 product	The proposed method
OA for all testing polygons	55%	67%
Kappa coefficient for all testing polygons	0.47	0.61
OA of all built types	33%	48%
OA of all built types (excluding LCZs 3 and 9)	38%	54%

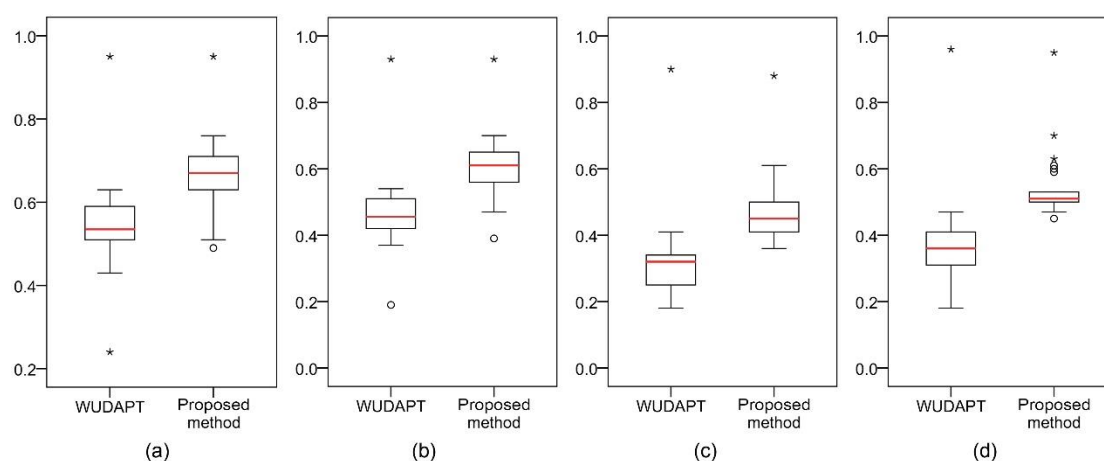


Figure 55. Boxplots of the distribution of the accuracy measures across the 25 iterations. (a) Overall accuracy for all testing polygons; (b) Kappa coefficient for all testing polygons; (c) Overall accuracy of all built polygons; and (d) Overall accuracy of all built polygons (excluding LCZs 3 and 9).

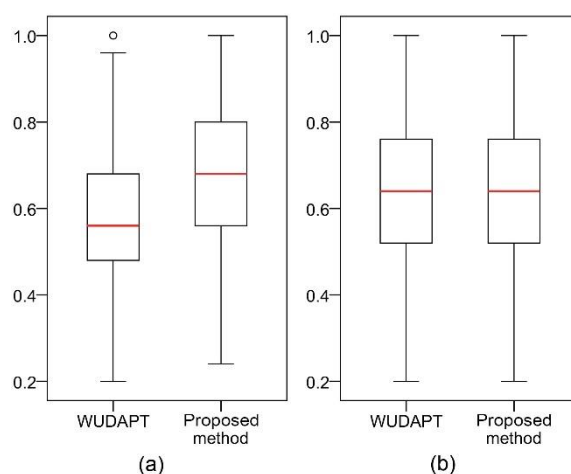


Figure 56. Boxplots for the certainty of the results over the entire domain. (a) Built LCZs; (b) Non-built LCZs.

Figure 57 shows the producer accuracy (%) for each LCZ type where the proposed method achieves remarkable improvements in seven LCZ types (i.e. 1, 5, 6, 7, 10, E, and F) and a slight improvement in other four types (i.e. LCZs 2, 9, A and D). However, almost no or very little improvements were achieved in the LCZs 4 and B. Figure 57 shows also that the WUDAPT level 0 product is performing slightly better in four LCZ types (i.e. 3, 8, C and G) which can be returned to the presence of the thermal

information that can provide further differentiation between these LCZ types since the surface permeability is negatively well correlated with land surface temperature (Bechtel et al., 2019a; Weng, 2009; Weng et al., 2004).

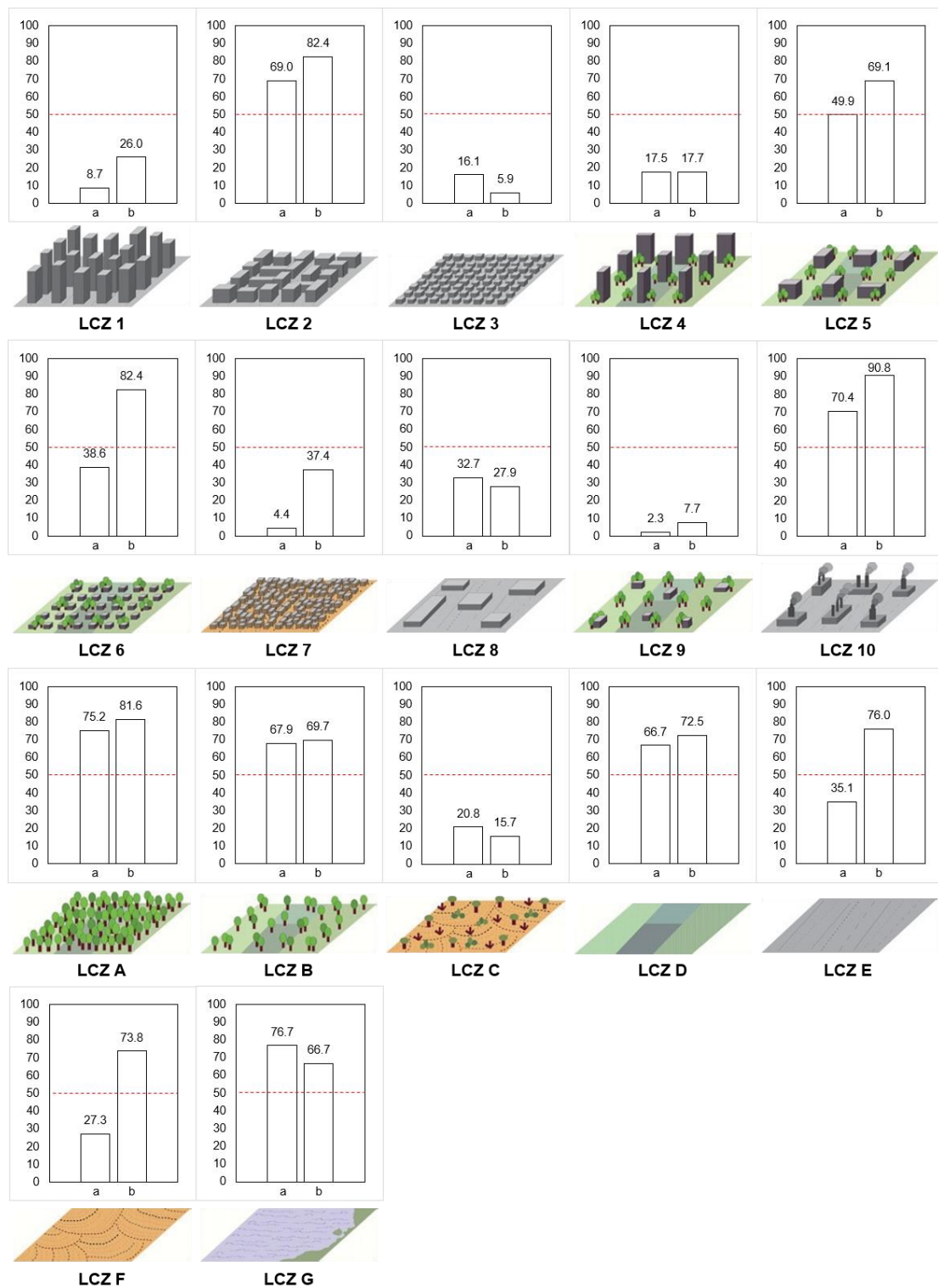


Figure 57. The producer accuracy (%) for each LCZ type. (a) The WUDAPT level 0 product; (b) The proposed method.

6.4 Discussion: The potentials and limitations of the proposed method and future improvements

In this chapter, we have provided an overview of the different methods for mapping cities into LCZs and proposed a new method for improving their output (in terms of scale and accuracy). In particular, we have combined multi-spectral indices, calculated using freely available satellite imagery (30 m), with morphological indices, calculated using a DTDB of building footprints, with the aim of conducting a pixel-based supervised LCZ classification. Further, we have digitized relatively small-sized training samples, using very high-resolution aerial imagery, to generate a fine-scale LCZ classification map suitable for better studying the urban climate phenomena at the micro- and local scale (e.g. the urban heat island effect).

The results of the accuracy assessment showed a noticeable improvement in the classification output of the proposed method, with respect to the WUDAPT level 0 product, for both the overall accuracy (OA) and the Kappa coefficient by 12% and 0.14, respectively. It was also found that the OA, considering only the built classes, is higher by 15%, which demonstrates the effectiveness of the proposed method in mapping fine-scale LCZs without additional thermal information. This also ascertains the morphological nature of the LCZs which are intrinsically related to certain temperature regimes and comfort levels (Stewart and Oke, 2012). Hence, one may conclude that the WUDAPT level 0 method is best suitable for mapping coarse-scale LCZs ($> 1 \text{ km}^2$); however, mapping finer resolution LCZ maps, while maintaining a minimum average accuracy, requires a better description of the surface cover and the morphological/geometric features of the urban environment.

On the other hand, there are still limitations in identifying some individual LCZ types using the proposed method, where the OA is less than 50% (e.g. LCZs 9, 4 and C). This is mainly, either because of the size and the quality of the training samples, which can vary from one user to another and require further expert knowledge (Bechtel et al., 2015; Ren et al., 2016), or because of the non-representativeness of some LCZ types, considering the generalization of the standard LCZ scheme. Therefore, it would be of interest, in future work, to evaluate the effect of using different sets of training samples (e.g. in terms of area, perimeter and quantity) on the OA of the output maps. Also, multi-seasonal satellite imagery and higher quality elevation models, such as Light Detection and Ranging (LIDAR-) derived digital surface model, could be utilized for better reliability of the results, especially when classifying land cover types.

Finally, considering the universality of the LCZ classification scheme (Stewart and Oke, 2012; R. Wang et al., 2018; Wicki and Parlow, 2017) with respect to the heterogeneity of the internal urban structure among cities of different sizes and locations (Bechtel et al., 2015), the possibility of readapting the standard LCZ scheme, by describing site-specific LCZ types or subtypes that are related to certain micro- and local climate conditions, should be investigated.

Part III

**Testing methods and techniques, gap of knowledge
and proposed innovation: The integrated
multi-dimensional typomorphological
classification**

Chapter 7

How well does the local climate zone classification scheme discern the thermal differences between different areas in Sixth of October, Egypt?

In the previous chapter, we have introduced the most common methods for applying the local climate zone (LCZ) classification scheme to cities and proposed a method for improving its application in general. This was demonstrated in a test case study that is representative of all the LCZ types and where there is the availability of complete Geographical Information Systems (GIS) building data, namely the metropolitan city of Milan, Italy.

In this chapter, we continue the discussion about the LCZ classification scheme; however, with the aim to assess its suitability for studying the impact of urban form on urban temperatures in contemporary cities in arid areas, exemplified by Sixth of October, Egypt, and thus the possibility, in a next step, of determining its impact on people's health and thermal sensation (i.e. the environmental/engineering dimension of heat-stress resilience). Because “each LCZ has a characteristic screen height temperature regime that is most apparent over dry surfaces, on calm, clear nights, and in areas of simple relief” (Stewart and Oke, 2012, p. 1884), by applicability here we mean similarity in air temperature characteristics among identical LCZ types (i.e. little variability in air temperature within the same LCZ type) but, more importantly, a different impact on air temperature when compared to other LCZ types (i.e. statistically significant differences between LCZ types in terms of air temperature).

The chapter consists of four main sections. In Section 7.1, we give a short overview of the few previous studies that have applied the LCZ classification scheme to contemporary arid cities. Section 7.2 presents the different data and methods that will be used for statistically analyzing the air temperature characteristics of the LCZ types present in Sixth of October. Section 7.3 presents the results of the statistical analysis; and finally, the results are discussed in Section 7.4.

7.1 The LCZ classification scheme in contemporary arid cities

Since its development, the LCZ classification scheme has been widely applied to many cities across the world to characterize the effect of urban form on their micro- and local climates. However, its specific application to contemporary arid cities has not received that great deal of attention. Examples of the few previous studies that have applied the LCZ scheme to contemporary arid cities include: Manandhar (2019) to Abu Dhabi (UAE), Bande et al. (2020a) to Al Ain (UAE), Fricke et al. (2020) to Beer Sheva (Israel), Jamali et al. (2021) to Tehran (Iran), Middel et al. (2014) to Phoenix (USA) and Nassar et al. (2016) and Bande et al. (2020b) to Dubai (UAE).

Nevertheless, most of the aforementioned studies have focused primarily on using the LCZ scheme to study the micro- and local climate of cities, and less on assessing its applicability to arid cities, for instance, in terms of whether the LCZ geometric and surface cover properties in arid cities match the proposed value ranges from the literature, or whether there are significant differences between the different LCZ types in terms of air or land surface temperatures (LST). The latter is an inherent (and probably the most important) feature of the LCZ scheme, and its assessment cannot be overlooked if it is to be useful for urban temperature studies in arid cities.

Among the few studies that have evaluated the LCZ scheme in arid cities is the one by C. Wang et al. (2018) who classified—using the World Urban Database and Access Portal Tools (WUDAPT) method—and evaluated LCZs for two arid U.S. cities, namely Phoenix, Arizona and Las Vegas, Nevada. Most importantly, they found that, in these two sprawled desert cities, some LCZ types are hardly distinguishable from each other such as the sparsely built (LCZ 9) and the bare soil or sand (LCZ F) or the lightweight low-rise (LCZ 7) and open low-rise (LCZ 6). They also found that the geometric (e.g. street aspect ratio and sky view factor) and surface cover properties of some LCZ types do not match with the proposed value range and guidelines provided in (e.g. Stewart and Oke, 2012). Therefore, they recommended that ancillary datasets should be used to further distinguish between LCZs, and that the upper boundaries of some geometric parameters could be adjusted so that they apply to arid cities.

7.2 Data and methods

7.2.1. LCZ sample sites

As discussed in Chapter 6, there are several methods for applying the LCZ scheme to cities such as manual sampling, to classify field sites into LCZs relying on secondary sources (e.g. aerial imagery), and GIS- and/or remote sensing-based methods. However, considering the unavailability of a high-quality digital topographic database (DTDB) for the study area to conduct a GIS-based classification, and the fact that remote sensing-based methods may lead to misclassification errors, as discussed in Chapter 6; here, we opted for manually classifying a sample of representative field sites in the study area into LCZs based on our local knowledge and experience. This classification method, although time-consuming, ensures a high classification accuracy of the LCZ sites as well as minimizes any potential source of methodological bias in the subsequent air temperature analysis, which can arise, for example, from using a LCZ classification that is obtained based on thermal data from satellites (e.g. the WUDAPT product).

In particular, we digitized, using Google Earth, a number of polygons that are representative of each of the LCZ types present in the study area²⁴. These are LCZ 2

²⁴ The dataset of the digitized LCZ polygons is licensed under CC BY-SA, and is available at https://lcz-generator.rub.de/factsheets/eca033d11e9bb4e1f1282169ee084223d1e3eac3/eca033d11e9bb4e1f1282169ee084223d1e3eac3_facsheet.html

(compact mid-rise), LCZ 5 (open mid-rise), LCZ 6 (open low-rise), LCZ 8 (large low-rise), LCZ C (bush, scrub) and LCZ F (bare soil or sand). The LCZ polygons were digitized following the procedure and the guidelines provided by the WUDAPT project²⁶, where the total number of polygons digitized per LCZ type is shown in Figure 58.

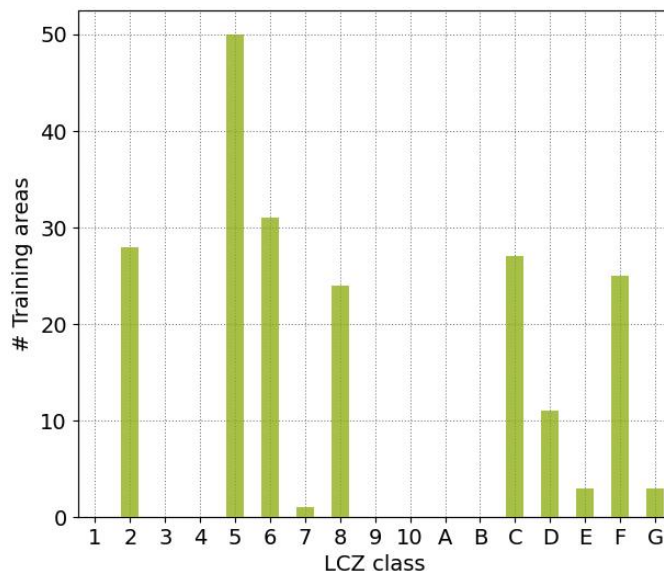


Figure 58. The total number of digitized polygons per LCZ type in Sixth of October, Egypt.

7.2.2. Air temperature data

In this chapter, in order to analyze the air temperature characteristics of the different LCZ types present in the study area and determine whether there is a statistically significant difference between them, we used screen-level (~ 1.5 m above ground) air temperature data obtained at different dates/times, including both daytime and nighttime.

The data were obtained through the empirical modelling procedure, proposed and described in detail in Chapter 5, and have an accuracy of about ± 0.2 °C and a spatial resolution of 30 m. The data are available online at [10.1088/1742-6596/2042/1/012045](https://www.wudapt.org/digitize-training-areas/) in GeoTIFF format for September 2nd, 29th and 30th, 2020. The LCZ polygons digitized in Section 7.2.1 were overlaid with the air temperature maps and each LCZ polygon was assigned an average air temperature value based on all the pixels that it overlays.

7.2.3. Statistical analysis

The main objective of the statistical analysis is to assess how well the LCZ scheme discerns the thermal differences between different areas in the study area by analyzing

²⁶ Available at <https://www.wudapt.org/digitize-training-areas/>

whether there is a significant difference between LCZ types in terms of air temperature at the different dates/times considered in the analysis.

In order to do so, first, we produced box plots of the distribution of the air temperature for each LCZ type. Box plots, showing the five-number summary (i.e. the minimum, the first quartile, the median, the third quartile and the maximum) of the air temperature values for each LCZ type lined up side-by-side, help to visually identify whether there might be a significant difference between LCZ types in terms of air temperature. As a rule of thumb, when the median line of one LCZ type lies entirely out of the box of another type, it is more likely that these two types differ significantly.

However, considering the subjectivity in interpreting box plots, the difference between LCZs was tested more formally using Welch's Heteroscedastic F Test with Trimmed Means and Winsorized Variances (Welch, 1951). Welch's Heteroscedastic F Test with Trimmed Means and Winsorized Variances is a robust alternative against the combined effect of non-normality and heteroscedasticity, which violate the main assumptions required to run a parametric one-way analysis of variance (ANOVA), and has high control and power over the Type I error (Cribbie et al., 2012; Dag et al., 2018; Keselman et al., 2008, 2002). Trimming and winsorizing (or winsorization) are statistical procedures to substitute the normal mean and variance by trimmed and winsorized ones so that the test is insensitive to the effect of the extreme values in the data. Good practices have shown that a symmetric trimming percentage of around 20% has good control over the Type I error (Cribbie et al., 2012; Wilcox, 1998a, 1998b, 1996). The normality assumption was assessed using Shapiro–Wilk test (Shapiro and Wilk, 1965) and histograms, while the homogeneity of variance was tested using the Fligner–Killeen test (Fligner and Killeen, 1976). The results (see Appendix B) indicated that there is a significant departure from normality in most of the independent groups and that the homogeneity of variance assumption was not met for all the designs. All the aforementioned tests were implemented using the `onewaytest` package (Dag et al., 2018) in R (Team, 2019).

When a statistically significant difference was found, a post-hoc analysis has followed to make pairwise comparisons and determine which specific groups (or LCZ types) make the difference in every design. This was done using the Games–Howell test (Games and Howell, 1976). The level of statistical significance is expressed as a p -value and the test results are significant at ($p < .05$). The post-hoc tests were conducted in R using the `rstatix` package (Alboukadel Kassambara, 2020). When comparing LCZs at a specific date/time, the number of pairwise comparisons showing a significant difference for each LCZ type is an indicator of how well a type is differentiated from all the other types in terms of air temperature as suggested by Geletič et al (2019, 2016). This number was calculated twice: once, considering all the LCZ types (minimum 0 and maximum 5) and once considering only the urban/built LCZ types (minimum 0 and maximum 3). Likewise, the degree to which the LCZ classification scheme discerns the air temperature differences among LCZ types at a specific date/time can be determined by calculating the overall percentage of the pairwise comparison tests showing a significant difference from the total number of pairwise comparisons.

7.3 Results: The significance of the air temperature differences between LCZ types

Figure 59 shows the box plots of the distribution of the air temperature values for each LCZ type at the different dates/times analyzed. By comparing these box plots, it is observed that for most of the LCZ pairwise comparisons during the nighttime, boxes either do not overlap or overlap but do not extend beyond both median lines. This indicates that the majority of the LCZ types are likely to be different in terms of air temperature during the nighttime, which is not the case during the daytime, where most of the boxes do overlap.

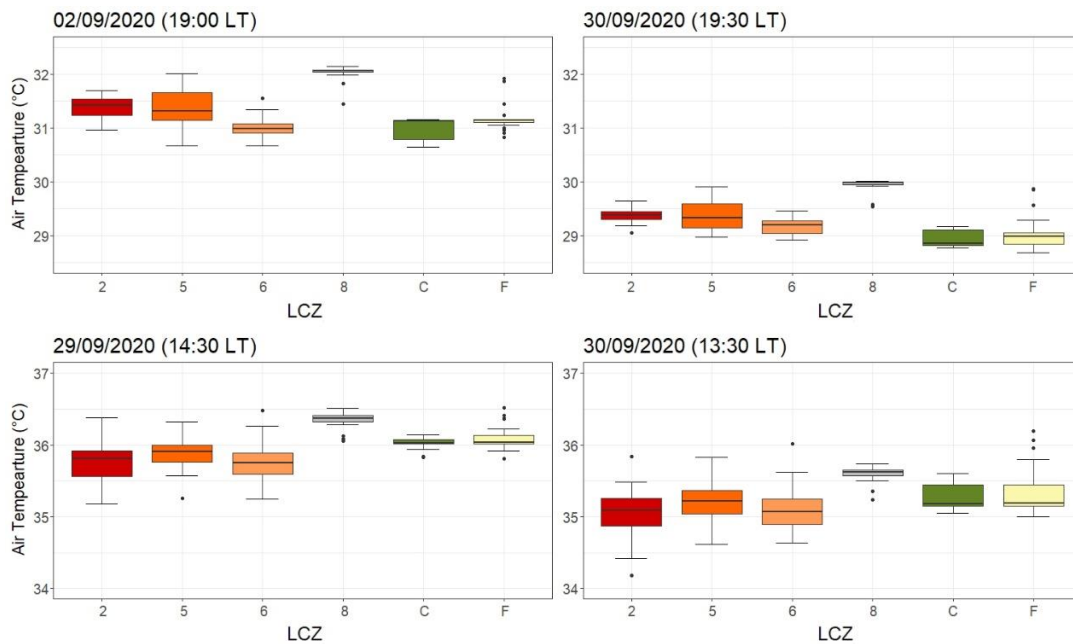


Figure 59. Box plots of the distribution of the air temperature for each LCZ type during nighttime (top) and daytime (bottom).

In general, the results of the preliminary analyses of variance using the Welch's Heteroscedastic F Test with Trimmed Means and Winsorized Variances show that we can reject the null hypothesis ($p < .05$) and that there is a statistically significant difference between LCZ types in terms of air temperature for all the dates/times analyzed, where smaller p -values show stronger evidence to reject the null hypothesis (Table 12).

Table 12. Summary of the preliminary analyses of variance showing the significance of the difference between LCZ types in terms of air temperature for each date/time analyzed.

Date (HH:MM)	statistic	p-value	Significant?
2 September 2020 (19:00 LT)	$F= 1879.011$	$1.347439e-55$	Yes
29 September 2020 (14:30 LT)	$F = 121.6002$	$2.353227e-27$	Yes
30 September 2020 (13:30 LT)	$F = 67.00813$	$1.036777e-20$	Yes
30 September 2020 (19:30 LT)	$F = 498.6541$	$1.649359e-40$	Yes

More specifically, the results of the Games–Howell post-hoc test show which groups (or LCZ types) differ significantly from others in terms of air temperature by performing pairwise comparisons between all the possible combinations of groups. The calculated p -values from the pairwise comparisons are reported in the form of a heatmap (Figure 60), where the total number of pairwise comparisons showing a significant difference for each LCZ type is reported at the end of each row (number of hits). Figure 60 shows that the overall percentage of pairwise comparison tests showing a significant difference is 86.7%, 73.3%, 53.3% and 80% for September 2nd (19:00 LT), 29th (14:30 LT), 30th (13:30 LT) and 30th (19:30 LT), 2020, respectively. These percentages are changed to 83.3%, 50%, 50% and 83.3%, respectively when comparing only the urban/built LCZ types (i.e. 2, 5, 6 and 8). In particular, during nighttime, all LCZ types are relatively well differentiated (i.e. with a high number of hits), while during the daytime, all the urban/built LCZ types, except LCZ 8, are indistinguishable from each other.

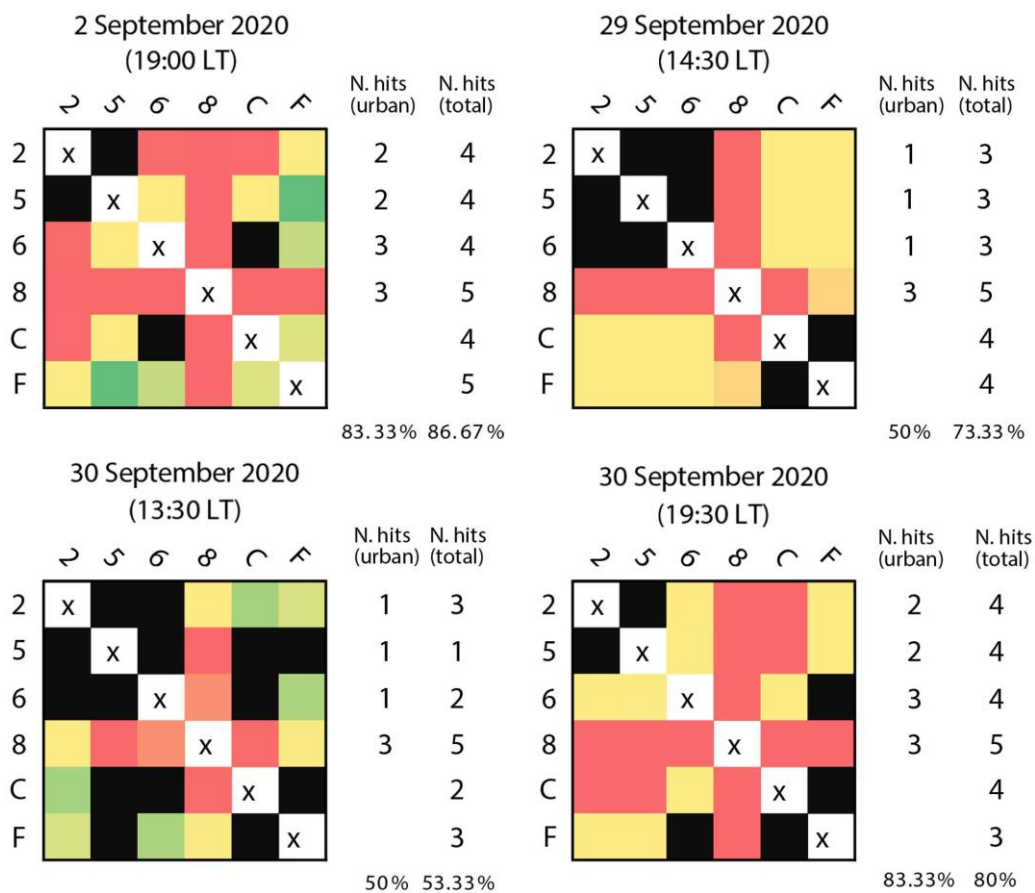


Figure 60. Results of the post-hoc tests to compare LCZ types for the different dates/times considered in the analysis. Black cells indicate no significant difference between LCZ types ($p > .05$), while colors ranging from red to yellow via green indicate higher to lower significance levels at ($p < .05$). The number of hits (N. hits) in significance per LCZ type is reported twice at the end of each row: once considering all the LCZ types and once considering only the urban/built LCZ types. The percentage of hits in all pairwise comparison tests is indicated for each date/time as a (%) value in the bottom right corner.

7.4 Conclusions: The need for a wider suitability assessment of the LCZ classification scheme

In this short chapter, we have assessed how well the LCZ classification scheme discerns the thermal differences between different areas in Sixth of October, Egypt, as a typical example of a contemporary city in an arid area. This was done by statistically analyzing whether there is a significant difference between LCZ types in terms of air temperature for different days and times (including both daytime and nighttime).

The results showed that during nighttime, all LCZ types are relatively well-differentiated from each other, while during the daytime, almost none of the urban/built LCZ types is indistinguishable from another. This finding, in light of a few studies that have applied the LCZ scheme to arid cities and where an assessment of the statistical significance of the thermal difference between LCZ types was often not performed or was incompletely reported, highlights a possible limitation that needs to be further investigated regarding the applicability of the LCZ scheme to arid cities. This limitation cannot be confirmed without conducting a wider suitability assessment, including a large number of field sites that are representative of all the LCZ types.

Therefore, in the next chapter, a wider study to confirm the suitability of the LCZ scheme, not only in arid but also in other macroclimate regions (where no previous in-depth studies were conducted), will be carried out. This is an important step if the LCZ typomorphological classification is to be useful for urban planning and design practices not only in arid areas but also globally.

Chapter 8

Assessing the suitability of the local climate zone classification scheme for urban temperature studies in distinct macroclimate regions²⁷

In the previous chapter, we have assessed how well the local climate zone (LCZ) typomorphological classification discerns the thermal differences between different areas in Sixth of October, Egypt, as a typical example of a contemporary desert city. The results suggested the need for conducting a wider study to confirm the suitability of the LCZ scheme for urban temperature studies in arid areas and, in turn, for addressing the environmental/engineering dimension of heat-stress resilience.

In addition to that, there is evidence from previous studies that the performance of the LCZ scheme in discerning the local thermal environment of cities varies per macroclimate region (Bechtel et al., 2019b; Chakraborty and Lee, 2019; Demuzere et al., 2019; Imhoff et al., 2010; Schwarz et al., 2011; Zhao et al., 2014); however, no previous studies have examined this in detail. Therefore, it is also important in this chapter to expand our knowledge about the suitability of the LCZ scheme not only in arid but also in other macroclimate regions. This is an essential methodological step if the LCZ scheme is to be useful for urban planning and design practices globally.

8.1 Introduction to the aim and scope of the assessment

In this chapter, by suitability we mean similarity in the temperature characteristics among identical LCZs in the same macroclimate region (i.e. little variability in the temperature within the same LCZ type), but more importantly, a different impact on the temperature when compared to other LCZ types in the same macroclimate region (i.e. statistically significant differences between LCZ types in terms of their temperature).

In particular, two questions are addressed in this chapter:

- Do identical LCZ types exhibit similar temperature characteristics within the same macroclimate region and how well does the standard LCZ scheme discern the temperature differences between LCZ types within the same macroclimate region?
- How do identical LCZ types change their temperature and heat island characteristics with changing macroclimate and does the standard LCZ scheme exhibit a similar temperature profile in different macroclimate regions?

While the first question addresses the general suitability of the LCZ scheme, the second one offers the possibility to test aspects of its performance as a typomorphological classification useful to inform urban planning and design, in this case, regarding the

²⁷ A version of this chapter has been peer-reviewed and published: **Eldesoky, A.H.**, Gil, J., Berghauser Pont, M., 2021. The suitability of the urban local climate zone classification scheme for surface temperature studies in distinct macroclimate regions. *Urban Clim* 37, 100823. <https://doi.org/10.1016/j.uclim.2021.100823>

expected impacts of global climate change on the climate of local urban areas. This is an important question as there is strong evidence that the world macroclimate regions have shifted and are quickly changing with global warming, where some regions are changing more than others toward a warmer or drier climate (Fraedrich et al., 2001; Jylhä et al., 2010; Mahlstein et al., 2013). The goal is not only to understand the impact of global warming on the absolute temperatures of the different LCZ types (i.e. how high/low temperatures are likely to be) but also on their relative temperature when compared with a reference (cool) LCZ type, e.g. LCZ D (low plants). The latter is particularly important to make the comparison consistent across macroclimate regions regardless of the differences in radiation, geology or latitude.

In order to answer these questions, a macroclimate region-based study is conducted, including a large number of LCZ sites from different cities across four different macroclimate regions, namely, the tropical, the arid, the temperate and the cold. Considering that obtaining global multi-year screen-level air temperature data at high spatial resolution is challenging as discussed in Chapters 4 and 5, multi-year land surface temperature (LST) data, obtained from Landsat satellites, are used in this study. However, it should be noted that the LCZ scheme was initially designed for air temperature studies and that air temperature and LST, although closely related (Schwarz et al., 2012), are significantly different. Yet, an analysis of the LST characteristics of LCZs can give valuable insights into the general suitability of the LCZ scheme for urban temperature studies in different macroclimate regions.

The focus here is on the built (or urban) LCZ types (i.e. LCZ 1–10), not because we want to supplant the non-built (or land cover) types from the discussion about LCZs, but because the built types are the most central to urban planning and design. Also, the relationship among built types is the most challenging due to minor differences in the geometric, surface cover and thermal properties of some LCZ types, e.g. between LCZ 3 (compact low-rise) and LCZ 7 (lightweight low-rise) or between LCZ 6 (open low-rise) and LCZ 9 (sparsely built) (Bechtel et al., 2017; Johnson and Jozdani, 2019). Furthermore, LST variations among LCZ built types are less studied under different macroclimatological conditions, compared to land cover types which have gained a lot of attention in the surface urban heat island (SUHI) literature in general (Geletič et al., 2019).

The chapter is structured as follows: firstly, the different datasets utilized, and the methods applied to acquire, process and statistically analyze the data are introduced in Section 8.2. Section 8.3 presents the results of the experiments, followed by a discussion of the findings in Section 8.4; and finally, in Section 8.5 the main conclusions are presented.

8.2. Data and methods

This section comprises four subsections that introduce the datasets used and explain the different methods applied in this work. Section 8.2.1 introduces the macroclimate classification system underlying our study, while Section 8.2.2 explains the basis on

which global LCZ site metadata were collected and processed. In Section 8.2.3, the methodology for retrieving multi-year LST data at the LCZ level is explained and Section 8.2.4 explains the different statistical procedures that have been applied to analyze the LCZ–LST relationship.

8.2.1. World macroclimate regions

The Köppen–Geiger climate classification system (Köppen and Geiger, 1936), first developed in the 19th century by Wladimir Köppen, is among the most used climate classification systems to study earth's climate and biome at a large scale based on vegetation characteristics and precipitation–temperature relationship. The classification combines five main classes and 30 subclasses (Figure 61) and it is widely used for, but not limited to, assessing the impacts of climate change, ecological modeling and evaluating the output of global climate models (H. E. Beck et al., 2018; Peel et al., 2007). The five main macroclimate classes are the tropical (A), the arid (B), the temperate (C), the cold (D) and the polar (E). Subclasses are described by adding to the main classification, a second and a third letter to denote the monthly and annual precipitation and temperature characteristics, respectively. More details about the criteria and threshold values for defining each of the main and subclasses can be found, e.g. in (H. E. Beck et al., 2018, p. 5) or in (Peel et al., 2007, p. 462).

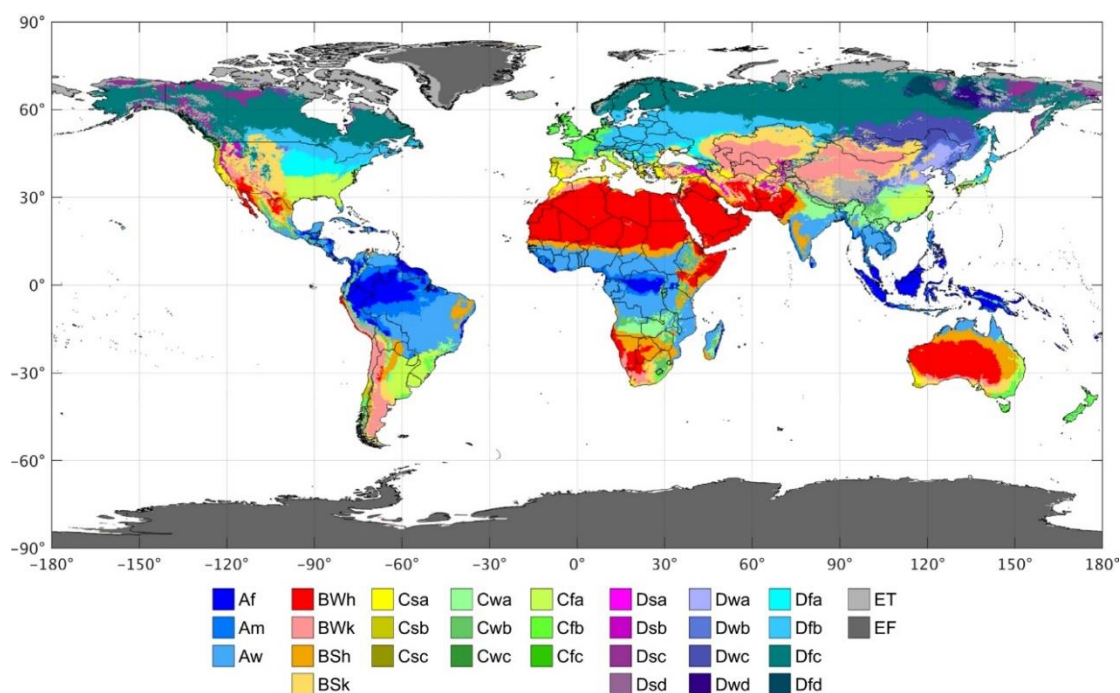


Figure 61. Köppen–Geiger climate classification map (1980–2016) at 1-km spatial resolution. Reproduced from (H. E. Beck et al., 2018, p. 3).

Recently, different versions of the Köppen–Geiger map were developed and made available, at different spatial resolutions and with different classification accuracies, using global precipitation and air temperature datasets, (e.g. H. E. Beck et al., 2018; Kottek et al., 2006; Kriticos et al., 2012; Peel et al., 2007). In particular, the updated Köppen–Geiger map of Beck et al. (2018) provides the highest spatial resolution (~

1000 m) and classification accuracy (80%) among all the other maps, as it is based on a large number of stations from different topographically-corrected datasets. The map is freely available online at <http://www.gloh2o.org/koppen> in GeoTIFF format and comes with the World Geodetic Reference System 1984 (WGS 84) ellipsoid and will be used in this study for the subsequent analysis to attribute the macroclimate class to the LCZ sites.

8.2.2. LCZ sample sites

As discussed in Chapter 6, classifying local areas into LCZs is not an easy task as it requires collecting enough site metadata about the urban surface properties empirically defined by Stewart and Oke (2012). This becomes even more challenging and time consuming in a wider study that includes a large number of local sites. Stewart and Oke (2012) suggested that if it is not possible to collect relevant geometric and surface cover properties information, other secondary sources can be useful to obtain site metadata (e.g. aerial photographs, land use/land cover classifications, satellite images).

In Chapter 6, we gave an introduction to the World Urban Database and Access Portal Tools (WUDAPT) participatory project (Bechtel et al., 2015), which aims to build a global climate-relevant urban database and generate LCZ remote sensing-based classifications for cities worldwide based on training data collected via crowdsourcing. However, we indicated that the output LCZ maps of WUDAPT are generally of moderate overall accuracy (50%–60%), mainly due to limitations in the input training data in terms of accuracy and sufficiency (Bechtel et al., 2019a). We also highlighted that the LCZ maps of WUDAPT are generated based on Landsat multi-spectral and thermal imagery, which implies some uncertainty over using the WUDAPT dataset in subsequent studies to analyze the relationship between LCZs and satellite-derived LSTs. Nevertheless, the WUDAPT raw training data, as originally provided by the community and collected using a standardized protocol, can be a valuable source of neighborhood information if systemically processed and checked for accuracy.

Therefore, we use the WUDAPT raw training data as a basis for this study, where each training polygon is considered a LCZ sample site. However, considering that the data are available on an as-is basis, without any prior quality check, several quality control and processing steps have been applied before the data are utilized for the subsequent analysis. This includes four main steps: (1) completeness and formatting check in Google Earth; (2) data pre-processing in Geographical Information Systems (GIS); (3) accuracy assessment, data cleansing and correction; and (4) data post-processing in GIS. Table 13 describes these steps in more detail and Figure 62 shows some examples of the processed data.

Table 13. Quality control and processing steps for the WUDAPT training data.

Steps	Description
1. Data collection	A. WUDAPT training raw data were downloaded from http://www.wudapt.org/raw-training-area-download/ . The data are freely available in KMZ format under the CC-BY-NC-SA license.
2. Completeness and formatting check in Google Earth	B. The data files were checked for completeness and consistency. Incomplete or missing data files were excluded. C. The built LCZ polygons were checked on a case-by-case basis for the proper formatting in Google Earth, i.e. whether the training polygons have the correct names following the standard LCZ scheme for the built types (1–10).
3. Data pre-processing in GIS	D. The data were exported to GIS, assigned a projection and merged into a single table. E. The data were checked for duplicates, critical intersects and overlaps. Some polygons were merged where possible, while others were excluded. F. Small ¹ or unrepresentative polygons (e.g. those that focus on single buildings or miss the neighborhood context) were excluded (Figure 62a).
4. Accuracy assessment, data cleansing and correction	G. The data were assessed several times by visual interpretation on a case-by-case basis using secondary sources (e.g. multi-year Google satellite imagery, Google street view, georeferenced images), where: <ul style="list-style-type: none"> i. Training polygons of sites that could be hardly interpreted or are too heterogenous were excluded (Figure 62a). The same was applied to training polygons of sites that are not persistent over time (e.g. those that have recently changed in structure or no longer exist) (Figure 62b). ii. Training polygons that were misinterpreted by original operators and were assigned a certain LCZ type, were reclassified (Figure 62c). iii. Training polygons that needed minor boundary line adjustment for more homogeneity and better match with LCZ types were modified.

(continued)

Table 13 (continued)

Steps	Description
5. Data post-processing in GIS	<p data-bbox="582 580 2051 687">H. Training polygons with too large areas relative to their LCZ mean area², were selected and reduced in area or split, where possible, into multiple polygons with radius consistent with the other training polygons. The LCZ polygons have an average area of about 0.61 Km².</p> <p data-bbox="582 711 2051 746">I. Polygons with very complex shapes were selected³ and simplified or split into multiple polygons where possible.</p> <p data-bbox="582 770 2051 836">J. In order to obtain more homogenous polygons of at least 200-m diameter, narrow extensions in polygons were removed by creating a 100-m-radius inward buffer followed by an outward buffer of the same radius.</p>

¹ LCZs span from one hundred meters to several kilometers (10^2 to 10^4 m) (Stewart and Oke, 2012). Polygons with a diameter less than 200 m are too small for the subsequent analysis to interpolate the Landsat-derived LST data (obtained at 100 m and resampled to 30 m) to the LCZ polygons (see Section 8.2.3).

² Values outside the range (± 3.5 times the standard deviation) were considered data outliers (Tsiptsis and Choriantopoulos, 2010).

³ Polygons with very complex shapes were selected by using a threshold value (defined on a trial basis) of a shape index (Reock, 1961).

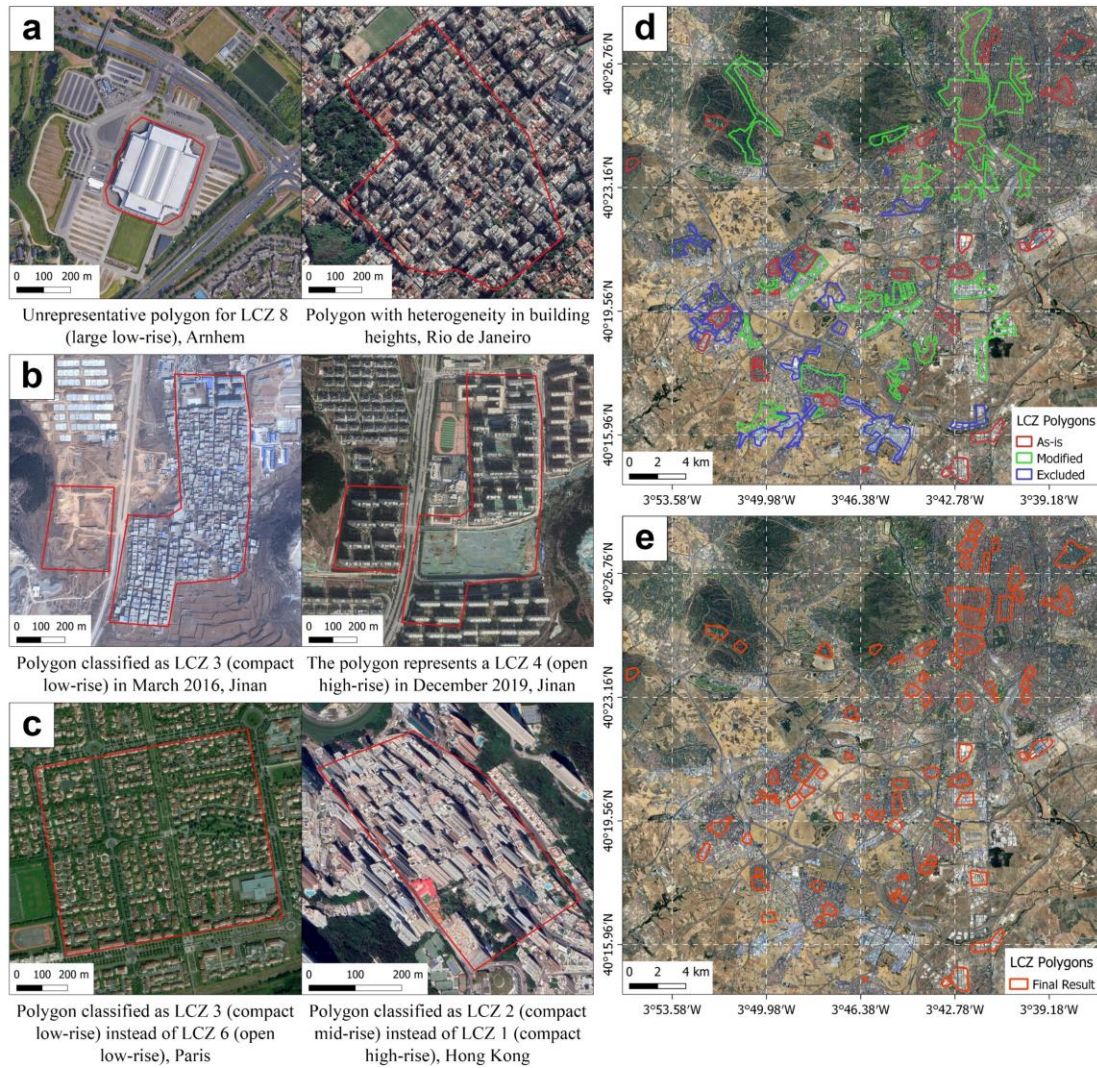


Figure 62. Examples of the quality control and the processed WUDAPT raw training data. (a) Excluded unrepresentative/heterogeneous LCZ polygons; (b) Excluded LCZ polygon representing site that is not persistent over time; (c) Reclassified LCZ polygons; (d) Range of LCZ polygons across Madrid, Spain distinguished for processing; (e) Final LCZ polygons after quality control and processing.

From a total of 7117 built LCZ polygons (the raw data collected from 86 cities available in the WUDAPT database), 5013 were obtained after applying all the aforementioned steps (Table 13). Next, considering that the number of polygons is biased toward certain macroclimate regions, we have added additional LCZ polygons in the less represented regions in order to obtain an adequate sample size and distribution per LCZ and macroclimate region. More specifically, additional 409 LCZ polygons were digitized following the standard WUDAPT protocol and the criteria described in Table 13. The new LCZ polygons were digitized mostly in cities or regions where the author has familiarity with the local context, or the types were easily identifiable. These are Brasilia, Brazil (tropical); Bucharest, Romania (cold); Dubai, United Arab Emirates (arid); Cairo, Egypt (arid); Luanda, Angola (arid); Miami, United States of America (tropical); Nile delta, Egypt (arid); Sharjah, United Arab Emirates (arid); Tehran, Iran (arid); and Toronto, Canada (cold). Furthermore, additional LCZ D (low plants) polygons were digitized in the newly added locations (126 polygons) or were retrieved from the WUDAPT database (1017 polygons) without further quality control or processing as this LCZ type is easily identifiable and it is usually recognized consistently by operators (Bechtel et al., 2017). The LCZ D polygons will be used as a reference (cool) LCZ type to estimate the SUHI intensity and consistently compare LCZs across macroclimate regions (see Section 8.3.3). The macroclimate class (described in Section 8.2.1) was attributed to each built LCZ polygon that is completely contained within, and polygons overlapping two or more macroclimate regions were excluded (30 polygons). The distribution of the total number of polygons per LCZ and macroclimate region and the geographic distribution of LCZ polygons, grouped by city, are given in Figure 63 and Figure 64, respectively.

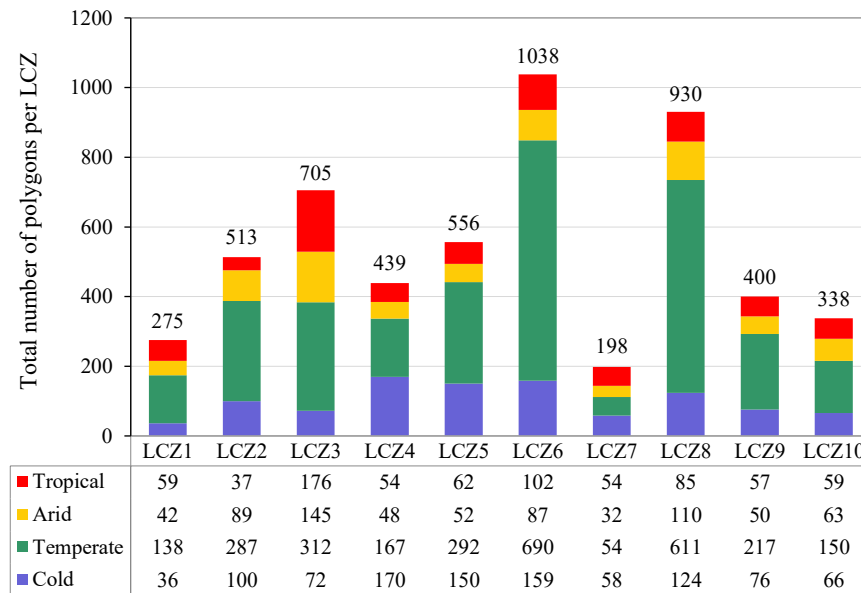


Figure 63. The distribution of the total number of polygons (5392) per LCZ and macroclimate region; the tropical (745), the arid (718), the temperate (2918) and the cold (1011).

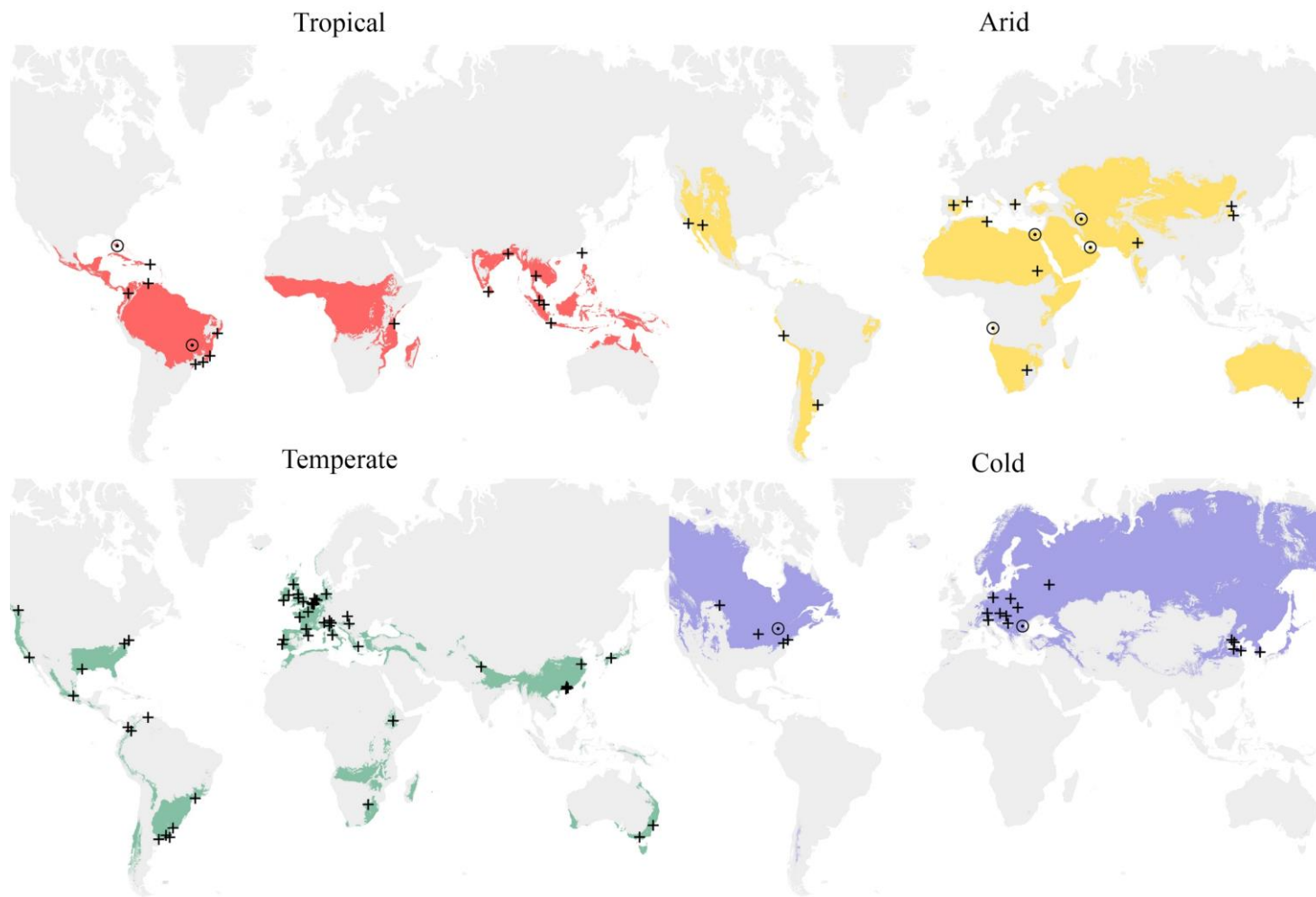


Figure 64. The geographic distribution of LCZ polygons (grouped by city) for each macroclimate region. Circled dots indicate the newly added locations.

8.2.3. LST retrieval

To ensure good representation of LST data and, in turn, greater certainty over the results of LCZs' surface temperature studies, it is recommended to use long time series of satellite imagery to calculate LST rather than only a single or few satellite images (Bechtel et al., 2019b). Therefore, for this study, we retrieved multi-year LST data. LST can be calculated from top of atmosphere (TOA) radiances measured by thermal infrared (TIR) sensors onboard satellites after correcting for the effects of the atmosphere, the viewing angles and the surface emissivity (Tomlinson et al., 2011). The Single-Channel (SC) algorithm developed by Jiménez-Munoz and Sobrino (2003) and updated and extended in (Jimenez-Munoz et al., 2014, 2009) applies a generalized formula to retrieve LST from Landsat satellite imagery assuming that the surface emissivity is known and can be calculated based on the Normalized Difference Vegetation Index (NDVI). As discussed in the previous chapters, the NDVI is a measure of vegetation intensity and it ranges from -1 to 1. High NDVI values ($\sim .60-.90$) indicate dense vegetation, while low values, close to zero, correspond to built-up areas, bare soil or sand.

Based on the above principles, multi-year LST data were automatically retrieved from Landsat imagery by running the SC algorithm, implemented by Nill et al. (2019) in Google Earth Engine. The python script²⁸ was customized to automate image extraction and LST calculation using a user-defined CSV file with the coordinates of the bounding boxes containing LCZ polygons belonging to the same city or region. Furthermore, the script was used to calculate multi-year NDVI to support the subsequent discussion in Section 8.4.2. For this study, all the Landsat 7 and Landsat 8 raw images available on Google cloud, acquired from January to December of 2017 to 2019, and with a 60% maximum cloud cover were utilized to calculate LST and NDVI. Figure 65 shows some examples of the retrieved LST and NDVI images. The LCZ polygons obtained in Section 8.2.2 were overlaid with the LST and NDVI images and each polygon was assigned an average LST and NDVI value based on all the pixels that it overlays. A SUHI value was then calculated for each built LCZ polygon as the difference between the LST of this polygon and the average LST of all the LCZ D polygons falling within the same city or region.

In fact, combining both Landsat 7 and Landsat 8 imagery allows for reducing the 16-days Landsat revisit time as the two satellites have an eight-day offset and thus more images are obtained (three to four per month). However, it should be noted that since 2003, Landsat 7 images have some gaps due to the failure of the Scan Line Corrector (SLC). In this study, the effect of the SLC-off problem can be considered minimal due to: (1) the concurrent use of Landsat 8 imagery; (2) the long time span analyzed; and (3) the fact that the spatial unit of our study is defined by “zones” (or LCZs) and not by individual pixels. Furthermore, Landsat-derived data calculated over a time period are susceptible to cloud contamination, especially when the underlying region has strong seasonality in cloud cover. Indeed, Figure 66a shows that the percentage of missing data in LCZ polygons is particularly high in some months, with an extreme in the cold climate region during winter (e.g. 83% in January). On the other hand, as expected, the lowest percentage of missing data is found in the arid climate region, which is

²⁸ Available online at https://github.com/leonsnill/lst_landsat

also in agreement with Chakraborty et al. (2020). Overall, in the tropical, the arid and the temperate climate regions, the percentage of missing data in the period from February to November (which still represents the four meteorological seasons in both the northern and the southern hemispheres) is relatively low (less than 20%).

In order to assess the influence of the monthly missing data on the mean annual LST calculated for each LCZ type per macroclimate region, we have calculated and compared the mean LST values obtained using five different samples of LCZ polygons with varying levels of missing data (Figure 66b. See Figure 1 in Appendix C for more details). These are: (1) the full dataset (including all polygons); (2) polygons with up to 80% missing data; (3) polygons with 60% missing data or less; (4) polygons with 40% missing data or less; and (5) polygons with 20% missing data or less. In general, the mean difference (for all LCZ types and macroclimate regions) between the full dataset and the dataset of polygons with 20% missing data or less is 0.8 °C. In particular, for the majority of the LCZ types across the tropical, the arid and the temperate climate regions, the mean LST differs 1 °C or less between the two datasets. On the other hand, as expected, in the cold climate region, the effect of missing data on the robustness of the mean LST is more pronounced, where the LST difference exceeds 1 °C in several LCZ types (2, 7, 8 and 9). Moreover, in LCZ 1 and LCZ 4, the percentage of missing data in all polygons is over 60% and 40%, respectively, which makes their LST estimates more uncertain. Overall, in the large majority of cases, the mean LST values of the full dataset are quite stable despite the missing data; and the uncertainty of the LST estimates in some LCZ types, especially in the cold climate region, should be kept in mind when analyzing the findings of this work.

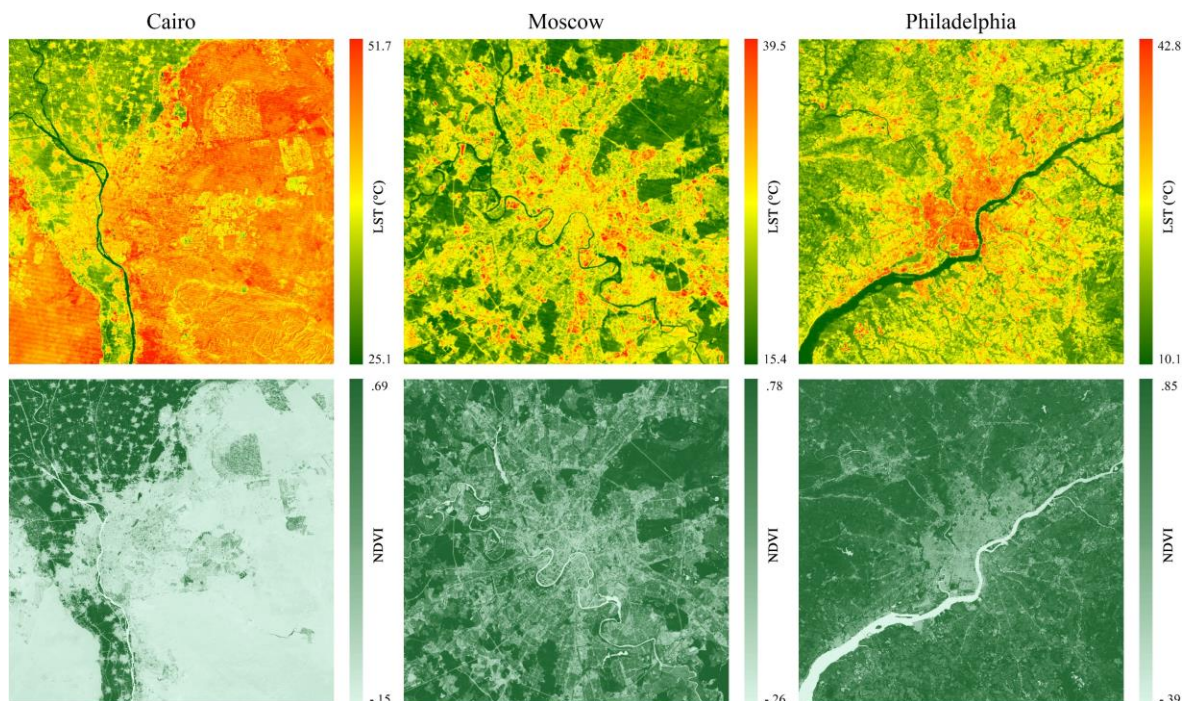


Figure 65. Examples of multi-year LST images (top) and NDVI images (bottom) calculated from Landsat 7 and Landsat 8 imagery between 2017 and 2019 by applying a SC algorithm in Google Earth Engine.

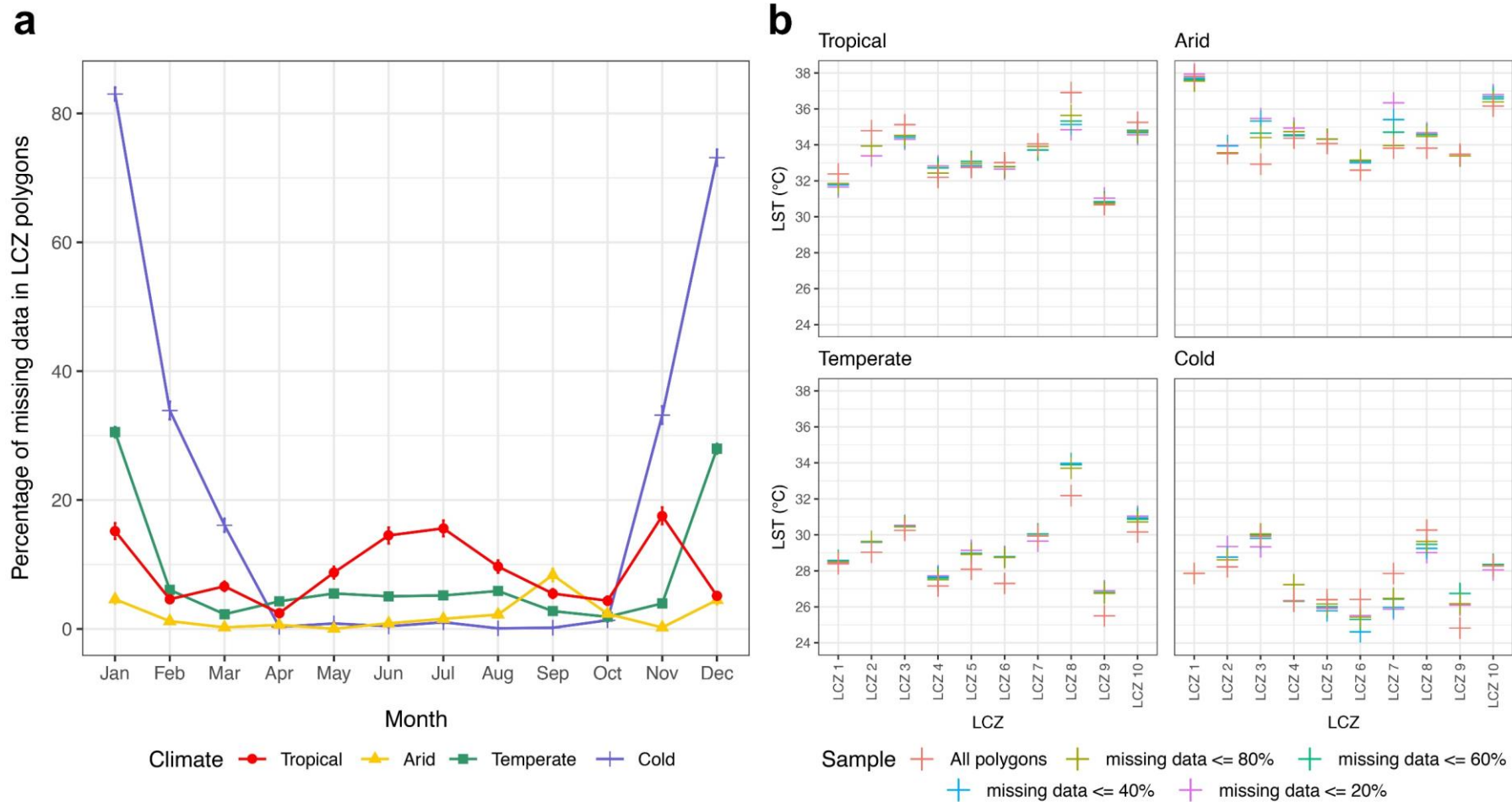


Figure 66. (a) Average percentage of monthly missing data in LCZ polygons per macroclimate region, calculated for every polygon as the ratio between the number of cloudy pixels in a polygon and the total number of pixels in that polygon. Bars represent the standard error of the mean. (b) Comparison between the mean LST values calculated per LCZ type and macroclimate region using different samples of LCZ polygons with varying levels of missing data, from no more than 20% up to 80% of missing data in all months (see Figure 1 in Appendix C for a more detailed plot).

8.2.4. Statistical analysis

The main objective of the statistical analysis is to answer the research questions, by examining independent groups to analyze how high/low their within-group variation is or to make inferences about whether there is a significant difference between them in terms of LST or SUHI magnitude. In particular, groups can be defined for two cases, depending on the research question. In the first case, groups are the LCZ types and they are analyzed and compared within each macroclimate region independently. In the second case, groups represent the four macroclimate regions and they are compared within each LCZ type.

Firstly, in order to describe the LST variability within each of the LCZ types in a macroclimate region and to determine whether there might be a significant difference between LCZ types in terms of LST within the same macroclimate region, box plots were produced. Box plots showing the five-number summary (i.e. the minimum, the first quartile, the median, the third quartile and the maximum) of the LST observations for each LCZ type per macroclimate region can give an indication of the spread or the variability of the observations within each of the LCZ types. In particular, the interquartile range (IQR), i.e. the difference between the first and the third quartiles (represented by the height of the box), reveals the variability of LST values within a given LCZ type. IQR is a robust measure of spread as it contains 50% of the observations and it is not affected by the outliers. Long boxes indicate large IQR and thus more spread or variability, while short boxes indicate small IQR values and less variability. On the other hand, box plots for each of the LCZ types lined up side-by-side help to visually identify whether there might be a significant difference between LCZ types in terms of LST. As a rule of thumb, when the median line of one LCZ type lies entirely out of the box of another type, it is more likely that these two types differ significantly.

However, considering the subjectivity in interpreting box plots, the difference between LCZs (within the same and across different macroclimate regions) was tested more formally using the Kruskal–Wallis test (Kruskal and Wallis, 1952) and the Welch's Heteroscedastic F Test with Trimmed Means and Winsorized Variances (Welch, 1951). The Kruskal–Wallis test is a non-parametric method that does not assume the normality of the data and it is less sensitive to outliers; however, it does assume homoscedasticity. On the other hand, Welch's Heteroscedastic F Test with Trimmed Means and Winsorized Variances is a robust alternative against the combined effect of non-normality and heteroscedasticity, which violate the main assumptions required to run a parametric one-way analysis of variance (ANOVA), and has high control and power over the Type I error (Cribbie et al., 2012; Dag et al., 2018; Keselman et al., 2008, 2002). Trimming and winsorizing (or winsorization) are statistical procedures to substitute the normal mean and variance by trimmed and winsorized ones so that the test is insensitive to the effect of the extreme values in the data. Good practices have shown that a symmetric trimming percentage of around 20% has good control over the Type I error (Cribbie et al., 2012; Wilcox, 1998a, 1998b, 1996). The normality

assumption was assessed using Shapiro–Wilk test (Shapiro and Wilk, 1965) and histograms, while the homogeneity of variance was tested using the Fligner–Killeen test (Fligner and Killeen, 1976). Tables 1 and 2 in Appendix C show that there is a significant departure from normality in most of the independent groups and that the homogeneity of variance assumption was not met for the majority of the designs. All the aforementioned tests were implemented using the `onewaytest` package (Dag et al., 2018) in R (Team, 2019).

When a statistically significant difference was found, a post-hoc analysis has followed to make pairwise comparisons and determine which specific groups make the difference in every design. This was done using either the Dunn test (Dunn, 1961) following the Kruskal–Wallis test or the Games–Howell test (Games and Howell, 1976) following the Welch's Heteroscedastic F Test with Trimmed Means and Winsorized Variances. The level of statistical significance is expressed as a p -value and the test results are significant at ($p < .05$). The post-hoc tests were conducted in R using the `rstatix` package (Alboukadel Kassambara, 2020). When comparing LCZs within macroclimate regions, the number of pairwise comparisons showing a significant difference for each LCZ type is an indicator of how well a type is differentiated from all the other types (minimum 0 and maximum 9) in terms of LST as suggested by Geletič et al (2019, 2016). Likewise, the degree to which the LCZ scheme discerns the LST differences among LCZ types in a specific macroclimate region can be determined by calculating the overall percentage of the pairwise comparison tests showing a significant difference from the total number of pairwise comparisons.

Finally, in order to understand the LST profile of identical LCZ types in different macroclimate regions, LCZs were compared in terms of their rank, from highest to lowest mean LST, within each of the macroclimate regions. This helps to identify the LCZ types that have the same ranking position irrespective of macroclimate region or those that change rank in relation to the climate warming trend. The results are presented in Section 8.3.

8.3. Results of the statistical analyses

The results are presented in three separate subsections addressing the research questions. In particular, Sections 8.3.1 and 8.3.2 relate to the first research question regarding the LST variability and difference within and between LCZs in the same macroclimate region, respectively. Section 8.3.3 describes the influence of the macroclimate region on the LST and SUHI characteristics of LCZs based upon comparing the four macroclimate regions for significant differences in LST and SUHI within each LCZ type.

8.3.1. Intra-macroclimate region variability of LST within LCZs

Box plots of the distribution of the LST for each LCZ type per macroclimate region (Figure 67) show that LCZ types in the arid climate region have larger variability compared to all the other macroclimate regions, where the IQR is 4 °C or more, with

an extreme in LCZ 3 of about 13 °C. In contrast, in tropical and cold climate regions, the narrower boxes indicate much lower variability with IQR less than 3.5 °C in all the LCZ types. Likewise, LCZs in the temperate climate region show low variability (IQR < 3.5 °C), but with more exceptions in LCZs 3, 6, 8 and 9, where variability is higher, but not on the same order as in the arid climate region. It is apparent that LSTs of LCZ types are not representative in the arid climate region but are representative in most LCZs in the other macroclimate regions.

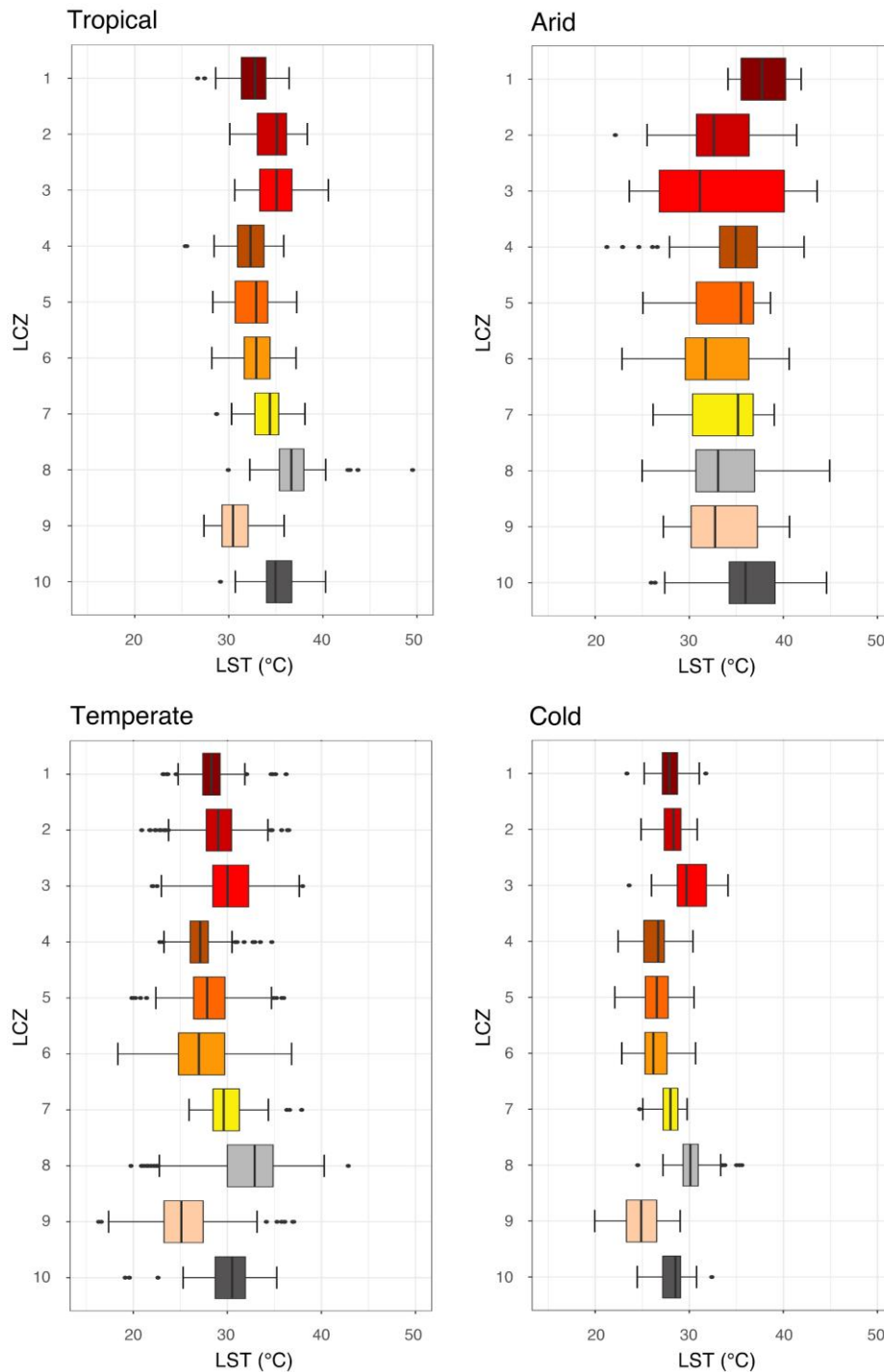


Figure 67. Box plots of the distribution of the LST for each LCZ type per macroclimate region.

8.3.2. Intra-macroclimate region LST differences between LCZs

When comparing the box plots for each of the LCZ types within the same macroclimate region (see Figure 67), it is observed that in the arid climate region, the boxes of most LCZ types overlap, where the median lines are inside the overlap range, suggesting a higher probability for non-significant differences between most LCZ types. In contrast, for many of the LCZ pairwise comparisons within the tropical, the temperate and the cold climate regions, boxes either do not overlap or overlap but do not extend beyond both median lines, indicating that many LCZ types are likely to be different in terms of LST.

In general, the results of the preliminary analyses of variance using the Kruskal–Wallis test and Welch's Heteroscedastic F Test with Trimmed Means and Winsorized Variances show that we can reject the null hypothesis ($p < .05$) and that there is a statistically significant difference between LCZ types in terms of LST in all the macroclimate regions, where smaller p -values show stronger evidence to reject the null hypothesis (Table 14).

Table 14. Summary of the preliminary analyses of variance showing the significance of the difference between LCZ built types in terms of LST within each macroclimate region, where statistic is the test statistics, reported as χ^2 in case of Kruskal–Wallis test and F in case of Welch's Heteroscedastic F Test with Trimmed Means and Winsorized Variances.

Macroclimate region	statistic	p -value	Significant?
Tropical	$\chi^2 = 291.4086$	1.731519e-57	Yes
Arid	$F = 9.42124$	4.235857e-11	Yes
Temperate	$F = 149.9059$	2.269153e-123	Yes
Cold	$F = 92.79138$	5.944351e-64	Yes

More specifically, the results of the Dunn and Games–Howell post-hoc tests show which groups (or LCZ types) differ significantly from others in terms of LST by performing pairwise comparisons between all the possible combinations of groups. The calculated p -values from the pairwise comparisons are reported in the form of a heatmap (Figure 68), where the total number of pairwise comparisons showing a significant difference for each LCZ type is reported at the end of each row (number of hits). Furthermore, Figure 68 shows that the overall percentage of pairwise comparison tests showing a significant difference is 66.67%, 28.89%, 84.44% and 77.78% for the tropical, the arid, the temperate and the cold climate regions, respectively. In particular, in the temperate and the cold climate regions, all types are relatively well differentiated (i.e. with a high number of hits), while in the tropical climate region, the most differentiated types are LCZ 8 and LCZ 9 and the least differentiated one is LCZ 7. In the arid climate region, all the LCZ types are indistinguishable, except LCZ 1 and LCZ 10; these two types have a number of hits equaling eight and five, respectively.

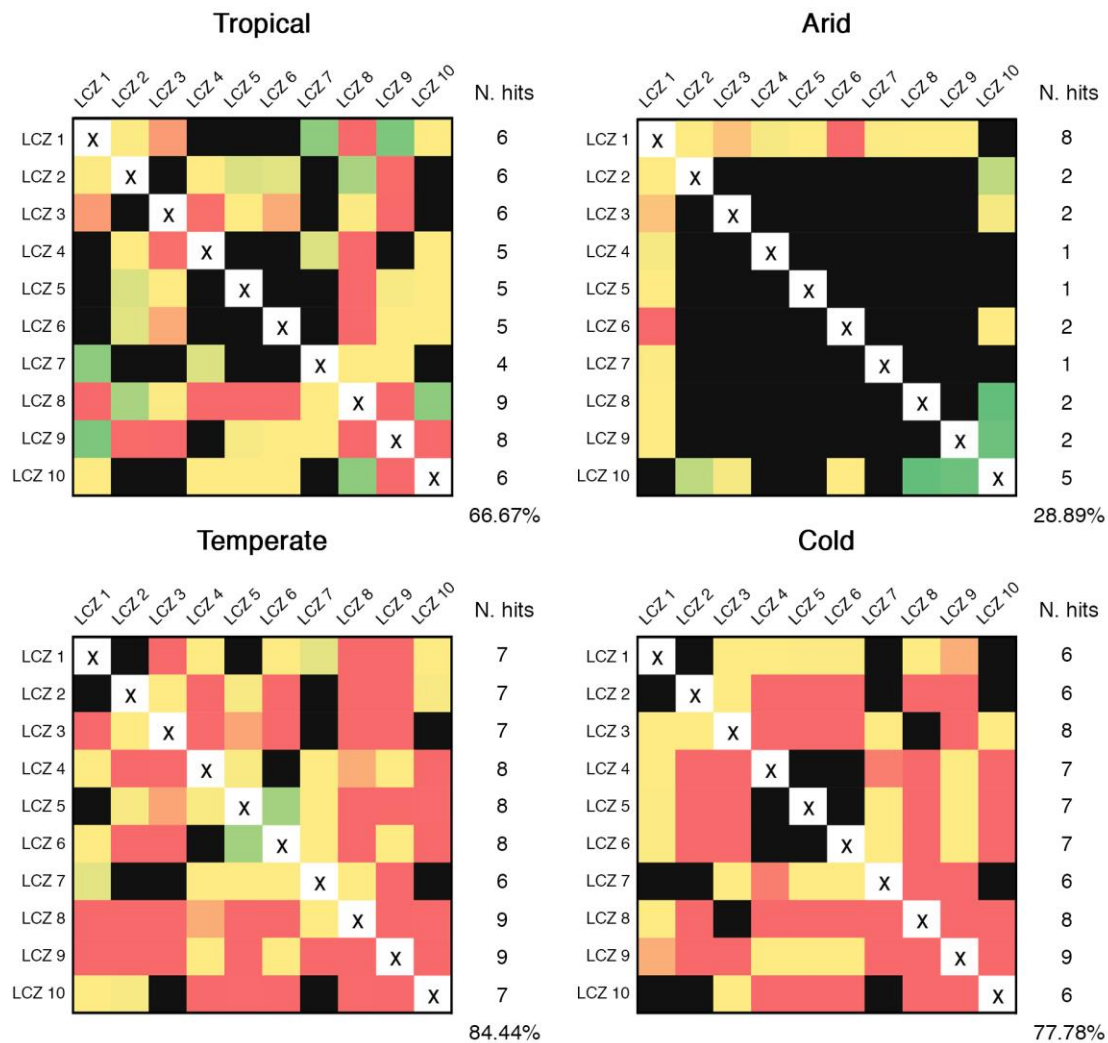


Figure 68. Results of the post-hoc tests to compare LCZ types within each macroclimate region. Black cells indicate no significant difference between LCZ types ($p > .05$), while colors ranging from red to yellow via green indicate higher to lower significance levels at ($p < .05$). The number of hits (N. hits) in significance per LCZ type is indicated at the end of each row. The percentage of hits in all pairwise comparison tests is indicated for each macroclimate region as a (%) value in the bottom right corner.

8.3.3. Influence of macroclimate on the LST/SUHI characteristics of LCZs

As for understanding the impact of climate change and global warming upon the LST and SUHI characteristics of the different LCZ built types, the results from the Kruskal–Wallis test and Welch's Heteroscedastic F Test with Trimmed Means and Winsorized Variances exhibit overall significant differences of LST and SUHI magnitude in identical LCZ types between the different macroclimate regions other than the arid (Tables 15 and 16). The relatively small number of LCZ pairwise comparisons showing a significant difference in the arid climate region (see Figure 68) makes its comparison with other macroclimate regions hard to interpret, and therefore it is disregarded in this part of the study.

Table 15. Summary of the preliminary analyses of variance showing the significance of the difference between the macroclimate regions, other than the arid, in terms of LST within each LCZ built type, where statistic is the test statistics, reported as χ^2 in case of Kruskal–Wallis test and F in case of Welch's Heteroscedastic F Test with Trimmed Means and Winsorized Variances.

LCZ	statistic	p -value	Significant?
LCZ 1	$\chi^2 = 91.65675$	1.250227e-20	Yes
LCZ 2	$F = 113.9555$	2.807201e-20	Yes
LCZ 3	$F = 198.9181$	4.206739e-40	Yes
LCZ 4	$F = 178.0843$	3.126028e-30	Yes
LCZ 5	$F = 130.6348$	1.730471e-28	Yes
LCZ 6	$F = 351.5512$	4.4269e-62	Yes
LCZ 7	$F = 198.7589$	9.625253e-27	Yes
LCZ 8	$F = 353.7566$	6.656014e-56	Yes
LCZ 9	$F = 132.8978$	3.721279e-28	Yes
LCZ 10	$F = 162.3325$	2.267425e-29	Yes

Table 16. Summary of the preliminary analyses of variance showing the significance of the difference between the macroclimate regions, other than the arid, in terms of SUHI within each LCZ built type, where statistic is the test statistics, reported as χ^2 in case of Kruskal–Wallis test and F in case of Welch's Heteroscedastic F Test with Trimmed Means and Winsorized Variances

LCZ	statistic	p -value	Significant?
LCZ 1	$F = 11.98948$	4.146439e-05	Yes
LCZ 2	$F = 6.453098$.002930074	Yes
LCZ 3	$F = 13.79835$	2.960568e-06	Yes
LCZ 4	$F = 9.09373$.0002900644	Yes
LCZ 5	$F = 4.267188$.01691539	Yes
LCZ 6	$F = 14.17087$	2.286361e-06	Yes
LCZ 7	$F = 0.3963259$.6748202	No
LCZ 8	$\chi^2 = 17.07781$.000195704	Yes
LCZ 9	$F = 1.286808$.282721	No
LCZ 10	$F = 8.449515$.0004818551	Yes

Results from the Dunn and Games–Howell post-hoc tests show that the LST of most LCZ types has changed significantly from one macroclimate region to another (Figure 69). The only exceptions are for LCZs 1, 3 and 9; these three types do not show significant differences between the temperate and the cold climate regions. As expected, the LSTs of all LCZ types are significantly peaked in the tropical climate region, as tropics receive a considerable amount of solar radiation compared to all the other macroclimate regions. More specifically, there is an overall increase in the LST of all the LCZ types of about 4 °C or more from the cold or the temperate climate regions to the tropical climate region compared to a maximum increase of about 2 °C from the cold to the temperate climate region.

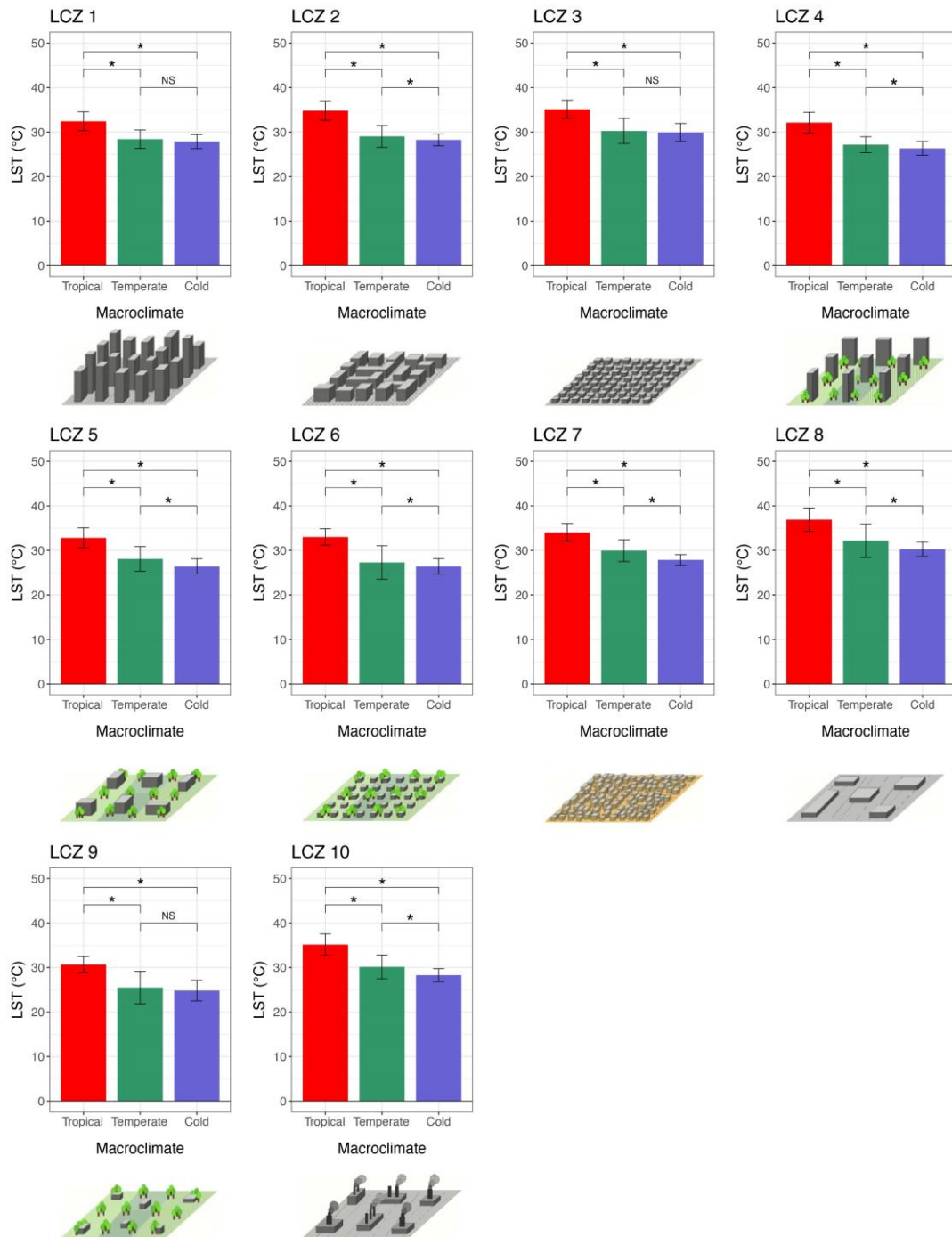


Figure 69. The mean LST of each LCZ type across the tropical (red), the temperate (sea green) and the cold (slate blue) climate regions. Bars represent standard deviation, NS stands for not significant and asterisks indicate significant differences between group pairs at ($p < .05$), as calculated by the post-hoc tests.

On the other hand, Figure 70 shows that in six out of 10 LCZs, the SUHI intensity significantly increases by 0.6 °C or more with a warmer climate. More specifically, in LCZs 2, 3, 6 and 8, there is a significant increase in SUHI intensity from the temperate or the cold climate regions to the tropical climate region, while, in LCZ 5 and LCZ 10 the only significant differences are found between the temperate and the cold climate

regions. In contrast, in LCZ 1, the SUHI intensity significantly decreases by 1 °C or more as global temperature increases from the cold climate region to the temperate or the tropical climate regions. Similarly, in LCZ 4 the SUHI intensity significantly decreases from the cold to the temperate climate region, but not on the same order as in LCZ 1, where the magnitude of the difference is only 0.4 °C. In the case of LCZ 7 and LCZ 9, the warmer climate has no significant impact on the SUHI intensity.

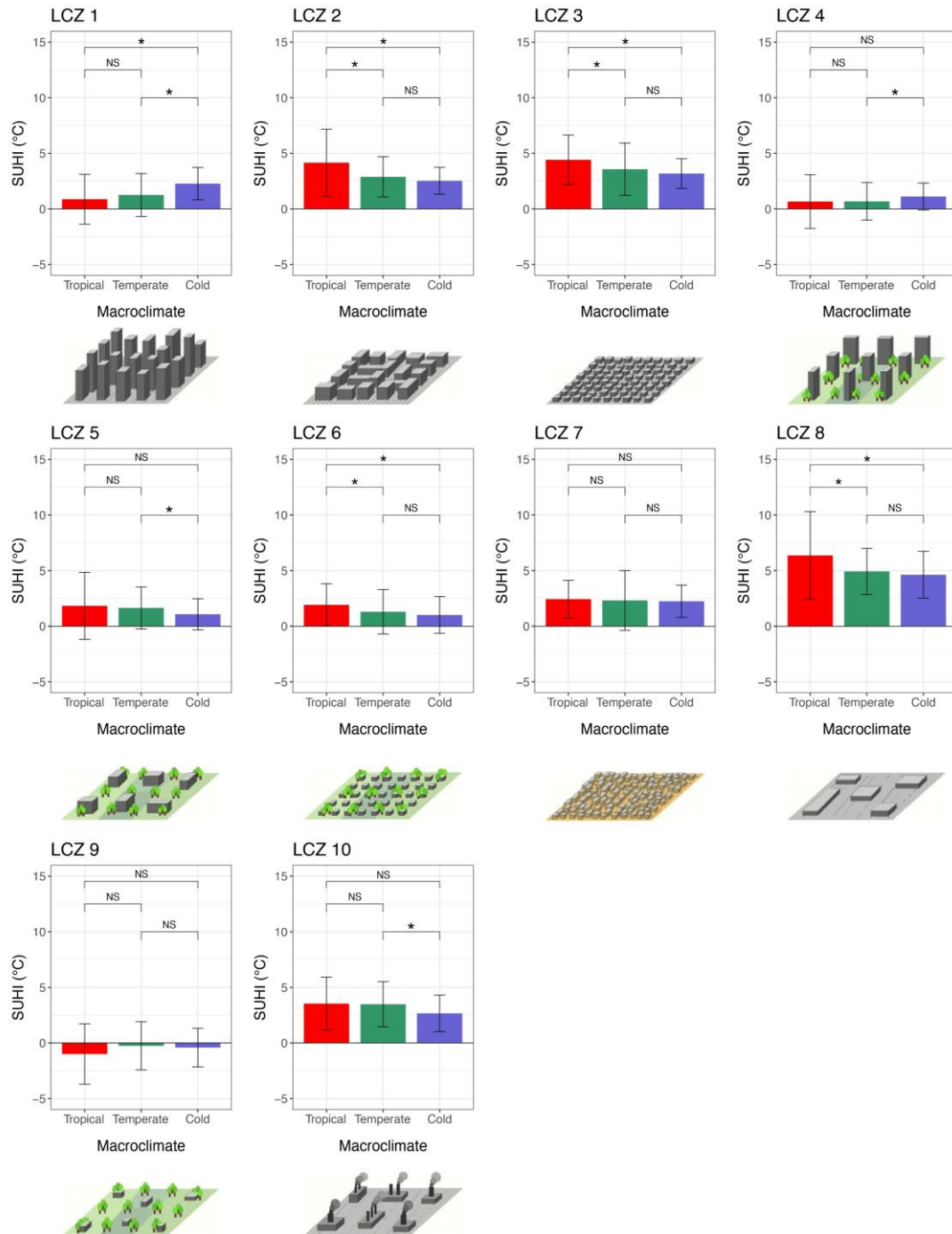


Figure 70. The mean SUHI intensity of each LCZ type across the tropical (red), the temperate (sea green) and the cold (slate blue) climate regions. Bars represent standard deviation, NS stands for not significant and asterisks indicate significant differences between group pairs at ($p < .05$), as calculated by the post-hoc tests.

Furthermore, when comparing identical LCZs ranked by mean LST, from highest to lowest, within each of the three macroclimate regions (Table 17), it is observed that most LCZ types tend to have a similar or very close ranking position, independent of the macroclimate region. For instance, LCZs 4, 8 and 9 keep the same rank across the three macroclimate regions. In particular, LCZ 8 is ranked first, whereas LCZ 9 and LCZ 4 exhibit the lowest and the second-lowest LSTs, respectively. On the other hand, there is a variation of one ranking position in the case of LCZs 2, 3, 5 and 10 and two ranking positions in the case of LCZ 6 and LCZ 7. LCZ 1 exhibits a larger variation in rank (from fifth in cold to sixth and eighth in temperate and tropical climate regions, respectively). However, despite this variation, most LCZ types can be expected to have a similar LST rank irrespective of the macroclimate region, so planning and design guidelines are consistent and applicable in different regions.

Table 17. LCZs' rank in terms of mean LST from 1 (highest) to 10 (lowest) within the tropical, the temperate and the cold climate regions.

Rank	Tropical		Temperate		Cold	
	LCZ	Mean LST (°C)	LCZ	Mean LST (°C)	LCZ	Mean LST (°C)
1	LCZ 8	36.92	LCZ 8	32.18	LCZ 8	30.27
2	LCZ 10	35.15	LCZ 3	30.25	LCZ 3	29.92
3	LCZ 3	35.12	LCZ 10	30.16	LCZ 10	28.28
4	LCZ 2	34.79	LCZ 7	29.95	LCZ 2	28.23
5	LCZ 7	34.05	LCZ 2	29.03	LCZ 1	27.87
6	LCZ 6	33.01	LCZ 1	28.39	LCZ 7	27.86
7	LCZ 5	32.82	LCZ 5	28.09	LCZ 6	26.42
8	LCZ 1	32.42	LCZ 6	27.30	LCZ 5	26.41
9	LCZ 4	32.12	LCZ 4	27.16	LCZ 4	26.35
10	LCZ 9	30.67	LCZ 9	25.50	LCZ 9	24.83

8.4. Discussion

8.4.1. LCZs and LSTs

The main finding of this study suggests that the urban LCZ scheme is suitable, with varying degrees, for urban (surface) temperature studies in all the macroclimate regions other than the arid. This is an important finding for urban planning and design as we can conclude that LCZs can provide an evidence-based tool to guide decisions on urban form and function in cities in three out of four macroclimate regions. LCZs are described using climate-influencing parameters that are typically used by architects, urban designers and planners, e.g. building heights, street aspect ratio, building density (Stewart and Oke, 2012). Hence, they can be applied during the different planning or design stages to provide valuable urban climate information at the local scale (Perera and Emmanuel, 2018). For example, in the early planning or design processes, LCZ maps can help to identify heat-stressed areas and critical hot spots within the city in terms of absolute temperatures or UHI magnitudes (e.g. LCZ 8, 3 and 10). Furthermore,

the LCZ scheme provides quantifiable metadata about the morphological, surface cover, thermal, radiative and metabolic properties of local urban areas, which can be incorporated into local building regulations and design/planning codes.

The results showed that there is a larger variability in LST within each of the LCZ types in the arid climate region compared to all the other macroclimate regions, which means that LSTs of LCZ types are not representative in arid climate regions, but are representative in most LCZs in the other macroclimate regions. Furthermore, when the different LCZ built types were compared for differences in LST within each of the macroclimate regions, it was found that in the tropical, the temperate and the cold climate regions, there are statistically significant differences between most of the LCZ types, whereas in the arid climate region, the differences between almost all the LCZ pairs are insignificant.

The second question raised in this chapter concerned the expected impacts of climate change on LST and SUHI characteristics of the standard LCZ built types in urban areas and their relative exposure to high-temperature hazards if no action is taken. Results showed, not surprisingly, that LSTs and SUHI magnitudes of the majority of the LCZ built types have significantly increased with warmer macroclimates. In the light of shifting world macroclimate regions, where some regions are changing more than others toward a warmer or drier climate (Fraedrich et al., 2001; Jylhä et al., 2010; Mahlstein et al., 2013), this is a result that should be investigated in more depth in further studies. Furthermore, results showed that in three out of four macroclimate regions, the commercial/light industrial, compact and heavy industry LCZ types are associated with relatively higher LST patterns compared to the other built types, which is in agreement with previous studies (e.g. Bartesaghi Koc et al., 2018; Budhiraja et al., 2017; Geletič et al., 2016; Ochola et al., 2020). More specifically, LCZ 8 (large low-rise), LCZ 3 (compact low-rise) and LCZ 10 (heavy industry) exhibit the highest LSTs in the tropical, the temperate and the cold climate regions. This can be explained by the abundance of impervious surface cover and the increased solar gains with the low building heights and thus minimal shadow casting. The latter also explains the lower LSTs of the compact high-rise type (LCZ 1) during daytime compared to all other compact types (i.e. LCZ 2 and LCZ 3), where shadows cast by tall buildings reduce the amount of solar radiation received by ground surfaces, and confirms previous studies (e.g. Bechtel et al., 2019b; Carnahan and Larson, 1990; Nassar et al., 2016; Nichol, 2005; Sobrino et al., 2013). LCZ 1 seems to be particularly a persistent type to high diurnal LSTs as it exhibits a lower SUHI magnitude and drops in LST rank as the global surface temperature rises (ranked fifth in the cold climate region versus eighth in the tropical climate region), as opposed to, e.g. LCZ 7 (lightweight low-rise) that increases in rank as it gets warmer from cold (ranked sixth) to temperate (ranked fourth) or tropical (ranked fifth) climate regions. LCZ 9 (sparsely built), on the other hand, is the built type with the lowest LST and negative SUHI in all the three macroclimate regions, as this type is mostly located in peripheral areas (e.g. suburbs) with very low built density (10%–20%) and abundance of natural cover.

8.4.2. Extending LCZs with land cover properties to address arid regions

More research is needed to complement or adapt the standard LCZ types that do not perform well in arid or desert regions for urban (surface) temperature studies. Such a study should identify the urban surface properties (i.e. fabric, land cover, morphology and urban metabolism) that are needed to better explain the varying local climates of these regions. Our current hypothesis is that soil moisture might be one variable that needs to be considered to better capture variations in LST in arid regions, and is discussed below.

In the LCZ scheme, land cover is mainly described as either paved or hard packed with few or no trees in case of the compact types or with an abundance of plant cover and scattered trees in case of open types, all under intermediate soil moisture levels (Stewart and Oke, 2012). However, in arid or desert areas, the same surface cover can vary extremely in terms of water content. For instance, Gamo et al. (2013) identified four categories of land that can exist in arid areas based on the annual degree of aridity and vegetation cover, and which range from severe deserts and semi-arid areas to relatively more humid areas, but with poor vegetation or areas with an abundance of vegetation cover despite aridity (e.g. in river basins). Furthermore, in arid areas, soil moisture significantly depends on air humidity (Ravi et al., 2004). This can result in very different LST profiles from those associated with the standard LCZ types as LST is greatly influenced by changes in soil moisture, especially in arid regions (Rasul et al., 2016). Dry soil has low heat capacity which leads to higher LST during the daytime and lower temperatures during the nighttime, whereas relatively higher soil moisture levels can significantly reduce LST through evaporative cooling. This LST–soil moisture relationship explains the reason for the urban cool island observed in many arid areas during the daytime, where built-up areas are less warm than the surrounding dry desert areas due to relatively higher soil moisture from the greening activities in urban areas (Frey et al., 2007; Haashemi et al., 2016; Lazzarini et al., 2015, 2013; Nassar et al., 2016; Rasul et al., 2016).

The LST and NDVI scatter plot, universally known as the surface temperature–vegetation index space (Lambin and Ehrlich, 1996; Sandholt et al., 2002) helps to better highlight this relationship. The LST–NDVI triangular/trapezoidal space (Figure 71) is a conceptual diagram that explains the status of soil moisture or water content based on the relationship between surface temperature and vegetation intensity. The leftmost part represents bare soil cover or built-up areas with an abundance of dry bare soil (upper part of the chart) and saturated bare soil (lower part), while the middle to the rightmost parts of the chart represent areas with partial to full vegetation cover. The upper and lower lines denote the dry and wet edges, respectively. Figure 71 shows that as vegetation is sparse in arid regions, most of the observations lie in the left part of the trapezoidal space; however, they extend vertically between the dry and the wet edges supporting the hypothesis that the large variability in LST per LCZ is mainly due to changes in soil moisture; a factor which is not accounted for in the standard LCZ scheme. In fact, Stewart and Oke (2012) highly recommended utilizing a

subclassification in such cases by using a higher parent class and one or more subclasses, e.g. LCZ 3₄ (compact low-rise with open high-rise) or LCZ 8_B (large low-rise with scattered trees) as well as, if applicable, an additional variable to describe the land cover property (e.g. with bare trees (*b*), snow cover (*s*), dry ground (*d*) or wet ground (*w*)). Nevertheless, this is often neglected or avoided due to the unavailability of surface properties values for the subclasses or due to the difficulty of communication in case of making complex combinations, which interferes with the whole idea of the LCZ scheme. Our study shows that this generalization is acceptable in the tropical, the temperate and the cold climate regions but not in arid climate regions.

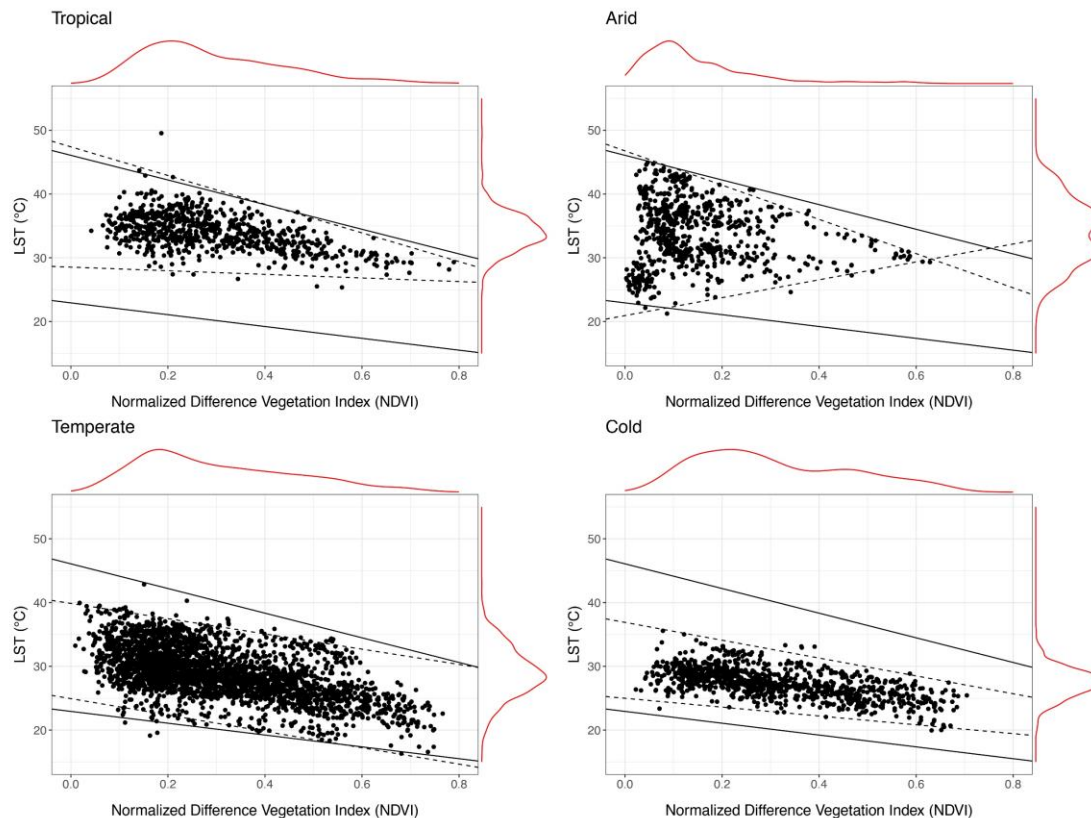


Figure 71. The LST–NDVI scatterplots with marginal histograms for the different macroclimate regions. The black solid lines are the dry (upper) and wet (lower) limiting edges considering all the observations from all macroclimate regions, while the black dashed lines are the limiting edges considering only observations from the underlying macroclimate region.

8.4.3. Limitations of the study

This study has been limited by three main factors, which are related to the quality and resolution of the data used. These are: (1) the aggregation level of the macroclimate classification maps underlying this study; (2) the accuracy of the LCZ site metadata collected; and (3) the temporal resolution of the satellite data employed.

Firstly, although the Köppen–Geiger climate classification maps used (H. E. Beck et al., 2018) are of high classification accuracy (80%) and provide more detail and full

subclassification (i.e. the 30 subclasses), we have only used the four aggregated main classes (i.e. the tropical, the arid, the temperate and the cold) due to limitations in the spatial coverage of the available LCZ data used. In fact, the shortcomings found in applying the LCZ classification scheme to arid regions, can in part be related to the missing macroclimate subclassification, where to some extent the influence of coastlines or oceans and of elevation is accounted for.

Secondly, although the LCZ site metadata, collected via crowdsourcing, have been systematically processed and checked for accuracy following the steps in Table 13, it is possible that some mistakes remain, especially given the large number of LCZs employed. In fact, this is a typical problem of crowdsourcing relying on human interpretation which can be biased particularly with certain LCZ types, e.g. between LCZ 3 (compact low-rise) and LCZ 7 (lightweight low-rise), where the interpretation of compact development versus lightweight development can be challenging, or between LCZ 6 (open low-rise) and LCZ 9 (sparsely built) (Bechtel et al., 2019a, 2017).

Thirdly, although satellites have achieved remarkable advances for studying urban climate, there are still limitations in their application, at least when using the freely available data. For instance, most satellite sensors do not provide a full view of the urban surface, where usually vertical surfaces (e.g. building walls) and other shadowed areas are not represented (Bechtel et al., 2019b; Coutts et al., 2016; Keramitsoglou et al., 2012; Oke et al., 2017; Sobrino et al., 2012; Tomlinson et al., 2011). Furthermore, there is a big trade-off between spatial and temporal resolutions of the freely available satellite data (Bechtel et al., 2019b; Sismanidis et al., 2015). For instance, although the Moderate Resolution Imaging Spectroradiometer (MODIS) imagery is available on a daily basis (for both daytime and nighttime), it has a coarse spatial resolution (~ 1000 m). On the other hand, Landsat 7 and Landsat 8 satellites (which were used in this study) can be used to derive LST data at a moderate spatial resolution (~ 30 m after resampling); however, they have low imaging frequency or revisit time (one image every 16 days), which makes the data sample particularly susceptible to cloud contamination, especially in regions that witness strong seasonality in cloud cover. Although we have tried to overcome this limitation by combining multi-year imagery from both satellites (which have an eight-day offset), the percentage of missing data in LCZ polygons is high in some months. In particular, in the cold climate region, there is a strong seasonality in the cloud cover compared to all the other macroclimate regions which implies some uncertainty over the results obtained for this climate region. More specifically, the low variability in LST measured in the cold climate region can be in part a result of a sampling bias due to the higher percentage of missing data in the winter months, and hence some seasonal variation in LST not being represented. Likewise, the finding that LCZ 1 and LCZ 4 exhibit lower SUHI magnitudes as the global temperature increases from the cold to the temperate or the tropical climate regions is uncertain considering the higher percentage of missing data in the winter months in these two specific LCZ types in the cold climate region. Although one could have considered only the months with minimum cloud cover (from April to October) to avoid the problem, in a global comparative study the seasons are different between hemispheres and hence

the comparison within the same and across different macroclimate regions would be inconsistent.

Furthermore, the LST data are only for daytime (at around 10:00 AM, local time), which is a disadvantage of Landsat imagery in general. The urban climate phenomena vary widely between day and night and across seasons and that is why it is necessary to account for such variability when studying the LST characteristics of LCZs by employing both daytime and nighttime LST data.

8.4.4. Further investigations

Future research on the relationship between macroclimate regions and LCZs' surface temperatures should first investigate whether using a macroclimate subclassification implies significantly different findings from what was concluded in this study. However, this will require employing more LCZ samples. Additionally, considering that several studies have demonstrated that LCZs exhibit significant diurnal and seasonal variation of LST (Geletič et al., 2019, 2016; Gémes et al., 2016; C. Wang et al., 2018), a more comprehensive study that accounts for diurnality and seasonality should be considered to confirm the findings of this chapter regarding the global suitability of the LCZ scheme for urban (surface) temperature studies. On the one hand, seasonality should be studied considering a longer time span to obtain enough monthly satellite images and preferably using a composite LST product to minimize the percentage of missing data due to clouds. For example, using the MODIS 8-day composite LST product can relatively improve the clear sky coverage and reduce noise (Chakraborty et al., 2020; Hu and Brunsell, 2013); however, this will require a new LCZ dataset due to the mismatch between MODIS spatial resolution (~ 1000 m) and the LCZ data (area ~ 0.61 Km²). In any case, one can expect a good agreement between MODIS and Landsat LST/SUHI estimates. In a study analyzing the SUHIs across 50 cities using the LCZ scheme, Bechtel et al. (2019b) used and compared multi-year acquisitions from both MODIS Terra and Landsat 8, and found a high correlation ($R = .87$) between the daytime SUHI intensities (using all cities and all LCz types). On the other hand, studying diurnal/nocturnal variations will require a new LST dataset, where nighttime TIR satellite imagery, at an adequate spatial resolution, should be employed (e.g. ASTER satellite imagery). Finally, further research is needed to confirm the hypothesis discussed in Section 8.4.2 about extending the LCZ scheme with other local variables (e.g. degree of soil moisture) to complement the standard LCZ scheme for urban (surface) temperature studies in arid regions.

Chapter 9

Combining environmental and social dimensions in the typomorphological study of urban resilience to heat stress in Sixth of October, Egypt²⁹

So far, we have discussed different climatological-/environmental-based and typomorphological methods (with a focus on the local climate zone [LCZ] classification scheme) for studying the impact of urban form on urban climate and, in turn, on people's health and thermal sensation (i.e. the environmental/engineering dimension of heat-stress resilience). In this chapter, we propose a new approach to the typomorphological study of heat-stress resilience that adds an important, however missing, social dimension of heat-stress resilience to the current framework used in urban climatology, thus better studying the broader impact of urban form on urban resilience to heat stress.

9.1. Inadequacies of the existing typomorphological classifications for studying heat-stress resilience

As discussed in Chapter 4, typomorphological research has been growing within urban climatology and several typomorphological classifications (e.g. the LCZ scheme) have been developed to describe the urban form characteristics that can exacerbate heat stress and influence people's health and thermal sensation negatively (i.e. the environmental/engineering dimension of heat-stress resilience). Although these typomorphological classifications, including the LCZ scheme, have contributed to the advancement of urban heat studies, from a broader perspective of understanding and describing urban resilience to heat stress, they are limited.

Evidence from past heatwave disasters indicates that people's degree of vulnerability and capacity to resist, adapt to and recover from a heatwave hazard is a complex interplay between different conditions in the places they inhabit, e.g. environmental, social, economic and institutional (see Table 1, Chapter 1). The aim of this chapter is to complement the current LCZ scheme and other typomorphological classifications that mainly focus on the environmental conditions, by addressing other conditions that have shown to be related to urban form characteristics and significantly affect people's adaptation capacity during heatwaves. These are the conditions of social interaction and the state of social ties and solidarities in urban neighborhoods (Klinenberg, 2018, 2002, 2001, 1999; Naughton et al., 2002; Seebaß, 2017).

This chapter thus proposes a broader multi-dimensional approach combining environmental and social dimensions that are important for heat-stress resilience in the

²⁹ A version of this chapter has been peer-review and published: **Eldesoky, A.H.**, Gil, J., Berghauer Pont, M., 2022. Combining environmental and social dimensions in the typomorphological study of urban resilience to heat stress. *Sustain Cities Soc* 83, 103971. <https://doi.org/10.1016/j.scs.2022.103971>

classification of urban form types. On the one hand, this approach includes the urban form characteristics that directly influence the urban micro- and local climate and, in turn, people's health and sensation (i.e. the environmental dimension). These characteristics are currently embedded in, for instance, the LCZ scheme.

On the other hand, the proposed approach adds other urban form characteristics that influence urban resilience to heat stress through the way people interact with each other and with the urban environment (i.e. the social dimension). This multi-dimensional approach is put forth through: firstly, proposing a conceptual morphological framework of urban resilience to heat stress that adds the missing social dimension to the current framework used in urban climatology; secondly, identifying the urban form characteristics that are important for this social dimension as well as the quantitative measures that best describe them; thirdly, employing a Geographic Information Systems (GIS-) and machine learning (ML-) based method using these measures to develop typomorphological classifications of the social dimension that complement existing classifications such as the LCZ scheme.

The latter step operates on large-scale datasets of multiple urban form measures simultaneously and systematically, thus allowing the typomorphological description of urban form in multiple dimensions, as well as enabling the discovery of urban form types that are not yet known or are hard to identify by manual means as was done, for instance, to derive the 17 standard LCZ types. Examples of previous studies that have combined GIS- and ML-based methods to develop typomorphological classifications for different applications include (Barthelemy, 2017; Berghauser Pont et al., 2019a, 2019b; Bobkova et al., 2019b, 2019a; Colaninno et al., 2011; Fleischmann et al., 2021; Fusco and Araldi, 2018; Gil et al., 2012; Hausleitner and Berghauser Pont, 2017; Lee et al., 2019; Maiullari et al., 2021; Song and Knaap, 2007; Steiniger et al., 2008).

The remainder of the chapter is structured as follows. Firstly, the proposed multi-dimensional approach to the typomorphological study of heat-stress resilience is presented in Section 9.2. In Section 9.3, we describe the quantitative GIS- and ML-based method to develop typomorphological classifications that complement the existing ones (e.g. the LCZ scheme) for describing heat-stress resilience. The method is then exemplified in the case study (i.e. Sixth of October new desert city, Egypt). Section 9.4 discusses the applicability and limitations of the proposed approach and the developed case-specific typomorphological classification, as well as possible future work. And finally, Section 9.5 presents the main conclusions of the study.

9.2. A multi-dimensional approach to the typomorphological study of heat-stress resilience

This section presents a multi-dimensional approach to the classification of urban form types combining the urban form characteristics that support both environmental and social dimensions of heat-stress resilience. The environmental dimension's relation to urban form is well developed in the existing typomorphological classifications, such as the LCZ scheme, as discussed in Chapter 4. However, the social dimension is missing

and therefore we will, first, add this dimension to the current framework used in urban climatology; and, second, identify the urban form characteristics that are important for this social dimension and the quantitative measures that best describe them.

9.2.1. A conceptual morphological framework to study heat-stress resilience

Many deadly heatwaves have occurred over the years, with a recent example of the 2021 summer heatwave in Western North America resulting in around 800 confirmed deaths. The midsummer heatwave that stroke Chicago in 1995 is one of the most studied and deadliest heatwaves, leaving more than 700 dead (Figure 72). In exploring what made Chicago so vulnerable during the 1995 heatwave, sociologist Eric Klinenberg has provided in his book *Heatwave: A Social Autopsy of Disaster in Chicago* a revealing and persuasive analysis, starting from his conception of the heatwave as “an environmentally stimulated but socially organized catastrophe” (2002, p. 21). Through an in-depth ethnographic study, spatial and statistical analyses, Klinenberg has demonstrated that the severity of the catastrophe in Chicago was, in great part, a result of a breakdown in the social structure amplified by specific urban conditions. More specifically, the highest death tolls were recorded in abandoned neighborhoods with decayed social infrastructure, commercial depletion and with the absence of businesses, vibrant street life or any quality public spaces. The urban conditions of these neighborhoods have not only reduced people’s possibility to find physical relief (or thermally comfortable conditions) during the heatwave, but also they did not support different forms of physical co-presence (also known as bodily co-presence) to take place. The latter is particularly important for both focused and unfocused face-to-face social interactions to occur, creating the conditions for developing social networks, ties and solidarities of different kinds. These can provide direct social support (e.g. emotional, informational, instrumental, financial) to vulnerable individuals in times of crisis (Collins, 2004; Legeby, 2013; Seebaß, 2017). In Chicago, neighborhoods that supported and encouraged these social processes were more resilient during the 1995 heatwave (Klinenberg, 2018, 2002, 2001, 1999).



Figure 72. Refrigerated trucks stored bodies during the 1995 heatwave (left); Chicagoans sleeping outdoor during the heatwave (right). Source: Chicago Sun-Times.

Based on the above, we propose a conceptual framework that describes the contribution of urban form to heat-stress resilience including both environmental and social dimensions (Figure 73). In this framework, urban form, through its geometric (e.g. building dimensions) and surficial (e.g. construction materials properties) characteristics, modifies the urban climate leading to the formation of urban heat islands (UHIs) and increased heat stress (see arrow a, Figure 73). This, in turn, impacts people’s health and comfort (arrow b, Figure 73). These two relationships are dominant in current urban heat studies and constitute the current framework of typomorphological research within urban climatology. For the multi-dimensional approach, three new relationships (i.e. arrows) are added to the conceptual framework, allowing for a broader understanding and description of urban resilience to heat stress. Firstly, face-to-face social interactions in urban neighborhoods and the development of different kinds of social ties and solidarities can enhance people’s adaptation capacity in times of climate crisis (arrow c, Figure 73). This capacity depends not only on people’s ability and willingness to interact, but it is also highly influenced by urban form characteristics that promote or discourage these social processes (arrow d, Figure 73). Lastly, people can modify urban form through redesign or management interventions at the micro-/local scale (e.g. at residential yards) not only to reduce the impacts of extreme heat and create better climate conditions (e.g. by increasing vegetation cover) but also to create better conditions for face-to-face social interactions among neighbors (e.g. by placing outdoor furniture such as seats and grills) (arrow e, Figure 73).

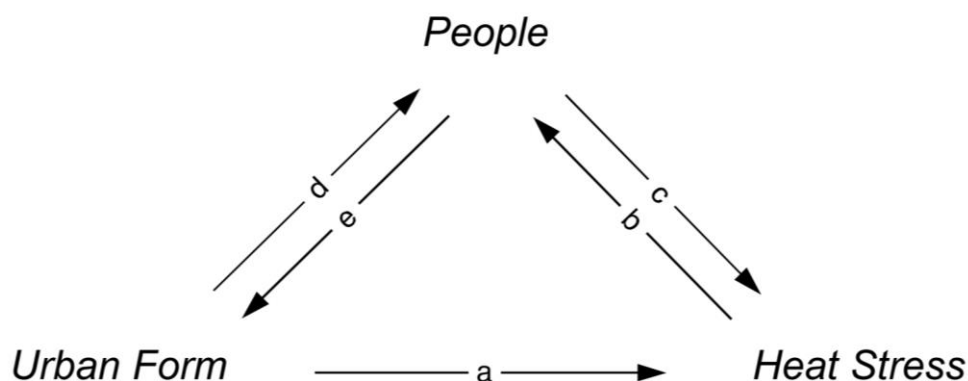


Figure 73. Conceptual framework representing the contribution of urban form to heat-stress resilience: (a) urban form characteristics modify urban climate and result in increased heat stress; (b) excessive heat stress impacts people’s health and comfort; (c) various social processes can increase people’s adaptation capacity to heat stress; (d) urban form characteristics influence these social processes; and (e) people can redesign/manage urban form to better mitigate or adapt to heat stress.

9.2.2. Urban form characteristics and measures associated with the social dimension of heat-stress resilience

In this section, we present the urban form characteristics associated with the social processes that play an important role in urban resilience to heat stress (arrows d and e, Figure 73) enhancing people’s adaptation capacity during heatwaves (arrow c, Figure

73). These social processes are influenced by urban form in three ways: (1) characteristics of public spaces at the meso-scale (neighborhood/district); (2) characteristics of semi-private/semi-public spaces at the micro-scale (urban block/cluster of blocks); and (3) characteristics of accessibility to social infrastructure. For each of these characteristics, we identify in the literature relevant quantitative measures that best describe them.

Characteristics and measures of public spaces

Configurational characteristics of streets and other public spaces (Hillier and Hanson, 1984) and building density (Jacobs, 1961) are urban form characteristics that influence the patterns of co-presence of people and impact their intensity (i.e. amount) and diversity (Legeby, 2013). On the one hand, the high intensity of co-present people creates vibrant and active urban life and increases the opportunity for face-to-face social interactions, thus combating social isolation and insecurity in urban neighborhoods that were so deadly during the Chicago heatwave (Klinenberg, 2001). On the other hand, the diversity of co-presence, and more specifically the mix of locals and non-locals, is essential to support what is known as “secondary relationships” or “weak ties” (Granovetter, 1983, 1973). These are important for building urban social networks that support information flow and knowledge exchange between different neighborhoods and, in turn, bridge the different social groups within the city (Granovetter, 1973; Legeby, 2013; Putnam, 2000). The latter is important for the management of collective resources and actions in times of crisis (Adger, 2003b; Seebaß, 2017) and can be strongly related to the broader issue of urban segregation in cities (Legeby, 2013), which was associated with higher death tolls in Chicago during the 1995 heatwave (Klinenberg, 2018).

To quantitatively describe the aforementioned urban form characteristics, Legeby (2013) has found that two urban form measures could significantly explain the variation in pedestrian flows, and more specifically the inflow of non-locals, in several neighborhoods in Stockholm, Sweden. These are spatial integration (Hillier and Hanson, 1984) and intelligibility (or integration interface) (Hillier, 1996; Hillier and Hanson, 1984). Spatial integration is a measure of network centrality that determines how close a space is to all other spaces, where more integrated spaces are visited more frequently and by a more diverse group of people. Intelligibility is a measure of the spatial integration of a place at different scales, attracting both local and global flows. Places with strong intelligibility (i.e. with a high correlation between local and global integration values) generate “multiplier effects” resulting in a more vibrant and diverse urban life, while places with weak intelligibility (i.e. low correlation between local and global integration values) represent a “mismatch” between local and global scales and lead to a separation between locals and non-locals (Hillier, 1996; Legeby, 2013; Peponis et al., 1997). Furthermore, Berghauer Pont et al. (2019b) and Bolin et al. (2021) have shown that the combination of two density measures, namely the accessible ground space index (AGSI) and accessible floor space index (AFSI) can be effective in describing the intensity of pedestrian flows. These are calculated by dividing the total

area of built land (in the case of AGSI) or built floor space (in the case of AFSI) that can be reached within a specific distance from a location by the total area of accessible land.

Characteristics and measures of semi-private/semi-public spaces

The semi-private/semi-public domain of urban space is important for neighbors to meet and interact and, hence, develop trust, mutual solidarity and a feeling of togetherness (Castell, 2010). Therefore, these spaces are particularly important for reinforcing the resilience of local communities in times of crisis by providing direct social support to vulnerable individuals (Elcheroth and Drury, 2020; Klinenberg, 2018, 2002, 2001, 1999). Semi-private/semi-public domain refers to the transitional or “interpersonal” (Madanipour, 2003) spaces between the private and the public. These can be either group-controlled spaces, e.g. residential enclosed yards exclusively used by residents, or semi-public spaces belonging to a certain group of residents but still publicly accessible, e.g. municipal green spaces in a cluster of multifamily housing or semi-enclosed/open residential yards (Olsson et al., 1997). The residents’ co-presence and social interaction in semi-private/semi-public spaces are partly influenced by the extent to which the characteristics of urban form, namely the enclosure/openness (i.e. the degree to which open space is defined by buildings), size and spaciousness, encourage residents’ sense of ownership, use and appropriation of such spaces (Castell, 2010; Minoura, 2016; Mousavinia et al., 2019; Olsson et al., 1997). For instance, in several multi-family residential yards in Malmö and Stockholm, Sweden, the residents’ sense of ownership and appropriation of space were higher in more enclosed and smaller yards with higher building coverage (GSI), while the frequency of use was higher in less enclosed and large yards with low built density (FSI) (Minoura, 2016). Besides these characteristics, also formal institutional characteristics, such as land ownership (e.g. public or private) and rights, determine who is allowed to use the space and to appropriate or modify it even without materialized boundaries (Minoura, 2016).

Characteristics and measures of accessibility to social infrastructure

By facilitating or impeding accessibility to social infrastructure, urban form influences the social interaction and the development of social ties and solidarities that are important for heat-stress resilience. In Chicago, neighborhoods with robust and healthy social infrastructure were more resilient during the 1995 heatwave (Klinenberg, 2018, 2002, 2001, 1999). According to Klinenberg, social infrastructure is “the physical places and organizations that shape the way people interact” (2018, p. 5). This includes: public institutions, e.g. libraries, schools, playgrounds, swimming pools, parks and open green spaces; community organizations, places of worship and other civic associations; and “third spaces” (Oldenburg, 2001), e.g. coffee shops, barbershops and bookstores. Certain types of social infrastructure, especially those related to green infrastructure (e.g. parks, community gardens), can become places where residents get physical and mental relief (Sugiyama et al., 2018; Wang et al., 2021). This is because vegetation not only regulates processes related to micro- and local climate reducing the

impact of extreme heat, but it also provides other cultural ecosystem services such as recreation, aesthetic enjoyment, physical and mental health benefits and spiritual experiences.

One can measure social infrastructure based on its individual characteristics, such as type, function, size, shape (in the case of open/green spaces), number per capita and strategic location in space, which can enhance urban resilience to different disturbances (Sharifi, 2019b). But one can also measure accessibility to social infrastructure, i.e. how urban form characteristics, such as the density and distribution of intersections and street segments, give access to social infrastructure within walking distance, the focus in this chapter. Attraction distance and attraction reach (Ståhle et al., 2007) can be used to calculate the accessibility to existing social infrastructure based on geometric or topological distances. In particular, attraction distance calculates the minimum distance from a set of origins (e.g. building entrances or addresses) to a set of attractions (e.g. schools, libraries) through the street network, while attraction reach calculates the total amount (e.g. number, area) of attractions that can be reached within a distance threshold.

9.3. A quantitative GIS- and ML-based method for typomorphological classification of the social dimension of heat-stress resilience

The conceptual framework's mechanisms (Figure 73), the urban form characteristics and the quantitative measures presented in Section 9.2 provide a description of the social dimension of heat-stress resilience in relation to urban form. One approach to apply this framework is through the typomorphological classification of urban form. This section describes a quantitative GIS- and ML-based method for systematic typomorphological classification of this social dimension, thus complementing the existing classifications used in urban climatology and urban planning and design. Here, a selection of urban form measures associated with the social dimension of heat-stress resilience, introduced in Section 9.2.2, is used as input variables to cluster residential neighborhoods in the case study, by means of GIS spatial analysis and statistical clustering methods. The section is organized as follows: firstly, the study neighborhoods are introduced in Section 9.3.1; then, the data and methods used for developing the typomorphological classification are presented in Section 9.3.2; and finally, the resulting classification and the description of the identified neighborhood clusters are given in Section 9.3.3.

9.3.1. Introduction to the study neighborhoods in Sixth of October

For this study, a sample of 78 of these so-called neighborhoods, defined by zoning in Sixth of October's master plan, was selected to develop a typomorphological classification that better describes their heat-stress resilience (Figure 74). This sample was selected so that neighborhoods represent LCZs, i.e. "regions of uniform surface

cover, structure, material, and human activity that span hundreds of meters to several kilometers in horizontal scale” (Stewart and Oke, 2012, p. 1884).

The LCZ scheme is chosen as a departure point because it is, as discussed in Chapter 4, the most developed typomorphological classification in urban climatology representing the environmental dimension of heat-stress resilience, and we aim to complement it with other typomorphological classifications representing the social dimension. In this study, considering that the focus is not on mapping LCZs and analyzing their thermal characteristics, the sample neighborhoods were classified into LCZ types using the expert knowledge-based method, which relies on the local knowledge of the author, and secondary resources (e.g. Google satellite imagery, land use/land cover maps) (Lehnert et al., 2021). Furthermore, in this study, the subtypes representing a combination of built and land cover types were used instead of the standard LCZ types as recommended in the previous chapter for cities in arid climates.



Figure 74. The case study area and the neighborhoods selected for the analysis and the typomorphological classification. Study neighborhoods were classified into LCZ types based on the local knowledge of the author and using subtypes that represent a combination of built and land cover types.

9.3.2. Data and methods

To cluster neighborhoods using statistical methods, we generally follow the steps recommended by Witten et al. (2016) and demonstrated in (Gil et al., 2012). Namely,

preparation of relevant data, spatial analysis to calculate relevant urban form measures, and statistical clustering of neighborhoods using the calculated measures.

As a first step, different GIS data layers were prepared for the study area. This included: (1) road centerlines and pedestrian paths; (2) neighborhood boundaries; (3) building blocks; (4) plots (property lines) with the state of ownership; (5) building footprints with height attribute; (6) open green spaces; (7) points of interest (POI), e.g. public libraries, places of worship, shopping malls, etc.; and (8) land use. The data were obtained from different sources, including official and open-source digital topographic databases, and pre-processed. The data sources and the pre-processing steps applied to the different data layers are summarized in Appendix D, and the resulting GIS model is presented in Figure 75.

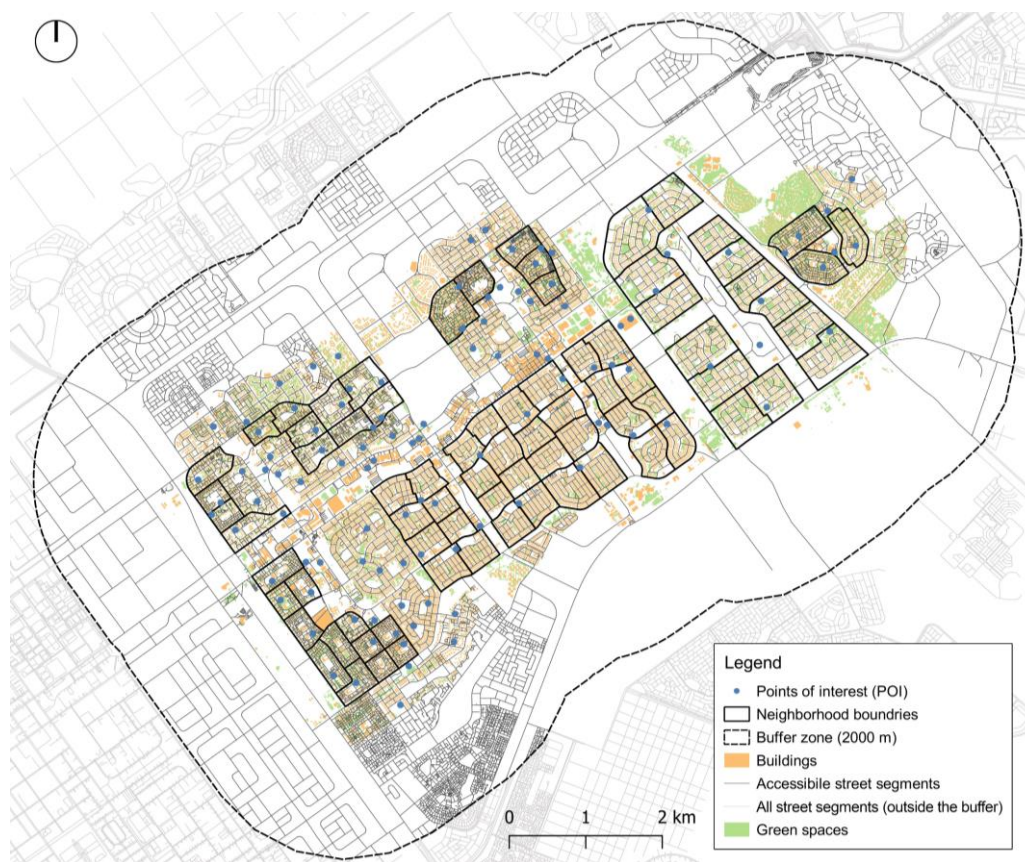


Figure 75. The GIS model of the study area showing the main layers included in the analysis and the typomorphological classification.

Next, we have performed spatial analysis operations on the GIS model to calculate, process and aggregate (at the neighborhood level) a selection of relevant urban form measures, described in Table 18 and with more details in Appendix D. To meet the prerequisites of the statistical clustering methods and reduce classification biases, the calculated numeric measures were post-processed to (1) exclude highly dependent measures; (2) standardize all measures to be on the same scale; and (3) remove data outliers (Gil et al., 2012; Serra, 2013). This resulted in a sample size of 76 (out of 78) neighborhoods and in ten (out of 14) clustering variables, i.e. AI (2k), SEGIN, AFSI, AFSI (SD), AGRA, DSINF, DSINF (SD), ENC, GSI and OWN.

Table 18. Overview of the urban form measures selected for the statistical clustering of neighborhoods. More details are provided in Appendix D.

Theme	Measure	Code	Unit of calculation (entity)	Measure type	Aggregation method	Notes
Characteristics of public spaces	Angular integration ¹	AI	Street segment	Numeric	Mean and Standard Deviation (SD)	Calculated within 500 m (local) and 2000 m (global) walking distances ²
	Segment intelligibility ³	SEGIN	Neighborhood	Numeric	-	Correlation between local and global AI values is calculated using Spearman's correlation coefficient
	Accessible ground space index	AGSI	Building	Numeric	Mean and SD	Within 500 m walking distance
	Accessible floor space index	AFSI	Building	Numeric	Mean and SD	Within 500 m walking distance
Characteristics of semi-private/semi-public spaces ⁴	Space enclosure	ENC	Block	Nominal based on numeric	Mean	A = Open/Less enclosed (below the mean) B = More enclosed (above the mean) C = N/A (rows of plots)
	Ground space index	GSI	Block	Nominal based on numeric	Mean	A = Relatively low density (below the mean) B = Relatively high density (above the mean) C = N/A (rows of plots)
	Land ownership ⁵	OWN	Block	Nominal	Majority	A = Public B = Private C = N/A (rows of plots)

(continued)

Table 18 (continued)

Theme	Measure	Code	Unit of calculation (entity)	Measure type	Aggregation method	Notes
Characteristics of accessibility to social infrastructure	Accessible area of green space (m ²)	AGRA	Building	Numeric	Mean and SD	Within 500 m walking distance
	Minimum distance to indoor social infrastructure (m)	DSINF	Building	Numeric	Mean and SD	Indoor social infrastructure includes (1) big shopping malls; (2) worship places (mosques and churches); and (3) libraries ⁶

¹ Spatial integration was calculated based on a line-segment map that was derived by splitting road centerlines and pedestrian paths, at junctions/intersections or pseudo nodes, into line segments. Because the distance between line segments was measured geometrically by calculating the angular change in direction, spatial integration is referred to here as angular integration (Hillier and Iida, 2005).

² 500 m and 2000 m represent the typical and maximum distance thresholds that people are willing to walk, respectively.

³ Segment intelligibility was calculated for each neighborhood based on all the line segments that are completely contained within. Because intelligibility is measured based on local and global angular integration values, it is referred to here as segment intelligibility (Alghatam, 2012).

⁴ Measures of semi-private/semi-public space characteristics apply only to part of the dataset (i.e. neighborhoods with urban blocks, where there is an open space surrounded by buildings) and do not apply to neighborhoods with rows of plots (i.e. individual parcels of land generated by land subdivision). Hence, for clustering purposes, numeric measures were discretized into two classes using Z-scores and all the left-out data points (rows of plots) were considered a third, separate class (N/A).

⁵ Land ownership is used as a measure of the formal institutional characteristics that determine, besides urban form characteristics, who is allowed to use the semi-private/semi-public space and to appropriate or modify it.

⁶ This choice is case-specific, and one can choose any other set of places that act as social infrastructure in other contexts.

Finally, cluster analysis was performed using the ten selected measures to partition the 76 neighborhoods into clusters. The agglomerative hierarchical clustering (AHC) algorithm was used, which partitions data points (in this case neighborhoods) into clusters based on their dissimilarity in an agglomerative bottom-up process (Nielsen, 2016). The process starts with each data point as an individual cluster, then combines the two most similar clusters, and this process is repeated until all data points are grouped in a single cluster. AHC was chosen for three main reasons. Firstly, it can handle different measures of dissimilarity or distance, and hence it can be used to cluster mixed-type data (e.g. numeric, ordinal and nominal) as is the case of this study (see Table 18). Secondly, AHC is an unsupervised ML algorithm that does not require the number of clusters to be defined beforehand which is particularly important for exploratory studies. Finally, AHC is visualized using a tree-like diagram called a dendrogram, which is effective to understand the clustering structure and determine a suitable number of clusters. AHC was performed in R using the `hclust` function of the `stats` package, applying Gower's dissimilarity/distance measure for mixed-type data (Gower, 1971) and Ward's linkage criterion for combining clusters (Ward, 1963). A suitable number of clusters was determined by identifying large changes in the height of the dendrogram (on the y-axis) as the number of clusters increases. Finally, a heatmap and boxplots were produced to provide quantitative and qualitative descriptions of the neighborhood clusters based on their characteristics.

9.3.3. Resulting typomorphological classification describing the social dimension of heat-stress resilience

The results of the cluster analysis suggest a division of the 76 neighborhoods into five clusters with different profiles, as shown in the dendrogram and the heatmap in Figure 76. The neighborhoods can be generally divided into two main clusters with different urban layouts where one is characterized by rows of plots and the other by urban blocks.

Rows of plots are individual parcels of land resulting mainly from land subdivision and are usually arranged along linear or curved streets, where each parcel belongs to a private entity with clear property boundaries. They are represented by neighborhood clusters 1 and 2 (NC1 and NC2) and include the majority of neighborhoods (59.2%). NC1 includes neighborhoods with mid-rise private apartment buildings, relatively high FSI and integration, and hence it has the potential for enhancing heat-stress resilience through physical co-presence and vibrancy in the public space (referred to as *urban life resilience*) (Figure 77a). NC2 includes neighborhoods with low- to mid-rise single-family houses aimed at high-income dwellers where, interestingly, none of the measured urban form characteristics contribute positively to heat-stress resilience (the vast majority of values are below the mean), which suggests that this cluster has *no resilience potential* compared to all the other neighborhood clusters (Figure 77b).

Urban blocks refer to layouts with a group of buildings (on public or private land) surrounding an open space that can be either semi-private or semi-public. They are represented by neighborhood clusters 3, 4 and 5 (NC3, NC4 and NC5) and include 40.8% of the neighborhoods. NC3 is characterized by relatively enclosed, high-density

blocks on private land and in the proximity of potential social infrastructure (both indoor and outdoor) (Figure 77c). Thus, this cluster has the potential for enhancing heat-stress resilience through both physical co-presence in the semi-private/semi-public space and social infrastructure (referred to as *baseline resilience*). NC4 and NC5 include neighborhoods with open, low-density blocks on private and public land, respectively. NC4 has relatively high intelligibility and low distance to potential social infrastructure, and hence it has the potential for enhancing heat-stress resilience through physical co-presence in public space and social infrastructure (referred to as *open/indoor space resilience*) (Figure 77d). NC5 exhibits a *limited resilience potential* compared to all the other neighborhood clusters, as none of the measured urban form characteristics stand out (Figure 77e). The latter includes neighborhoods with public housing particularly targeted at low-income dwellers.

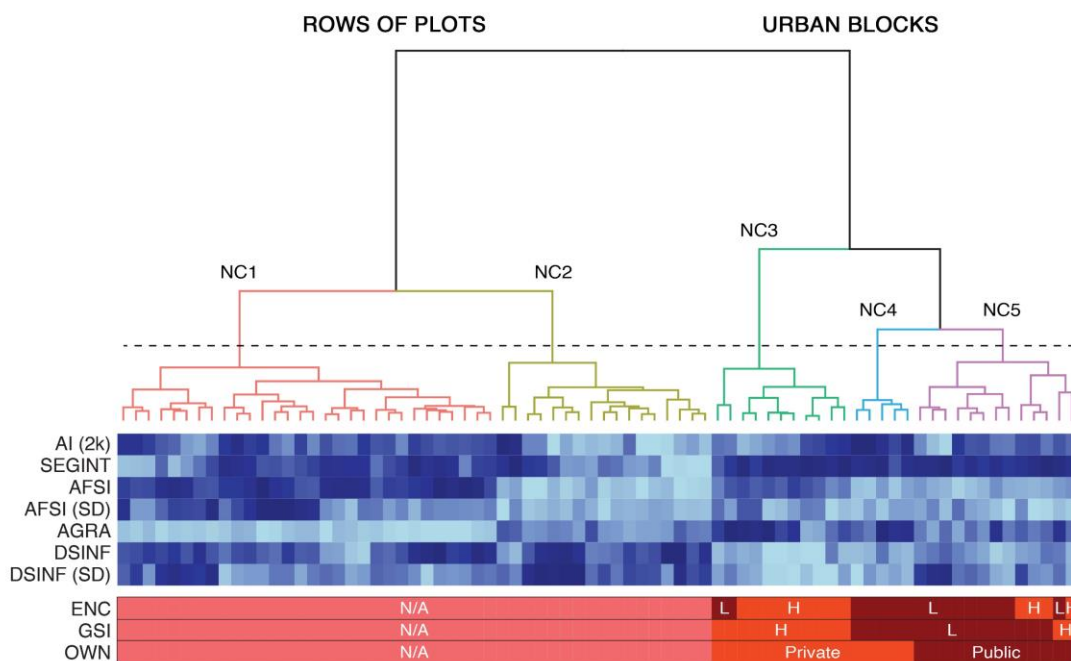


Figure 76. Hierarchical clustering dendrogram with a heatmap. Colors ranging from dark to light blue indicate higher to lower values. The dendrogram suggests a division of the neighborhoods into five clusters. H, L and N/A stand for high, low and not applicable, respectively.

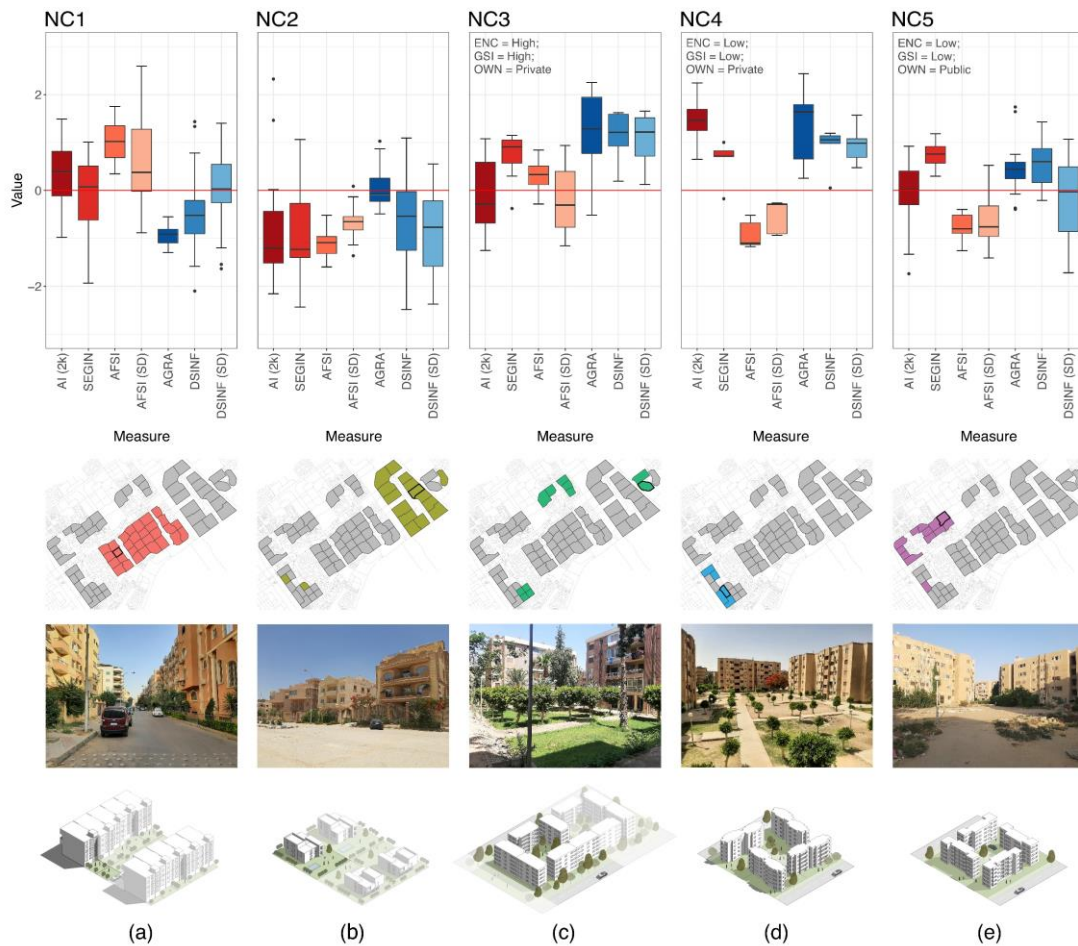


Figure 77. Box plots showing the distribution of urban form numeric measures per neighborhood cluster (top), the spatial distribution of clusters (middle) and examples of representative neighborhoods with schematic visualizations (bottom). Boxes in red colors represent the measures of public space characteristics and in blue colors accessibility to social infrastructure. Boxplot values are standardized using Z-scores, where the values of DSINF and DSINF (SD) are inverted so that positive values (above the mean) indicate a positive contribution to heat-stress resilience.

9.4. Discussion

This chapter has addressed the shortcomings of the existing typomorphological classifications within urban climatology that primarily focus on the environmental dimension of heat-stress resilience and overlook important social dimensions. We have proposed a broader approach combining these two dimensions in the classification of urban form types. Departing from evidence from the deadly 1995 Chicago heatwave, we have identified, in the literature, urban form characteristics that influence the way people interact with each other and with the urban environment in various social processes associated with heat-stress resilience (i.e. the social dimension). These, in combination with the other well-established urban form characteristics embedded in, for instance, the LCZ scheme (i.e. the environmental dimension), allow for a broader understanding and description of heat-stress resilience through typomorphology.

Further, we have employed a quantitative GIS- and ML-based method to develop typomorphological classifications that complement the existing ones, by describing the social dimension of heat-stress resilience. This systematic method relies on statistical clustering (AHC) of a set of relevant urban form measures that are associated with the social dimension of heat-stress resilience. Sixth of October new desert city in Egypt was used to exemplify the method, but it can be applied in different contexts.

The results showed the possibility of numerically identifying neighborhood clusters that, through distinct urban form characteristics, have different potentials for enhancing the social dimension of heat-stress resilience. This means that the developed typomorphology has a direct planning and design relevance since it can help urban planners and designers to identify vulnerable neighborhoods in case of extreme heat events. Not only those neighborhoods at risk of high temperatures (i.e. the environmental dimension), using for example the LCZ scheme but also those that offer little support to the relevant social processes (i.e. the social dimension). Furthermore, the quantifiable characteristics of the identified neighborhood clusters can be translated into guidelines and rules and incorporated into local planning and design regulations. Therefore, the combination of the developed typomorphological classification and the existing ones offers promising opportunities for urban planners and designers to know not only where to intervene in cities but also what should be done to enhance heat-stress resilience through urban form.

9.4.1. An integrated multi-dimensional typomorphological classification

By comparing the developed classification and the LCZ classification of the study neighborhoods (Table 19), it becomes clear that the description of urban neighborhoods in terms of heat-stress resilience can be enhanced, for example through new composite types, since one LCZ type focusing on the environmental dimension (rows) can correspond to one or more of the identified neighborhood clusters focusing on the social dimension of heat-stress resilience (columns). For example, a neighborhood whose LCZ type is *open mid-rise* (LCZ 5) and whose cluster representing the social dimension

of heat-stress resilience is *baseline resilience* (NC3) can be notated as LCZ 5_{NC3} to denote both the environmental and social dimensions of heat-stress resilience in the composite type. Table 19 shows that LCZ 2 (compact mid-rise) corresponds to NC1 (urban life resilience), while LCZ 6 (open low-rise) and LCZ 6_F (open low-rise with bare soil/sand) correspond to NC2 (no resilience potential). On the other hand, LCZ 5 (open mid-rise) and LCZ 5_F (open mid-rise with bare soil/sand) correspond to four neighborhood clusters, i.e. NC2 (no resilience potential), NC3 (baseline resilience), NC4 (open/indoor space resilience) and NC5 (limited resilience potential) with a dominance of NC3 in LCZ 5 (53.8%) and NC5 in LCZ 5_F (41.6%).

Table 19. Contingency table between the LCZ types and the identified neighborhood clusters.

	NC1		NC2		NC3		NC4		NC5		Total
	count	%	count	%	count	%	count	%	count	%	
LCZ 2	30	100	0	0	0	0	0	0	0	0	30
LCZ 5	0	0	1	7.7	7	53.8	2	15.4	3	23.1	13
LCZ 5 _F	0	0	7	29.2	4	16.7	3	12.5	10	41.6	24
LCZ 6	0	0	1	100	0	0	0	0	0	0	1
LCZ 6 _F	0	0	8	100	0	0	0	0	0	0	8
Total	30		17		11		5		13		76

9.4.2. The scope and role of the developed typomorphological classification

As discussed throughout this chapter, the neighborhood classification developed in Section 9.3 is inherently typomorphological. This means, first, that it does not describe all the conditions that influence heat-stress resilience referred to in Table 1 (Chapter 1), such as the economic, health and demographic conditions. Rather, the focus is on those conditions that have shown to be associated with urban form, i.e. social interaction and the state of social ties and solidarities in urban neighborhoods, and are not included in the LCZ scheme or any other typomorphological classifications. Second, that it does not include every aspect complementary to urban form that can influence urban resilience to heat stress. For example, denser neighborhoods (with relatively higher AFSI and AGSI values) will not necessarily be more vibrant without mixed land uses and an adequate level of commercial activity. Similarly, highly integrated streets will not attract more pedestrian flows if they have decayed, unshaded sidewalks or incomplete infrastructure. This is the case in the neighborhoods of NC1 (urban life resilience) that have the urban form characteristics to enhance heat-stress resilience through physical co-presence and vibrancy of urban life, but building regulations strictly prohibit the opening of businesses, offices or services in most buildings. Furthermore, many of the sidewalks have been occupied and privatized by the adjacent property owners with the absence of any municipal control. Likewise, one should also understand that proximity to social infrastructure (e.g. as in NC3 and NC4) is not an advantage for heat-stress resilience if such services are unmaintained and unequipped with the necessary facilities (e.g. air conditioning and furniture) and staff.

Therefore, in urban planning and design practice, one can consider typomorphology as the first assessment layer to determine whether fundamental urban form characteristics supporting heat-stress resilience are in place. If these are missing, the built environment should be reshaped first. This can include, for instance, making residential yards more enclosed to encourage social interaction among neighbors (e.g. NC4 and NC5), densifying neighborhoods and upgrading public space to ensure vibrant and active urban life (e.g. NC5) or, more radically, unbuilding/demolishing parts of the built environment that are obsolete or have no resilience potential (e.g. NC2). Once this is satisfied, other instruments might be needed to make sure the affordances already present in the built environment can also be used by citizens. This can include, for example: legal instruments to provide a degree of flexibility in zoning plans and facilitate urban land reallocation; financial instruments to encourage private investments in the public sector and reduce government spending (e.g. the maintenance and management of social infrastructure); and organizational instruments to get users/residents and other stakeholders involved in the decision-making process of the urban development and in the running and management of public space (Bergeroet and van Tuijl, 2016).

9.4.3. Towards general typomorphological classifications

Finally, one should keep in mind that the typomorphological classification developed in this study using a GIS- and ML-based method is only a demonstration of the proposed multi-dimensional approach, to complement the existing classifications with the missing social dimension of heat-stress resilience, applied in a specific and limited case. The approach and the method should be applied in other new desert cities, which can result in the identification of more neighborhood clusters, to eventually arrive at a set of general types useful for urban planning and design practices in these contexts. Moreover, the capability of the identified neighborhood clusters to explain the variation in resilience performance to heat stress should be empirically validated in future studies, e.g. by using data about death tolls from extreme heatwaves. Also, the identified neighborhood clusters are comparable only in terms of their relative resilience to heat stress, and hence future research should aim at establishing benchmarks to better measure the heat-resilience performance of different neighborhood types.

Chapter 10

Discussion of research results and conclusions

This thesis has focused on one of the emerging research topics within the field of urban morphology that investigates how the concept of resilience, which has recently become a buzzword very favored to address the complexity and future uncertainty in cities, can be integrated into the study of urban form, as the raw material of urban design and a key element that can guide cities towards more sustainable trajectories.

More specifically, the thesis has focused on some of the theoretical/conceptual and methodological challenges (with more focus on the latter) for integrating resilience thinking into urban morphology (or the study of urban form), where two main research problems were identified. These are:

- The need to understand the core meaning of resilience in urban morphology and examine its underlying politics in light of growing literature on the topic (e.g. resilience of what? To what? For whom? When? And where?) so that it can be effectively operationalized.
- The need to support urban planning and design decisions with tools and methods that provide an improved understanding of the impact of urban form on urban resilience to different stresses and shocks.

To adequately address the latter research problem within the space and the time set for this thesis, the research topic was narrowed down to focus, more specifically, on urban resilience to heat stress as one of the most pressing challenges in cities nowadays that has been demonstrated to be strongly influenced by urban form.

In this final chapter, we bring together the conclusions of the various chapters to (1) summarize the theoretical/conceptual and methodological contributions of the thesis (Section 10.1); (2) discuss the implications of the work carried out for urban planning and design practice (Section 10.2); and (3) make some final reflections and propose directions for future research on the topic (Section 10.3).

10.1. Theoretical and methodological contributions

In this section, we highlight the theoretical/conceptual and methodological contributions of this thesis to existing knowledge by revisiting and trying to provide an answer to each of the initial research questions formulated in Chapter 1 and addressed throughout the various chapters of the thesis. It is worth highlighting that some of these research questions were formulated/reformulated during the study as the research evolved. By theoretical/conceptual contributions, we refer to those contributions that have increased our understanding and knowledge about the topic (e.g. syntheses/reviews to summarize existing knowledge in the field and provide improved definitions of existing constructs or the identification and conceptual definition of additional constructs to be added to existing theoretical frameworks). On the other

hand, methodological contributions are those contributions that have advanced the existing methods in the field either by identifying their limits (i.e. boundary conditions) or by making incremental improvements and extending their application to new contexts.

What is the core meaning of resilience in urban morphology?

This preliminary research question was formulated in response to a growing interest in recent years to understand how resilience thinking can be integrated into the study of urban form as the main object of study in urban morphology. However, because resilience is a polysemic concept and can be addressed from different perspectives (e.g. engineering, ecological or social-ecological), one needs to understand and adjust its meaning “depending on the specific research question(s)” (Sharifi and Yamagata, 2018a) so that it can be effectively operationalized. In this thesis, this required thinking critically and systematically through a set of important wh-questions such as what elements of urban form can be resilient (or can provide resilience) to what? Resilience for whom or whose resilience is addressed/prioritized? Who does determine (plan/design for) the resilience? And how or in which mechanism? Where (in which geographical context)? And when?

To adequately answer these questions, in Chapter 3 a comprehensive systematic literature review was conducted based on 106 peer-reviewed publications (288 before screening and assessment) that were retrieved from two scientific databases (i.e. Scopus and Web of Science). The reading of the full articles, which was guided by the aforementioned questions, in addition to a few others, has provided an improved understanding of the nature of the relationship between urban form and urban resilience from many different aspects. Moreover, it offered a detailed overview of how the combination of urban form and urban resilience has been used across disciplines and fields of study, where around 41 different definitions of urban form resilience, or resilient urban forms, were identified (see Table 8, Chapter 3).

Most importantly, the review has shown that the relationship between urban form and urban resilience is rather complex and multifaceted. For example, there are a great many urban form elements (ranging from the marco- to the meso- and micro-scales) that can enhance the resilience of the urban population (both general and specified) to a great many disturbances (general/specified and slow-/rapid-onset). Furthermore, in responding to these disturbances, urban form elements were found to exhibit different resilience performances (i.e. persistence, adaptability and transformability) depending on the kind of disturbance, and where they can be resilient in themselves (i.e. resilience *of* urban form) or can increase people’s adaptation capacity during a disturbance (i.e. resilience *through* urban form). Also, several actors, with different points of view, priorities and powers, were found to be involved in the planning/design process of urban form resilience. Lastly, the review highlighted that there are some pitfalls in applying resilience thinking in urban morphology (or to the study of urban form) and pointed out that urban form resilience might not be always perceived as a good thing.

Based on this complexity, we favored not to give one definition or provide a single understanding of the meaning of urban form resilience (or resilient urban forms), which may indeed undermine this desired complexity. Rather, to offer the readers a rich glimpse of the many perspectives on the topic so that they may decide which perspective may be most appropriate for their specific research question(s) and aim(s). But also to stimulate new ideas of how urban form can contribute to urban resilience.

What are the existing quantitative methods that can be used for studying the impact of urban form on urban heating and, in turn, on people's health and thermal sensation (i.e. the environmental/engineering dimension of heat-stress resilience)? What are their potentials and limitations?

Although this research question may not seem pertinent to the thesis's main research problems, it is considered an important, opening question to the second set of chapters (4–9), where we investigate the different quantitative methods for studying the impact of urban form on urban climate (with a focus on urban heating) and, in turn, the possibility of determining its impact on people's health and thermal sensation (i.e. what we coined as the environmental/engineering dimension of heat-stress resilience following the systematic literature review conducted in Chapter 3). More specifically, answering this question has helped to set the ground for all the chapters that followed and contributed to cognitive studies in urban morphology (i.e. those that aim to produce knowledge or develop theoretical and analytical tools to produce such knowledge) by achieving a better understanding of why these quantitative methods are relevant for urban planning/design decision-making and how they can be used appropriately and effectively.

This question was addressed in Chapter 4 after having presented, in Chapter 2, a strong argument of why urban form should be studied quantitatively or measured. In a nutshell, quantification offers the possibility of formulating urban policies and regulations based on empirical evidence or measurable design outcomes (Berghauser Pont, 2018; Moudon and Lee, 2009).

In particular, we have identified and distinguished between two groups of quantitative methods: climatological-/environmental-based methods and typomorphological methods. An important conclusion of this chapter is that these methods should be viewed as complementary rather than substitutes since they aim to, respectively, answer the following two different questions in urban climatology:

- Do urban climate effects (of urban form) in terms of heating exist and, if so, what is their nature?
- What are the specific causes (or the urban form characteristics responsible for) of such effects?

More specifically, in this thesis, we coined climatological-/environmental-based methods as *descriptive* methods aiming at describing the phenomenon under question (e.g. urban heating and its related health/thermal sensation consequences) and providing relevant empirical information on it (i.e. emphasizing *what is the problem*).

On the other hand, typomorphological methods were coined as *analytical* (explanatory) methods aiming at explaining the causes (or the urban form characteristics) responsible for this phenomenon (i.e. emphasizing the *why* and/or *how* urban heating happens). Furthermore, typomorphological methods were suggested to be also normative/prescriptive methods (i.e. emphasizing *what should be*). This is because types within typomorphologies perform and function in specific ways, and hence they are very useful to inform urban planning and design practices, as was discussed in Chapter 2. In this regard, the so-called local climate zone (LCZ) classification scheme (Stewart and Oke, 2012) was introduced as an example of the most developed typomorphological classifications in urban climatology from which this thesis departs and aims to add to.

How can we improve the output of these methods in terms of scale and accuracy to better support urban planning and design decisions?

This question was addressed throughout the second set of chapters (4–9) but with particular emphasis in Chapters 5 and 6 to address the shortcomings of the existing methods in terms of scale and accuracy, where scale here refers to both the level of detail, i.e. spatial resolution, and extent, i.e. size of the study area (Smith and Crooks, 2010). More specifically, in Chapter 5 we have proposed a method to better *describe* the impact of urban form on urban temperatures and, in turn, the possibility, in a next step, of determining its impact on people’s health and thermal sensation (i.e. the environmental/engineering dimension of heat-stress resilience). In particular, the method combines two different climatological techniques, i.e. field observations (using mobile measurements) and empirical modelling (using supervised machine learning approaches) to provide gridded air temperature data (i.e. air temperature maps) for entire cities and urban areas at a high spatial resolution (30 m) and good accuracy ($R^2 > 0.87$ and $RMSE < 0.18$ °C). The novelty of this method is that it is systematic and relies on low-cost instrumentation and freely-available satellite data. Hence, it can be replicated in any city or urban area (including meteorologically data-scarce areas) for various applications, among which the most important to this thesis is supporting urban heat-resilience planning and design decisions as will be discussed in Section 10.2.

On the other hand, in Chapter 6, we have proposed a method for improving the application of the LCZ typomorphological classification to entire cities and urban areas at a fine spatial resolution and accuracy where it can be time-consuming and, sometimes, not possible to carry out typical in-situ measurements to classify field sites into LCZs based on their geometric and surface cover parameters. This is an important step to consistently provide urban climate-relevant descriptions of the urban form and function of cities around the world, which, in turn, allows for city comparisons and facilitates knowledge transfer between urban climatologists, planners and designers globally.

The proposed method uses a combination of two existing LCZ mapping techniques, namely remote sensing- and Geographical Information Systems (GIS-) based techniques to create LCZ maps at a fine scale and accuracy based on a combination of

LCZ-relevant multi-spectral and morphological indices. The multi-spectral indices that were used are the surface albedo (both narrow and broadband albedo) and the Normalized Difference Vegetation Index (NDVI) and were derived from freely-available, multi-spectral satellite imagery. On the other hand, the morphological indices included building heights and the sky view factor (SVF) and were calculated using GIS building data.

The accuracy of the LCZ map produced using the proposed method was compared with that of a LCZ map produced using a widely-used LCZ mapping tool, namely WUDAPT (World Urban Database and Access Portal Tools), which uses a remote sensing-based mapping technique employing freely available multi-spectral and thermal satellite data (to account for the thermal properties of the LCZ types). The results showed a noticeable improvement in the overall accuracy of the LCZ map produced using the proposed method by 12% (67% overall accuracy) and in the accuracy of the built LCZ types by 15% (48% overall accuracy). This demonstrates the effectiveness of the proposed method in mapping LCZs at a fine scale and accuracy without the need for high-quality GIS data (that are not always available or open-sourced) or thermal satellite data. The latter is an important methodological advancement because if we want to use the LCZ typomorphological classification for analytical purposes to study the relationship between urban form and urban temperatures or urban heat-related issues, it is necessary to isolate the cause (i.e. the geometric and surface cover characteristics of LCZs) from the effect (i.e. their thermal properties).

What is the applicability of the aforementioned methods in contemporary cities in arid areas (e.g. Cairo desert cities)?

This question was formulated in light of the documented exponential growth of newly-built cities in arid areas, which besides being already located in a highly heat-vulnerable climate region, are usually planned and designed based on outdated global western (modernist) models that are not suitable for arid conditions. Hence, there was a need to understand the applicability of the aforementioned methods in these cities (on which little research has been conducted) to better support the development and implementation of their heat-resilience plans.

In order to answer this question, both the climatological-/environmental-based and typomorphological (LCZs) methods discussed in Chapter 4 were applied to Sixth of October, Egypt, as a typical example of a contemporary city located in an arid area. In fact, the climatological-/environmental-based method proposed in Chapter 5 was already tested in Sixth of October, hence its applicability can be confirmed in light of the findings of Chapter 5.

As for the typomorphological methods and, more specifically, understanding the applicability of the LCZ scheme for urban temperature studies in contemporary arid cities, in Chapter 7 we have assessed how well the LCZ typomorphological classification discerns the thermal differences between different areas in Sixth of October. This was done by statistically analyzing whether there is a significant

difference between LCZ types in terms of air temperature for different days and times (including both daytime and nighttime). The results showed that during nighttime, all LCZ types are relatively well-differentiated from each other, while during the daytime, almost none of the urban/built LCZ types is indistinguishable from another. This, in light of a few studies that have applied the LCZ scheme to arid cities and where an assessment of the statistical significance of the thermal difference between LCZ types was often not performed, highlighted a possible limitation that needed to be further investigated regarding the applicability of the LCZ scheme in arid areas. In this regard, it was also considered important to expand our knowledge about the suitability of the LCZ typomorphological classification in other macroclimate regions, where no previous studies examined this topic in detail. This is an essential step if the LCZ scheme is to be useful for urban planning and design practices not only in arid areas but also globally.

Therefore, in Chapter 8 we have conducted a global study to determine the suitability of the LCZ scheme in four main macroclimate regions, namely the tropical, the arid, the temperate and the cold climates. We defined suitability as the similarity in the temperature characteristics among identical LCZ types in the same macroclimate region (i.e. little variability in temperature within the same LCZ type), but more importantly, a different impact on temperatures when compared to other LCZ types in the same macroclimate region (i.e. statistically significant temperature differences between LCZs). Most importantly, it was confirmed that the LCZ standard scheme is applicable, with varying degrees, to all macroclimate regions other than the arid, where the standard LCZ classification scheme needs to be adapted or complemented with other variables. One recommended solution was to consider adding a LCZ subclassification to describe with more precision the large variability in land cover and property typical for arid areas. We see these findings as important advancements in the typomorphological research within urban climatology.

What other important urban form characteristics and quantitative measures (not considered in existing typomorphological methods) do we need to consider when studying the broader perspective of heat-stress resilience (e. considering both its environmental/engineering and social/ecological dimensions)?

This question was formulated following the insights gained from the systematic literature review conducted in Chapter 3 and which gave us the opportunity to think more broadly about the possible ways through which urban form can contribute to enhancing urban resilience to heat stress. In particular, we could identify at least two possible pathways through which urban form characteristics can enable urban populations to survive (persist/adapt to) extreme heat events:

- By maintaining desirable (within the acceptable ranges) outdoor/indoor thermal sensation conditions (both physiological and psychological). In fact, the systematic literature review conducted in Chapter 3 has shown that this is the most common approach used in the literature when addressing the relationship between urban form and urban resilience to heat stress. This corresponds to the *engineering* definition

of resilience (i.e. to maintain the system's status quo against a disturbance), and it was regarded as the baseline on which the concept of resilience was addressed in this thesis.

- By encouraging various social processes that have been demonstrated to affect people's adaptation capacity during extreme heat events. This, in principle, corresponds to the *ecological* definition of resilience, which focuses on the ability to maintain the function of the system without necessarily changing its physical state.

Based on the above, in Chapter 9, we have proposed a new approach to the typomorphological study of heat-stress resilience. This approach combines the urban form characteristics that support both environmental and social dimensions of heat-stress resilience in the classification of urban form types. The environmental dimension's relation to urban form is well developed in the existing typomorphological classifications, such as the LCZ scheme, as discussed in detail in Chapter 4. However, the social dimension is missing. Hence, in Chapter 9, first, we have added this dimension to the current framework used in urban climatology (see the proposed conceptual framework depicted in Figure 73); and, second, identified the urban form characteristics and quantitative measures that are associated with the social processes that play an important role in the heat-stress resilience. These social processes were found to be influenced by urban form in three ways:

- The configurational characteristics of streets and other public spaces at the meso-scale (neighborhood/district), which influence the patterns of co-presence of people and have an impact on their intensity and diversity. These patterns of co-presence generate various social processes that are important for heat-stress resilience. For instance, high-intensity co-presence creates vibrant and active urban life and increases the opportunity for face-to-face social interactions, thus combating social isolation and insecurity in urban neighborhoods that proved so deadly during previous extreme heat events.
- The geometric characteristics of semi-private/semi-public spaces at the micro-/local scale (urban block/cluster of blocks), which influence residents' physical co-presence and social interaction in such transitional spaces and hence facilitating/impeding the possibility to develop trust, mutual solidarity and a feeling of togetherness. The later processes have been demonstrated to be particularly important for reinforcing the resilience of local communities in times of crisis such as during extreme heat events.
- Characteristics of accessibility to social (soft) infrastructure, which was defined as "the physical places and organizations that shape the way people interact" (2018, p. 5) such as libraries, schools, playgrounds, swimming pools, parks and open green spaces. These places are important for social interaction and the development of social ties and solidarities similar to the public and semi-private/semi-public spaces.

Furthermore, we have identified, based on a survey of the literature, a relevant set of quantitative measures that best describe each of these aforementioned urban form

characteristics. These urban form measures were described in detail in Chapter 9 (see Table 18, Section 9.2.2) and more information about how they are calculated is provided in Appendix D. Examples of these measures include spatial integration (Hillier and Hanson, 1984) and intelligibility (or integration interface) (Hillier, 1996; Hillier and Hanson, 1984) to describe the configurational characteristics of streets and other public spaces; space enclosure and ground space index (GSI) to describe the geometric characteristics of semi-private/semi-public spaces; and the measures of attraction accessibility to calculate accessibility to vital social infrastructure based on either geometric or topological distances (Stähle et al., 2007), such as attraction distance and attraction reach.

How can these urban form characteristics and quantitative measures be employed to develop complementary typomorphological classifications of heat-stress resilience that have a better reach into urban planning and design practices?

The answer to this question is provided in the second part of Chapter 9 (Section 9.3) where we have employed a GIS- and machine learning-based method to develop typomorphological classifications of the social dimension of heat-stress resilience that complement existing classifications focusing on the environmental dimension, such as the LCZ scheme. This method operates on large-scale datasets of multiple urban form measures simultaneously and systematically, thus allowing the typomorphological description of urban form in multiple dimensions, and enabling the discovery of urban form types that are not yet known or are hard to identify by manual means.

More specifically, the method uses GIS spatial analysis to calculate, for a sample of neighborhoods (or LCZs), a set of the aforementioned urban form measures that are associated with the social dimension of heat-stress resilience, and then uses statistical clustering (Agglomerative Hierarchical Clustering) to partition these neighborhoods into clusters based on the calculated measures. In Chapter 9, Sixth of October, Egypt, was used to exemplify this method as a typical example of a contemporary city in arid areas, but it can be applied in different contexts. The results were very encouraging as it was possible to identify neighborhood types that, through distinct urban form characteristics, have different potentials for heat-stress resilience. These neighborhood types are useful for various applications, among which the most important is supporting urban planning and design decisions as will be discussed in the next section.

10.2. Implications for urban planning and design practice

In addition to the theoretical/conceptual and methodological advancement highlighted in the previous section, the work carried out in this thesis, especially on the quantitative methods for studying the impact of urban form on urban temperatures, has various implications for the urban planning and design practice, which “focus[es] not merely on the professional and technical aspects of planning but also on the impact of the [other] involved interests on the planning process and its outcome” (Auerbach, 2012, p. 49). These include, for instance, bureaucrats, politicians, entrepreneurs, stakeholders

as well as the general public who “engage in persuasion, power struggle, and negotiations” (Auerbach, 2012, p. 49).

Therefore, the empirically-derived and valid evidence that these methods aim to provide is useful not only for *neutral* urban planners/designers, who focus on conventional professional aspects, to support their technical decisions when intervening in cities or planning/designing new ones. But also, they are useful for urban planners/designers who are involved in planning decisions and policy-making (e.g. consultants and overt activists) to confront and communicate with the aforementioned actors who are involved in the decision-making process.

Design guidelines and regulations of the built environment

On the one hand, there are several implications of the quantitative methods discussed in this thesis for urban planning and design practice from professional and technical perspectives. For instance, the use of the typomorphological methods in this work to study the impact of urban form on heat-stress resilience (from both environmental and social dimensions), has yielded concrete and precise information about some urban (form) types that can facilitate/hinder heat-stress resilience in cities. These types are effective tools to inform urban planning and design practice because, as repeatedly discussed in this thesis, they perform and function in specific ways; hence, they can be used directly by professionals to achieve specific desired outcomes when they intervene in cities or plan/design new ones. Furthermore, their quantifiable characteristics can be directly translated into rules and guidelines and incorporated into local building regulations and planning/design codes.

For instance, the use of the LCZ typomorphological classification in Chapter 8 to study the impact of universally-recognized urban/built forms (i.e. standard urban/built LCZ types) on urban temperatures (i.e. the environmental/engineering dimension of heat-stress resilience) in different macroclimate regions, has shown that:

- Not surprisingly, in three out of four macroclimate regions, the commercial/light industrial (LCZ 8), compact low-rise (LCZ 3) and heavy industry types (LCZ 10) are usually associated with relatively higher temperature characteristics than the other built types. This means that urban planners and designers globally should pay special attention to the planning and design of these areas and think of new ways and more sustainable solutions to reduce their micro-and local climate impacts.
- Interestingly, the compact high-rise urban development type (i.e. LCZ 1) was turned out to be a highly resilient (from an environmental/engineering dimension) type to high diurnal temperatures as it exhibits a lower surface urban heat island (SUHI) magnitude and drops in surface temperature rank as the global surface temperature rises (ranked fifth in the cold climate region versus eighth in the tropical climate region), as opposed to, e.g. the lightweight low-rise type (LCZ 7) that increases in rank as it gets warmer from cold (ranked sixth) to temperate (ranked fourth) or tropical (ranked fifth) climate regions. This, in light of shifting world macroclimate

regions towards a warmer and drier climate, is an important finding that advocates compact living and the containment of urban sprawl.

Another example of the practical application of the typomorphological methods addressed in this thesis is the study conducted in Chapter 9 to inform urban planning and design professionals in contemporary arid cities about the possible impacts of some of the urban (form) types that they widely use in their planning/design proposals in terms of heat-stress resilience. In particular, in this study, we have identified five neighborhood types in the Sixth of October, Egypt, based on a set of urban form quantitative measures that have empirically demonstrated to be associated with social processes important for heat-stress resilience. These types were discussed to have different potentials for heat-stress resilience as follows:

- Neighborhoods with mid-rise private apartment buildings, relatively high floor space density and highly-integrated streets and public spaces have the potential for providing resilience to heat stress through social co-presence and vibrancy in the public space (referred to as *urban life resilience*).
- Neighborhoods with low- to mid-rise single-family houses aimed at high-income dwellers (gated communities) have *no resilience potential* compared to all the other neighborhood types as none of their measured urban form characteristics contribute positively to resilience to heat stress (the vast majority of values are below the mean). This constitutes an important implication for urban planning and design practice in contemporary arid cities where this development type is usually seen and promoted as providing luxury, privacy and security.
- Neighborhoods characterized by relatively enclosed, high-density blocks on private land and in the proximity of potential social infrastructure (both indoor and outdoor) have the potential for providing *baseline resilience* to heat stress through both social co-presence in the semi-private/semi-public space and social infrastructure.
- Neighborhoods with open, low-density blocks on private lands with relatively high intelligibility and low distance to potential social infrastructure have the potential for providing resilience to heat stress through social co-presence in public space and social infrastructure (referred to as *open/indoor space resilience*).
- Neighborhoods with open, low-density blocks on public lands have *limited resilience potential* compared to all the other neighborhood types as none of their measured urban form characteristics stand out.

Planning decisions and policymaking

On the other hand, the output of the quantitative methods discussed in this thesis can also reduce the gap between research and practice of urban planning and design by helping to communicate and confront empirical evidence about complex phenomena/relationships, such as the impact of urban form (or, more generally, the built environment) on urban temperatures and, in turn, on people's health and thermal sensation, to different urban actors in an accessible and persuasive language such as

through maps. Maps are powerful tools to convey spatial information and have proven to be a good way of communicating environmental exposures and health risks while, at the same time, showing relationships with the surrounding environment, thus increasing public awareness about the possible environmental impacts of the built environment (Stieb et al., 2019).

For instance, one can use the high-resolution air temperature maps, which were produced in Chapter 5, and produce others during summertime over longer periods, to find the association between ambient air temperature and observed heat-related deaths and develop statistical models based on that to produce heat-related mortality maps at the local scale. Also, one can model/map other environmental variables such as relative humidity by applying a similar procedure to the one presented in Chapter 5 for modelling air temperature. And use a simple combination of air temperature and relative humidity to calculate and map simple thermal comfort indices such as the heat index or the humidex. These indices can be translated into multi-categorical heat-related morbidity maps to describe, in simple terms, possible heat-related illnesses (e.g. fatigue, heat cramps, heat exhaustion, heatstroke).

Because morbidity and mortality maps convey complex information about the built environment-health nexus in layman's terms or plain language (e.g. the number of heat-related deaths and heat-related illnesses), they are very useful tools to inform and raise the awareness of policymakers and planning/design professionals, who "are limited in addressing public health concerns" (Moudon and Lee, 2009, p. 75), about the impacts of the built environment on health and well being; but also foster the awareness of citizens and private parties, who are now more actively involved in the urban planning and design decision making with increased power than in the past.

10.3. Final considerations and directions for future research

In this thesis, we have addressed the topic of urban resilience to heat stress primarily from the perspective of space-morphology. Of course, this is not a claim that urban resilience to heat stress is dependent on urban form alone nor that their relationship is based on deterministic causality, which is, undoubtedly, not the case. Indeed, urban resilience is influenced by many other factors, e.g. social, economic, geographic, and institutional/governmental (Bueno et al., 2021; Cardinale, 2019; Oliva and Lazzeretti, 2018; Patel et al., 2020), which are not the focus of this work. However, the key message that we wanted to convey in this thesis is that space matters and can make a difference for several reasons. Firstly, as Andrew Sayer mentioned in his book *Realism and Social Science* and cited in (Felicciotti, 2018, p. 401) "social processes do not occur tabula rasa but always 'take place' within an inherited space constituted by different processes and objects, each of which have their own spatial extension, physical exclusivity and configuration" (2000, p. 115). Secondly, from an urban planning and design perspective, "we know that urban problems are manifest in the first instance in physical and spatial terms. We also know that many, if not most, of the instruments that we have at our disposal for designing better cities are physical in form and intent" (Batty

and Longley, 1994, p. 1). Therefore, if making cities more resilient to heat stress is on the top of the global and local agenda, the role of urban planners and designers in shaping the built environment cannot be overlooked.

Another point of importance that deserves emphasis here is that in applying a space-morphological approach to the analysis and understanding of urban resilience to heat stress, we have used typomorphology (or typomorphological classifications) as means. The use of these typomorphological classifications should not be understood here in the way that they are used in *typology-morphology* studies—another area of concentration in urban design that “grounds analysis and explanation of space on the history and evolution of material space” (Moudon, 1992, p. 344)—to describe the urban forms of cities and explain their mutations over space and time to advance city making. Types within typology-morphology studies are, as such, “conceived as cultural entities rooted in, and specific to, the local process of cultural development” (Kropf, 2009, p. 112), which undoubtedly introduces a cultural bias into the analysis of space. Rather, in space-morphology, which remains essentially an *a-historical* area of concentration in urban design, types are used, as repeatedly discussed in this thesis, as means to describe urban environments purely based on their shared physical characteristics (e.g. geometric, configurational and surficial) to express aspects of the performance and function of urban form regardless of place or culture.

Having highlighted this, it should be clear now for the reader of this work, be it urban researchers or planning and design professionals, the considerations and caveats that should be taken into account when applying the methods discussed in this thesis or using their outputs in urban heat-resilience planning and design decision-making.

Finally, it should be noted that after all, and albeit the work presented in this thesis has contributed to the advancement of both research and practice in urban planning and design, further research is still needed in several directions, especially on the methods for studying the impact of urban form on urban resilience to heat stress. For instance, to address the various technical and methodological challenges that were highlighted in Chapters 5, 6 and 8 to further improve the output of the climatological-based and typomorphological methods and achieve a better understating of their suitability under different conditions and in different contexts. And, most importantly, to answer the many questions left open in Chapter 9 about the new proposed typomorphological approach to study the environmental and social dimensions of heat-stress resilience. Obviously, this approach is at its initial stages of development due to the time limit of this thesis and the limited access (and sometimes the unavailability) to empirical data on health and well-being to validate the developed typomorphological classification. Therefore, our long-term endeavor is to better establish this approach and take it further by, firstly, adding more test case studies, not only in arid cities but also globally, which can result in the identification of more neighborhood clusters, to eventually arrive at a set of general types and, probably, a universal classification system useful for urban planning and design practices globally. Secondly, to conduct an empirical validation, e.g. using data on health and well-being, to confirm the association between different neighborhood types and heat-stress resilience. The selection of these data should be

based on the criteria of relevance, validity and reliability, sensitivity to differences across space and repeatability (traceable over time). Last possible but not least, an interesting next step could be the identification of benchmark values of the urban form measures that are associated with certain health and well-being conditions in cities, which can be used to formulate urban planning and design guidelines/standards.

References

- Abdulkareem, M., Elkadi, H., 2018. From engineering to evolutionary, an overarching approach in identifying the resilience of urban design to flood. *Int J Disaster Risk Reduct* 28, 176–190. <https://doi.org/10.1016/j.ijdr.2018.02.009>
- Adger, W.N., 2016. Social and ecological resilience: are they related?: <http://dx.doi.org/10.1191/030913200701540465> 24, 347–364. <https://doi.org/10.1191/030913200701540465>
- Adger, W.N., 2003a. Building Resilience to Promote Sustainability: An Agenda for Coping with Globalisation and Promoting Justice. *Updat A Newsl Int Hum Dimens Program Glob Environ Chang*.
- Adger, W.N., 2003b. Social Capital, Collective Action, and Adaptation to Climate Change. *Econ Geogr* 79, 387–404. <https://doi.org/10.1111/J.1944-8287.2003.TB00220.X>
- Alboukadel Kassambara, 2020. rstatix: Pipe-Friendly Framework for Basic Statistical Tests [WWW Document]. R Packag version 050. URL <https://cran.r-project.org/package=rstatix>
- Albrechts, L., Barbanente, A., Monno, V., 2020. Practicing transformative planning: the territory-landscape plan as a catalyst for change. *City, Territ Archit*. <https://doi.org/10.1186/s40410-019-0111-2>
- Aldous, T., 1992. *Urban villages : a concept for creating mixed-use urban developments on a sustainable scale*. [London] : Urban Villages Group.
- Alexander, D.E., 2013. Resilience and disaster risk reduction: An etymological journey. *Nat Hazards Earth Syst Sci*. <https://doi.org/10.5194/nhess-13-2707-2013>
- Alexander, P.J., Mills, G., 2014. Local climate classification and Dublin’s urban heat island. *Atmosphere (Basel)*. <https://doi.org/10.3390/atmos5040755>
- Alghatam, W., 2012. Cultural movement patterns and social implications in space of villages absorbed by cities in Bahrain, in: 8th International Space Syntax Symposium.
- Allan, P., Bryant, M., Wirsching, C., Garcia, D., Teresa Rodriguez, M., 2013. The Influence of Urban Morphology on the Resilience of Cities Following an Earthquake. *J Urban Des* 18, 242–262. <https://doi.org/10.1080/13574809.2013.772881>
- Alonso, L., Renard, F., 2020. A new approach for understanding urban microclimate by integrating complementary predictors at different scales in regression and machine learning models. *Remote Sens*. <https://doi.org/10.3390/RS12152434>
- Anderies, J.M., 2014. Embedding built environments in social-ecological systems: Resilience-based design principles. *Build Res Inf* 42, 130–142. <https://doi.org/10.1080/09613218.2013.857455>

- Ando, M., Katagiri, K., Yamamoto, S., Wakamatsu, K., Kawahara, I., Asanuma, S., Usuda, M., Sasaki, K., 1997. Age-related effects of heat stress on protective enzymes for peroxides and microsomal monooxygenase in rat liver. *Environ Health Perspect* 105, 726–733. <https://doi.org/10.1289/EHP.97105726>
- Angélil, M., Malterre-Barthes, C. (Eds.), 2018. *Cairo Desert Cities*. Ruby press.
- Arup, 2018. *Cities Alive: Rethinking cities in arid environments*. Dubai.
- Asikin, D., Antariksa, Wulandari, L.D., Rukmi, W.I., 2017. Spatial adaptation as the Madurese migrant resilience form at urban informal sector workers settlement: a case study of Kotalama settlement - Malang. *IOP Conf Ser Earth Environ Sci* 99, 012027. <https://doi.org/10.1088/1755-1315/99/1/012027>
- Auer, A.H., 1978. Correlation of Land Use and Cover with Meteorological Anomalies. *J Appl Meteorol*. [https://doi.org/10.1175/1520-0450\(1978\)017<0636:coluac>2.0.co;2](https://doi.org/10.1175/1520-0450(1978)017<0636:coluac>2.0.co;2)
- Auerbach, G., 2012. Urban planning: Politics vs. Planning and Politicians vs. Planners. *Horizons Geogr / אופקים בגאוגרפיה*.
- Auliciems, A., 1981. Towards a psycho-physiological model of thermal perception. *Int J Biometeorol* 1981 252 25, 109–122. <https://doi.org/10.1007/BF02184458>
- Avogo, F.A., Wedam, E.A., Opoku, S.M., 2017. Housing transformation and livelihood outcomes in Accra, Ghana. *Cities* 68, 92–103. <https://doi.org/10.1016/j.cities.2017.05.009>
- Baccini, M., Biggeri, A., Accetta, G., Kosatsky, T., Katsouyanni, K., Analitis, A., Anderson, H.R., Bisanti, L., D'Ippoliti, D., Danova, J., Forsberg, B., Medina, S., Paldy, A., Rabczenko, D., Schindler, C., Michelozzi, P., 2008. Heat effects on mortality in 15 European cities. *Epidemiology* 19, 711–719. <https://doi.org/10.1097/EDE.0B013E318176BFCD>
- Bande, L., Manandhar, P., Ghazal, R., Marpu, P., 2020a. Characterization of local climate zones using ENVI-met and site data in the city of Al-Ain, UAE. *Int J Sustain Dev Plan* 15, 751–760. <https://doi.org/10.18280/IJSDP.150517>
- Bande, L., Manandhar, P., Marpu, P., Battah, M. Al, 2020b. Local Climate Zones Definition in Relation to ENVI-met in the City of Dubai, UAE. *IOP Conf Ser Mater Sci Eng* 829, 012013. <https://doi.org/10.1088/1757-899X/829/1/012013>
- Barbour, G., Romice, O., Porta, S., 2016. Sustainable Plot-Based Urban Regeneration and Traditional Master Planning Practice in Glasgow. *Open House Int* 41, 15–22. <https://doi.org/10.1108/OHI-04-2016-B0003>
- Bartesaghi Koc, C., Osmond, P., Peters, A., Irger, M., 2018. Understanding Land Surface Temperature Differences of Local Climate Zones Based on Airborne Remote Sensing Data. *IEEE J Sel Top Appl Earth Obs Remote Sens*. <https://doi.org/10.1109/JSTARS.2018.2815004>
- Barthelemy, M., 2017. From paths to blocks: New measures for street patterns.

- Barton, H., 2000. Conflicting perceptions of neighborhood: In Sustainable Communities. Earthscan.
- Batty, M., 2008. The size, scale, and shape of cities. *Science* (80-). <https://doi.org/10.1126/science.1151419>
- Batty, M., Longley, P., 1994. Fractal cities : a geometry of form and function 394.
- Bechtel, B., Alexander, P.J., Beck, C., Böhner, J., Brousse, O., Ching, J., Demuzere, M., Fonte, C., Gál, T., Hidalgo, J., Hoffmann, P., Middel, A., Mills, G., Ren, C., See, L., Sismanidis, P., Verdonck, M.L., Xu, G., Xu, Y., 2019a. Generating WUDAPT Level 0 data – Current status of production and evaluation. *Urban Clim*. <https://doi.org/10.1016/j.uclim.2018.10.001>
- Bechtel, B., Alexander, P.J., Böhner, J., Ching, J., Conrad, O., Feddema, J., Mills, G., See, L., Stewart, I., 2015. Mapping local climate zones for a worldwide database of the form and function of cities. *ISPRS Int J Geo-Information*. <https://doi.org/10.3390/ijgi4010199>
- Bechtel, B., Demuzere, M., Mills, G., Zhan, W., Sismanidis, P., Small, C., Voogt, J., 2019b. SUHI analysis using Local Climate Zones—A comparison of 50 cities. *Urban Clim*. <https://doi.org/10.1016/j.uclim.2019.01.005>
- Bechtel, B., Demuzere, M., Sismanidis, P., Fenner, D., Brousse, O., Beck, C., Van Coillie, F., Conrad, O., Keramitsoglou, I., Middel, A., Mills, G., Niyogi, D., Otto, M., See, L., Verdonck, M.-L., 2017. Quality of Crowdsourced Data on Urban Morphology—The Human Influence Experiment (HUMINEX). *Urban Sci*. <https://doi.org/10.3390/urbansci1020015>
- Beck, C., Straub, A., Breitner, S., Cyrus, J., Philipp, A., Rathmann, J., Schneider, A., Wolf, K., Jacobeit, J., 2018. Air temperature characteristics of local climate zones in the Augsburg urban area (Bavaria, southern Germany) under varying synoptic conditions. *Urban Clim*. <https://doi.org/10.1016/j.uclim.2018.04.007>
- Beck, H.E., Zimmermann, N.E., McVicar, T.R., Vergopolan, N., Berg, A., Wood, E.F., 2018. Present and future köppen-geiger climate classification maps at 1-km resolution. *Sci Data*. <https://doi.org/10.1038/sdata.2018.214>
- Benjamin, K., Luo, Z., Wang, X., 2021. Crowdsourcing Urban Air Temperature Data for Estimating Urban Heat Island and Building Heating/Cooling Load in London. *Energies* 14, 5208. <https://doi.org/10.3390/en14165208>
- Bergevoet, T., van Tuijl, M., 2016. The flexible city sustainable solutions for a Europe in transition. nai010 publishers, Rotterdam.
- Berghauser Pont, M., 2018. An analytical approach to urban form, in: *Urban Book Series*. https://doi.org/10.1007/978-3-319-76126-8_7
- Berghauser Pont, M., Stavroulaki, G., Bobkova, E., Gil, J., Marcus, L., Olsson, J., Sun, K., Serra, M., Hausleitner, B., Dhanani, A., Legeby, A., 2019a. The spatial

- distribution and frequency of street, plot and building types across five European cities. *Environ Plan B Urban Anal City Sci*.
<https://doi.org/10.1177/2399808319857450>
- Berghauer Pont, M., Stavroulaki, G., Gil, J., Marcus, L., Serra, M., Hausleitner, B., Olsson, J., Abshirini, E., Dhanani, A., 2017. Quantitative comparison of cities: Distribution of street and building types based on density and centrality measures, in: *Proceedings - 11th International Space Syntax Symposium, SSS 2017*.
- Berghauer Pont, M., Stavroulaki, G., Marcus, L., 2019b. Development of urban types based on network centrality, built density and their impact on pedestrian movement. *Environ Plan B Urban Anal City Sci*.
<https://doi.org/10.1177/2399808319852632>
- Berkes, F., Folke, C., 1998. Linking social and ecological systems for resilience and sustainability, in: Berkes, F., Folke, C. (Eds.), *Linking Social and Ecological Systems*. Cambridge University Press, Cambridge, UK, pp. 13–20.
- Bobkova, E., Berghauer Pont, M., Marcus, L., 2019a. Towards analytical typologies of plot systems: Quantitative profile of five European cities. *Environ Plan B Urban Anal City Sci*. <https://doi.org/10.1177/2399808319880902>
- Bobkova, E., Marcus, L., Berghauer Pont, M., Stavroulaki, I., Bolin, D., 2019b. Structure of Plot Systems and Economic Activity in Cities: Linking Plot Types to Retail and Food Services in London, Amsterdam and Stockholm. *Urban Sci* 3, 66. <https://doi.org/10.3390/urbansci3030066>
- Bolin, D., Verendel, V., Berghauer Pont, M., Stavroulaki, I., Ivarsson, O., Håkansson, E., 2021. Functional ANOVA modelling of pedestrian counts on streets in three European cities. *J R Stat Soc Ser A Stat Soc*.
<https://doi.org/10.1111/rssa.12646>
- Bozza, A., Asprone, D., Fiasconaro, A., Latora, V., Manfredi, G., 2015. Catastrophe resilience related to urban network shape: Preliminary analysis, in: Papadarakakis M. Papadopoulos V., P. V (Ed.), *COMPADYN 2015 - 5th ECCOMAS Thematic Conference on Computational Methods in Structural Dynamics and Earthquake Engineering*. National Technical University of Athens, pp. 1513–1531.
- Bradter, U., Kunin, W.E., Altringham, J.D., Thom, T.J., Benton, T.G., 2013. Identifying appropriate spatial scales of predictors in species distribution models with the random forest algorithm. *Methods Ecol Evol*.
<https://doi.org/10.1111/j.2041-210x.2012.00253.x>
- Breiman, L., 2001. Random forests. *Mach Learn*.
<https://doi.org/10.1023/A:1010933404324>
- Brody, S., Kim, H., Gunn, J., 2013. Examining the Impacts of Development Patterns on Flooding on the Gulf of Mexico Coast. *Urban Stud* 50, 789–806.
<https://doi.org/10.1177/0042098012448551>
- Brousse, O., Georganos, S., Demuzere, M., Vanhuysse, S., Wouters, H., Wolff, E.,

- Linard, C., van Lipzig, N.P.M., Dujardin, S., 2019. Using Local Climate Zones in Sub-Saharan Africa to tackle urban health issues. *Urban Clim* 27, 227–242. <https://doi.org/10.1016/j.uclim.2018.12.004>
- Brown, A., Dayal, A., Rumbaitis Del Rio, C., 2012. From practice to theory: Emerging lessons from Asia for building urban climate change resilience. *Environ Urban* 24, 531–556. <https://doi.org/10.1177/0956247812456490>
- Brown, K., 2014. Global environmental change I. *Prog Hum Geogr* 38, 107–117. <https://doi.org/10.1177/0309132513498837>
- Bruzzone, L., Melgani, F., 2005. Robust multiple estimator systems for the analysis of biophysical parameters from remotely sensed data. *IEEE Trans Geosci Remote Sens* 43, 159–173. <https://doi.org/10.1109/TGRS.2004.839818>
- Budhiraja, B., Pathak, P., Agrawal, G., 2017. Spatio-temporal variability of urban heat islands in local climate zones of Delhi-NCR. <https://doi.org/10.1117/12.2280253>
- Bueno, S., Bañuls, V.A., Gallego, M.D., 2021. Is urban resilience a phenomenon on the rise? A systematic literature review for the years 2019 and 2020 using textometry. *Int J Disaster Risk Reduct* 66, 102588. <https://doi.org/10.1016/J.IJDRR.2021.102588>
- Bunker, A., Wildenhain, J., Vandenberg, A., Henschke, N., Rocklöv, J., Hajat, S., Sauerborn, R., 2016. Effects of Air Temperature on Climate-Sensitive Mortality and Morbidity Outcomes in the Elderly; a Systematic Review and Meta-analysis of Epidemiological Evidence. *EBioMedicine* 6, 258–268. <https://doi.org/10.1016/j.ebiom.2016.02.034>
- Buttstädt, M., Sachsen, T., Ketzler, G., Merbitz, H., Schneider, C., 2011. A new approach for highly resolved air temperature measurements in urban areas. *Atmos Meas Tech Discuss* 4.
- Byahut, S., Mittal, J., 2017. Using Land Readjustment in Rebuilding the Earthquake-Damaged City of Bhuj, India. *J Urban Plan Dev* 143, 05016012. [https://doi.org/10.1061/\(ASCE\)UP.1943-5444.0000354](https://doi.org/10.1061/(ASCE)UP.1943-5444.0000354)
- Cai, M., Ren, C., Xu, Y., Lau, K.K.L., Wang, R., 2018. Investigating the relationship between local climate zone and land surface temperature using an improved WUDAPT methodology – A case study of Yangtze River Delta, China. *Urban Clim*. <https://doi.org/10.1016/j.uclim.2017.05.010>
- Calthorpe, P., 1993. *The next American metropolis: ecology, community, and the American dream*. Princeton Architectural Press, New York.
- Camps-Valls, G., Bruzzone, L., Rojo-Álvarez, J.L., Melgani, F., 2006. Robust support vector regression for biophysical variable estimation from remotely sensed images. *IEEE Geosci Remote Sens Lett* 3, 339–343. <https://doi.org/10.1109/LGRS.2006.871748>
- Cardinale, I., 2019. Vulnerability, Resilience and ‘Systemic Interest’: a Connectivity

- Approach. *Networks Spat Econ* 1–17. <https://doi.org/10.1007/S11067-019-09462-9/TABLES/2>
- Cariolet, J.-M., Colombert, M., Vuillet, M., Diab, Y., 2018. Assessing the resilience of urban areas to traffic-related air pollution: Application in Greater Paris. *Sci Total Environ* 615, 588–596. <https://doi.org/10.1016/j.scitotenv.2017.09.334>
- Carmona, M., 2021. Public places urban spaces: The dimensions of urban design, *Public Places Urban Spaces: The Dimensions of Urban Design*. Routledge. <https://doi.org/10.4324/9781315158457>
- Carnahan, W.H., Larson, R.C., 1990. An analysis of an urban heat sink. *Remote Sens Environ*. [https://doi.org/10.1016/0034-4257\(90\)90056-R](https://doi.org/10.1016/0034-4257(90)90056-R)
- Carpenter, S., Walker, B., Anderies, J.M., Abel, N., 2001. From Metaphor to Measurement: Resilience of What to What? *Ecosystems* 4, 765–781. <https://doi.org/10.1007/s10021-001-0045-9>
- Carpenter, S.R., Ludwig, D., Brock, W.A., 1999. Management of eutrophication for lakes subject to potentially irreversible change. *Ecol Appl* 9. [https://doi.org/10.1890/1051-0761\(1999\)009\[0751:MOEFLS\]2.0.CO;2](https://doi.org/10.1890/1051-0761(1999)009[0751:MOEFLS]2.0.CO;2)
- Cassano, J.J., 2014. Weather bike: A bicycle-based weather station for observing local temperature variations. *Bull Am Meteorol Soc*. <https://doi.org/10.1175/BAMS-D-13-00044.1>
- Castell, P., 2010. Managing yards and togetherness: living conditions and social robustness through tenant involvement in open space management. Chalmers University of Technology.
- Cervero, R., 1998. *The transit metropolis : a global inquiry*. Island Press, Washington, DC.
- Chakraborty, T., Hsu, A., Manya, D., Sheriff, G., 2020. A spatially explicit surface urban heat island database for the United States: Characterization, uncertainties, and possible applications. *ISPRS J Photogramm Remote Sens*. <https://doi.org/10.1016/j.isprsjprs.2020.07.021>
- Chakraborty, T., Lee, X., 2019. A simplified urban-extent algorithm to characterize surface urban heat islands on a global scale and examine vegetation control on their spatiotemporal variability. *Int J Appl Earth Obs Geoinf*. <https://doi.org/10.1016/j.jag.2018.09.015>
- Chandler, T.J., 1965. *The Climate of London*. Hutchinson & Co, London.
- Chelleri, L., Kunath, A., Minucci, G., Olazabal, M., Waters, J.J., Yumalogava, L., 2012. Multidisciplinary perspectives on urban resilience. BC3, Basque Centre for Climate Change.
- Choay, F., Merlin, P. (Eds.), 1986. *A propos de la morphologie urbaine: Rapport pour le Ministère de l'Urbanisme, du Logement et des Transports*. Institut d'Urbanisme de l'Academie de Paris, Université de Paris VIII, Paris.

- Cimellaro, G.P., Marasco, S., Zamani Noori, A., Kammouh, O., Mahin, S., 2018. A new tool to assess the resilience of an urban environment under an earthquake scenario, in: 11th National Conference on Earthquake Engineering 2018, NCEE 2018: Integrating Science, Engineering, and Policy. Earthquake Engineering Research Institute, pp. 5606–5617.
- Cohen, J., 1960. A Coefficient of Agreement for Nominal Scales. *Educ Psychol Meas.* <https://doi.org/10.1177/001316446002000104>
- Colaninno, N., Cladera, J., Pfeffer, K., 2011. An automatic classification of urban texture: form and compactness of morphological homogeneous structures in Barcelona, in: *New Challenges for European Regions and Urban Areas in a Globalised World.*
- Colaninno, N., Morello, E., 2019. Modelling the impact of green solutions upon the urban heat island phenomenon by means of satellite data. *J Phys Conf Ser* 1343, 012010. <https://doi.org/10.1088/1742-6596/1343/1/012010>
- Collins, R., 2004. *Interaction Ritual Chains.* Princeton University Press.
- Combeau, F., Greco, G., 2018. Desert urbanization: the planning of the neglect, in: Angélil, M., Malterre-Barthes, C. (Eds.), *Cairo Desert Cities.* Ruby press, p. 418.
- Conzen, M.R.G., 1960. Alnwick, Northumberland: A Study in Town-Plan Analysis. *Trans Pap (Institute Br Geogr.* <https://doi.org/10.2307/621094>
- Cote, M., Nightingale, A.J., 2012. Resilience thinking meets social theory. *Prog Hum Geogr* 36, 475–489. <https://doi.org/10.1177/0309132511425708>
- Coutts, A.M., Harris, R.J., Phan, T., Livesley, S.J., Williams, N.S.G., Tapper, N.J., 2016. Thermal infrared remote sensing of urban heat: Hotspots, vegetation, and an assessment of techniques for use in urban planning. *Remote Sens Environ.* <https://doi.org/10.1016/j.rse.2016.09.007>
- Cribbie, R.A., Fiksenbaum, L., Keselman, H.J., Wilcox, R.R., 2012. Effect of non-normality on test statistics for one-way independent groups designs. *Br J Math Stat Psychol.* <https://doi.org/10.1111/j.2044-8317.2011.02014.x>
- Cristóbal, J., Ninyerola, M., Pons, X., 2008. Modeling air temperature through a combination of remote sensing and GIS data. *J Geophys Res Atmos.* <https://doi.org/10.1029/2007JD009318>
- Curriero, F.C., Heiner, K.S., Samet, J.M., Zeger, S.L., Strug, L., Patz, J.A., 2002. Temperature and Mortality in 11 Cities of the Eastern United States. *Am J Epidemiol* 155, 80–87. <https://doi.org/10.1093/AJE/155.1.80>
- Cutini, V., Pezzica, C., 2020. Street Network Resilience Put to the Test: The Dramatic Crash of Genoa and Bologna Bridges. *Sustainability* 12, 4706. <https://doi.org/10.3390/su12114706>
- Cutter, S.L., 2016. The landscape of disaster resilience indicators in the USA. *Nat Hazards* 80, 741–758. <https://doi.org/10.1007/s11069-015-1993-2>

- D'Ippoliti, D., Michelozzi, P., Marino, C., De' Donato, F., Menne, B., Katsouyanni, K., Kirchmayer, U., Analitis, A., Medina-Ramón, M., Paldy, A., Atkinson, R., Kovats, S., Bisanti, L., Schneider, A., Lefranc, A., Iñiguez, C., Perucci, C.A., 2010. The impact of heat waves on mortality in 9 European cities: Results from the EuroHEAT project. *Environ Heal A Glob Access Sci Source* 9, 1–9. <https://doi.org/10.1186/1476-069X-9-37/FIGURES/2>
- da Silva, J., Kernaghan, S., Luque, A., 2012. A systems approach to meeting the challenges of urban climate change. *Int J Urban Sustain Dev*. <https://doi.org/10.1080/19463138.2012.718279>
- Dag, O., Dolgun, A., Konar, N.M., 2018. Onewaytests: An R package for one-way tests in independent groups designs. *R J*. <https://doi.org/10.32614/RJ-2018-022>
- Das, M., Das, A., Mandal, S., 2020. Outdoor thermal comfort in different settings of a tropical planning region: A study on Sriniketan-Santiniketan Planning Area (SSPA), Eastern India. *Sustain Cities Soc* 63, 102433. <https://doi.org/10.1016/j.scs.2020.102433>
- Davoudi, S., Shaw, K., Haider, L.J., Quinlan, A.E., Peterson, G.D., Wilkinson, C., Fünfgeld, H., McEvoy, D., Porter, L., 2012. Resilience: A Bridging Concept or a Dead End? “Reframing” Resilience: Challenges for Planning Theory and Practice Interacting Traps: Resilience Assessment of a Pasture Management System in Northern Afghanistan Urban Resilience: What Does it Mean in Planni. *Plan Theory Pract*. <https://doi.org/10.1080/14649357.2012.677124>
- Demuzere, M., Bechtel, B., Mills, G., 2019. Global transferability of local climate zone models. *Urban Clim*. <https://doi.org/10.1016/j.uclim.2018.11.001>
- Demuzere, M., Kittner, J., Bechtel, B., 2021. LCZ Generator: A Web Application to Create Local Climate Zone Maps. *Front Environ Sci* 9, 112. <https://doi.org/10.3389/FENV.2021.637455/BIBTEX>
- Dhar, T.K., Khirfan, L., 2017. A multi-scale and multi-dimensional framework for enhancing the resilience of urban form to climate change. *Urban Clim* 19, 72–91. <https://doi.org/10.1016/j.uclim.2016.12.004>
- Di Martino, B., Rak, M., Ficco, M., Esposito, A., Maisto, S.A., Nacchia, S., 2018. Internet of things reference architectures, security and interoperability: A survey. *Internet of Things (Netherlands)* 1–2, 99–112. <https://doi.org/10.1016/j.iot.2018.08.008>
- Du Plessis, C., Landman, K., Nel, D., Peres, E., 2015. A “resilient” urban morphology: TRUST. *Urban Morphol* 19, 183–184.
- Dunn, O.J., 1961. Multiple Comparisons Among Means. *J Am Stat Assoc*. <https://doi.org/10.2307/2282330>
- Durbha, S.S., King, R.L., Younan, N.H., 2007. Support vector machines regression for retrieval of leaf area index from multiangle imaging spectroradiometer. *Remote Sens Environ* 107, 348–361. <https://doi.org/10.1016/J.RSE.2006.09.031>

- Ebi, K.L., Teisberg, T.J., Kalkstein, L.S., Robinson, L., Weiher, R.F., 2004. Heat Watch/Warning Systems Save Lives: Estimated Costs and Benefits for Philadelphia 1995–98. *Bull Am Meteorol Soc* 85, 1067–1074. <https://doi.org/10.1175/BAMS-85-8-1067>
- Elcheroth, G., Drury, J., 2020. Collective resilience in times of crisis: Lessons from the literature for socially effective responses to the pandemic. *Br J Soc Psychol*. <https://doi.org/10.1111/bjso.12403>
- Eldesoky, A.H.M., Colaninno, N., Morello, E., 2020. Mapping Urban ventilation corridors and assessing their impact upon the cooling effect of greening solutions, in: *International Archives of the Photogrammetry, Remote Sensing and Spatial Information Sciences - ISPRS Archives*. pp. 665–672. <https://doi.org/10.5194/isprs-archives-XLIII-B4-2020-665-2020>
- Ellefsen, R., 1991. Mapping and measuring buildings in the canopy boundary layer in ten U.S. cities. *Energy Build.* [https://doi.org/10.1016/0378-7788\(91\)90097-M](https://doi.org/10.1016/0378-7788(91)90097-M)
- Ellin, N., 2007. *Postmodern Urbanism*. Princeton Architectural Press, New York.
- Fahed, J., Kinab, E., Ginestet, S., Adolphe, L., 2020. Impact of urban heat island mitigation measures on microclimate and pedestrian comfort in a dense urban district of Lebanon. *Sustain Cities Soc.* <https://doi.org/10.1016/j.scs.2020.102375>
- Fanger, P.O., 1972. Thermal comfort: Analysis and applications in environmental engineering, *Applied Ergonomics*. [https://doi.org/10.1016/S0003-6870\(72\)80074-7](https://doi.org/10.1016/S0003-6870(72)80074-7)
- Farris, J.T., 2001. The barriers to using urban infill development to achieve smart growth. *Hous Policy Debate* 12. <https://doi.org/10.1080/10511482.2001.9521395>
- Felicioni, L., Lupíšek, A., Hájek, P., 2020. Major European Stressors and Potential of Available Tools for Assessment of Urban and Buildings Resilience. *Sustainability* 12, 7554. <https://doi.org/10.3390/su12187554>
- Feliciotti, A., 2018. Resilience and urban design: A systems approach to the study of resilience in urban form. Learning from the case of Gorbals. University of Strathclyde.
- Feliciotti, A., Romice, O., Porta, S., 2016. Design for Change: Five Proxies for Resilience in the Urban Form. *Open House Int* 41, 23–30. <https://doi.org/10.1108/OHI-04-2016-B0004>
- Fenner, D., Meier, F., Bechtel, B., Otto, M., Scherer, D., 2017. Intra and inter “local climate zone” variability of air temperature as observed by crowdsourced citizen weather stations in Berlin, Germany. *Meteorol Zeitschrift*. <https://doi.org/10.1127/metz/2017/0861>
- Ferreira, T.M., Maio, R., Vicente, R., Costa, A., 2016. Earthquake risk mitigation: the impact of seismic retrofitting strategies on urban resilience. *Int J Strateg Prop Manag* 20, 291–304. <https://doi.org/10.3846/1648715X.2016.1187682>

- Fischer, K., Hiermaier, S., Riedel, W., Häring, I., 2018. Morphology Dependent Assessment of Resilience for Urban Areas. *Sustainability* 10, 1800. <https://doi.org/10.3390/su10061800>
- Fleischmann, M., Feliciotti, A., Romice, O., Porta, S., 2021. Methodological foundation of a numerical taxonomy of urban form: <https://doi.org/10.1177/23998083211059835> 0, 1–17. <https://doi.org/10.1177/23998083211059835>
- Fligner, M.A., Killeen, T.J., 1976. Distribution-Free Two-Sample Tests for Scale. *J Am Stat Assoc* 71, 210–213. <https://doi.org/10.1080/01621459.1976.10481517>
- Folke, C., 2006. Resilience: The emergence of a perspective for social–ecological systems analyses. *Glob Environ Chang* 16, 253–267. <https://doi.org/10.1016/j.gloenvcha.2006.04.002>
- Folke, C., Biggs, R., Norström, A. V., Reyers, B., Rockström, J., 2016. Social-ecological resilience and biosphere-based sustainability science. *Ecol Soc* 21. <https://doi.org/10.5751/ES-08748-210341>
- Folke, C., Carpenter, S., Elmqvist, T., Gunderson, L., Holling, C.S., Walker, B., 2002. Resilience and sustainable development: Building adaptive capacity in a world of transformations. *Ambio*. <https://doi.org/10.1579/0044-7447-31.5.437>
- Folke, C., Carpenter, S.R., Walker, B., Scheffer, M., Chapin, T., Rockström, J., 2010. Resilience thinking: Integrating resilience, adaptability and transformability. *Ecol Soc* 15. <https://doi.org/10.5751/ES-03610-150420>
- Forgaci, C., van Timmeren, A., 2014. Urban Form and Fitness: A Space-Morphological Approach to General Urban Resilience, in: *Proceedings of the 20th International Sustainable Development Research Conference*.
- Fotheringham, A.S., Charlton, M.E., Brunson, C., 1998. Geographically weighted regression: a natural evolution of the expansion method for spatial data analysis. *Environ Plan A*. <https://doi.org/10.1068/a301905>
- Fraedrich, K., Gerstengarbe, F.W., Werner, P.C., 2001. Climate shifts during the last century. *Clim Change*. <https://doi.org/10.1023/A:1010699428863>
- Frey, C.M., Rigo, G., Parlow, E., 2007. Urban radiation balance of two coastal cities in a hot and dry environment. *Int J Remote Sens*. <https://doi.org/10.1080/01431160600993389>
- Frey, H., 2003. *Designing the city: Towards a more sustainable urban form*, *Designing the City: Towards a More Sustainable Urban Form*. Taylor & Francis. <https://doi.org/10.4324/9780203362433>
- Fricke, C., Pongrácz, R., Gál, T., Savić, S., Unger, J., 2020. Using local climate zones to compare remotely sensed surface temperatures in temperate cities and hot desert cities. *Morav Geogr Reports* 28, 48–60. <https://doi.org/10.2478/mgr-2020-0004>

- Friedman, J.H., 1991. *Multivariate Adaptive Regression Splines*.
<https://doi.org/10.1214/aos/1176347963> 19, 1–67.
<https://doi.org/10.1214/AOS/1176347963>
- Friend, R., Moench, M., 2013. What is the purpose of urban climate resilience? Implications for addressing poverty and vulnerability. *Urban Clim* 6, 98–113.
<https://doi.org/10.1016/J.UCLIM.2013.09.002>
- Fung, W.Y., Lam, K.S., Nichol, J., Wong, M.S., 2009. Derivation of nighttime urban air temperatures using a satellite thermal image. *J Appl Meteorol Climatol*.
<https://doi.org/10.1175/2008JAMC2001.1>
- Fusco, G., Araldi, A., 2018. The Nine Forms of the French Riviera: Classifying Urban Fabrics from the Pedestrian Perspective.
<https://doi.org/10.4995/isuf2017.2017.5219>
- Fusco, G., Venerandi, A., 2020. Assessing Morphological Resilience. *Methodological Challenges for Metropolitan Areas*, in: *Lecture Notes in Computer Science (Including Subseries Lecture Notes in Artificial Intelligence and Lecture Notes in Bioinformatics)*. pp. 593–609. https://doi.org/10.1007/978-3-030-58820-5_44
- Galderisi, A., Limongi, G., Salata, K.D., 2020. Strengths and weaknesses of the 100 Resilient Cities Initiative in Southern Europe: Rome and Athens' experiences. *City, Territ Archit*. <https://doi.org/10.1186/s40410-020-00123-w>
- Games, P.A., Howell, J.F., 1976. Pairwise Multiple Comparison Procedures with Unequal N's and/or Variances: A Monte Carlo Study. *J Educ Stat*.
<https://doi.org/10.3102/10769986001002113>
- Gamo, M., Shinoda, M., Maeda, T., 2013. Classification of arid lands, including soil degradation and irrigated areas, based on vegetation and aridity indices. *Int J Remote Sens*. <https://doi.org/10.1080/01431161.2013.805281>
- Gauthier, P., Gilliland, J., 2006. Mapping urban morphology: A classification scheme for interpreting contributions to the study of urban form. *Urban Morphol*.
- Geletič, J., Lehnert, M., Dobrovolný, P., 2016. Land surface temperature differences within local climate zones, Based on two central European cities. *Remote Sens*.
<https://doi.org/10.3390/rs8100788>
- Geletič, J., Lehnert, M., Savić, S., Milošević, D., 2019. Inter-/intra-zonal seasonal variability of the surface urban heat island based on local climate zones in three central European cities. *Build Environ* 156, 21–32.
<https://doi.org/10.1016/j.buildenv.2019.04.011>
- Gémes, O., Tobak, Z., Leeuwen, B. van, 2016. Satellite Based Analysis of Surface Urban Heat Island Intensity. *J Environ Geogr*. <https://doi.org/10.1515/jengeo-2016-0004>
- Gibson, J., 1986. *The Ecological Approach to Visual Perception*. Psychology Press, New York, NY.

- Gibson, J., 1977. The theory of affordances, in: Shaw, R., Bransford, J. (Eds.), *Perceiving, Acting, and Knowing: Toward an Ecological Psychology*. Erlbaum, Hillsdale NJ, p. 67.
- Gil, J., Beirão, J.N., Montenegro, N., Duarte, J.P., 2012. On the discovery of urban typologies: Data mining the many dimensions of urban form. *Urban Morphol*.
- Gower, J.C., 1971. A General Coefficient of Similarity and Some of Its Properties. *Biometrics*. <https://doi.org/10.2307/2528823>
- Granovetter, M., 1983. The Strength of Weak Ties: A Network Theory Revisited. *Sociol Theory*. <https://doi.org/10.2307/202051>
- Granovetter, M.S., 1973. The Strength of Weak Ties. *Am J Sociol*. <https://doi.org/10.1086/225469>
- Grigg, D., 1965. THE LOGIC OF REGIONAL SYSTEMS¹. *Ann Assoc Am Geogr* 55, 465–491. <https://doi.org/10.1111/J.1467-8306.1965.TB00529.X>
- Gunderson, L.H., 2003. Ecological Resilience—In Theory and Application. <http://dx.doi.org/10.1146/annurev.ecolsys.31.1.425> 31, 425–439. <https://doi.org/10.1146/ANNUREV.ECOLSYS.31.1.425>
- Gunderson, L.H., Holling, C.S. (Eds.), 2002. *Panarchy: understanding transformations in human and natural systems*. Island Press, Washington DC.
- Guo, Y., Gál, T., Tian, G., Unger, J., 2020. Model development for the estimation of urban air temperature based on surface temperature and NDVI. *Acta Climatol Chorol* 54, 29–40. <https://doi.org/10.14232/ACTA.CLIM.2020.54.3>
- Haashemi, S., Weng, Q., Darvishi, A., Alavipanah, S.K., 2016. Seasonal variations of the surface urban heat Island in a semi-arid city. *Remote Sens*. <https://doi.org/10.3390/rs8040352>
- Habraken, J., 1961. *De dragers en de mensen : het einde van de massawoningbouw*. Scheltema & Holkema, Amsterdam.
- Habraken, N.J., 1972. *Supports: An Alternative to Mass Housing*. Architectural Press, London.
- Hahn, B., 2000. Power centres: A new retail format in the United States of America. *J Retail Consum Serv* 7. [https://doi.org/10.1016/S0969-6989\(00\)00015-1](https://doi.org/10.1016/S0969-6989(00)00015-1)
- Hansen, O., 1961. La forme ouverte dans l'architecture – l'art du grand nombre. *Le Carré Bleu* 1, 4–5.
- Harlan, S.L., Brazel, A.J., Prashad, L., Stefanov, W.L., Larsen, L., 2006. Neighborhood microclimates and vulnerability to heat stress. *Soc Sci Med* 63, 2847–2863. <https://doi.org/10.1016/J.SOCSCIMED.2006.07.030>
- Hassler, U., Kohler, N., 2014. Resilience in the built environment. *Build Res Inf* 42, 119–129. <https://doi.org/10.1080/09613218.2014.873593>

- Hatvani-Kovacs, G., Belusko, M., Skinner, N., Pockett, J., Boland, J., 2016. Heat stress risk and resilience in the urban environment. *Sustain CITIES Soc* 26, 278–288. <https://doi.org/10.1016/j.scs.2016.06.019>
- Hausleitner, B., Berghauser Pont, M., 2017. Development of a configurational typology for micro-businesses integrating geometric and configurational variables, in: *Proceedings - 11th International Space Syntax Symposium, SSS 2017*.
- Heaviside, C., Macintyre, H., Vardoulakis, S., 2017. The Urban Heat Island: Implications for Health in a Changing Environment. *Curr Environ Heal reports*. <https://doi.org/10.1007/s40572-017-0150-3>
- Hertel, S., Le Tertre, A., Jöckel, K.H., Hoffmann, B., 2009. Quantification of the heat wave effect on cause-specific mortality in Essen, Germany. *Eur J Epidemiol* 24, 407–414. <https://doi.org/10.1007/S10654-009-9359-2/FIGURES/3>
- Hertzberger, H., 1991. *Lessons for Students in Architecture*. nai010 publishers.
- Hillier, B., 1996. *Space is the machine*, Design Studies.
- Hillier, B., Hanson, J., 1984. *The social logic of space*. <https://doi.org/10.1017/cbo9780511597237>
- Hillier, B., Iida, S., 2005. Network and psychological effects in urban movement, in: *Lecture Notes in Computer Science (Including Subseries Lecture Notes in Artificial Intelligence and Lecture Notes in Bioinformatics)*. https://doi.org/10.1007/11556114_30
- Hjort, J., Suomi, J., Käyhkö, J., 2011. Spatial prediction of urban–rural temperatures using statistical methods. *Theor Appl Climatol* 2011 1061 106, 139–152. <https://doi.org/10.1007/S00704-011-0425-9>
- Ho, H.C., Knudby, A., Sirovyak, P., Xu, Y., Hodul, M., Henderson, S.B., 2014. Mapping maximum urban air temperature on hot summer days. *Remote Sens Environ*. <https://doi.org/10.1016/j.rse.2014.08.012>
- Ho, T.K., 1998. The random subspace method for constructing decision forests. *IEEE Trans Pattern Anal Mach Intell*. <https://doi.org/10.1109/34.709601>
- Holling, C.S., 1996a. Engineering resilience versus ecological resilience, in: *Engineering within Ecological Constraints*.
- Holling, C.S., 1996b. Engineering resilience versus ecological resilience, National Academy of Engineering. *Eng Within Ecol Constraints*.
- Holling, C.S., 1973. Resilience and Stability of Ecological Systems. *Annu Rev Ecol Syst* 4, 1–23. <https://doi.org/10.1146/annurev.es.04.110173.000245>
- Hooker, J., Duveiller, G., Cescatti, A., 2018. Data descriptor: A global dataset of air temperature derived from satellite remote sensing and weather stations. *Sci Data*. <https://doi.org/10.1038/sdata.2018.246>

- Höppe, P., 2002. Different aspects of assessing indoor and outdoor thermal comfort. *Energy Build* 34, 661–665. [https://doi.org/10.1016/S0378-7788\(02\)00017-8](https://doi.org/10.1016/S0378-7788(02)00017-8)
- Hu, L., Brunsell, N.A., 2013. The impact of temporal aggregation of land surface temperature data for surface urban heat island (SUHI) monitoring. *Remote Sens Environ*. <https://doi.org/10.1016/j.rse.2013.02.022>
- Hu, L., Wilhelmi, O. V., Uejio, C., 2019. Assessment of heat exposure in cities: Combining the dynamics of temperature and population. *Sci Total Environ* 655, 1–12. <https://doi.org/10.1016/J.SCITOTENV.2018.11.028>
- Huete, A.R., 1988. A soil-adjusted vegetation index (SAVI). *Remote Sens Environ*. [https://doi.org/10.1016/0034-4257\(88\)90106-X](https://doi.org/10.1016/0034-4257(88)90106-X)
- Huynen, M.M.T.E., Martens, P., Schram, D., Weijenberg, M.P., Kunst, A.E., 2001. The impact of heat waves and cold spells on mortality rates in the Dutch population. *Environ Health Perspect* 109, 463–470. <https://doi.org/10.1289/EHP.01109463>
- Imhoff, M.L., Zhang, P., Wolfe, R.E., Bounoua, L., 2010. Remote sensing of the urban heat island effect across biomes in the continental USA. *Remote Sens Environ*. <https://doi.org/10.1016/j.rse.2009.10.008>
- Jabareen, Y., 2013. Planning the resilient city: Concepts and strategies for coping with climate change and environmental risk. *Cities* 31, 220–229. <https://doi.org/10.1016/j.cities.2012.05.004>
- Jabareen, Y.R., 2006. Sustainable Urban Forms: Their Typologies, Models, and Concepts. *J Plan Educ Res* 26, 38–52. <https://doi.org/10.1177/0739456X05285119>
- Jacobs, J., 1961. *The Death and Life of Great American Cities*. Random House, New York.
- Jamali, F.S., Khaledi, S., Razavian, M.T., 2021. Seasonal impact of urban parks on land surface temperature (LST) in semi-arid city of Tehran. *Int J Urban Sustain Dev* 13, 248–264. <https://doi.org/10.1080/19463138.2021.1872083>
- Jang, J.S.R., 1993. ANFIS: Adaptive-Neural-Based Fuzzy Inference System. *IEEE Trans Syst Man Cybern* 23, 665–685. <https://doi.org/10.1109/21.256541>
- Jayakody, R.R.J.C., Amaratunga, D., 2020. Guiding factors for planning public open spaces to enhance coastal cities' disaster resilience to tsunamis. *Int J Disaster Resil Built Environ ahead-of-p*. <https://doi.org/10.1108/IJDRBE-06-2020-0058>
- Jenks, M., Burton, E., Williams, K. (Eds.), 1996. *The Compact City: A Sustainable Urban Form?* E & FN Spon, London.
- Jiang, S., Huang, F., Zhan, W., Bechtel, B., Liu, Z., Demuzere, M., Huang, Y., Xu, Y., Quan, J., Xia, W., Ma, L., Hong, F., Jiang, L., Lai, J., Wang, C., Kong, F., Du, H., Miao, S., Chen, Y., Zhang, X., 2021. Mapping Local Climate Zones: A Bibliometric Meta-Analysis and Systematic Review.

<https://doi.org/10.31219/osf.io/c2bez>

- Jimenez-Munoz, J.C., Cristobal, J., Sobrino, J.A., Sòria, G., Ninyerola, M., Pons, X., 2009. Revision of the single-channel algorithm for land surface temperature retrieval from landsat thermal-infrared data. *IEEE Trans Geosci Remote Sens.* <https://doi.org/10.1109/TGRS.2008.2007125>
- Jiménez-Munoz, J.C., Sobrino, J.A., 2003. A generalized single-channel method for retrieving land surface temperature from remote sensing data. *J Geophys Res D Atmos.* <https://doi.org/10.1029/2003jd003480>
- Jimenez-Munoz, J.C., Sobrino, J.A., Skokovic, D., Mattar, C., Cristobal, J., 2014. Land surface temperature retrieval methods from landsat-8 thermal infrared sensor data. *IEEE Geosci Remote Sens Lett.* <https://doi.org/10.1109/LGRS.2014.2312032>
- Johnson, B.A., Jozdani, S.E., 2019. Local climate zone (LCZ) map accuracy assessments should account for land cover physical characteristics that affect the local thermal environment. *Remote Sens.* <https://doi.org/10.3390/rs11202420>
- Jylhä, K., Tuomenvirta, H., Ruosteenoja, K., Niemi-Hugaerts, H., Keisu, K., Karhu, J.A., 2010. Observed and Projected Future Shifts of Climatic Zones in Europe and Their Use to Visualize Climate Change Information. *Weather Clim Soc.* <https://doi.org/10.1175/2010wcas1010a.1>
- Kabano, P., Lindley, S., Harris, A., 2021. Evidence of urban heat island impacts on the vegetation growing season length in a tropical city. *Landsc Urban Plan* 206, 103989. <https://doi.org/10.1016/j.landurbplan.2020.103989>
- Kawashima, S., Ishida, T., Minomura, M., Miwa, T., 2000. Relations between surface temperature and air temperature on a local scale during winter nights. *J Appl Meteorol.* [https://doi.org/10.1175/1520-0450\(2000\)039<1570:RBSTAA>2.0.CO;2](https://doi.org/10.1175/1520-0450(2000)039<1570:RBSTAA>2.0.CO;2)
- Kelbaugh, D. (Ed.), 1989. *The Pedestrian pocket book : a new suburban design strategy.* Princeton Architectural Press in association with the University of Washington.
- Keramitsoglou, I., Daglis, I.A., Amiridis, V., Chrysoulakis, N., Ceriola, G., Manunta, P., Maiheu, B., De Ridder, K., Lauwaet, D., Paganini, M., 2012. Evaluation of satellite-derived products for the characterization of the urban thermal environment. *J Appl Remote Sens.* <https://doi.org/10.1117/1.jrs.6.061704>
- Keselman, H.J., Algina, J., Lix, L.M., Wilcox, R.R., Deering, K.N., 2008. A Generally Robust Approach for Testing Hypotheses and Setting Confidence Intervals for Effect Sizes. *Psychol Methods.* <https://doi.org/10.1037/1082-989X.13.2.110>
- Keselman, H.J., Wilcox, R.R., Othman, A.R., Fradette, K., 2002. Trimming, transforming statistics, and bootstrapping: Circumventing the biasing effects of heteroscedasticity and nonnormality. *J Mod Appl Stat Methods.* <https://doi.org/10.22237/jmasm/1036109820>

- Kim, H., Macdonald, E., 2016. Does Wind Discourage Sustainable Transportation Mode Choice? Findings from San Francisco, California, USA. *Sustainability* 8, 257. <https://doi.org/10.3390/su8030257>
- Kim, Y., Joh, S., 2006. A vulnerability study of the low-income elderly in the context of high temperature and mortality in Seoul, Korea. *Sci Total Environ* 371, 82–88. <https://doi.org/10.1016/J.SCITOTENV.2006.08.014>
- Kittana, A.M.G., Meulder, B. De, 2019. Architecture as an agency of resilience in urban armed conflicts. *Archnet-IJAR Int J Archit Res* 13, 698–717. <https://doi.org/10.1108/ARCH-03-2019-0065>
- Klein, R.J.T., Nicholls, R.J., Thomalla, F., 2003. Resilience to natural hazards: How useful is this concept? *Environ Hazards*. <https://doi.org/10.1016/j.hazards.2004.02.001>
- Klinenberg, E., 2018. *Palaces for the People: How Social Infrastructure Can Help Fight Inequality, Polarization, and the Decline of Civic Life*. NY: Crown, New York.
- Klinenberg, E., 2002. *Heat Wave: A Social Autopsy of Disaster in Chicago*. University of Chicago Press, Chicago.
- Klinenberg, E., 2001. *Dying Alone: The Social Production of Urban Isolation*. *Ethnography*. <https://doi.org/10.1177/14661380122231019>
- Klinenberg, E., 1999. Denaturalizing disaster: A social autopsy of the 1995 Chicago heat wave. *Theory Soc* 1999 282 28, 239–295. <https://doi.org/10.1023/A:1006995507723>
- Köppen, W., Geiger, R., 1936. *Handbuch der Klimatologie: Das geographische System der Klimate*, Verlag von Gebrüder Borntraeger. <https://doi.org/10.3354/cr01204>
- Kotharkar, R., Bagade, A., 2018. Local Climate Zone classification for Indian cities: A case study of Nagpur. *Urban Clim*. <https://doi.org/10.1016/j.uclim.2017.03.003>
- Kotharkar, R., Ghosh, A., Kapoor, S., Reddy, D.G.K., 2022. Approach to local climate zone based energy consumption assessment in an Indian city. *Energy Build* 259, 111835. <https://doi.org/10.1016/j.enbuild.2022.111835>
- Kottek, M., Grieser, J., Beck, C., Rudolf, B., Rubel, F., 2006. World map of the Köppen-Geiger climate classification updated. *Meteorol Zeitschrift*. <https://doi.org/10.1127/0941-2948/2006/0130>
- Kriticos, D.J., Webber, B.L., Leriche, A., Ota, N., Macadam, I., Bathols, J., Scott, J.K., 2012. CliMond: Global high-resolution historical and future scenario climate surfaces for bioclimatic modelling. *Methods Ecol Evol*. <https://doi.org/10.1111/j.2041-210X.2011.00134.x>
- Kropf, K., 2011. *Morphological investigations: Cutting into the substance of urban*

- form. *Built Environ.* <https://doi.org/10.2148/benv.37.4.393>
- Kropf, K., 2009. Aspects of urban form. *Urban Morphol* 13, 105–120. <https://doi.org/10.1002/9781118747711.ch3>
- Kruskal, W.H., Wallis, W.A., 1952. Use of Ranks in One-Criterion Variance Analysis. *J Am Stat Assoc* 47, 583–621. <https://doi.org/10.1080/01621459.1952.10483441>
- Kumar, V., Bandhyopadhyay, S., Ramamritham, K., Jana, A., 2020. Optimizing the Redevelopment Cost of Urban Areas to Minimize the Fire Susceptibility of Heterogeneous Urban Settings in Developing Nations: a Case from Mumbai, India. *Process Integr Optim Sustain* 4, 361–378. <https://doi.org/10.1007/s41660-020-00124-9>
- Kwok, Y.T., Schoetter, R., Lau, K.K., Hidalgo, J., Ren, C., Pigeon, G., Masson, V., 2019. How well does the local climate zone scheme discern the thermal environment of Toulouse (France)? An analysis using numerical simulation data. *Int J Climatol* 39, 5292–5315. <https://doi.org/10.1002/joc.6140>
- Lak, A., Asl, S.S., Maher, A., 2020. Resilient urban form to pandemics: Lessons from COVID-19. *Med J Islam Repub Iran* 34, 1–9. <https://doi.org/10.34171/mjiri.34.71>
- Lambin, E.F., Ehrlich, D., 1996. The surface temperature-vegetation index space for land cover and land-cover change analysis. *Int J Remote Sens.* <https://doi.org/10.1080/01431169608949021>
- Lau, K.K.L., Chung, S.C., Ren, C., 2019. Outdoor thermal comfort in different urban settings of sub-tropical high-density cities: An approach of adopting local climate zone (LCZ) classification. *Build Environ* 154, 227–238. <https://doi.org/10.1016/j.buildenv.2019.03.005>
- Lazzarini, M., Marpu, P.R., Ghedira, H., 2013. Temperature-land cover interactions: The inversion of urban heat island phenomenon in desert city areas. *Remote Sens Environ.* <https://doi.org/10.1016/j.rse.2012.11.007>
- Lazzarini, M., Molini, A., Marpu, P.R., Ouarda, T.B.M.J., Ghedira, H., 2015. Urban climate modifications in hot desert cities: The role of land cover, local climate, and seasonality. *Geophys Res Lett.* <https://doi.org/10.1002/2015GL066534>
- Leconte, F., Bouyer, J., Claverie, R., Pétrissans, M., 2015. Using Local Climate Zone scheme for UHI assessment: Evaluation of the method using mobile measurements. *Build Environ* 83, 39–49. <https://doi.org/10.1016/j.buildenv.2014.05.005>
- Lee, D., Oh, K., Jung, S., 2019. Classifying Urban Climate Zones (UCZs) Based on Spatial Statistical Analyses. *Sustainability* 11, 1915. <https://doi.org/10.3390/su11071915>
- Legeby, A., 2013. Patterns of co-presence: Spatial configuration and social segregation, Usab.

- Lehnert, M., Savić, S., Milošević, D., Dunjić, J., Geletič, J., 2021. Mapping local climate zones and their applications in european urban environments: A systematic literature review and future development trends. *ISPRS Int J Geo-Information* 10, 260. <https://doi.org/10.3390/IJGI10040260/S1>
- Leichenko, R., 2011. Climate change and urban resilience. *Curr Opin Environ Sustain* 3, 164–168. <https://doi.org/10.1016/j.cosust.2010.12.014>
- Lennon, M., Scott, M., O’Neill, E., 2014. Urban Design and Adapting to Flood Risk: The Role of Green Infrastructure. *J Urban Des* 19, 745–758. <https://doi.org/10.1080/13574809.2014.944113>
- Lenzholzer, S., Klemm, W., Vasilikou, C., 2018. Qualitative methods to explore thermo-spatial perception in outdoor urban spaces. *Urban Clim* 23, 231–249. <https://doi.org/10.1016/J.UCLIM.2016.10.003>
- León, J., March, A., 2014. Urban morphology as a tool for supporting tsunami rapid resilience: A case study of Talcahuano, Chile. *Habitat Int* 43, 250–262. <https://doi.org/10.1016/j.habitatint.2014.04.006>
- Levy, A., 1999. Urban morphology and the problem of the modern urban fabric: Some questions for research. *Urban Morphol*.
- Lhomme, S., Serre, D., Diab, Y., Laganier, R., 2013. Urban technical networks resilience assessment, in: *Resilience and Urban Risk Management - Proceedings of the Conference “How the Concept of Resilience Is Able to Improve Urban Risk Management? A Temporal and a Spatial Analysis.”* <https://doi.org/10.1201/b12994-18>
- Liang, S., 2001. Narrowband to broadband conversions of land surface albedo I algorithms. *Remote Sens Environ*. [https://doi.org/10.1016/S0034-4257\(00\)00205-4](https://doi.org/10.1016/S0034-4257(00)00205-4)
- Liao, K.-H., 2012. A Theory on Urban Resilience to Floods--A Basis for Alternative Planning Practices. *Ecol Soc* 17, art48. <https://doi.org/10.5751/ES-05231-170448>
- Liaw, A., Wiener, M., 2002. Classification and Regression by randomForest. *R News*.
- Ligtelijn, V., Strauven, F. (Eds.), 2008. *Aesthetic of Number. Statement at CIAM 9, Aix-en-Provence, 1953*, in: *Aldo Van Eyck Writings. Collected Articles and Other Writings 1947-1998*. Sun Publishers, Amsterdam.
- Lim, H.K., Kain, J.-H., 2016. Compact Cities Are Complex, Intense and Diverse but: Can We Design Such Emergent Urban Properties? *Urban Plan* 1, 95–113. <https://doi.org/10.17645/up.v1i1.535>
- Lin, C.H., Liou, D.Y., Wu, K.W., 2007. Opportunities and challenges created by terrorism. *Technol Forecast Soc Change* 74, 148–164. <https://doi.org/10.1016/j.techfore.2006.02.004>
- Lin, Z., Xu, H., 2016. A study of Urban heat island intensity based on “local climate zones”: A case study in Fuzhou, China, in: *4th International Workshop on Earth*

- Observation and Remote Sensing Applications, EORSA 2016 - Proceedings. <https://doi.org/10.1109/EORSA.2016.7552807>
- Lo, Y.T.E., Mitchell, D.M., Thompson, R., O'Connell, E., Gasparri, A., 2022. Estimating heat-related mortality in near real time for national heatwave plans. *Environ Res Lett* 17, 024017. <https://doi.org/10.1088/1748-9326/AC4CF4>
- Lu, T., Marshall, J.D., Zhang, W., Hystad, P., Kim, S.Y., Bechle, M.J., Demuzere, M., Hankey, S., 2021. National Empirical Models of Air Pollution Using Microscale Measures of the Urban Environment. *Environ Sci Technol* 55, 15519–15530. <https://doi.org/10.1021/acs.est.1c04047>
- Madanipour, A., 2003. Public and private spaces of the city, *Public and Private Spaces of the City*. <https://doi.org/10.4324/9780203402856>
- Madrigano, J., Ito, K., Johnson, S., Kinney, P.L., Matte, T., 2015. A case-only study of vulnerability to heat wave-related mortality in New York City (2000–2011). *Environ Health Perspect* 123, 672–678. <https://doi.org/10.1289/EHP.1408178>
- Mahlstein, I., Daniel, J.S., Solomon, S., 2013. Pace of shifts in climate regions increases with global temperature. *Nat Clim Chang*. <https://doi.org/10.1038/nclimate1876>
- Maiullari, D., Pijpers-Van Esch, M., van Timmeren, A., 2021. A Quantitative Morphological Method for Mapping Local Climate Types. *Urban Plan* 6, 240–257. <https://doi.org/10.17645/UP.V6I3.4223>
- Manandhar, P., Bande, L., Tsoupos, A., Marpu, P.R., Armstrong, P., 2019. A Study of Local Climate Zones in Abu Dhabi with Urban Weather Stations and Numerical Simulations. *Sustain* 2020, Vol 12, Page 156 12, 156. <https://doi.org/10.3390/SU12010156>
- Marcus, L., 2018. Overcoming the subject-object dichotomy in urban modeling: Axial maps as geometric representations of affordances in the built environment. *Front Psychol*. <https://doi.org/10.3389/fpsyg.2018.00449>
- Marcus, L., Colding, J., 2014. Toward an integrated theory of spatial morphology and resilient urban systems. *Ecol Soc* 19, art55. <https://doi.org/10.5751/ES-06939-190455>
- Marcus, L., Colding, J., 2011. Towards a Spatial Morphology of Urban Social-Ecological Systems. *Conf Proc 18th Int Conf Urban Form ISUF 2011* 1–20.
- Marshall, S., 2012. Science, pseudo-science and urban design. *Urban Des Int*. <https://doi.org/10.1057/udi.2012.22>
- Marshall, S., Çalişkan, O., 2011. A joint framework for urban morphology and design. *Built Environ*. <https://doi.org/10.2148/benv.37.4.409>
- Martin, L., March, L., 1975. Urban space and structures 272.
- Martins, T.A.L., Adolphe, L., Bonhomme, M., Bonneaud, F., Faraut, S., Ginestet, S.,

- Michel, C., Guyard, W., 2016. Impact of Urban Cool Island measures on outdoor climate and pedestrian comfort: Simulations for a new district of Toulouse, France. *Sustain Cities Soc* 26, 9–26. <https://doi.org/10.1016/j.scs.2016.05.003>
- Masnavi, M.R., Gharai, F., Hajibandeh, M., 2019. Exploring urban resilience thinking for its application in urban planning: a review of literature. *Int J Environ Sci Technol*. <https://doi.org/10.1007/s13762-018-1860-2>
- Masson-Delmotte, V., Zhai, P., Pirani, A., Connors, S.L., Péan, C., Berger, S., Caud, N., Chen, Y., Goldfarb, L., Gomis, M.I., Huang, M., Leitzell, K., Lonnoy, E., Matthews, J.B.R., Maycock, T.K., Waterfield, T., Yelekçi, O., Yu, R., Zhou, B., (eds.), 2021. IPCC: Climate Change 2021: The Physical Science Basis. Cambridge Univ Press Press.
- Masterton, J.M., Richardson, F.A., 1979. Humidex, A Method of Quantifying Human Discomfort Due to Excessive Heat and Humidity. *Service de l'environnement atmospherique*.
- Matzarakis, A., Mayer, H., Iziomon, M.G., 1999. Applications of a universal thermal index: physiological equivalent temperature. *Int J Biometeorol* 1999 432 43, 76–84. <https://doi.org/10.1007/S004840050119>
- Mayer, H., Höppe, P., 1987. Thermal comfort of man in different urban environments. *Theor Appl Climatol* 1987 381 38, 43–49. <https://doi.org/10.1007/BF00866252>
- McHugh, M.L., 2012. Interrater reliability: The kappa statistic. *Biochem Medica*.
- Meerow, S., Newell, J.P., 2016. Urban resilience for whom, what, when, where, and why? *Urban Geogr* 40, 309–329. <https://doi.org/10.1080/02723638.2016.1206395>
- Meerow, S., Newell, J.P., Stults, M., 2016. Defining urban resilience: A review. *Landsc Urban Plan*. <https://doi.org/10.1016/j.landurbplan.2015.11.011>
- Middel, A., Häb, K., Brazel, A.J., Martin, C.A., Guhathakurta, S., 2014. Impact of urban form and design on mid-afternoon microclimate in Phoenix Local Climate Zones. *Landsc Urban Plan* 122, 16–28. <https://doi.org/10.1016/J.LANDURBPLAN.2013.11.004>
- Miguez, M.G., Veról, A.P., Battemarco, B.P., Yamamoto, L.M.T., de Brito, F.A., Fernandez, F.F., Merlo, M.L., Queiroz Rego, A., 2019. A framework to support the urbanization process on lowland coastal areas: Exploring the case of Vargem Grande – Rio de Janeiro, Brazil. *J Clean Prod* 231, 1281–1293. <https://doi.org/10.1016/j.jclepro.2019.05.187>
- Mills, G., Bechtel, B., Ching, J., See, L., Feddema, J., Foley, M., Alexander, P., O'Connor, M., 2015. An Introduction to the WUDAPT project. *Proc ICUC9 Meteo Fr*.
- Minoura, E., 2016. *Uncommon Ground: Urban Form and Social Territory*. KTH Royal Institute of Technology.

- Moneo, R., 1978. On Typology. *Oppositions*, n 13 23–45.
- Mota, R., Tavares, A., Santos, P., 2017. Urban vulnerability to fires and the efficiency of hydrants. Improving resource positioning and institutional response, in: Cepin M., B.R. (Ed.), *Safety and Reliability – Theory and Applications*. CRC Press, CRC Press Taylor & Francis Group 6000 Broken Sound Parkway NW, Suite 300 Boca Raton, FL 33487-2742, pp. 178–178.
<https://doi.org/10.1201/9781315210469-152>
- Moudon, A., 1986. *Built for change: neighborhood architecture in San Francisco*. MIT Press, Cambridge, MA.
- Moudon, A.V., 1997. Urban morphology as an emerging interdisciplinary field. *Urban Morphol.*
- Moudon, A.V., 1992. A Catholic Approach to Organizing What Urban Designers Should Know. *J Plan Lit.* <https://doi.org/10.1177/088541229200600401>
- Moudon, A.V., Lee, C., 2009. *Making the Metropolitan Landscape, Making the Metropolitan Landscape: Standing Firm on Middle Ground*. Routledge.
<https://doi.org/10.4324/9780203872048>
- Moudon, A. V., 1994. Getting to know the built landscape: Typomorphology, in: Franck, K.A., Schneekloth, L.H. (Eds.), *Ordering Space: Types in Architecture and Design*. Van Nostrand Reinhold, New York, pp. 289–311.
- Mousavinia, S.F., Pourdeihimi, S., Madani, R., 2019. Housing layout, perceived density and social interactions in gated communities: Mediation role of territoriality. *Sustain Cities Soc.* <https://doi.org/10.1016/j.scs.2019.101699>
- Muratori, S., 1959. *Studi per una operante storia urbana di Venezia*. Istituto Poligrafico dello Stato, Roma.
- Muratori, S., Bollati, R., Bollati, S., Marinucci, G., 1963. *Studi per un operante storia urbana di Roma*. Consiglio nazionale delle ricerche, Roma.
- Nassar, A.K., Blackburn, G.A., Whyatt, J.D., 2016. Dynamics and controls of urban heat sink and island phenomena in a desert city: Development of a local climate zone scheme using remotely-sensed inputs. *Int J Appl Earth Obs Geoinf.* <https://doi.org/10.1016/j.jag.2016.05.004>
- Naughton, M.P., Henderson, A., Mirabelli, M.C., Kaiser, R., Wilhelm, J.L., Kieszak, S.M., Rubin, C.H., McGeehin, M.A., 2002. Heat-related mortality during a 1999 heat wave in Chicago. *Am J Prev Med* 22, 221–227.
[https://doi.org/10.1016/S0749-3797\(02\)00421-X](https://doi.org/10.1016/S0749-3797(02)00421-X)
- Nelson, D.R., Adger, W.N., Brown, K., 2007. Adaptation to environmental change: contributions of a resilience framework. *Annu Rev Environ Resour* 32, 395–419.
<https://doi.org/10.1146/annurev.energy.32.051807.090348>
- Newell, J.P., Cousins, J.J., 2015. The boundaries of urban metabolism: Towards a political–industrial ecology. *Prog Hum Geogr* 39, 702–728.

<https://doi.org/10.1177/0309132514558442>

- Nichol, J., 2005. Remote sensing of urban heat islands by day and night. *Photogramm Eng Remote Sensing*. <https://doi.org/10.14358/PERS.71.5.613>
- Nichol, J.E., Fung, W.Y., Lam, K., Wong, M.S., 2009. Urban heat island diagnosis using ASTER satellite images and ‘in situ’ air temperature. *Atmos Res* 94, 276–284. <https://doi.org/10.1016/j.atmosres.2009.06.011>
- Nielsen, F., 2016. Hierarchical Clustering BT - Introduction to HPC with MPI for Data Science, in: Springer.
- Nielsen, T.A.S., 2015. Changes in transport behavior during the financial crisis. An analysis of urban form, location and transport behavior in the greater Copenhagen area 2006–2011. *Res Transp Econ* 51, 10–19. <https://doi.org/10.1016/j.retrec.2015.07.003>
- Nil, L., Ullmann, T., Kneisel, C., Sobiech-Wolf, J., Baumhauer, R., 2019. Assessing spatiotemporal variations of landsat land surface temperature and multispectral indices in the Arctic Mackenzie Delta Region between 1985 and 2018. *Remote Sens*. <https://doi.org/10.3390/rs11192329>
- Norris, F.H., Stevens, S.P., Pfefferbaum, B., Wyche, K.F., Pfefferbaum, R.L., 2008. Community resilience as a metaphor, theory, set of capacities, and strategy for disaster readiness. *Am J Community Psychol*. <https://doi.org/10.1007/s10464-007-9156-6>
- Ochola, E.M., Fakharizadehshirazi, E., Adimo, A.O., Mukundi, J.B., Wesonga, J.M., Sodoudi, S., 2020. Inter-local climate zone differentiation of land surface temperatures for Management of Urban Heat in Nairobi City, Kenya. *Urban Clim*. <https://doi.org/10.1016/j.uclim.2019.100540>
- Oke, T.R., 2004. Initial guidance to obtain representative meteorological observations at urban sites. *World Meteorol Organ*.
- Oke, T.R., Mills, G., Christen, A., Voogt, J.A., 2017. *Urban Climates*. Cambridge University Press, Cambridge. <https://doi.org/10.1017/9781139016476>
- Oldenburg, R., 2001. *Celebrating the Third Place: Inspiring Stories About the “Great Good Places” at the Heart of Our Communities*. Marlowe & Company.
- Oliva, S., Lazzeretti, L., 2018. Measuring the economic resilience of natural disasters: An analysis of major earthquakes in Japan. *City, Cult Soc* 15, 53–59. <https://doi.org/10.1016/J.CCS.2018.05.005>
- Oliveira, V., 2018. *Teaching Urban Morphology, The Urban Book Series*.
- Oliveira, V., 2016. *Urban Morphology: An Introduction to the Study of the Physical Form of Cities (The Urban Book Series)*, Springer.
- Olsson, S., Sondén, G.C., Ohlander, M., 1997. *Det lilla grannskapet: gårdar, trapphus & socialt liv. Centrum för byggnadskultur i västra Sverige, Chalmers &*

Göteborgs universitet, Göteborg.

- Oshiro, T.M., Perez, P.S., Baranauskas, J.A., 2012. How many trees in a random forest?, in: *Lecture Notes in Computer Science (Including Subseries Lecture Notes in Artificial Intelligence and Lecture Notes in Bioinformatics)*.
https://doi.org/10.1007/978-3-642-31537-4_13
- Pan, X., Zhu, X., Yang, Y., Cao, C., Zhang, X., Shan, L., 2018. Applicability of Downscaling Land Surface Temperature by Using Normalized Difference Sand Index. *Sci Rep*. <https://doi.org/10.1038/s41598-018-27905-0>
- Parlette, V., Cowen, D., 2011. Dead Malls: Suburban Activism, Local Spaces, Global Logistics. *Int J Urban Reg Res* 35. <https://doi.org/10.1111/j.1468-2427.2010.00992.x>
- Paschoalin, R., Pace, R., Isaacs, N., 2020. Urban resilience: Potential for rainwater harvesting in a heritage building, in: *Proceedings of the International Conference of Architectural Science Association*. pp. 1331–1340.
- Patel, R., Sanderson, D., Sitko, P., De Boer, J., 2020. Investigating urban vulnerability and resilience: a call for applied integrated research to reshape the political economy of decision-making: <https://doi.org/10.1177/0956247820909275> 32, 589–598. <https://doi.org/10.1177/0956247820909275>
- Peel, M.C., Finlayson, B.L., McMahon, T.A., 2007. Updated world map of the Köppen-Geiger climate classification. *Hydrol Earth Syst Sci*.
<https://doi.org/10.5194/hess-11-1633-2007>
- Pendall, R., Foster, K.A., Cowell, M., 2010. Resilience and regions: building understanding of the metaphor. *Cambridge J Reg Econ Soc* 3, 71–84.
<https://doi.org/10.1093/CJRES/RSP028>
- Penning de Vries, B.B.L., van Smeden, M., Rosendaal, F.R., Groenwold, R.H.H., 2020. Title, abstract, and keyword searching resulted in poor recovery of articles in systematic reviews of epidemiologic practice. *J Clin Epidemiol* 121, 55–61.
<https://doi.org/10.1016/j.jclinepi.2020.01.009>
- Peponis, J., 2013. Investigative Modeling and Spatial Analysis A commentary on directions. *Archit Morphol Investig Model Spat Anal Res Work*.
- Peponis, J., Ross, C., Rashid, M., 1997. The Structure of Urban Space, Movement and Co-presence: The Case of Atlanta. *Geoforum*. [https://doi.org/10.1016/s0016-7185\(97\)00016-x](https://doi.org/10.1016/s0016-7185(97)00016-x)
- Perera, N.G.R., Emmanuel, R., 2018. A “Local Climate Zone” based approach to urban planning in Colombo, Sri Lanka. *Urban Clim*.
<https://doi.org/10.1016/j.uclim.2016.11.006>
- Perkins-Kirkpatrick, S.E., Lewis, S.C., 2020. Increasing trends in regional heatwaves. *Nat Commun*. <https://doi.org/10.1038/s41467-020-16970-7>
- Pigliautile, I., Pisello, A.L., 2018. A new wearable monitoring system for

- investigating pedestrians' environmental conditions: Development of the experimental tool and start-up findings. *Sci Total Environ* 630, 690–706. <https://doi.org/10.1016/j.scitotenv.2018.02.208>
- Pizzo, B., 2015. Problematizing resilience: Implications for planning theory and practice. *Cities* 43, 133–140. <https://doi.org/10.1016/j.cities.2014.11.015>
- Putnam, R.D., 2000. *Bowling Alone: The Collapse and Revival of American Community*. New York: Simon und Schuster, 2001. ISBN. Policy Anal.
- Pyrgou, A., Santamouris, M., 2018. Increasing probability of heat-related mortality in a mediterranean city Due to urban warming. *Int J Environ Res Public Health*. <https://doi.org/10.3390/ijerph15081571>
- Ragheb, S.A., Ayad, H.M., Galil, R.A., 2017. An energy-resilient city, an appraisal matrix for the built environment, in: Brebbia, C.A., Longhurst, J., Marco, E., Booth, C. (Eds.), *WIT Transactions on Ecology and the Environment*. pp. 667–678. <https://doi.org/10.2495/SDP170581>
- Rajkovich, N.B., Larsen, L., 2016. A bicycle-based field measurement system for the study of thermal exposure in Cuyahoga county, Ohio, USA. *Int J Environ Res Public Health*. <https://doi.org/10.3390/ijerph13020159>
- Raman, S., 2010. Designing a liveable compact city physical forms of city and social life in urban neighbourhoods. *Built Environ*. <https://doi.org/10.2148/benv.36.1.63>
- Rao, F., Dovey, K., Pafka, E., 2018. Towards a genealogy of urban shopping: types, adaptations and resilience. *J Urban Des* 23, 544–557. <https://doi.org/10.1080/13574809.2017.1405726>
- Rao, F., Summers, R.J., 2016. Planning for retail resilience: Comparing Edmonton and Portland. *Cities* 58, 97–106. <https://doi.org/10.1016/j.cities.2016.05.002>
- Rasul, A., Balzter, H., Smith, C., 2016. Diurnal and seasonal variation of surface Urban Cool and Heat Islands in the semi-arid city of Erbil, Iraq. *Climate*. <https://doi.org/10.3390/cli4030042>
- Ratti, C., Raydan, D., Steemers, K., 2003. Building form and environmental performance: archetypes, analysis and an arid climate. *Energy Build* 35, 49–59. [https://doi.org/10.1016/S0378-7788\(02\)00079-8](https://doi.org/10.1016/S0378-7788(02)00079-8)
- Ravi, S., D'Odorico, P., Over, T.M., Zobeck, T.M., 2004. On the effect of air humidity on soil susceptibility to wind erosion: The case of air-dry soils. *Geophys Res Lett*. <https://doi.org/10.1029/2004GL019485>
- Ray, B., Shaw, R., 2018. Changing built form and implications on urban resilience: loss of climate responsive and socially interactive spaces. *Procedia Eng* 212, 117–124. <https://doi.org/10.1016/j.proeng.2018.01.016>
- Ren, C., Wang, R., Cai, M., Xu, Y., Zheng, Y., Ng, E., 2016. The accuracy of LCZ maps generated by the World Urban Database and Access Portal Tools

- (WUDAPT) Method: A Case Study of Hong Kong, in: The Fourth International Conference on Countermeasure to Urban Heat Islands.
<https://doi.org/10.1093/mnras/stv403>
- Reock, E.C., 1961. A Note: Measuring Compactness as a Requirement of Legislative Apportionment. *Midwest J Polit Sci.* <https://doi.org/10.2307/2109043>
- Requena-Ruiz, I., Drozd, C., Leduc, T., Rodler, A., Servières, M., Siret, D., 2019. A Review on interdisciplinary methods for the characterization of thermal perception in public spaces. *J Phys Conf Ser* 1343, 012007.
<https://doi.org/10.1088/1742-6596/1343/1/012007>
- Rezende, O.M., Miranda, F.M., Haddad, A.N., Miguez, M.G., 2019. A Framework to Evaluate Urban Flood Resilience of Design Alternatives for Flood Defence Considering Future Adverse Scenarios. *Water* 11, 1485.
<https://doi.org/10.3390/w11071485>
- Richard, Y., Emery, J., Dudek, J., Pergaud, J., Chateau-Smith, C., Zito, S., Rega, M., Vairet, T., Castel, T., Thévenin, T., Pohl, B., 2018. How relevant are local climate zones and urban climate zones for urban climate research? Dijon (France) as a case study. *Urban Clim* 26, 258–274.
<https://doi.org/10.1016/j.uclim.2018.10.002>
- Rocklöv, J., Forsberg, B., Ebi, K., Bellander, T., 2014. Susceptibility to mortality related to temperature and heat and cold wave duration in the population of Stockholm County, Sweden. *Glob Health Action* 7.
https://doi.org/10.3402/GHA.V7.22737/SUPPL_FILE/ZGHA_A_11818077_SM0007.PDF
- Rode, S., Gralepois, M., 2017. Towards an Urban Design Adapted to Flood Risk?, in: *Floods*. Elsevier, pp. 365–380. <https://doi.org/10.1016/B978-1-78548-269-4.50024-X>
- Rode, S., Guevara, S., Bonnefond, M., 2018. Resilience in urban development projects in flood-prone areas: a challenge to urban design professionals. *Town Plan Rev* 89, 167–190. <https://doi.org/10.3828/tpr.2018.10>
- Roggema, R., 2018. Design with voids: how inverted urbanism can increase urban resilience. *Archit Sci Rev* 61, 349–357.
<https://doi.org/10.1080/00038628.2018.1502153>
- Roggema, R., 2014. Towards Enhanced Resilience in City Design: A Proposition. *Land* 3, 460–481. <https://doi.org/10.3390/land3020460>
- Roggema, R., Kabat, P., van den Dobbelsteen, A., 2012. Towards a spatial planning framework for climate adaptation. *Smart Sustain Built Environ* 1, 29–58.
<https://doi.org/10.1108/20466091211227043>
- Romano, R., Bologna, R., Hasanaj, G., Arnetoli, M.V., 2020. Adaptive Design to Mitigate the Effects of UHI: The Case Study of Piazza Togliatti in the Municipality of Scandicci, in: Littlewood J. Howlett R.J., H.R.J.J.L.C.C.A.J.L.C.J.L.C.J.L.C. (Ed.), *Smart Innovation, Systems and*

- Technologies. Springer, pp. 531–541. https://doi.org/10.1007/978-981-32-9868-2_45
- Romice, O., Porta, S., Feliciotti, A., 2018. Urban form Resilience Urban Design Practice: Masterplanning for Change. <https://doi.org/10.3390/ifou2018-05976>
- Roosta, M., Javadpoor, M., Ebadi, M., 2022. A study on street network resilience in urban areas by urban network analysis: comparative study of old, new and middle fabrics in shiraz. *Int J Urban Sci* 26, 309–331. <https://doi.org/10.1080/12265934.2021.1911676>
- Rose, A., 2007. Economic resilience to natural and man-made disasters: Multidisciplinary origins and contextual dimensions. *Environ Hazards* 7, 383–398. <https://doi.org/10.1016/j.envhaz.2007.10.001>
- Rouse, J.W., Hass, R.H., Schell, J.A., Deering, D.W., Harlan, J.C., 1974. Monitoring the vernal advancement and retrogradation (green wave effect) of natural vegetation. Final Report, RSC 1978-4, Texas A M Univ Coll Station Texas.
- Rudlin, D., Falk, N., 1999. The process of urban generation and regeneration [chapter 14], *Building the 21st century home: the sustainable urban neighbourhood*. Architectural Press, Oxford.
- Salat, S., 2017. A systemic approach of urban resilience: power laws and urban growth patterns. *Int J Urban Sustain Dev* 9, 107–135. <https://doi.org/10.1080/19463138.2016.1277227>
- Salata, F., Golasi, I., Petitti, D., de Lieto Vollaro, E., Coppi, M., de Lieto Vollaro, A., 2017. Relating microclimate, human thermal comfort and health during heat waves: An analysis of heat island mitigation strategies through a case study in an urban outdoor environment. *Sustain Cities Soc*. <https://doi.org/10.1016/j.scs.2017.01.006>
- Salem, O., 2021. Adapting Cities for Mediterranean Migration Influxes: The Arrival City. *Civ Eng Archit* 9, 760–769. <https://doi.org/10.13189/cea.2021.090317>
- Samad, A., Vogt, U., 2020. Investigation of urban air quality by performing mobile measurements using a bicycle (MOBAIR). *Urban Clim* 33, 100650. <https://doi.org/10.1016/j.uclim.2020.100650>
- Samuelsson, K., Colding, J., Barthel, S., 2019. Urban resilience at eye level: Spatial analysis of empirically defined experiential landscapes. *Landsc Urban Plan* 187, 70–80. <https://doi.org/10.1016/j.landurbplan.2019.03.015>
- Sanders, A.E., Lim, S., Sohn, W., 2008. Resilience to Urban Poverty: Theoretical and Empirical Considerations for Population Health. *Am J Public Health* 98, 1101–1106. <https://doi.org/10.2105/AJPH.2007.119495>
- Sandholt, I., Rasmussen, K., Andersen, J., 2002. A simple interpretation of the surface temperature/vegetation index space for assessment of surface moisture status. *Remote Sens Environ*. [https://doi.org/10.1016/S0034-4257\(01\)00274-7](https://doi.org/10.1016/S0034-4257(01)00274-7)

- Santos, L.G.R., Singh, V.K., Mughal, M.O., Nevat, I., Norford, L.K., Fonseca, J.A., 2020. Estimating building's anthropogenic heat: a joint local climate zone and land use classification metho, in: ESIM 2021 Conference. pp. 12–19. <https://doi.org/https://doi.org/10.3929/ethz-b-000445814,2020>
- Saunders, D., 2012. *Arrival City: How the Largest Migration in History Is Reshaping Our World*. Vintage Books.
- Sayer, R.A., 2000. Realism and social science 211.
- Scheer, B.C., 2016. The epistemology of urban morphology. *Urban Morphol.*
- Scheffer, M., 2009. *Critical Transitions in Nature and Society*.
- Scheffer, M., Hosper, S.H., Meijer, M.L., Moss, B., Jeppesen, E., 1993. Alternative equilibria in shallow lakes. *Trends Ecol Evol*. [https://doi.org/10.1016/0169-5347\(93\)90254-M](https://doi.org/10.1016/0169-5347(93)90254-M)
- Scherer, D., Fehrenbach, U., Beha, H.D., Parlow, E., 1999. Improved concepts and methods in analysis and evaluation of the urban climate for optimizing urban planning processes. *Atmos Environ*. [https://doi.org/10.1016/S1352-2310\(99\)00161-2](https://doi.org/10.1016/S1352-2310(99)00161-2)
- Schinke, R., Kaidel, A., Golz, S., Naumann, T., López-Gutiérrez, J., Garvin, S., 2016. Analysing the Effects of Flood-Resilience Technologies in Urban Areas Using a Synthetic Model Approach. *ISPRS Int J Geo-Information* 5, 202. <https://doi.org/10.3390/ijgi5110202>
- Schwarz, N., Lautenbach, S., Seppelt, R., 2011. Exploring indicators for quantifying surface urban heat islands of European cities with MODIS land surface temperatures. *Remote Sens Environ*. <https://doi.org/10.1016/j.rse.2011.07.003>
- Schwarz, N., Schlink, U., Franck, U., Großmann, K., 2012. Relationship of land surface and air temperatures and its implications for quantifying urban heat island indicators - An application for the city of Leipzig (Germany). *Ecol Indic*. <https://doi.org/10.1016/j.ecolind.2012.01.001>
- Seebaß, K., 2017. Who Is Feeling the Heat?: Vulnerabilities and Exposures to Heat Stress--Individual, Social, and Housing Explanations. *Nat Cult* 12, 137–161. <https://doi.org/10.3167/nc.2017.120203>
- Semenza, J.C., Rubin, C.H., Falter, K.H., Selanikio, J.D., Flanders, W.D., Howe, H.L., Wilhelm, J.L., 1996. Heat-Related Deaths during the July 1995 Heat Wave in Chicago. *N Engl J Med* 335, 84–90. <https://doi.org/10.1056/NEJM199607113350203>
- Serra, M., 2013. *Anatomy of Emerging Metropolitan Territory: Towards an Integrated Analytical Framework for Metropolitan Morphology*. Faculdade de Engenharia da Universidade do Porto.
- Shahraiyni, H., Ghafouri, M., Shouraki, S., Saghafian, B., Nasser, M., 2012. Comparison between active learning method and support vector machine for

- runoff modeling. *J Hydrol Hydromechanics* 60, 16–32.
<https://doi.org/10.2478/V10098-012-0002-7>
- Shahraiyani, H.T., Shahsavani, D., Sargazi, S., Habibi–Nokhandan, M., 2015. Evaluation of MARS for the spatial distribution modeling of carbon monoxide in an urban area. *Atmos Pollut Res* 6, 581–588.
<https://doi.org/10.5094/APR.2015.065>
- Shahraiyani, H.T., Sodoudi, S., 2017. High-resolution air temperature mapping in urban areas a review on different modelling techniques. *Therm Sci*.
<https://doi.org/10.2298/TSCI150922094T>
- Shandas, V., Voelkel, J., Williams, J., Hoffman, J., 2019. Integrating satellite and ground measurements for predicting locations of extreme urban heat. *Climate*.
<https://doi.org/10.3390/cli7010005>
- Shapiro, S.S., Wilk, M.B., 1965. An Analysis of Variance Test for Normality (Complete Samples). *Biometrika* 52, 591. <https://doi.org/10.2307/2333709>
- Shareef, S., Abu-Hijleh, B., 2020. The effect of building height diversity on outdoor microclimate conditions in hot climate. A case study of Dubai-UAE. *Urban Clim* 32, 100611. <https://doi.org/10.1016/J.UCLIM.2020.100611>
- Sharifi, A., 2019a. Resilient urban forms: A macro-scale analysis. *Cities* 85, 1–14.
<https://doi.org/10.1016/J.CITIES.2018.11.023>
- Sharifi, A., 2019b. Urban form resilience: A meso-scale analysis. *Cities* 93, 238–252.
<https://doi.org/10.1016/J.CITIES.2019.05.010>
- Sharifi, A., 2019c. Resilient urban forms: A review of literature on streets and street networks. *Build Environ* 147, 171–187.
<https://doi.org/10.1016/j.buildenv.2018.09.040>
- Sharifi, A., 2019d. Resilient urban forms: A macro-scale analysis. *Cities* 85, 1–14.
<https://doi.org/10.1016/j.cities.2018.11.023>
- Sharifi, A., 2019e. Resilient urban forms: A review of literature on streets and street networks. *Build Environ* 147, 171–187.
<https://doi.org/10.1016/J.BUILDENV.2018.09.040>
- Sharifi, A., Yamagata, Y., 2018a. Resilient Urban Form: A Conceptual Framework, in: Yamagata, Y., Sharifi, A. (Eds.), *Resilience-Oriented Urban Planning: Theoretical and Empirical Insights*. Springer Verlag, pp. 167–179.
https://doi.org/10.1007/978-3-319-75798-8_9
- Sharifi, A., Yamagata, Y., 2018b. Resilience-Oriented Urban Planning, in: Yamagata, Y., Sharifi, A. (Eds.), *Resilience-Oriented Urban Planning: Theoretical and Empirical Insights*. Springer, Cham, pp. 3–27. https://doi.org/10.1007/978-3-319-75798-8_1
- Sharifi, A., Yamagata, Y., 2016a. Urban Resilience Assessment: Multiple Dimensions, Criteria, and Indicators, in: Yamagata, Y., Maruyama, H. (Eds.),

- URBAN RESILIENCE: A TRANSFORMATIVE APPROACH. pp. 259–276.
https://doi.org/10.1007/978-3-319-39812-9_13
- Sharifi, A., Yamagata, Y., 2016b. Principles and criteria for assessing urban energy resilience: A literature review. *Renew Sustain Energy Rev* 60, 1654–1677.
<https://doi.org/10.1016/j.rser.2016.03.028>
- Sharifi, E., Boland, J., 2017. Heat Resilience in Public Space and Its Applications in Healthy and Low Carbon Cities, in: Osmond P. Ding L., F.F. (Ed.), *Procedia Engineering*. Elsevier Ltd, pp. 944–954.
<https://doi.org/10.1016/j.proeng.2017.04.254>
- Sharifi, E., Larbi, M., Omrany, H., Boland, J., 2020. Climate change adaptation and carbon emissions in green urban spaces: Case study of Adelaide. *J Clean Prod* 254, 120035. <https://doi.org/10.1016/j.jclepro.2020.120035>
- Shi, Y., Lau, K.K.L., Ren, C., Ng, E., 2018. Evaluating the local climate zone classification in high-density heterogeneous urban environment using mobile measurement. *Urban Clim*. <https://doi.org/10.1016/j.uclim.2018.07.001>
- Shi, Z., Yang, J., Zhang, Y., Xiao, X., Xia, J.C., 2022. Urban ventilation corridors and spatiotemporal divergence patterns of urban heat island intensity: a local climate zone perspective. *Environ Sci Pollut Res* 1–13. <https://doi.org/10.1007/s11356-022-21037-9>
- Shih, W., 2017. The impact of urban development patterns on thermal distribution in Taipei, in: 2017 Joint Urban Remote Sensing Event, JURSE 2017.
<https://doi.org/10.1109/JURSE.2017.7924634>
- Siksna, A., 1997. The effects of block size and form in North American and Australian city centres. *Urban Morphol* 1, 19–33.
- Sismanidis, P., Keramitsoglou, I., Kiranoudis, C.T., 2015. A satellite-based system for continuous monitoring of Surface Urban Heat Islands. *Urban Clim*.
<https://doi.org/10.1016/j.uclim.2015.06.001>
- Siu, L.W., Hart, M.A., 2013. Quantifying urban heat island intensity in Hong Kong SAR, China. *Environ Monit Assess* 185, 4383–4398.
<https://doi.org/10.1007/s10661-012-2876-6>
- Smith, D. a, Crooks, A.T., 2010. *From Buildings to Cities: Techniques for the Multi-Scale Analysis of Urban Form and Function*. *Built Environ* 44.
- Smithson, A., 1974. How to Recognize and read Mat-Building. *Mainstream architecture as it developed towards mat-building*. *Archit Des* 9.
- Sobrino, J.A., Ultra-Carrió, R., Sòria, G., Bianchi, R., Paganini, M., 2012. Impact of spatial resolution and satellite overpass time on evaluation of the surface urban heat island effects. *Remote Sens Environ*.
<https://doi.org/10.1016/j.rse.2011.04.042>
- Sobrino, J.A., Ultra-Carrió, R., Sòria, G., Jiménez-Muñoz, J.C., Franch, B., Hidalgo,

- V., Mattar, C., Julien, Y., Cuenca, J., Romaguera, M., Gómez, J.A., de Miguel, E., Bianchi, R., Paganini, M., 2013. Evaluation of the surface urban heat island effect in the city of Madrid by thermal remote sensing. *Int J Remote Sens.* <https://doi.org/10.1080/01431161.2012.716548>
- Song, J., Li, W., 2019. Linkage Between the Environment and Individual Resilience to Urban Flooding: A Case Study of Shenzhen, China. *Int J Environ Res Public Health* 16, 2559. <https://doi.org/10.3390/ijerph16142559>
- Song, Y., Knaap, G.J., 2007. Quantitative Classification of Neighbourhoods: The Neighbourhoods of New Single-family Homes in the Portland Metropolitan Area. <http://dx.doi.org/10.1080/13574800601072640> 12, 1–24. <https://doi.org/10.1080/13574800601072640>
- Stähle, A., Marcus, L., Karlstrom, L.A., 2007. Place Syntax Tool—GIS Software for Analysing Geographic Accessibility with Axial Lines. *New Dev Sp Syntax Softw* 35–42.
- Steadman, R.G., 1979. The assessment of sultriness. Part I. A temperature-humidity index based on human physiology and clothing science. *J Appl Meteorol* 18. [https://doi.org/10.1175/1520-0450\(1979\)018<0861:TAOSPI>2.0.CO;2](https://doi.org/10.1175/1520-0450(1979)018<0861:TAOSPI>2.0.CO;2)
- Steenefeld, G.-J., Klompaker, J.O., Groen, R.J.A., Holtslag, A.A.M., 2018. An urban climate assessment and management tool for combined heat and air quality judgements at neighbourhood scales. *Resour Conserv Recycl* 132, 204–217. <https://doi.org/10.1016/j.resconrec.2016.12.002>
- Steiniger, S, Lange, T, Burghardt, D, Weibel, R, Steiniger, Stefan, Burghardt, Dirk, Lange, Tilman, Weibel, Robert, 2008. An Approach for the Classification of Urban Building Structures Based on Discriminant Analysis Techniques. *Trans GIS* 12, 31–59. <https://doi.org/10.1111/J.1467-9671.2008.01085.X>
- Stevens, M.R., Song, Y., Berke, P.R., 2010. New Urbanist developments in flood-prone areas: Safe development, or safe development paradox? *Nat Hazards* 53, 605–629. <https://doi.org/10.1007/s11069-009-9450-8>
- Stewart, I.D., 2011. Redefining the Urban Heat Island. October.
- Stewart, I.D., Oke, T.R., 2012. Local Climate Zones for Urban Temperature Studies. *Bull Am Meteorol Soc* 93, 1879–1900. <https://doi.org/10.1175/BAMS-D-11-00019.1>
- Stewart, I.D., Oke, T.R., Krayenhoff, E.S., 2014. Evaluation of the “local climate zone” scheme using temperature observations and model simulations. *Int J Climatol.* <https://doi.org/10.1002/joc.3746>
- Stieb, D.M., Huang, A., Hocking, R., Crouse, D.L., Osornio-Vargas, A.R., Villeneuve, P.J., 2019. Using maps to communicate environmental exposures and health risks: Review and best-practice recommendations. *Environ Res* 176, 108518. <https://doi.org/10.1016/J.ENVRES.2019.05.049>
- Sugiyama, T., Carver, A., Koohsari, M.J., Veitch, J., 2018. Advantages of public

- green spaces in enhancing population health. *Landsc Urban Plan.*
<https://doi.org/10.1016/j.landurbplan.2018.05.019>
- Swapan, A.Y., 2017. HOLISTIC STRATEGY FOR URBAN DESIGN: A MICROCLIMATIC CONCERN TO SUSTAINABILITY. *J Urban Environ Eng* 10, 221–232. <https://doi.org/10.4090/juee.2016.v10n2.221232>
- Tablada, A., Zhao, X., 2016. Sunlight availability and potential food and energy self-sufficiency in tropical generic residential districts. *Sol Energy* 139, 757–769. <https://doi.org/10.1016/j.solener.2016.10.041>
- Taheri Shahraiyini, H., Sodoudi, S., Kerschbaumer, A., Cubasch, U., 2015. A new structure identification scheme for ANFIS and its application for the simulation of virtual air pollution monitoring stations in urban areas. *Eng Appl Artif Intell* 41, 175–182. <https://doi.org/10.1016/J.ENGAPPAI.2015.02.010>
- Talen, E., 1999. Sense of community and neighbourhood form: An assessment of the social doctrine of new urbanism. *Urban Stud* 36, 1361–1379. <https://doi.org/10.1080/0042098993033>
- Tayebi, S., Mohammadi, H., Shamsipoor, A., Tayebi, S., Alavi, S.A., Hoseinioun, S., 2019. Analysis of land surface temperature trend and climate resilience challenges in Tehran. *Int J Environ Sci Technol* 16, 8585–8594. <https://doi.org/10.1007/s13762-019-02329-z>
- Team, R.C., 2019. R: A Language and Environment for Statistical Computing. Vienna, Austria.
- Tipple, A.G., 1992. Self-help transformations to low-cost housing: initial impressions of cause, context and value. *Third World Plann Rev* 14. <https://doi.org/10.3828/twpr.14.2.004201k76w523323>
- Tomlinson, C.J., Chapman, L., Thornes, J.E., Baker, C., 2011. Remote sensing land surface temperature for meteorology and climatology: A review. *Meteorol Appl.* <https://doi.org/10.1002/met.287>
- Tsin, P.K., Knudby, A., Krayenhoff, E.S., Ho, H.C., Brauer, M., Henderson, S.B., 2016. Microscale mobile monitoring of urban air temperature. *Urban Clim* 18, 58–72. <https://doi.org/10.1016/j.uclim.2016.10.001>
- Tsipsis, K., Chorianopoulos, A., 2010. Data Mining Techniques in CRM: Inside Customer Segmentation, Data Mining Techniques in CRM: Inside Customer Segmentation. <https://doi.org/10.1002/9780470685815>
- Tumini, I., Villagra-Islas, P., Herrmann-Lunecke, G., 2017. Evaluating reconstruction effects on urban resilience: a comparison between two Chilean tsunami-prone cities. *Nat Hazards* 85, 1363–1392. <https://doi.org/10.1007/s11069-016-2630-4>
- Unger, J., Sümeghy, Z., Zoboki, J., 2001. Temperature cross-section features in an urban area. *Atmos Res.* [https://doi.org/10.1016/S0169-8095\(01\)00087-4](https://doi.org/10.1016/S0169-8095(01)00087-4)
- United Nations, 2019. World Urbanization Prospects: The 2018 Revision

- (ST/ESA/SER.A/420). New York.
- USGS, 2015. Landsat 8 (L8) Data Users Handbook. Earth Resour Obs Sci Cent.
- Vale, L.J., 2014. The politics of resilient cities: whose resilience and whose city? *Build Res Inf* 42, 191–201. <https://doi.org/10.1080/09613218.2014.850602>
- van Eck, N.J., Waltman, L., 2010. Software survey: VOSviewer, a computer program for bibliometric mapping. *Scientometrics* 84, 523–538. <https://doi.org/10.1007/s11192-009-0146-3>
- van Loenhout, J.A.F., le Grand, A., Duijm, F., Greven, F., Vink, N.M., Hoek, G., Zuurbier, M., 2016. The effect of high indoor temperatures on self-perceived health of elderly persons. *Environ Res* 146, 27–34. <https://doi.org/10.1016/J.ENVRES.2015.12.012>
- Venerandi, A., Zanella, M., Romice, O., Dibble, J., Porta, S., 2017. Form and urban change – An urban morphometric study of five gentrified neighbourhoods in London. *Environ Plan B Urban Anal City Sci* 44, 1056–1076. <https://doi.org/10.1177/0265813516658031>
- Villagra, P., Rojas, C., Ohno, R., Xue, M., Gómez, K., 2014. A GIS-base exploration of the relationships between open space systems and urban form for the adaptive capacity of cities after an earthquake: The cases of two Chilean cities. *Appl Geogr* 48, 64–78. <https://doi.org/10.1016/j.apgeog.2014.01.010>
- Voelcke, J., 1959. D'Aix-en-Provence à Otterlo ou l'agonie et la mort du C.I.A.M. *Le Carré Bleu* 4.
- Voelkel, J., Shandas, V., 2017. Towards systematic prediction of urban heat islands: Grounding measurements, assessing modeling techniques. *Climate*. <https://doi.org/10.3390/cli5020041>
- Voelkel, J., Shandas, V., Haggerty, B., 2016. Developing high-resolution descriptions of urban heat islands: A public health imperative. *Prev Chronic Dis*. <https://doi.org/10.5888/pcd13.160099>
- Vogt, J. V., Viau, A.A., Paquet, F., 1997. Mapping regional air temperature fields using satellite-derived surface skin temperatures. *Int J Climatol* 17. [https://doi.org/10.1002/\(sici\)1097-0088\(19971130\)17:14<1559::aid-joc211>3.3.co;2-x](https://doi.org/10.1002/(sici)1097-0088(19971130)17:14<1559::aid-joc211>3.3.co;2-x)
- Walker, B., Holling, C.S., Carpenter, S.R., Kinzig, A., 2004. Resilience, adaptability and transformability in social-ecological systems. *Ecol Soc* 9. <https://doi.org/10.5751/ES-00650-090205>
- Walker, B., Salt, D., 2012. Resilience practice: Building capacity to absorb disturbance and maintain function, *Resilience Practice: Building Capacity to Absorb Disturbance and Maintain Function*. Island Press-Center for Resource Economics. <https://doi.org/10.5822/978-1-61091-231-0>
- Walker, B., Salt, D., 2006. *Resilience Thinking: Sustaining Ecosystems and People in*

a Changing World, Peace and Conflict.

- Wang, C.-H., 2020. Does compact development promote a seismic-resistant city? Application of seismic-damage statistical models to Taichung, Taiwan. *Environ Plan B Urban Anal City Sci* 47, 84–101.
<https://doi.org/10.1177/2399808318770454>
- Wang, C., Middel, A., Myint, S.W., Kaplan, S., Brazel, A.J., Lukasczyk, J., 2018. Assessing local climate zones in arid cities: The case of Phoenix, Arizona and Las Vegas, Nevada. *ISPRS J Photogramm Remote Sens* 141, 59–71.
<https://doi.org/10.1016/j.isprsjprs.2018.04.009>
- Wang, J., Foley, K., 2021. Assessing the performance of urban open space for achieving sustainable and resilient cities: A pilot study of two urban parks in Dublin, Ireland. *Urban For Urban Green* 62, 127180.
<https://doi.org/10.1016/j.ufug.2021.127180>
- Wang, L., Zhou, Y., Wang, F., Ding, L., Love, P.E.D., Li, S., 2021. The Influence of the Built Environment on People’s Mental Health: An Empirical Classification of Causal Factors. *Sustain Cities Soc.* <https://doi.org/10.1016/j.scs.2021.103185>
- Wang, R., Ren, C., Xu, Y., Lau, K.K.L., Shi, Y., 2018. Mapping the local climate zones of urban areas by GIS-based and WUDAPT methods: A case study of Hong Kong. *Urban Clim.* <https://doi.org/10.1016/j.uclim.2017.10.001>
- Wang, Y., Berardi, U., Akbari, H., 2016. Comparing the effects of urban heat island mitigation strategies for Toronto, Canada. *Energy Build* 114, 2–19.
<https://doi.org/10.1016/j.enbuild.2015.06.046>
- Wang, Y., Berardi, Umberto, Akbari, H., 2015. The Urban Heat Island Effect in the City of Toronto, in: Chong, W.O., Chang, J., Parrish, K., Berardi, U (Eds.), *Procedia Engineering*. pp. 137–144.
<https://doi.org/10.1016/j.proeng.2015.08.412>
- Wang, Y., Zhan, Q., Ouyang, W., 2017. Impact of Urban climate landscape patterns on land surface temperature in Wuhan, China. *Sustain.*
<https://doi.org/10.3390/su9101700>
- Ward, J.H., 1963. Hierarchical Grouping to Optimize an Objective Function. *J Am Stat Assoc.* <https://doi.org/10.1080/01621459.1963.10500845>
- Wardekker, J.A., de Jong, A., Knoop, J.M., van der Sluijs, J.P., 2010. Operationalising a resilience approach to adapting an urban delta to uncertain climate changes. *Technol Forecast Soc Change* 77, 987–998.
<https://doi.org/10.1016/j.techfore.2009.11.005>
- Weichselgartner, J., Kelman, I., 2015. Geographies of resilience: Challenges and opportunities of a descriptive concept. *Prog Hum Geogr.*
<https://doi.org/10.1177/0309132513518834>
- Weichselgartner, J., Kelman, I., 2014. Geographies of resilience: Challenges and opportunities of a descriptive concept.

- <http://dx.doi.org/10.1177/0309132513518834> 39, 249–267.
<https://doi.org/10.1177/0309132513518834>
- Welch, B.L., 1951. On the Comparison of Several Mean Values: An Alternative Approach. *Biometrika*. <https://doi.org/10.2307/2332579>
- Weng, Q., 2009. Thermal infrared remote sensing for urban climate and environmental studies: Methods, applications, and trends. *ISPRS J Photogramm Remote Sens*. <https://doi.org/10.1016/j.isprsjprs.2009.03.007>
- Weng, Q., Lu, D., Schubring, J., 2004. Estimation of land surface temperature-vegetation abundance relationship for urban heat island studies. *Remote Sens Environ*. <https://doi.org/10.1016/j.rse.2003.11.005>
- Whitehand, J.W.R., 2001. British urban morphology: The Conzenian tradition. *Urban Morphol*.
- Wicki, A., Parlow, E., 2017. Attribution of local climate zones using a multitemporal land use/land cover classification scheme. *J Appl Remote Sens*. <https://doi.org/10.1117/1.jrs.11.026001>
- Wilcox, R.R., 1998a. How Many Discoveries Have Been Lost by Ignoring Modern Statistical Methods? *Am Psychol*. <https://doi.org/10.1037/0003-066X.53.3.300>
- Wilcox, R.R., 1998b. The goals and strategies of robust methods. *Br J Math Stat Psychol*. <https://doi.org/10.1111/j.2044-8317.1998.tb00659.x>
- Wilcox, R.R., 1996. A note on testing hypotheses about trimmed means. *Biometrical J*. <https://doi.org/10.1002/bimj.4710380205>
- Williams, A.A., Allen, J.G., Catalano, P.J., Spengler, J.D., 2020. The role of individual and small-area social and environmental factors on heat vulnerability to mortality within and outside of the Home in Boston, MA. *Climate* 8. <https://doi.org/10.3390/cli8020029>
- Wilmers, F., 1990. Effects of vegetation on urban climate and buildings. *Energy Build*. [https://doi.org/10.1016/0378-7788\(90\)90028-H](https://doi.org/10.1016/0378-7788(90)90028-H)
- Witten, I.H., Frank, E., Hall, M.A., Pal, C.J., 2016. Data Mining: Practical Machine Learning Tools and Techniques, Data Mining: Practical Machine Learning Tools and Techniques. <https://doi.org/10.1016/c2009-0-19715-5>
- Wu, J., Wu, T., 2014. Ecological Resilience as a Foundation for Urban Design and Sustainability, in: *The Ecological Design and Planning Reader*. https://doi.org/10.5822/978-1-61091-491-8_49
- Wu, Y., Sharifi, A., Yang, P., Borjigin, H., Murakami, D., Yamagata, Y., 2018. Mapping building carbon emissions within local climate zones in Shanghai. *Energy Procedia* 152, 815–822. <https://doi.org/10.1016/j.egypro.2018.09.195>
- Xu, C., Rahman, M., Haase, D., Wu, Y., Su, M., Pauleit, S., 2020. Surface runoff in urban areas: The role of residential cover and urban growth form. *J Clean Prod*

262, 121421. <https://doi.org/10.1016/j.jclepro.2020.121421>

- Yang, X., Peng, L.L.H., Jiang, Z., Chen, Y., Yao, L., He, Y., Xu, T., 2020. Impact of urban heat island on energy demand in buildings: Local climate zones in Nanjing. *Appl Energy* 260, 114279. <https://doi.org/10.1016/j.apenergy.2019.114279>
- Yang, Y., Cao, C., Pan, X., Li, X., Zhu, X., 2017. Downscaling land surface temperature in an arid area by using multiple remote sensing indices with random forest regression. *Remote Sens.* <https://doi.org/10.3390/rs9080789>
- Yokoyama, H., Ooka, R., Kikumoto, H., 2018. Study of mobile measurements for detailed temperature distribution in a high-density urban area in Tokyo. *Urban Clim.* <https://doi.org/10.1016/j.uclim.2017.06.006>
- Zha, Y., Gao, J., Ni, S., 2003. Use of normalized difference built-up index in automatically mapping urban areas from TM imagery. *Int J Remote Sens.* <https://doi.org/10.1080/01431160304987>
- Zhang, X., Li, H., 2018. Urban resilience and urban sustainability: What we know and what do not know? *Cities.* <https://doi.org/10.1016/j.cities.2017.08.009>
- Zhao, C., 2018. Linking the local climate zones and land surface temperature to investigate the surface urban heat island, a case study of San Antonio, Texas, U.S, in: *ISPRS Annals of the Photogrammetry, Remote Sensing and Spatial Information Sciences.* <https://doi.org/10.5194/isprs-annals-IV-3-277-2018>
- Zhao, L., Lee, X., Smith, R.B., Oleson, K., 2014. Strong contributions of local background climate to urban heat islands. *Nature.* <https://doi.org/10.1038/nature13462>
- Zhao, Z., Shen, L., Li, L., Wang, H., He, B.-J., 2020. Local Climate Zone Classification Scheme Can Also Indicate Local-Scale Urban Ventilation Performance: An Evidence-Based Study. *Atmosphere (Basel)* 11, 776. <https://doi.org/10.3390/atmos11080776>
- Zhou, Q., Wang, C., Fang, S., 2019. Application of geographically weighted regression (GWR) in the analysis of the cause of haze pollution in China. *Atmos Pollut Res* 10, 835–846. <https://doi.org/10.1016/J.APR.2018.12.012>

Appendices

Appendix A: A matrix of the relationship between the urban form elements/attributes (rows) and different disturbances (columns) that they provide resilience to

	General (N/A)	Floods	earthquakes	High temperatures	Climate change	Energy shortages	Disease outbreaks	Economic recessions	Immigration/Migration	Fires	Urban poverty	Air pollution	Ill-being	Warfares/armed conflicts	Water scarcity	Terrorist attacks	Gentrification	general structural collapses	Varied
General/Not-specified	(du Plessis et al., 2015, Ladiana et al., 2017, Irajifar et al., 2016)	(Connolly et al., 2020, Abdulka reem & Elkadi, 2018, Song & Li, 2019, Asad et al., 2021)		(Ottone et al., 2019)	(Dhar & Khirfan, 2017, da Silva et al., 2012, Bigio, 2015)		(Lak et al., 2020)		(Salem, 2021, Asikin et al., 2018)			(Cariolet et al., 2018)							(Eltinay & Egbu, 2017, Brunetta & Salata, 2019, Pitidis et al., 2018, Caputo et al., 2015)
Development type	(Pessoa et al., 2016, Lim & Kain, 2016, Cao & Shi, 2020)	(Brody et al., 2013, Mycoo et al., 2021, Palencia et al., 2017, Xu et al., 2020)	(Bozza et al., 2017, Habibi et al., 2016, Bozza et al., 2015, C.-H. Wang, 2020, Giuliani et al., 2020)		(Eckert & Huynh, 2015, Gleeson, 2008)	(Rauland et al., 2011)										(Fischer et al., 2018)			(Cruz et al., 2013)
Building	(Bouzarovski et al., 2011)	(Rezende et al., 2019, Schinke et al., 2016, Houghton & Castillo-Salgado, 2017)	(Cimellaro et al., 2018, Ingaramo & Pascale, 2020, Cerè et al., 2018)	(Hatvani-Kovacs et al., 2016)		(Caputo et al., 2013)		(Rao et al., 2018)		(Kumar et al., 2020)	(Avogadro et al., 2017, Sanders et al., 2008)				(Paschoalin et al., 2020)				

(continued)

	General (N/A)	Floods	earthquakes	High temperatures	Climate change	Energy shortages	Disease outbreaks	Economic recessions	Immigration/Migration	Fires	Urban poverty	Air pollution	Ill-being	Warfares/armed conflicts	Water scarcity	Terrorist attacks	Gentrification	general structural collapses	Varied
Open/Green space	(Roggema, 2018)	(Miguez et al., 2019, Jayakody & Amaratinga, 2020, Magliocchetti et al., 2021)	(Villagra et al., 2014, Allan et al., 2013)	(Romano et al., 2020, E. Sharifi et al., 2020, E. Sharifi & Boland, 2017)	(Gargiulo et al., 2018)								(Samuelsson et al., 2019)						
Neighborhood/Sanctuary area	(Kostourou & Karimi, 2017)			(Tayebi et al., 2019, Y. Wang et al., 2016, Williams et al., 2020, Y. Wang et al., 2015)		(Perera et al., 2021)											(Venardi et al., 2016)		(A. Sharifi et al., 2021)
Street		(Leon et al., 2020)	(Cutini et al., 2019)					(Nielsen, 2015)										(Cutini & Pezzica, 2020)	(Roosta et al., n.d.)
Land use			(Meshkini et al., 2021)																(Yamagata et al., 2016, Downes, N.k. et al., 2016)
Block		(Morschek et al., 2019)			(Tablada & Zhao, 2016)														

(continued)

	General (N/A)	Floods	earthquakes	High temperatures	Climate change	Energy shortages	Disease outbreaks	Economic recessions	Immigration/Migration	Fires	Urban poverty	Air pollution	Ill-being	Warfares/armed conflicts	Water scarcity	Terrorist attacks	Gentrification	general structural collapses	Varied
The urban project		(Rode et al., 2018) (Rode & Gralepois, 2017)																	
Underground space																			(Admiral & Cornaro, 2020)
Plot	(Barbour, G. et al., 2016)																		
Varied	(Feng et al., 2020, Fusco & Venerandi, 2020, Feliciotti et al., 2016, Marcus & Colding, 2014, Khirfan & El-Shayeb, 2020)	(Serre, 2018, Tumini et al., 2017, Abdulkarim et al., 2020, Barau et al., 2015)	(Ferreira et al., 2016, Hosseini, 2018, Atrachali et al., 2019)			(Ragheb et al., 2017, Yang & Quan, 2016)	(Monteiro et al., 2012)			(Mota et al., 2017)		(García-Esparza & Alcañiz, 2017)		(Kittana & Meulder, 2019)					(Fu & Wang, 2018, Ray & Shaw, 2018, Stangl, Paul, 2018)

References

- Abdulkareem, M., Elkadi, H., 2018. From engineering to evolutionary, an overarching approach in identifying the resilience of urban design to flood. *INTERNATIONAL JOURNAL OF DISASTER RISK REDUCTION* 28, 176–190. <https://doi.org/10.1016/j.ijdr.2018.02.009>
- Abdulkareem, M., Kenawy, I., Elkadi, H., 2020. Neo Ekistics for flood mitigation in cities. *WORLD JOURNAL OF SCIENCE TECHNOLOGY AND SUSTAINABLE DEVELOPMENT* 17, 167–181. <https://doi.org/10.1108/WJSTSD-01-2018-0008>
- Admiraal, H., Cornaro, A., 2020. Future cities, resilient cities – The role of underground space in achieving urban resilience. *Underground Space (China)* 5, 223–228. <https://doi.org/10.1016/j.undsp.2019.02.001>
- Allan, P., Bryant, M., Wirsching, C., Garcia, D., Teresa Rodriguez, M., 2013. The Influence of Urban Morphology on the Resilience of Cities Following an Earthquake. *Journal of Urban Design* 18, 242–262. <https://doi.org/10.1080/13574809.2013.772881>
- Asad, R., Ahmed, I., Vaughan, J., von Meding, J., 2021. Traditional water knowledge: challenges and opportunities to build resilience to urban floods. *International Journal of Disaster Resilience in the Built Environment*. <https://doi.org/10.1108/IJDRBE-08-2020-0091>
- Avogo, F.A., Wedam, E.A., Opoku, S.M., 2017. Housing transformation and livelihood outcomes in Accra, Ghana. *Cities* 68, 92–103. <https://doi.org/10.1016/j.cities.2017.05.009>
- Barau, A.S., Maconachie, R., Ludin, A.N.M., Abdulharnid, A., 2015. Urban morphology dynamics and environmental change in Kano, Nigeria. *LAND USE POLICY* 42, 307–317. <https://doi.org/10.1016/j.landusepol.2014.08.007>
- Bigio, A.G., 2015. Towards resilient and low-carbon cities. *Geneva Reports on the World Economy* 2015-November, 435–450.
- Bouzarovski, S., Salukvadze, J., Gentile, M., 2011. A socially resilient urban transition? The contested landscapes of apartment building extensions in two post-communist cities. *Urban Studies* 48, 2689–2714. <https://doi.org/10.1177/0042098010385158>
- Bozza, A., Asprone, D., Fiasconaro, A., Latora, V., Manfredi, G., 2015. Catastrophe resilience related to urban network shape: Preliminary analysis, in: Papadrakakis, M., Papadopoulos, V., Plevris, V. (Eds.), 5th ECCOMAS Thematic Conference on Computational Methods in Structural Dynamics and Earthquake Engineering, *COMPdyn 2015*. National Technical University of Athens, pp. 1513–1531. <https://doi.org/10.7712/120115.3482.1114>

- Bozza, A., Asprone, D., Manfredi, G., 2017. A methodological framework assessing disaster resilience of city ecosystems to enhance resource use efficiency. *International Journal of Urban Sustainable Development* 9, 136–150. <https://doi.org/10.1080/19463138.2016.1244538>
- Brody, S., Kim, H., Gunn, J., 2013. Examining the Impacts of Development Patterns on Flooding on the Gulf of Mexico Coast. *Urban Studies* 50, 789–806. <https://doi.org/10.1177/0042098012448551>
- Cao, Q., Shi, M., 2020. Research on spatial resilience characteristics and response mechanism of Chengdu-Chongqing urban agglomeration based on power-law, in: 2020 International Workshop on Green Energy, Environment and Sustainable Development, G2ESD 2020. IOP Publishing Ltd. <https://doi.org/10.1088/1755-1315/601/1/012028>
- Caputo, S., Caserio, M., Coles, R., Jankovic, L., Gaterell, M.R., 2015. Urban resilience: two diverging interpretations. *Journal of Urbanism* 8, 222–240. <https://doi.org/10.1080/17549175.2014.990913>
- Caputo, S., Caserio, M., Coles, R., Jankovic, L., Gaterell, M.R., 2013. A scenario-based analysis of building energy performance. *Proceedings of the Institution of Civil Engineers: Urban Design and Planning* 166, 326–348. <https://doi.org/10.1680/udap.12.00008>
- Cariolet, J.-M., Colombert, M., Vuillet, M., Diab, Y., 2018. Assessing the resilience of urban areas to traffic-related air pollution: Application in Greater Paris. *Science of the Total Environment* 615, 588–596. <https://doi.org/10.1016/j.scitotenv.2017.09.334>
- Cerè, G., Zhao, W., Rezgui, Y., 2018. Nurturing Virtual Collaborative Networks into Urban Resilience for Seismic Hazards Mitigation, 19th IFIP WG 5.5 Working Conference on Virtual Enterprises, PRO-VE 2018. Springer New York LLC.
- Cimellaro, G.P., Marasco, S., Zamani Noori, A., Kammouh, O., Mahin, S., 2018. A new tool to assess the resilience of an urban environment under an earthquake scenario, in: 11th National Conference on Earthquake Engineering 2018: Integrating Science, Engineering, and Policy, NCEE 2018. Earthquake Engineering Research Institute, pp. 5606–5617.
- Connelly, A., O’Hare, P., White, I., 2020. “The best flood I ever had”: Contingent resilience and the (relative) success of adaptive technologies. *Cities* 106. <https://doi.org/10.1016/j.cities.2020.102842>
- Cruz, S.S., Costa, J.P.T.A., de Sousa, S.Á., Pinho, P., 2013. *Urban Resilience and Spatial Dynamics*, GeoJournal Library. Springer Science and Business Media B.V.
- Cutini, V., de Falco, A., Giuliani, F., Syntax, B.I. of A.D. (BIAD); C.I. of U.P. and D.U.C.L.S., 2019. Urban grid and seismic prevention: A configurational approach to

- the emergency management of Italian historic centres, in: 12th International Space Syntax Symposium, SSS 2019. Beijing JiaoTong University.
- Cutini, V., Pezzica, C., 2020. Street Network Resilience Put to the Test: The Dramatic Crash of Genoa and Bologna Bridges. *SUSTAINABILITY* 12. <https://doi.org/10.3390/su12114706>
- da Silva, J., Kernaghan, S., Luque, A., 2012. A systems approach to meeting the challenges of urban climate change. *International Journal of Urban Sustainable Development* 4, 125–145. <https://doi.org/10.1080/19463138.2012.718279>
- Dhar, T.K., Khirfan, L., 2017. A multi-scale and multi-dimensional framework for enhancing the resilience of urban form to climate change. *URBAN CLIMATE* 19, 72–91. <https://doi.org/10.1016/j.uclim.2016.12.004>
- du Plessis, C., Landman, K., Nel, D., Peres, E., 2015. A “resilient” urban morphology: TRUST. *URBAN MORPHOLOGY* 19, 183–184.
- Eckert, R., Huynh, L.H.C., 2015. Climate responsive neighbourhoods for HCMC: Compact city vs. urban landscape, in: *Sustainable Ho Chi Minh City: Climate Policies for Emerg. Mega Cities*. Springer International Publishing, pp. 207–238.
- Eltinay, N., Egbu, C., 2017. Disaster risk reduction conceptual framework: Open data for building resilience in critical infrastructure, in: Chan, P.W., Neilson, C.J. (Eds.), 33rd Annual Association of Researchers in Construction Management Conference, ARCOM 2017. Association of Researchers in Construction Management, pp. 197–207.
- Feliciotti, A., Romice, O., Porta, S., 2016. DESIGN FOR CHANGE: FIVE PROXIES FOR RESILIENCE IN THE URBAN FORM. *OPEN HOUSE INTERNATIONAL* 41, 23–30.
- Feng, X., Lei, J., Xiu, C., Li, J., Bai, L., Zhong, Y., 2020. Analysis of Spatial Scale Effect on Urban Resilience: A Case Study of Shenyang, China. *Chinese Geographical Science* 30, 1005–1021. <https://doi.org/10.1007/s11769-020-1163-7>
- Ferreira, T.M., Maio, R., Vicente, R., Costa, A., 2016. Earthquake risk mitigation: the impact of seismic retrofitting strategies on urban resilience. *International Journal of Strategic Property Management* 20, 291–304. <https://doi.org/10.3846/1648715X.2016.1187682>
- Fischer, K., Hiermaier, S., Riedel, W., Haring, I., 2018. Morphology Dependent Assessment of Resilience for Urban Areas. *SUSTAINABILITY* 10. <https://doi.org/10.3390/su10061800>
- Fusco, G., Venerandi, A., 2020. Assessing Morphological Resilience. Methodological Challenges for Metropolitan Areas, 20th International Conference on Computational

Science and Its Applications, ICCSA 2020. Springer Science and Business Media Deutschland GmbH.

Fu, X., Wang, X., 2018. Developing an integrative urban resilience capacity index for plan making. *Environment Systems and Decisions* 38, 367–378.
<https://doi.org/10.1007/s10669-018-9693-6>

García-Esparza, J.A., Alcañiz, E., 2017. To rehabilitate the habitability. Scenario simulation for consolidated urban areas in Warm regions. *WSEAS Transactions on Environment and Development* 13, 291–303.

Giuliani, F., de Falco, A., Cutini, V., 2020. The role of urban configuration during disasters. A scenario-based methodology for the post-earthquake emergency management of Italian historic centres. *Safety Science* 127.
<https://doi.org/10.1016/j.ssci.2020.104700>

Gleeson, B., 2008. Critical commentary. Waking from the dream: An Australian perspective on urban resilience. *Urban Studies* 45, 2653–2668.
<https://doi.org/10.1177/0042098008098198>

Habibi, S.M., Nabavi Razavi, H.S., DRI International; Fonds National Suisse Schweizerischer National Fonds, F.S.R., 2016. Assessment of urban fabrics to increase resiliency against earthquake in Iran (Ghazvin), in: Sigrist, D., Wahlen, S., Bernabe, N., Stal, M., Portmann, J., M, D.V.D., Ammann, W.J., Glover, J. (Eds.), 6th International Disaster and Risk Conference: Integrative Risk Management - Towards Resilient Cities, IDRC Davos 2016. Global Risk Forum (GRF), pp. 256–263.

Hatvani-Kovacs, G., Belusko, M., Skinner, N., Pockett, J., Boland, J., 2016. Heat stress risk and resilience in the urban environment. *Sustainable Cities and Society* 26, 278–288. <https://doi.org/10.1016/j.scs.2016.06.019>

Houghton, A., Castillo-Salgado, C., 2017. Health co-benefits of green building design strategies and community resilience to urban flooding: A systematic review of the evidence. *International Journal of Environmental Research and Public Health* 14.
<https://doi.org/10.3390/ijerph14121519>

Ingaramo, R., Pascale, L., 2020. An interpretative matrix for an adaptive design approach. Italian school infrastructure: Safety and social restoration. *Sustainability (Switzerland)* 12, 1–22. <https://doi.org/10.3390/su12208354>

Irajifar, L., Sipe, N., Alizadeh, T., 2016. The impact of urban form on disaster resiliency A case study of Brisbane and Ipswich, Australia. *INTERNATIONAL JOURNAL OF DISASTER RESILIENCE IN THE BUILT ENVIRONMENT* 7, 259–275.
<https://doi.org/10.1108/IJDRBE-10-2014-0074>

- Khirfan, L., El-Shayeb, H., 2020. Urban climate resilience through socio-ecological planning: a case study in Charlottetown, Prince Edward Island. *Journal of Urbanism* 13, 187–212. <https://doi.org/10.1080/17549175.2019.1650801>
- Kittana, A.M.G., Meulder, B.D., 2019. Architecture as an agency of resilience in urban armed conflicts: The case of Nablus City/Palestine. *Archnet-IJAR* 13, 698–717. <https://doi.org/10.1108/ARCH-03-2019-0065>
- Kostourou, F., Karimi, K., 2017. The integration of new social housing in existing urban schemes: The case of Cité Manifeste in Mulhouse, France. *Urban Morphology* 21, 41–60.
- Kumar, V., Bandhyopadhyay, S., Ramamritham, K., Jana, A., 2020. Optimizing the Redevelopment Cost of Urban Areas to Minimize the Fire Susceptibility of Heterogeneous Urban Settings in Developing Nations: a Case from Mumbai, India. *PROCESS INTEGRATION AND OPTIMIZATION FOR SUSTAINABILITY* 4, 361–378. <https://doi.org/10.1007/s41660-020-00124-9>
- Ladiana, D., di Sivo, M., (CIOB), A.C.I. (ACI); A.I. of J. (AIJ); J.C.I. (JCI); J.S. of C.E. (JSCE); T.C.I. of B., 2017. Resilient communities for safe cities, in: Adam, J.M., Pellicer, E., Yazdani, S., Singh, A., Yepes, V. (Eds.), 9th International Structural Engineering and Construction Conference: Resilient Structures and Sustainable Construction, ISEC 2017. ISEC Press.
- Lak, A., Asl, S.S., Maher, A., 2020. Resilient urban form to pandemics: Lessons from COVID-19. *Medical Journal of the Islamic Republic of Iran* 34, 1–9. <https://doi.org/10.34171/mjiri.34.71>
- Leon, J., Castro, S., Mokrani, C., Gubler, A., 2020. Tsunami evacuation analysis in the urban built environment: a multi-scale perspective through two modeling approaches in Vina del Mar, Chile. *COASTAL ENGINEERING JOURNAL* 62, 389–404. <https://doi.org/10.1080/21664250.2020.1738073>
- Lim, H.K., Kain, J.H., 2016. Compact Cities Are Complex, Intense and Diverse but: Can We Design Such Emergent Urban Properties? *URBAN PLANNING* 1, 95–113. <https://doi.org/10.17645/up.v1i1.535>
- Magliocchetti, M., Adinolfi, V., Viccione, G., Grimaldi, M., Fasolino, I., 2021. Small rivers and landscape nbs to mitigate flood risk. *Sustainable Mediterranean Construction* 2021, 32–36.
- Marcus, L., Colding, J., 2014. Toward an integrated theory of spatial morphology and resilient urban systems. *ECOLOGY AND SOCIETY* 19. <https://doi.org/10.5751/ES-06939-190455>

- Meshkini, A., Hajilou, M., Jokar, S., Esmaeili, A., 2021. The role of land use patterns in earthquake resilience: a case study of the Ahvaz Manba Ab neighborhood. *Natural Hazards*. <https://doi.org/10.1007/s11069-021-04909-0>
- Miguez, M.G., Veról, A.P., Battemarco, B.P., Yamamoto, L.M.T., de Brito, F.A., Fernandez, F.F., Merlo, M.L., Queiroz Rego, A., 2019. A framework to support the urbanization process on lowland coastal areas: Exploring the case of Vargem Grande – Rio de Janeiro, Brazil. *Journal of Cleaner Production* 231, 1281–1293. <https://doi.org/10.1016/j.jclepro.2019.05.187>
- Monteiro, A., Carvalho, V., Velho, S., Sousa, C., 2012. Assessing and monitoring urban resilience using COPD in Porto. *SCIENCE OF THE TOTAL ENVIRONMENT* 414, 113–119. <https://doi.org/10.1016/j.scitotenv.2011.11.009>
- Morschek, J., König, R., Schneider, S., 2019. An integrated urban planning and simulation method to enforce spatial resilience towards flooding hazards, in: Rockcastle, S., Rakha, T., Davila, C.C., Papanikolaou, D., Zakula, T. (Eds.), 10th Annual Symposium on Simulation for Architecture and Urban Design, SimAUD 2019. The Society for Modeling and Simulation International, pp. 79–86.
- Mota, R., Tavares, A.O., Santos, P.P., 2017. Urban vulnerability to fires and the efficiency of hydrants. Improving resource positioning and institutional response, in: Cepin, M., Bris, R. (Eds.), 27th European Safety and Reliability Conference, ESREL 2017. CRC Press/Balkema, pp. 1207–1214. <https://doi.org/10.1201/9781315210469-152>
- Mycoo, M., Robinson, S.-A., Nguyen, C., Nisbet, C., Tonkel III, R., 2021. Human Adaptation to Coastal Hazards in Greater Bridgetown, Barbados. *Frontiers in Environmental Science* 9. <https://doi.org/10.3389/fenvs.2021.647788>
- Ottone, M.F., Grifoni, R.C., Marchesani, G.E., Riera, D., 2019. Density - intensity. Material and immaterial elements in assessing urban quality. *TECHNE-JOURNAL OF TECHNOLOGY FOR ARCHITECTURE AND ENVIRONMENT* 17, 278–288. <https://doi.org/10.13128/Techne-24022>
- Paschoalin, R., Pace, R., Isaacs, N., CIAT, A.U.T.U.N.Z., 2020. Urban resilience: Potential for rainwater harvesting in a heritage building, in: Ghaffarianhoseini, A., Ghaffarianhoseini, A., Naismith, N., Purushothaman, M.B., Doan, D., Aigwi, E., Rotimi, F., Ghodrati, N. (Eds.), 54th International Conference of the Architectural Science Association, ANZAScA 2020. Architectural Science Association, pp. 1331–1340.
- Perera, A.T.D., Javanroodi, K., Nik, V.M., 2021. Climate resilient interconnected infrastructure: Co-optimization of energy systems and urban morphology. *APPLIED ENERGY* 285. <https://doi.org/10.1016/j.apenergy.2020.116430>

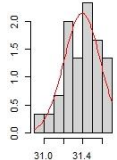
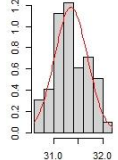
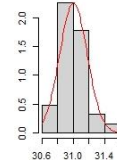
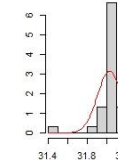
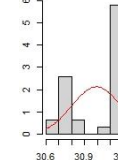
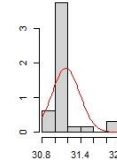
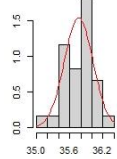
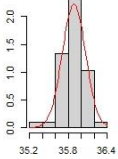
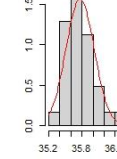
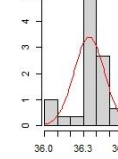
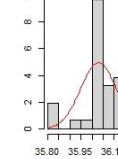
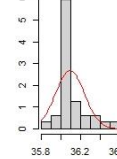
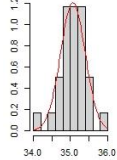
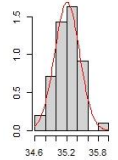
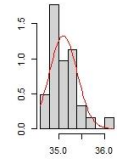
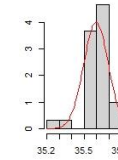
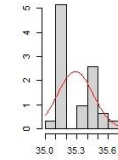
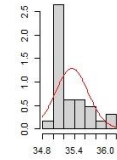
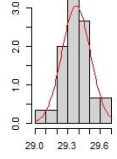
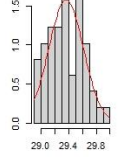
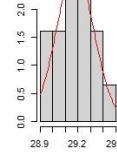
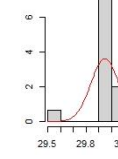
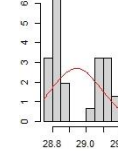
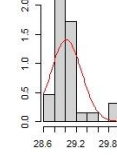
- Pessoa, I.M., Tasan-Kok, T., Altes, W.K., 2016. Brazilian urban porosity: Treat or threat? *Proceedings of the Institution of Civil Engineers: Urban Design and Planning* 169, 47–55. <https://doi.org/10.1680/udap.15.00009>
- Pitidis, V., Tapete, D., Coaffee, J., Kapetas, L., de Albuquerque, J.P., 2018. Understanding the implementation challenges of urban resilience policies: Investigating the influence of urban geological risk in Thessaloniki, Greece. *Sustainability (Switzerland)* 10. <https://doi.org/10.3390/su10103573>
- Ragheb, S.A., Ayad, H.M., Galil, R.A., 2017. An energy-resilient city, an appraisal matrix for the built environment. 9th International Conference on Sustainable Development and Planning, SDP 2017 226, 667–678. <https://doi.org/10.2495/SDP170581>
- Rao, F.J., Dovey, K., Pafka, E., 2018. Towards a genealogy of urban shopping: types, adaptations and resilience. *JOURNAL OF URBAN DESIGN* 23, 544–557. <https://doi.org/10.1080/13574809.2017.1405726>
- Rauland, V., Newman, P., University, C.A.G.-B. of M.P.C. and E.C.P.C.B.C., 2011. Decarbonising Australian cities: A new model for creating low carbon, resilient cities, in: 19th International Congress on Modelling and Simulation - Sustaining Our Future: Understanding and Living with Uncertainty, MODSIM2011. pp. 3073–3079.
- Ray, B., Shaw, R., 2018. Changing built form and implications on urban resilience: loss of climate responsive and socially interactive spaces, in: Amaratunga, D., Haigh, R. (Eds.), 7TH INTERNATIONAL CONFERENCE ON BUILDING RESILIENCE: USING SCIENTIFIC KNOWLEDGE TO INFORM POLICY AND PRACTICE IN DISASTER RISK REDUCTION. pp. 117–124.
- Rezende, O.M., Miranda, F.M., Haddad, A.N., Miguez, M.G., 2019. A framework to evaluate urban flood resilience of design alternatives for flood defence considering future adverse scenarios. *Water (Switzerland)* 11. <https://doi.org/10.3390/w11071485>
- Rode, S., Gralepois, M., 2017. Towards an Urban Design Adapted to Flood Risk?, in: *Floods*. Elsevier Inc., pp. 365–380.
- Rode, S., Guevara, S., Bonnefond, M., 2018. Resilience in urban development projects in flood-prone areas: A challenge to urban design professionals. *Town Planning Review* 89, 167–190. <https://doi.org/10.3828/tpr.2018.10>
- Roggema, R., 2018. Design with voids: how inverted urbanism can increase urban resilience. *Architectural Science Review* 61, 349–357. <https://doi.org/10.1080/00038628.2018.1502153>
- Romano, R., Bologna, R., Hasanaj, G., Arnetoli, M. v, 2020. Adaptive design to mitigate the effects of UHI: The case study of piazza togliatti in the municipality of scandicci, 11th International Conference on Sustainability and Energy in Buildings, SEB 2019. Springer.

- Roosta, M., Javadpoor, M., Ebadi, M., n.d. A study on street network resilience in urban areas by urban network analysis: comparative study of old, new and middle fabrics in shiraz. *INTERNATIONAL JOURNAL OF URBAN SCIENCES*.
<https://doi.org/10.1080/12265934.2021.1911676>
- Samuelsson, K., Colding, J., Barthel, S., 2019. Urban resilience at eye level: Spatial analysis of empirically defined experiential landscapes. *Landscape and Urban Planning* 187, 70–80. <https://doi.org/10.1016/j.landurbplan.2019.03.015>
- Schinke, R., Kaidel, A., Golz, S., Naumann, T., López-Gutiérrez, J.S., Garvin, S., 2016. Analysing the effects of flood-resilience technologies in urban areas using a synthetic model approach. *ISPRS International Journal of Geo-Information* 5.
<https://doi.org/10.3390/ijgi5110202>
- Serre, D., 2018. Ds3 model testing: Assessing critical infrastructure network flood resilience at the neighbourhood scale, *Urban Book Series*. Springer.
- Sharifi, A., Roosta, M., Javadpoor, M., 2021. Urban Form Resilience: A Comparative Analysis of Traditional, Semi-Planned, and Planned Neighborhoods in Shiraz, Iran. *URBAN SCIENCE* 5. <https://doi.org/10.3390/urbansci5010018>
- Sharifi, E., Boland, J., 2017. Heat Resilience in Public Space and Its Applications in Healthy and Low Carbon Cities, in: Ding, L., Fiorito, F., Osmond, P. (Eds.), *International High-Performance Built Environment Conference - A Sustainable Built Environment Conference 2016 Series SBE16, IHBE 2016*. Elsevier Ltd, pp. 944–954.
<https://doi.org/10.1016/j.proeng.2017.04.254>
- Sharifi, E., Larbi, M., Omrany, H., Boland, J., 2020. Climate change adaptation and carbon emissions in green urban spaces: Case study of Adelaide. *Journal of Cleaner Production* 254. <https://doi.org/10.1016/j.jclepro.2020.120035>
- Song, J., Li, W., 2019. Linkage between the environment and individual resilience to urban flooding: A case study of shenzhen, china. *International Journal of Environmental Research and Public Health* 16. <https://doi.org/10.3390/ijerph16142559>
- Tablada, A., Zhao, X., 2016. Sunlight availability and potential food and energy self-sufficiency in tropical generic residential districts. *Solar Energy* 139, 757–769.
<https://doi.org/10.1016/j.solener.2016.10.041>
- Tayebi, S., Mohammadi, H., Shamsipoor, A., Tayebi, S., Alavi, S.A., Hoseinioun, S., 2019. Analysis of land surface temperature trend and climate resilience challenges in Tehran. *International Journal of Environmental Science and Technology* 16, 8585–8594. <https://doi.org/10.1007/s13762-019-02329-z>
- Tumini, I., Villagra-Islas, P., Herrmann-Lunecke, G., 2017. Evaluating reconstruction effects on urban resilience: a comparison between two Chilean tsunami-prone cities. *NATURAL HAZARDS* 85, 1363–1392. <https://doi.org/10.1007/s11069-016-2630-4>

- Villagra, P., Rojas, C., Ohno, R., Xue, M., Gomez, K., 2014. A GIS-base exploration of the relationships between open space systems and urban form for the adaptive capacity of cities after an earthquake: The cases of two Chilean cities. *APPLIED GEOGRAPHY* 48, 64–78. <https://doi.org/10.1016/j.apgeog.2014.01.010>
- Wang, C.-H., 2020. Does compact development promote a seismic-resistant city? Application of seismic-damage statistical models to Taichung, Taiwan. *Environment and Planning B: Urban Analytics and City Science* 47, 84–101. <https://doi.org/10.1177/2399808318770454>
- Wang, Y., Berardi, U., Akbari, H., 2016. Comparing the effects of urban heat island mitigation strategies for Toronto, Canada. *Energy and Buildings* 114, 2–19. <https://doi.org/10.1016/j.enbuild.2015.06.046>
- Wang, Y., Berardi, U., Akbari, H., Engineers Without Borders USA; HOK; Kiss + Cathcart, A.T.A.S. of C.E., 2015. The Urban Heat Island Effect in the City of Toronto, in: Chong, W.O., Berardi, U., Parrish, K., Chang, J. (Eds.), *International Conference on Sustainable Design, Engineering and Construction, ICSDEC 2015*. Elsevier Ltd, pp. 137–144. <https://doi.org/10.1016/j.proeng.2015.08.412>
- Williams, A.A., Allen, J.G., Catalano, P.J., Spengler, J.D., 2020. The role of individual and small-area social and environmental factors on heat vulnerability to mortality within and outside of the Home in Boston, MA. *Climate* 8. <https://doi.org/10.3390/cli8020029>
- Xu, C., Rahman, M., Haase, D., Wu, Y., Su, M., Pauleit, S., 2020. Surface runoff in urban areas: The role of residential cover and urban growth form. *Journal of Cleaner Production* 262. <https://doi.org/10.1016/j.jclepro.2020.121421>
- Yamagata, Y., Seya, H., Murakami, D., 2016. *Urban Economics Model for Land-Use Planning, Advanced Sciences and Technologies for Security Applications*. Springer.
- Yang, P.P.J., Quan, S.J., 2016. *Urban Form and Energy Resilient Strategies: A Case Study of the Manhattan Grid, Advanced Sciences and Technologies for Security Applications*. Springer.

Appendix B: Results of the normality and homogeneity of variance tests conducted in Chapter 7

Frequency distribution histograms of air temperature for each LCZ type per each day/time analyzed with the p -value from Shapiro–Wilk normality test (below each) and Fligner–Killeen test for the homogeneity of variance. The distribution is considered normal and variances are homogenous at ($p > .05$).

Day (time)	LCZ 2	LCZ 5	LCZ 6	LCZ 8	LCZ C	LCZ F	Homogeneity of variance
02/09/2020 (19:00 LT)							$p = 5.035178e-07$
	$p = 6.323676e-01$	$p = 3.521526e-01$	$p = 1.639603e-01$	$p = 3.494563e-08$	$p = 6.188499e-06$	$p = 1.124049e-07$	
29/09/2020 (14:30 LT)							$p = 1.45414e-06$
	$p = 0.6799107655$	$p = 0.1068810658$	$p = 0.3868190892$	$p = 0.0006894062$	$p = 0.0019820774$	$p = 0.0001913463$	
30/09/2020 (13:30 LT)							$p = .0001674927$
	$p = 6.524923e-01$	$p = 7.515832e-01$	$p = 7.531267e-02$	$p = 1.293143e-04$	$p = 5.339849e-04$	$p = 5.797406e-05$	
30/09/2020 (19:30 LT)							$p = 2.890359e-07$
	$p = 8.465725e-01$	$p = 8.135701e-02$	$p = 2.863004e-01$	$p = 5.929122e-09$	$p = 7.819299e-05$	$p = 2.450235e-05$	

Appendix C: Results of the normality and homogeneity of variance tests conducted in Chapter 8

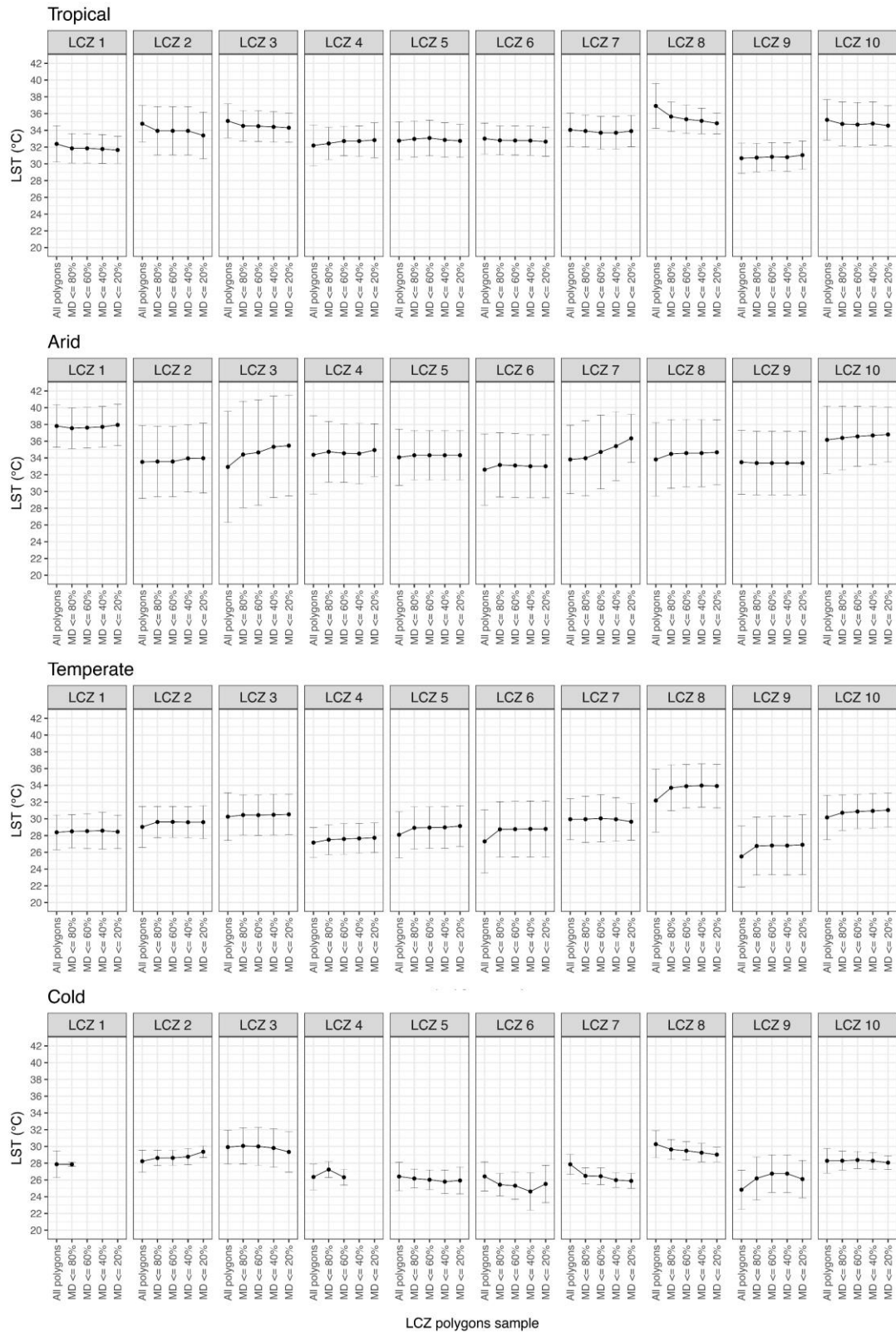


Figure 1. Comparison between the mean LST values calculated per LCZ type and macroclimate region using different samples of LCZ polygons with varying levels of missing data (MD), from no more than 20% up to 80% of missing data in all months. Bars represent standard deviation.

Table 1. Frequency distribution histograms of LST for each LCZ type per macroclimate region with the p -value from Shapiro–Wilk normality test (below each) and Fligner–Killeen test for the homogeneity of variance. The distribution is considered normal and variances are homogenous at ($p > .05$).

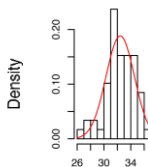
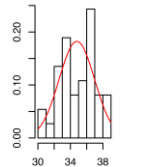
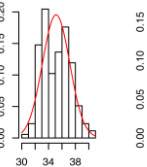
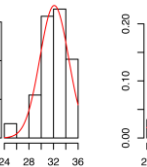
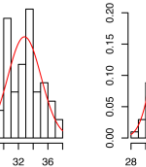
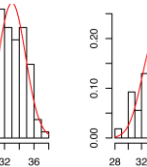
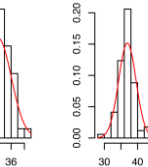
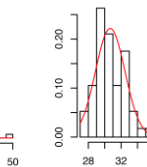
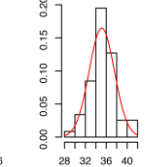
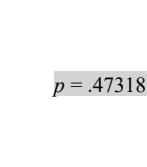
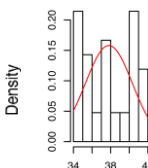
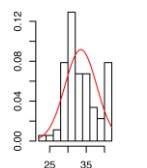
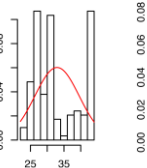
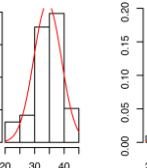
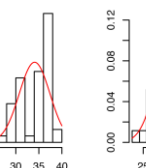
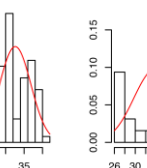
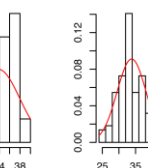
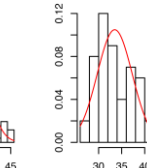
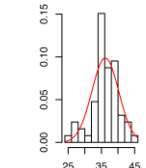
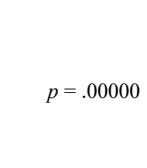
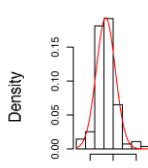
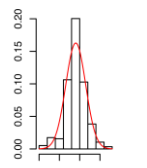
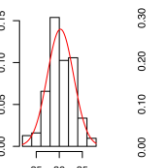
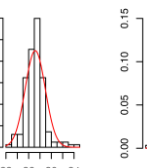
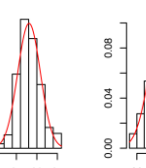
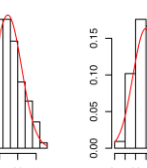
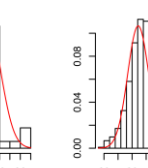
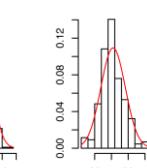
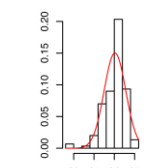
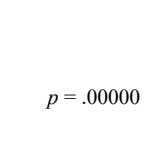
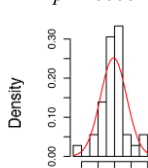
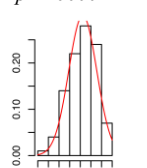
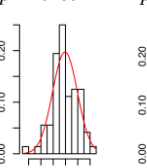
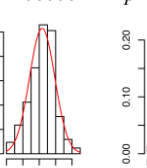
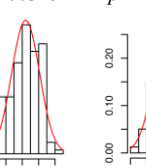
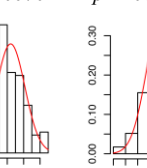
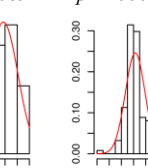
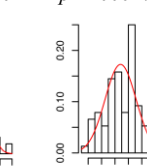
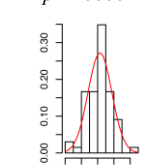
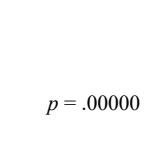
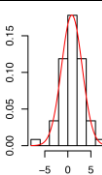
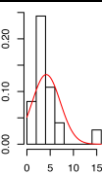
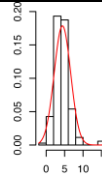
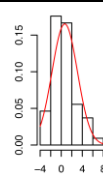
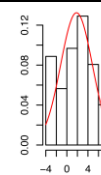
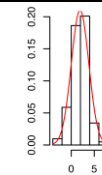
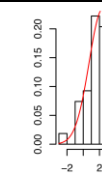
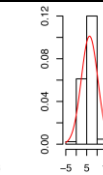
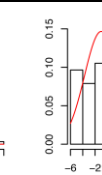
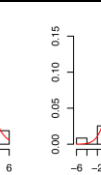
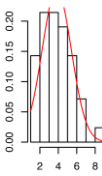
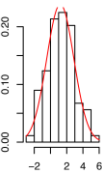
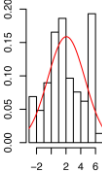
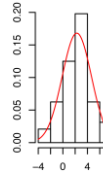
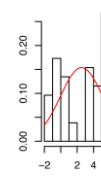
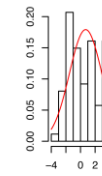
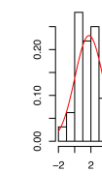
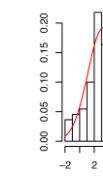
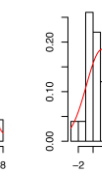
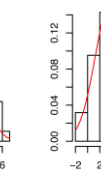
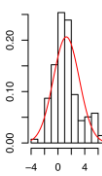
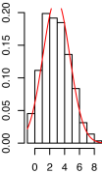
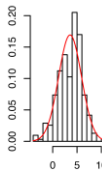
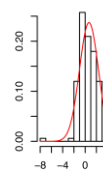
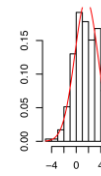
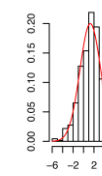
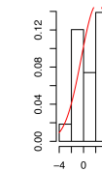
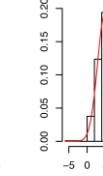
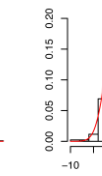
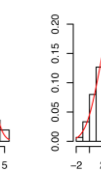
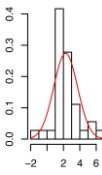
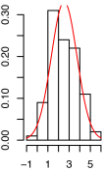
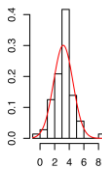
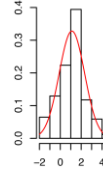
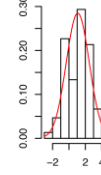
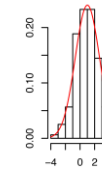
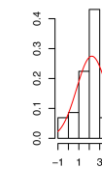
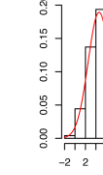
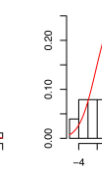
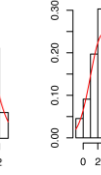
Macroclimate region	LCZ 1	LCZ 2	LCZ 3	LCZ 4	LCZ 5	LCZ 6	LCZ 7	LCZ 8	LCZ 9	LCZ 10	Homogeneity of variance
Tropical											$p = .47318$
	$p = .12187$	$p = .23131$	$p = .00035$	$p = .01995$	$p = .06360$	$p = .48315$	$p = .33185$	$p = .00001$	$p = .21435$	$p = .85048$	
Arid											$p = .00000$
	$p = .00354$	$p = .00045$	$p = .00000$	$p = .01105$	$p = .00006$	$p = .02208$	$p = .00050$	$p = .00459$	$p = .00847$	$p = .06267$	
Temperate											$p = .00000$
	$p = .00001$	$p = .00001$	$p = .02594$	$p = .00000$	$p = .00325$	$p = .00070$	$p = .00069$	$p = .00000$	$p = .00027$	$p = .00001$	
Cold											$p = .00000$
	$p = .13711$	$p = .38704$	$p = .19263$	$p = .04036$	$p = .01224$	$p = .00626$	$p = .04375$	$p = .00010$	$p = .06589$	$p = .47444$	
Homogeneity of variance	$p = .00119$	$p = .00000$	$p = .00000$	$p = .00000$	$p = .00001$	$p = .00000$	$p = .00001$	$p = .00000$	$p = .00000$	$p = .00000$	(all macroclimate regions included)
	$p = .10178$	$p = .00020$	$p = .00011$	$p = .01675$	$p = .00003$	$p = .00000$	$p = .00124$	$p = .00000$	$p = .00005$	$p = .00046$	(excluding the arid climate region)

Table 2. Frequency distribution histograms of SUHI for each LCZ type per macroclimate region with the p -value from Shapiro–Wilk normality test (below each) and Fligner–Killeen test for the homogeneity of variance. The distribution is considered normal and variances are homogenous at ($p > .05$).

Macroclimate region	LCZ 1	LCZ 2	LCZ 3	LCZ 4	LCZ 5	LCZ 6	LCZ 7	LCZ 8	LCZ 9	LCZ 10	Homogeneity of variance
Tropical											$p = .00000$
	$p = .28239$	$p = .00000$	$p = .00000$	$p = .00499$	$p = .11708$	$p = .00016$	$p = .82535$	$p = .00000$	$p = .04638$	$p = .16867$	
Arid											$p = .00001$
	$p = .08969$	$p = .48078$	$p = .00010$	$p = .66473$	$p = .00017$	$p = .00103$	$p = .09127$	$p = .13923$	$p = .04213$	$p = .47554$	
Temperate											$p = .00000$
	$p = .00019$	$p = .00373$	$p = .00080$	$p = .00013$	$p = .09338$	$p = .00554$	$p = .03487$	$p = .00072$	$p = .00007$	$p = .38274$	
Cold											$p = .00000$
	$p = .10583$	$p = .60004$	$p = .00056$	$p = .02026$	$p = .00430$	$p = .25808$	$p = .02135$	$p = .15661$	$p = .00081$	$p = .06017$	
Homogeneity of variance	$p = .04308$	$p = .00039$	$p = .00000$	$p = .00000$	$p = .00000$	$p = .00017$	$p = .00000$	$p = .81711$	$p = .00377$	$p = .00114$	(all macroclimate regions included)
	$p = .02825$	$p = .00015$	$p = .00000$	$p = .00001$	$p = .00000$	$p = .01505$	$p = .00000$	$p = .67439$	$p = .00140$	$p = .02597$	(excluding the arid climate region)

Appendix D: Data sources, processing steps and the calculation of the urban form measures selected in Chapter 9 for the statistical clustering of neighborhoods

1. Data sources and processing

1.1 Road centerlines and pedestrian paths

The map of road centerlines and pedestrian paths was created by combining official street network data (that are incomplete and low-detail) with OpenStreetMap (OSM) data that were manually processed on a line-by-line basis to correct some topology and geometric problems (Gil, 2015; Girres and Touya, 2010). This included:

- Removing duplicate lines.
- Removing overlaps between lines.
- Digitizing missing lines based on recent satellite imagery.
- Excluding unmeaningful objects (e.g. traffic islands, roundabouts and slip roads).
- Substituting multiple road lanes by one road centerline.
- Identifying and excluding lines in areas with public access restrictions (e.g. gated communities) based on land-use maps, satellite imagery and field visits.
- Extending/trimming unfinished lines.
- Connecting, where applicable, orphan lines to the rest of the network.

1.2 Neighborhood boundaries

Neighborhood boundaries were drawn based on the official master plan of the city.

1.3 Building blocks

Blocks were retrieved from the official digital topographic database (DTDB), where each block is defined by road centerlines. When blocks were not surrounded by road centerlines from all sides, pedestrian paths or plot boundaries (property lines) were used to delimit the block boundary (Berghauser Pont and Per, 2010; Minoura, 2016).

1.4 Plots (property lines)

Plot data with the state of ownership (e.g. public, private, etc.) were obtained from the official DTDB.

1.5 Building footprints

Buildings and building heights data were mainly obtained from the official DTDB; however, a few other buildings were manually digitized within a 500-m buffer zone from the boundaries of the study neighborhoods as described in Chapter 9.

1.6 Open green spaces

Open green spaces were obtained by means of remote sensing and spatial analysis. In particular, a Landsat 8 level-1 image of the study area (at 30-m spatial resolution), acquired during the growing season on October 10, 2020, was freely downloaded from the United States Geological Survey (USGS, 2015), atmospherically corrected and used to derive the Soil Adjusted Vegetation Index (SAVI) (Huete, 1988). SAVI is a measure of vegetation density that ranges from -1.0 to 1.0, and it is used in areas where vegetation cover is low (e.g. arid areas) to correct for the soil brightness. SAVI is defined as:

$$SAVI = \left(\frac{B5 - B4}{B5 + B4 + L} \right) \times (1 + L) \quad (1)$$

where:

B5 = the near-infrared (NIR) band

B4 = the visible red band

L = a soil brightness correction factor (L = 0.5)

Next, areas with intermediate to dense vegetation were extracted by setting different SAVI threshold values and choosing the one with the best results (i.e. SAVI = 0.15). Finally, private, non-accessible green spaces were excluded using the land property data from the official DTDB.

1.7 Points of interest (POI)

Points of interest (POI) that represent potential social infrastructure were retrieved from the official DTDB and included:

- Big shopping malls (when they have adequate physical space for people to meet).
- Worship places (mosques and churches).
- Cultural services (e.g. public libraries).

1.8 Land use

Land use data were obtained from the official DTDB.

2. Calculation of the urban form measures described in Table 18

2.1 Angular integration

Local and global normalized angular integration (NAIN) were calculated in the PST software (Stähle et al., 2007) based on a line-segment map using the following equation:

$$AI_{NAIN}(x) = \frac{N^{1.2}}{1 + \sum_{i \neq x} D(x, i)} \quad (2)$$

where:

N = node count or number of reached nodes (including origin node)

D(x, i) = angular depth of i in relation to x

2.2 Accessible ground/floor space index (AGSI/AFSI)

AGSI and AFSI were calculated at each building following the procedure described by Berghauser Pont et al. (2019). Firstly, the Reach tool in PST was used to calculate the total accessible land area within a 500-m walking distance from each building (referred to as the catchment area). Secondly, the Attraction Reach tool in PST was used to calculate the accessible built-up area (BA) and accessible gross floor area (GFA) within a 500-m walking distance from each building based on the following equation:

$$AR(o) = \sum_{a \in A} (f(a)) \quad (3)$$

where:

o = point of origin (i.e. buildings)

A = the set of reachable attractions (i.e. buildings) within a given radius (i.e. 500 m)

$f(a)$ = attraction value associated with attraction a (i.e. BA or GFA)

Finally, AGSI and AFSI were calculated by dividing the accessible BA and accessible GFA by the catchment area, respectively.

2.3 Space enclosure (block)

Space enclosure was calculated following the procedure described by Minoura (2016). Firstly, an inward buffer was created from each block perimeter using a specified distance (in this study, a 20-m inward buffer distance was found to achieve the best results). Secondly, buildings were intersected with the inward buffer and the area of the intersection was calculated. Finally, the enclosure value was calculated as the ratio of the area of buildings-buffer intersection over the area of the buffer, where a 100% enclosure indicates a fully built buffer.

2.4 Ground space index (block)

Ground space index (GSI) was calculated for each block as the ratio between the area of building footprints and the total area of the block.

2.5 Accessible area of green space (m²)

The accessible green space area within a 500-m walking distance from each building was calculated in a similar way to the calculation of AGSI and AFSI, i.e. using the Attraction Reach tool in PST based on equation 3, described above.

2.6 Minimum distance to indoor social infrastructure (m)

The minimum distance from each building to the closest POI (described in Section 1.7) was calculated in PST using the Attraction Distance tool based on the following function:

$$AD(o) = \min_{a \in A} (D(o, a)) \quad (4)$$

where:

A = the set of reachable attractions (i.e. POI) within a given radius (i.e. 500 m)

$D(o, a)$ = shortest distance from origin (i.e. building) o to attraction a (i.e. POI)

3. References

- Berghauer Pont, M., Per, H., 2010. *Spacematrix, Space, Density and Urban Form*. NAI Publishers, Rotterdam.
- Berghauer Pont, M., Stavroulaki, G., Bobkova, E., Gil, J., Marcus, L., Olsson, J., Sun, K., Serra, M., Hausleitner, B., Dhanani, A., Legeby, A., 2019. The spatial distribution and frequency of street, plot and building types across five European cities. *Environ Plan B Urban Anal City Sci*. <https://doi.org/10.1177/2399808319857450>
- Gil, J., 2015. Building a multimodal urban network model Using OpenStreetMap data for the analysis of sustainable accessibility. *Lect Notes Geoinf Cartogr*. https://doi.org/10.1007/978-3-319-14280-7_12
- Girres, J.F., Touya, G., 2010. Quality Assessment of the French OpenStreetMap Dataset. *Trans GIS*. <https://doi.org/10.1111/j.1467-9671.2010.01203.x>
- Huete, A.R., 1988. A soil-adjusted vegetation index (SAVI). *Remote Sens Environ*. [https://doi.org/10.1016/0034-4257\(88\)90106-X](https://doi.org/10.1016/0034-4257(88)90106-X)
- Minoura, E., 2016. *Uncommon Ground: Urban Form and Social Territory*. KTH Royal Institute of Technology.
- Ståhle, A., Marcus, L., Karlstrom, L.A., 2007. Place Syntax Tool—GIS Software for Analysing Geographic Accessibility with Axial Lines. *New Dev Sp Syntax Softw* 35–42.
- USGS, 2015. *Landsat 8 (L8) Data Users Handbook*. Earth Resour Obs Sci Cent.